SIDE CHAIN POLYMERS WITH PENDANT CHROMOPHORES FOR NONLINEAR OPTICS

A THESIS SUBMITTED TO THE

UNIVERSITY OF PUNE

FOR THE DEGREE OF

DOCTOR OF PHILOSOPHY

(IN CHEMISTRY)

BY

Mrs. VAISHALI RAGHU VOHRA

POLYMER SCIENCE AND ENGINEERING UNIT

CHEMICAL ENGINEERING DIVISION

NATIONAL CHEMICAL LABORATORY

PUNE 411 008, INDIA

Certificate

Certified that the work incorporated in this thesis "Side chain polymers with pendant chromophores for Nonlinear Optics" submitted by Mrs. Vaishali Raghu Vohra for the degree of Doctor of Philosophy, University of Pune, Pune was carried out by the candidate under my supervision at Polymer Science and Engineering Unit, Chemical Engineering Division, National Chemical Laboratory, Pune 411 008. Such material obtained from other sources has been duly acknowledged in this thesis.

Dr. Surendra Ponrathnam

Research Guide

Dedicated to my father

ACKNOWLEDGEMENT

I would like to express my deep sense of gratitude to my research guide Dr. Surendra Ponrathnam, Scientist, National Chemical Laboratory, Pune, for his invaluable guidance and help rendered throughout the course of this investigation, without which I would not have completed this thesis successfully.

I am very much obliged to Dr. C. R. Rajan and Dr. R. S. Ghadge for the co-operation extended and continuous professional help during the course of this investigation.

I am sincerely thankful to Prof. Dr. H. Finkelmann, Professor, University of Freiburg, Germany, for his immense help and guidance while working with him under DAAD fellowship program.

I am grateful to Dr. F. Kajzar for his professional help.

I thank Prof. S. K. Pakniker who inspired me to do my doctoral studies.

I am truly thankful to Dr. S. Suresh for his immense help and encouragement at every stage of my work.

I am very much personally obliged to all my colleagues and friends who have helped me during my work tenure. All of them and many other well-wishers have left an indelible mark in the preparation of this dissertation.

I take this opportunity to thank Dr. Maryanne Large for her invaluable help.

I thank Mr. S. N. Sathe for his help throughout the research work.

I would like to thank my friend Dr. A. N. Perumal for all his help.

I am greatly indebted to my beloved husband Raghu, for his constant help, morale boosting and for keeping a cheerful spirit around. Mere words cannot express my gratitude to my mother, brother and in-laws for their tremendous support at all times.

I am thankful to Dr. B. D. Kulkarni, Head, Chemical Engineering Division, National Chemical Laboratory and Dr. Paul Ratnaswamy, Director, National Chemical Laboratory, Pune for permitting me to submit this work in the form of thesis. I would also like to thank Council of Scientific and Industrial Research (CSIR) and Deutscher Akademischer Austauschdienst (DAAD) for the award of fellowship during the period of this work.

Vaishali Raghu Vohra

Table of Contents I – IX

List of Figures IX – XIII

List of Tables XIII

List of Schemes XIII – XV

Abstract of thesis XVI – XVIII

TABLE OF CONTENTS

CHAPTER 1

INTRODUCTION

Section No.	Content	Page no.
1	Introduction	1
1.1	History of nonlinear optics	1
1.2	**Basic aspects of nonlinear optical phenomena**	**2**
1.2.1	*Relation between molecular and macroscopic properties*	**7**
1.2.2	*NLO materials*	**7**
1.2.3	*Linear optical effects*	**8**
1.2.3.1	*Refractive index*	**8**
1.2.4	*Nonlinear optical effects*	**9**
1.2.5	*Second harmonic generation (SHG)*	**9**
1.2.5.1	*Frequency doubling*	**10**
1.3	**Optimisation of b**	**11**
1.3.1	*Donor-acceptor system*	**11**
1.3.2	*The nature of substituents*	**12**
1.3.3	*Conjugated psystems*	**14**
1.3.4	*Influence of planarity*	**15**
1.4	**Second order NLO materials**	**15**
1.4.1	*Inorganics*	**15**
1.4.2	*Organometallic compounds*	**16**
1.4.3	*Organics*	**16**

1.5	**Polymer films**	**19**
1.5.1	*Amorphous doped or "guest-host" polymers*	**20**
1.5.2	*Functionalised polymers*	**20**
1.6	**Liquid crystals**	**21**
1.6.1	*Classification*	**21**
1.6.1.1	*Nematic*	**21**
1.6.1.2	*Cholesteric*	**22**
1.6.1.3	*Smectic*	**22**
1.6.1.4	*Chiral Smectic C phase*	**22**
1.6.2	*Liquid crystalline polymers*	**26**
1.6.3	*Ferroelectric liquid crystals*	**26**
1.7	**Applications of NLO materials**	**28**
1.7.1	*Optical switches*	**28**
1.7.2	*Second order devices*	**29**
1.7.3	*Holographic optical element (HOE)*	**30**
1.8	**Scope of this work**	**30**
1.9	**References**	**34**

CHAPTER 2

SYNTHESIS OF MONOMERS

Section No.	Content	Page no.
2	**Synthesis of monomers**	**40**
2.1	**Azomethines**	**40**
2.1.1	*General synthesis of substituted azomethine*	**40**
2.1.1.1	*General procedure for synthesis of azomethine bases*	**40**
2.2	**Azomethines with spacer**	**43**
2.2.1	*General procedure for alkylation*	**44**
2.3	**4-(2-Methacryloyloxyethyloxy)-N-(4'-formyl/ methinebarbiturate benzylidene) aniline**	**46**
2.3.1	*Preparation of methacryloyl chloride*	**47**
2.3.2	*Synthesis of 4-(2-methacryloyloxy ethyloxy)-N-(4'-formyl benzylidene) aniline*	**47**
2.3.3	*Synthesis of 4-(2-methacryloyloxyethyloxy)-N-(4'-methinebarbiturate benzylidene)aniline*	**48**
2.4	*4-(2-Acryloyloxy ethyloxy)-N-(4'-formyl/methinebarbiturate benzylidene) aniline*	**49**
2.4.1	*Preparation of acryloyl chloride*	**49**

2.4.2	*Synthesis of 4-(2-acryloyloxy ethyloxy)-N-(4'-formyl benzylidene) aniline*	**50**
2.4.3	*Synthesis of 4-(2-acryloyloxy ethyloxy)-N-(4'-methinebarbiturate benzylidene) aniline*	**51**
2.5	**4-[2-(4-Vinylbenzyloxy) ethyloxy]-N-(4'-cyano/ nitro/ formyl/methinebarbiturate benzylidene) aniline**	**52**
2.5.1	*Synthesis of 4-[2-(4-vinylbenzyloxy) ethyloxy]-N-(4'-cyano/ nitro/formyl benzylidene) aniline*	**52**
2.5.2	*Synthesis of 4-[2-(4-vinylbenzyloxy) ethyloxy]-N-(4'-methinebarbiturate benzylidene)aniline*	**54**
2.6	**4-[2/6-(N-Maleimido)eth-1-yloxy/hex-1-yloxy)-N-(4'-cyano/nitro benzylidene)] aniline**	**55**
2.6.1	*Synthesis of 4-[2/6-(N-maleimido) eth-1-yloxy/ hex-1-yloxy)-N-(4'-cyano/ nitro benzylidene)]aniline*	**55**
2.7	**Azobenzenes**	**58**
2.7.1	*General synthesis of substituted azobenzene*	**58**
2.7.2	*Diazotisation with phenol*	**58**
2.8	**Azo compounds with spacer**	**59**
2.8.1	*General procedure for alkylation*	**59**
2.9	**4-(2-Methacryloyloxy ethyloxy)-4'-formyl/ methinebarbiturate azobenzene**	**60**
2.9.1	*Synthesis of 4-(2-methacryloyloxy ethyloxy)-4'-formyl azobenzene*	**61**
2.9.2	*Synthesis of 4-(2-methacryloyloxyethyloxy)-4'-methinebarbiturate azobenzene*	**61**
2.10	**4-(2-Acryloyloxyethyloxy)-4'-formyl/methinebarbiturate azobenzene**	**62**
2.10.1	*Synthesis of 4-(2-acryloyloxyethyloxy)-4'-formylphenylazobenzene*	**63**
2.10.2	*Synthesis of 4-(2-acryloyloxyethyloxy)-4'-methinebarbiturate azobenzene*	**64**
2.11	**4-[2-(3/4-Vinylbenzyloxy)ethyloxy]-4'-formyl/ methinebarbiturate azobenzene**	**65**
2.11.1	*Synthesis of 4-[2-(3/4-vinylbenzyloxy)ethyloxy]-4'-formyl azobenzene*	**65**
2.11.2	*Synthesis of 4-[2-(3/4-vinylbenzyloxy)ethyloxy]-4'-methinebarbiturate azobenzene*	**66**
2.12	**4-[2-(N-Maleimido) ethyloxy]-4'-formyl azobenzene**	**67**
2.12.1	*Synthesis of 4-[2-(N-maleimido)ethyloxy]-4'-formyl azobenzene*	**67**
2.13	**Heterocycles as chromophores**	**68**
2.13.1	*Synthesis of N-(3-hydroxypropyl)carbazole*	**69**
2.13.2	*Synthesis of 2-formyl-N-(3-hydroxypropyl)carbazole*	**70**

2.13.3	*2-Formyl-N-[3-(3/4-vinylbenzyloxy)propyl]carbazole*	**70**
2.13.3.1	*Synthesis of 2-formyl-N-[3-(3/4-vinylbenzyloxy)propyl] carbazole*	**71**
2.13.4	*2-(4-Cyano/nitro phenylene-1-azomethine)-N-(3-hydroxy propyl) carbazole*	**71**
2.13.4.1	*Synthesis of 2-(4-cyano/ nitro phenylene-1-azomethine)-N-(3-hydroxy propyl) carbazole*	**72**
2.13.5	*2-(4-Cyano/nitro phenylene-1-azomethine)-N-[3-(3/4-vinyl benzyloxy) propyl] carbazole*	**73**
2.13.5.1	*Synthesis of 2-(4-cyano/nitro phenylene-1-azomethine)-N-[3-(3/4-vinyl benzyloxy)propyl] carbazole*	**73**
2.14	**Synthesis of monomers from 5-amino-1,3,4-thiadiazole-2-thiol**	**75**
2.14.1	*Synthesis of 5-[N-(4'-cyano/nitro benzylidene)amine]-1,3,4-thiadiazole-2-thiol*	**75**
2.14.2	*Synthesis of 5-[N-(4'- cyano/nitro benzylidene)amine]-2-(2-hydroxyethylthio)-1,3,4-thiadiazole*	**76**
2.14.3	*5-[N-(4'-Cyano/nitro benzylidene)amine]-2-(2-methacryloyl oxyethylthio)-1,3,4-thiadiazole*	**77**
2.14.3.1	*Synthesis of 5-[N-(4'-cyano/nitro benzylidene)amine]-2-(2-methacryloyl oxyethylthio)-1,3,4-thiadiazole*	**78**
2.14.4	*5-[N-(4'-Nitro benzylidene) amine]-2-(2-acryloyloxy ethylthio)-1,3,4-thiadiazole*	**79**
2.14.4.1	*Synthesis of 5-[N-(4'-nitro benzylidene) amine]-2-(2-acryloyloxyethylthio)-1,3,4-thiadiazole*	**79**
2.14.5	*5-[N-(4'-Cyano/nitro benzylidene)amine]-2-[2-(3/4-vinyl benzyloxy)ethylthio]-1,3,4-thiadiazole*	**80**
2.14.5.1	*Synthesis of 5-[N-(4'-cyano/nitro benzylidene)amine]-2-[2-(3/4-vinyl benzyloxy) ethylthio]-1,3,4-thiadiazole*	**81**
2.15	**4-[g-(2,3-Dihydroxypropaneoxy)propyloxy]-4'-nitro/cyano azobenzene *and* N-(4'-nitro/cyano benzylidene)-4-[g-(2,3-dihydroxypropaneoxy) ethyloxy] aniline**	**82**
2.15.1	*Synthesis of 4-[g-(2,3-epoxypropaneoxy) propyloxy]-4'-nitro/cyano azobenzene* and *N-(4'-nitro/cyano benzylidene)-4-[b-(2,3-epoxypropane oxy) ethyloxy]aniline*	**83**
2.15.2	*Synthesis of 4-[g-(2,3-dihydroxypropaneoxy) propyloxy]-4'-nitro/cyano azobenzene and N-(4'-nitro/cyano benzylidene)-4-[g-(2,3-dihydroxypropaneoxy) ethyloxy]aniline*	**85**
2.16	**2-[3-(4-Nitro/cyano azobenzene-4'-oxy) propyl]-1,3-propanediol**	**86**
2.16.1	*Synthesis of 4-(3-bromopropyloxy)-4'-nitro/cyano azobenzene*	**87**

2.16.2	*Synthesis of 2-[3-(4-nitro/cyano azobenzene-4'-oxy)propyl] diethylmalonate*	**88**
2.16.3	*Synthesis of 2-[3-(4-nitro/cyano azobenzene-4'-oxy) propyl]-1,3-propanediol*	**89**
2.17	**4-[(S-1-Methylheptyloxy)-3-nitro-1,4-phenylene carbonyl oxy]-4'-(undec-10-enoxy) biphenyl (M34)**	**90**
2.17.1	*Synthesis of 4-hydroxy-4'-(undec-10-enoxy) biphenyl*	**91**
2.17.2	*Synthesis of 4-(S-1-methylheptyloxy)-3-nitro benzoic acid*	**92**
2.17.3	*Synthesis of 4-[(S-1-methylheptyloxy)-3-nitro-1,4-phenylene carbonyloxy]-4'-(undec-10-enoxy) biphenyl (M34)*	**93**
2.18	**1-[(S-2-Methylbutyl)oxycarbonyl-1,4-phenylene oxycarbonyl]-4-(hex-5-enoxy) phenylene (M35)**	**94**
2.18.1	*Synthesis of 4-(hex-5-enoxy) benzoic acid*	**94**
2.18.2	*Synthesis of 4-(S-2-methylbutyl oxycarbonyl) phenol*	**95**
2.18.3	*Synthesis of 1-[(S-2-methylbutyl) oxycarbonyl-1,4-phenylene oxycarbonyl]-4-(hex-5-enoxy) phenylene (M35)*	**95**
2.19	**1-[(S-1-Methylheptyloxy)-3-nitro-1,4-phenylene carbonyl oxy]-4-(undec-10-enoxy) phenylene (M36)**	**96**
2.19.1	*Synthesis of 4-(undec-10-enoxy) phenol*	**97**
2.19.2	*Synthesis of 1[(S-1-methylheptyloxy)-3-nitro-1,4-phenylene carbonyloxy]-4-(undec-10-enoxy) phenylene (M36)*	**97**
2.20	**4-Nitro/cyano-4'-(undec-10-enoxy) azobenzene (M37)/ (M39) *and* 2,5-dimethyl-4-nitro-4'-(undec-10-enoxy) azobenzene (M38)**	**98**
2.20.1	*Synthesis of 4-nitro/cyano-4'-(undec-10-enoxy) azobenzene (M37)/ (M39)/ and 2,5-dimethyl-4-nitro-4'-(undec-10-enoxy) azobenzene (M38)*	**98**
2.21	**1-{[(S-2-Chloro-4-methyl) pent-1-yloxy]-1,4-phenylene carbonyloxy}-4-(undec-10-enoxy) phenylene (M40)**	**99**
2.21.1	*Synthesis of S-2-chloro-4-methylpentan-1-oic acid*	**99**
2.21.2	*Synthesis of S-2-chloro-4-methylpentan-1-ol*	**100**
2.21.3	*Synthesis of 4-(S-2-chloro-4-methylpent-1-yloxy) benzoic acid*	**101**
2.21.4	*Synthesis of 1-{[(S-2-chloro-4-methyl)pent-1-yloxy]-1,4-phenylene carbonyl oxy}-4-(undec-10-enoxy) phenylene (M40)*	**101**
2.22	**1,4-Bis(undec-10-enoxy) phenylene (M41)**	**102**
2.23	**Physico-chemical characterisation of synthesised materials**	**103**

2.24	**References**	**105**

CHAPTER 3

SYNTHESIS OF POLYMERS

Section No.	Content	Page no.
3	**Synthesis of polymers**	**106**
3.1	**Introduction**	**106**
3.2	**Free radical polymerisation**	**106**
3.3	**Synthesis of polymethacrylates**	**108**
3.3.1	*Characterisation of polymethacrylates*	**109**
3.4	**Synthesis of polyacrylates**	**111**
3.4.1	*Characterisation of polyacrylates*	**112**
3.5	**Synthesis of polystyrenes**	**113**
3.5.1	*Characterisation of polystyrenes*	**114**
3.6	**Synthesis of polymaleimides**	**118**
3.6.1	*Characterisation of polymaleimides*	**118**
3.7	**Synthesis of copolymers of N-substituted maleimide with styrene and N-vinyl carbazole**	**120**
3.7.1	*Characterisation of copolymers of N-substituted maleimide with styrene and N-vinyl carbazole*	**121**
3.8	**Synthesis of polyurethanes**	**123**
3.8.1	*Synthesis of polyurethanes using 2,4-tolylene diisocyanate (TDI)*	**123**
3.8.2	*Synthesis of polyurethanes using methylene-4,4'-bis(phenyl isocyanate) (MDI)*	**124**
3.8.3	*Characterisation of polyurethanes*	**126**
3.9	**Synthesis of epoxy resins**	**139**
3.9.1	*Characterisation of epoxy resins*	**140**
3.10	**Synthesis of siloxane polymers**	**141**
3.11	**Synthesis of siloxane elastomers**	**143**
3.12	**References**	**149**

CHAPTER 4

RESULTS and DISCUSSION

Section No.	Content	Page no.
4	**Results and Discussion**	**150**
4.1	**Free-radical polymerisation**	**150**
4.1.1	*Azo initiator*	**150**
4.1.1.1	*2,2'-Azobis(2-methylpropanenitrile) [AIBN]*	**150**
4.1.2	*Reactivity of monomers towards radical*	**151**
4.2	**NLO chromophores**	**152**
4.2.1	*Azo chromophores*	**153**
4.2.2	*Azomethine chromophores*	**156**
4.2.3	*Heterocycles in NLO*	**157**
4.3	**Side chain NLO polymers**	**157**
4.4	**IR and NMR of polymers**	**162**
4.4.1	*Polymethacrylates*	**162**
4.4.2	*Polyacrylates*	**162**
4.4.3	*Polystyrenes*	**163**
4.4.4	*Polymaleimides*	**163**
4.4.5	*Copolymers of N-substituted maleimide with styrene and N-vinyl carbazole*	**163**
4.4.6	*Polyurethanes*	**163**
4.5	**Thermal properties**	**164**
4.5.1	*Glass Transition (T_g)*	**164**
4.5.1.1	*Polymethacrylates*	**166**
4.5.1.2	*Polyacrylates*	**166**
4.5.1.3	*Polystyrenes*	**166**
4.5.1.4	*Polymaleimides*	**167**
4.5.1.5	*Copolymers of N-substituted maleimide with styrene and N-vinyl carbazole*	**167**
4.5.1.6	*Polyurethanes*	**167**
4.5.2	*Thermogravimetric analysis (TGA) studies on polyurethanes*	**168**
4.6	**Molecular weights**	**169**
4.6.1	*Polymethacrylates*	**169**
4.6.2	*Polyacrylates*	**170**
4.6.3	*Polystyrenes*	**170**
4.6.4	*Polymaleimides*	**170**

4.6.5	*Copolymers of N-substituted maleimide with styrene and N-vinyl carbazole*	**170**
4.6.6	*Polyurethanes*	**170**
4.7	**Solubility**	**171**
4.8	**Spin coating**	**173**
4.9	**Polarisation**	**173**
4.10	**Poling**	**174**
4.11	**UV measurements**	**174**
4.12	**Order parameter $<P_2>$**	**176**
4.13	**Substituted epoxy resins**	**181**
4.14	**Synthesis of siloxane polymers and elastomers**	**188**
4.14.1	*4-[(S-1-Methylheptyloxy)-3-nitro-1,4-phenylene carbonyloxy]-4'-(undec-10-enoxy) biphenyl (**M34**) and poly{1-methyl-1-[4-(S-1-methylheptyloxy)-3-nitro-1,4-phenylene carbonyloxy-4'-(undecamethyleneoxy) biphenyl] siloxane} (**V 42**)*	**188**
4.14.2	*1-[(S-2-Methylbutyl) oxycarbonyl-1,4-phenyleneoxy carbonyl]-4-(hex-5-enoxy) phenylene (**M35**) and Poly{1-methyl-1-[1-(S-2-methylbutyloxycarbonyl-1,4-phenylene oxycarbonyl)-4-(hexamethyleneoxy) phenylene]siloxane} (**V 43**)*	**191**
4.14.3	*1-[(S-1-Methylheptyloxy)-3-nitro-1,4-phenylene-1-carbonyl oxy]-4-(undec-10-enoxy) phenylene (**M36**) and poly{1-methyl-1-[1-(S-1-methylheptyloxy)-3-nitro-1,4-phenylene carbonyloxy-4-(undecamethyleneoxy)biphenyl] siloxane} (**V 44**)*	**192**
4.14.4	*4-Nitro/cyano-4'-(undec-10-enoxy) azobenzene (**M37**)/ (**M39**) and 2,5-dimethyl-4-nitro-4'-(undec-10-enoxy) azobenzene (**M38**)*	**192**
4.14.5	*1-{[(S-2-Chloro-4-methyl) pent-1-yloxy]-1,4-phenylene carbonyloxy}-4-(undec-10-enoxy) phenylene (**M40**)*	**193**
4.14.6	*1,4-Bis(undec-10-enoxy) phenylene (**M41**)*	**193**
4.14.7	*Elastomer E1*	**193**
4.15	**Alignment of elastomer**	**195**
4.15.1	*Uniaxial deformation of elastomer*	**195**
4.15.2	*Shear deformation of elastomer*	**196**
4.16	**Characterisation of E1**	**197**
4.17	**Characterisation of E3**	**202**
4.18	**Second harmonic generation (SHG) studies**	**204**
4.18.1	*Experimental techniques*	**204**
4.18.1.1	*Kurtz-powder technique*	**204**
4.18.1.2	*Solvatochromism*	**205**

4.18.2.3	*Electric field induced second harmonic generation (EFISH)*	**205**
4.18.1.4	*Hyper Rayleigh scattering (HRS)*	**206**
4.18.1.5	*Maker-Fringe analysis*	**206**
4.19	**Mathematical models**	**207**
4.19.1	*Second order nonlinear optical properties of poled polymers*	**208**
4.20	**Statistical orientation models**	**209**
4.20.1	*Ising model*	**209**
4.20.2	*Isotropic model*	**210**
4.20.3	*Singer, Kuzyk and Sohn (SKS) model*	**210**
4.20.4	*Maier, Saupe, Vander Vorst and Picken (MSVP) model*	**210**
4.21	**SHG results of selected synthesised polymers**	**211**
4.22	**General conclusions**	**228**
4.23	**Outlook**	**229**
4.24	**References**	**232**

LIST OF FIGURES

INTRODUCTION

FIGURE NO.	CAPTION	PAGE NO.
1.1	**Schematic representation of the major themes in the history of research on organic nonlinear optical materials**	**3**
1.2	**Plot of polarisability of a material as a function of the frequency of applied field**	**4**
1.3	**Plot of induced polarisation against applied field**	**4**
1.4	**Plot of polarisation response to an incident electromagnetic field at frequency w and the Fourier components of that response**	**5**
1.5	**Frequency doubling effect for optical communications**	**10**
1.6	**Frequency doubling effect for optical data storage**	**11**
1.7	**Substituent-induced electronic perturbations**	**13**
1.8	**Schematic representation of the origin of asymmetric polarisation in donor-acceptor substituted benzene**	**14**

1.9	A co-ordination complex with large hyperpolarisability and an organometallic molecule which produces strong SHG	17
1.10	Structures of organic materials used for NLO	18
1.11	Tradeoffs between polymer and crystal organic nonlinear optical materials	19
1.12	Types of liquid crystals	22
1.13	A schematic representation of a smectic C* phase (left); and a view of the same phase, but along the axis (right)	23
1.14	Chiral smectic C molecule	24
1.15	Relation between the allowed point group symmetry operations and the appearance of ferroelectricity vanishing in the tilted smectic C* and C phases	25
1.16	Design of an optical switch	29
1.17	A Mach-Zender interferometer	30
1.18	Trans-cis isomerisation in azobenzene	31
3.1	Staudinger formula	106
4.1	Potential gain in aromaticity upon charge separation	155
4.2	A schematic representation of an amorphous side chain substituted NLO polymer	158
4.3	Structure of polyurethane PU	161
4.4	Optical texture of alkylated chromophore 4-(2-hydroxy ethyl oxy)-N-(4'-cyano benzylidene) aniline at 112^{o} C	166
4.5	TGA curves of polyurethane V 32 and V33 with a heating rate of 10^{o} C/min	168
4.6	A schematic representation of corona poling set-up	174
4.7	UV-visible spectrum of polymer V 1 before (—) and after (---) poling	177
4.8	UV-visible spectrum of polymer V 7 before (—) and after (---) poling	177
4.9	UV-visible spectrum of polymer V 10 before (—) and after (---) poling	177
4.10	UV-visible spectrum of polymer V 11 before (—) and after (---) poling	178

4.11	**UV-visible spectrum of polymer V 12 before (—) and after (--) poling**	**178**
4.12	**UV-visible spectrum of polymer V 14 before (—) and after (--) poling**	**178**
4.13	**UV-visible spectrum of polymer V 17 before (—) and after (--) poling**	**179**
4.14	**UV-visible spectrum of polymer V 18 before (—) and after (--) poling**	**179**
4.15	**UV-visible spectrum of polymer V 19 before (—) and after (--) poling**	**179**
4.16	**UV-visible spectrum of polymer V 20 before (—) and after (--) poling**	**180**
4.17	UV-visible spectrum of polymer V 22 before (—) and after (---) poling	**180**
4.18	**UV-visible spectrum of polymer V 23 before (—) and after (--) poling**	**180**
4.19	**UV-visible spectrum of polymer V 26 before (—) and after (--) poling**	**181**
4.20	**Development of order parameter against poling time for polymer V 10**	**182**
4.21	**Development of order parameter against poling time for polymer V 11**	**182**
4.22	**Development of order parameter against poling time for polymer V 17**	**183**
4.23	**Development of order parameter against poling time for polymer V 18**	**183**
4.24	Development of order parameter against poling time for polymer V 19	**184**
4.25	**Development of order parameter against poling time for polymer V 1**	**184**
4.26	**Development of order parameter against poling time for polymer V 20**	**185**
4.27	**Development of order parameter against poling time for polymer V 21**	**185**
4.28	**Development of order parameter against poling time for polymer V 26**	**186**
4.29	**Development of order parameter against poling time for polymer V 5**	**186**
4.30	**Development of order parameter against poling time for polymer V 12**	**187**
4.31	Development of order parameter against poling time for polymer V 9	**187**
4.32	**Finger-print texture and fan texture for polymer V 42; (a) at 75^{o} C and (b) at 82^{o} C.**	**190**
4.33	**Plot of temperature v/s layer distance**	**190**

4.34	**Composition of smectic elastomer E1**	**194**
4.35	**Set-up for uniaxial deformation**	**195**
4.36	**Orientation after uniaxial deformation in the swollen state**	**196**
4.37	**Photograph of the oriented S_C* elastomer corresponding to the unoriented polydomain sample**	**196**
4.38	**Shearing of the preoriented sample**	**197**
4.39	**Set-up for shear experiment**	**197**
4.40	**X-ray pattern of the chiral smectic polydomain**	**198**
4.41	**Mechanical alignment of S_C* elastomer (E1); (a) Uniaxial elongation results in an uniform orientation of the mesogens while the orientation of the smectic layers shows a conical distribution. The X-ray pattern shows four small angle reflections of equal intensity. (b) A second elongation at an angle Y w.r.t. the axis of the first deformation leads to an almost uniform orientation of the layers, indicated by suppression of two of the maxima in the X-ray pattern**	**199**
4.42	**X-ray diffractograms during first heating for elastomer E1 from room temperature [25^o C, (a)] to isotropic [75^o C, (k)]**	**200**
4.43	**Tilt angle against temperature**	**200**
4.44	**X-ray patterns of elastomer E1 after uniaxial deformation (a), of the nonannealed sample after the second deformation (b) and of the annealed sample (c)**	**201**
4.45	**Composition of smectic elastomer E3**	**202**
4.46	**X-ray pattern of elastomer E3 after second deformation**	**203**
4.47	**X-ray pictures during heating of elastomer E3 from room temperature [25^o C, (a)] to isotropic [100^o C, (s)]**	**203**
4.48	**Schematic representation of SHG set-up**	**212**
4.49	**Growth of SHG signal for polymer V 20 (p-p)**	**216**
4.50	**Growth of SHG signal for polymer V 20 (s-p)**	**216**
4.51	**Growth of SHG signal for polymer V 17 (p-p)**	**217**
4.52	**Growth of SHG signal for polymer V 17 (s-p)**	**217**
4.53	Growth of SHG signal for polymer V 22 (p-p)	**218**
4.54	**Growth of SHG signal for polymer V 22 (s-p)**	**218**
4.55	**Growth of SHG signal for polymer V 21 (p-p)**	**219**
4.56	**Growth of SHG signal for polymer V 21 (s-p)**	**219**
4.57	**Growth of SHG signal for polymer V 1 (p-p)**	**220**
4.58	**Growth of SHG signal for polymer V 1 (s-p)**	**220**
4.59	Growth of SHG signal for polymer V 18 (p-p)	**221**
4.60	**Growth of SHG signal for polymer V 18 (s-p)**	**221**
4.61	**Growth of SHG signal for polymer V 19 (p-p)**	**222**

4.62	**Growth of SHG signal for polymer V 19 (s-p)**	**222**
4.63	**Growth of SHG signal for polymer V 26 (p-p)**	**223**
4.64	**Growth of SHG signal for polymer V 26 (s-p)**	**223**
4.65	**Growth of SHG signal for polymer V 34 (p-p)**	**224**
4.66	**Growth of SHG signal for polymer V 34 (s-p)**	**224**
4.67	**Structure of the chiral smectic C elastomer after the second deformation step**	**227**

LIST OF TABLES

TABLE NO.	CAPTION	PAGE NO.
1.1	**b Value of substituted benzene system**	**12**
1.2	**Effect of donor-acceptor groups on b value**	**12**
1.3	**Effect of conjugation on b value**	**15**
1.4	**NLO coefficients of inorganic materials**	**16**
1.5	**NLO coefficients of organic materials**	**18**
4.1	**Linear and nonlinear properties of typical nonlinear optical chromophores as measured by EFISH**	**153**
4.2	**Solubility of polymers synthesised in the present investigation**	**172**
4.3	**Structures of selected polymers studied for SHG**	**213**
4.4	**SHG results of selected polymers**	**225**

LIST OF SCHEMES

SCHEME NO.	CAPTION	PAGE NO.
2.1	**Synthesis of azomethine**	**40**
2.2	**Alkylation of azomethine**	**43**
2.3	**Synthesis of 4-(2-methacryloyloxy ethyloxy)-N-(4'-formyl benzylidene) aniline**	**47**
2.4	**Coupling of 4-(2-methacryloyloxyethyloxy)-N-(4'-formyl benzylidene)aniline with barbituric acid**	**48**
2.5	Synthesis of 4-(2-acryloyloxy ethyloxy)-N-(4'-formyl benzylidene) aniline	**49**

2.6	**Coupling of 4-(2-acryloyloxyethyloxy)-N-(4'-formyl benzylidene)aniline with barbituric acid**	**51**
2.7	**Synthesis of 4-[2-(4-vinylbenzyloxy) ethyloxy]-N-(4'-cyano/nitro/formyl benzylidene) aniline**	**52**
2.8	**Coupling of 4-[2-(4-vinylbenzyloxy) ethyloxy]-N-(4'-formyl benzylidene)aniline with barbituric acid**	**54**
2.9	**4-[2/6-(N-maleimido)eth-1-yloxy/hex-1-yloxy)-N-(4'-cyano/nitro benzylidene)] aniline**	**55**
2.10	**Diazotisation methodology**	**58**
2.11	**Alkylation of azo phenol**	**59**
2.12	Synthesis of 4-(2-methacryloyloxyethyloxy)-4'-formyl azobenzene	**60**
2.13	**Coupling of 4-(2-methacryloyloxyethyloxy)-4'-formyl azobenzene with barbituric acid**	**62**
2.14	Synthesis of 4-(2-acryloyloxyethyloxy)-4'-formyl azobenzene	**63**
2.15	Coupling of 4-(2-acryloyloxyethyloxy)-4'-formyl azobenzene with barbituric acid	**64**
2.16	Synthesis of 4-[2-(3/4-vinylbenzyloxy)ethyloxy]-4'-formyl azobenzene	**65**
2.17	**Coupling of 4-[2-(3/4-vinylbenzyloxy) ethyloxy]-4'-formyl azobenzene with barbituric acid**	**66**
2.18	Synthesis of 4-[2-(N-maleimido)ethyloxy]-4'-formyl azobenzene	**67**
2.19	**Alkylation followed by formylation of carbazole**	**69**
2.20	Synthesis of 2-formyl-N-[3-(3/4-vinylbenzyloxy) propyl] carbazole	**70**
2.21	**Condensation of 2-formyl-N-(3-hydroxypropyl)carbazole with substituted aniline**	**72**
2.22	**Synthesis of 2-(4-cyano/nitro phenylene-1-azomethine)-N-[3-(3/4-vinylbenzyloxy) propyl] carbazole**	**73**
2.23	Condensation followed by alkylation of 5-amino-1,3,4-thiadiazole-2-thiol	**75**
2.24	**Synthesis of 5-[N-(4'-cyano/nitro benzylidene)amine]-2-(2-methacryloyloxyethylthio)-1,3,4-thiadiazole**	**77**
2.25	**Synthesis of 5-[N-(4'-nitro benzylidene)amine]-2-(2-acryloyloxy ethylthio)-1,3,4-thiadiazole**	**79**
2.26	**Synthesis of 5-[N-(4'-cyano/nitro benzylidene)amine]-2-[2-(3/4-vinylbenzyloxy) ethylthio]-1,3,4-thiadiazole**	**80**
2.27	**Epoxide formation and ring opening by base catalysed hydrolysis**	**82**
2.28	**Synthesis of diester followed by hydrolysis**	**87**
2.29	**Synthesis of 4-[(S-1-methylheptyl oxy)-3-nitro-1,4-phenylene carbonyloxy]-4'-(undec-10-enoxy) biphenyl (M34)**	**91**
2.30	**Synthesis of 1-[(S-2-methylbutyl) oxycarbonyl-1,4-phenylene oxycarbonyl]-4-(hex-5-enoxy) phenylene (M35)**	**94**

2.31	**Synthesis of 1-[(S-1-methylheptyloxy)-3-nitro-1,4-phenylene carbonyloxy]-4-(undec-10-enoxy) phenylene (M36)**	**96**
2.32	**Synthesis of 4-nitro/cyano-4'-(undec-10-enoxy) azobenzene (M37)/ (M39) *and* 2,5-dimethyl-4-nitro-4'-(undec-10-enoxy) azobenzene (M38)**	**98**
2.33	**Synthesis of 1-{[(S-2-chloro-4-methyl)pent-1-yloxy]-1,4-phenylenecarbonyloxy}-4-(undec-10-enoxy)phenylene (M40)**	**99**
2.34	**Synthesis of 1,4-bis(undec-10-enoxy) phenylene (M41)**	**102**
3.1	**Mechanism of free radical polymerisation**	**107**
3.2	**Primary radicals formed from initiators**	**107**
3.3	**Polymerisation of methacrylates**	**109**
3.4	**Polymerisation of acrylates**	**111**
3.5	**Polymerisation of styrenes**	**114**
3.6	**Polymerisation of maleimides**	**118**
3.7	**Synthesis of copolymers**	**120**
3.8	**Synthesis of polyurethanes from unsymmetrical diols**	**125**
3.9	**Synthesis of polyurethanes from symmetrical diols**	**126**
3.10	**Synthesis of epoxy resins**	**140**
3.11	**Synthesis of siloxane polymers**	**142**
4.1	**Decomposition mechanism of AIBN**	**151**
4.2	**Formation of peroxide linkages**	**151**
4.3	**Generalised procedures for the preparation of side chain NLO functionalised methacrylate and styrene polymers/copolymers by: (a) vinyl polymerisation of functionalised monomers and (b) polymer analogous reactions**	**159**

ABSTRACT

Nonlinear Optics is expected to play a major role in the technology of photonics. The need to process and store large amounts of data appears to be growing at an exponential rate, pushing existing technologies more and more towards their fundamental limits. Optical data processing and storage schemes, where light instead of electricity is the data carrier, offer the potential to revolutionise the way we handle information. A key element for the success of these emerging technologies is the availability of efficient nonlinear optical materials that mediate the interaction between light beams, i.e. materials whose optical properties change upon illumination. This is the driving force behind the strong interest shown in this area of science.

Reflection, refraction, diffraction and absorption are commonly observed interactions of light with matter. During these processes the optical properties of the material such as the refractive index and absorption coefficient remain unaffected by the electromagnetic radiation. However, when the light used is in the form of powerful laser beams, some materials manifest marked changes in their optical properties as a result of the interaction with the strong electromagnetic field of the radiation. This inturn effects a modification of the frequency, phase or amplitude of the light transmitted through the material. Such interactions arising out of multiphoton effects are known as nonlinear optical (NLO) processes and the materials in which such processes can be carried out efficiently are called NLO materials.

The field of nonlinear optics (NLO) has grown tremendously in recent years due to the technological potential of certain nonlinear optical effects for photonic technologies. The earliest NLO phenomenon to be discovered, in 1906, was the electrooptic (EO) effect. Second harmonic generation (SHG) in a single crystal was first established only in 1961. A beam of red light from a ruby laser was directed through a quartz crystal. The emerging light included both red and ultraviolet components. The frequency of the UV component was precisely double that of incident light. This doubled frequency is termed

as second harmonic generation. This was soon followed by the observation of a large number of NLO effects, the important one being wave-mixing in lithium niobate in 1965.

The main objectives of the present work are: (1) Synthesis of different molecular systems with head-tail arrangement of strong electron donor-acceptor groups connected by extended conjugation; (2) Coupling to different polymeric backbones through polymethylene spacers; (3) Crosslinking of polymers to form elastomers; (4) Characterisation of the monomers for UV, IR, NMR and Mass spectra; (5) Characterisation of polymers for UV, IR, NMR and molecular weights; (6) Study of thermal properties; (7) Spin coating of selected polymers from their solutions, poling and studying NLO response.

The thesis consists of 4 chapters.

Chapter I deals with current state of knowledge in side chain polymers and their importance in NLO applications. A review of fundamental and technical information on NLO of side chain polymers is also presented.

Chapter II discusses the multi-step syntheses of different donor-acceptor functionalised azo and azomethines moieties with different electron withdrawing groups such as nitro, cyano, aldehyde and barbiturate groups. In all cases, either phenolic or thio group is used as the donor end. These are treated with halo ethers to give alkylated products which are transformed into methacrylate, acrylate, styrenic, epoxy and maleimide monomers. This chapter also includes synthesis of some chiral monomers. These monomers were synthesised with the aim of synthesising some elastomers for SHG studies. This chapter also gives the complete physio-chemical characterisations (IR, NMR, Mass, m.p, DSC) for all the molecules synthesised in this study.

Chapter III consists of free-radical polymerisation of monomers and characterisation of polymers by UV, IR, NMR, DSC and molecular weights. Some polymers are also studied under optical microscope to understand their phase behaviour. This chapter also includes synthesis of some chiral polymers and elastomers. The elastomers were synthesised with the aim of applying novel techniques of orientation for alignment of the chiral elastomers so as to make them suitable for SHG studies.

Chapter IV consists of study of poling characteristics and optical nonlinear responses of poled polymers. Structure-property correlations and the importance of different

substituents, polymer backbones are also discussed. It also consists of orientation studies of new elastomers for NLO applications. It includes the orientation behaviour of chiral smectic C elastomers by suitable shear fields consistent with the phase symmetry. This chapter also gives a conclusion of the study done and gives a bird's-eye view on future prospects of this area of research.

1

Introduction

1 Introduction

1.1 History of nonlinear optics

The explosion of the Internet illustrates the need for rapid exchange and processing of information. More powerful data-systems including larger networks, faster processors and mass storage devices are under intensive research and development. As the need for larger data processing rates grows, the strength of optics and the potential of optoelectronic technology are increasingly being recognised. The high speed, high degree of parallelism of optics will gradually lead to optoelectronic systems in which an increasing number of functions will be implemented optically. The development of photonics technology, however, relies largely on advances in fabricating new and better performing optical materials.

Photonics is emerging as a multidisciplinary new frontier of science and technology that is capturing the imagination of scientists and engineers worldwide because of its potential applications to many areas of present and future information and image processing technologies (1-5). Non-linear optics is expected to play a major role in the technology of photonics. Photonics is the analogy of electronics in that it describes the technology in which photons instead of electrons are used to acquire, store, transmit and process information. The ability to alter the frequency or colour of light and to amplify one source of light with another, switch it or alter transmission characteristics through a medium, on the basis of its intensity, are examples of nonlinear optical (NLO) phenomena that are potentially useful (1).

It is this potential of providing these functions in suitable materials and devices that motivates much of the current fundamental and exploratory research in the field of NLO. This field offers challenging opportunities for fundamental research. The challenges are multidisciplinary, ranging from a basic understanding of physics of nonlinear optical interaction to molecular engineering and chemical synthesis of novel organic structures with enhanced optical nonlinearities.

The field of nonlinear optics (NLO) has grown tremendously in recent years due to the technological potential of certain nonlinear optical effects for photonic technologies. The earliest NLO phenomenon to be discovered, in 1906, was the

electrooptic (EO) effect. Second harmonic generation (SHG) in a single crystal was first established only in 1961 (6). A beam of red light from a ruby laser was directed through a quartz crystal. The emerging light included both red and ultraviolet components. The frequency of the UV component was precisely double that of incident light. This doubled frequency is termed as second harmonic generation (SHG). This was soon followed by the observation of a large number of NLO effects (7), the important one being wave-mixing in lithium niobate in 1965 (8).

Among organic materials, SHG was first observed in 1964 with benzpyrene (9), to be followed by observations on hippuric acid and benzil (10-12). Rapid and qualitative screening of NLO materials were made possible by the powder method developed earlier by Kurtz and Perry (13). In the past 15 years the NLO properties of organic and polymeric materials have been measured increasingly (12). This has led to concerted efforts to synthesise molecular materials with improved NLO properties (14-19). The application potential of these materials have also been evaluated widely (20-25).

Figure 1.1 schematically illustrates the history of research on second order organic NLO materials. Soon after the invention of the laser and the birth of the field on nonlinear optics, second harmonic generation and two photon absorption were observed in a variety of organic molecules. Systematic studies of the relationship of molecular structure to molecular nonlinearities done during the 1970's brought out the importance of electron delocalisation and charge transfer for high nonlinearity. In the 1980's research began on ways to incorporate these highly nonlinear organic molecules into orientationally ordered bulk materials that would exhibit useful bulk NLO properties. Two main approaches were initiated that are still being followed with great energy today: crystal growth and poled polymers.

1.2 Basic aspects of nonlinear optical phenomena

Feynman (26) pointed out that to understand physical laws, is to realise that these are approximate. While it is well known that the phenomenon is not linear, few understand what it is. A process is nonlinear when the response to input (i.e output) changes the process itself.

Nonlinear optics is concerned with how the electromagnetic field of light wave interacts with electromagnetic fields of matter and other light waves. The interaction of

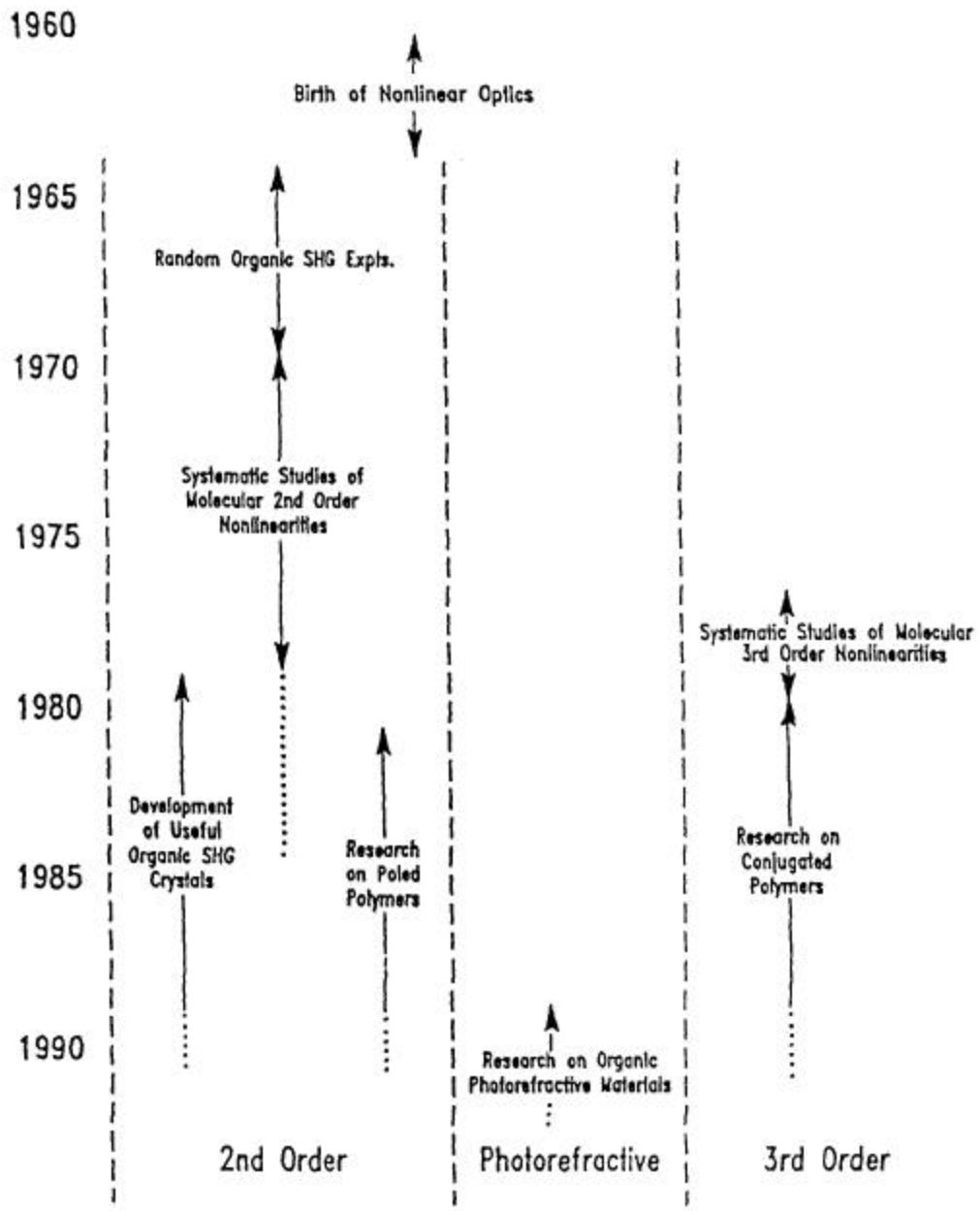

Figure 1.1 Schematic representation of the major themes in the history of research on organic nonlinear optical materials

light with a nonlinear optical (NLO) material will cause the material characteristics to change, and the next arriving photon will see a different material altogether. When electromagnetic radiation is incident on matter a variety of polarisations are induced depending on the frequency of the radiation. When the frequencies are relatively low (radiowave and microwave) three contributions to the total polarisation occur; orientation polarisation, vibrational polarisation and electronic polarisation. The first

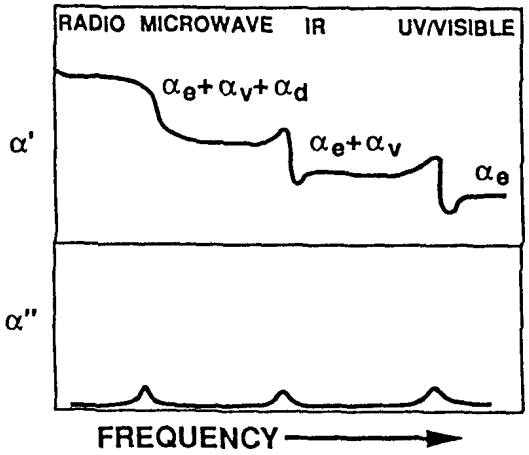

Figure 1.2 Plot of polarisability of a material as a function of the frequency of applied field. Top: Real polarisability. Bottom: Imaginary polarisability.

one involves reorientation of molecules in a field, whereas the second one is associated with the deformation of nuclear framework of the molecule by the applied field. When the radiation has wavelengths in the optical range, only electronic polarisation occurs because of the higher frequencies involved (Figure 1.2). When the electric field associated with the electromagnetic radiation is small, as is usually the case with ordinary light, the polarisation varies linearly with the electric field and the constant of proportionality is the familiar polarisability, α, in the case of molecules and the linear electric susceptibility $\chi^{(1)}$ in the case of bulk solids. However, when laser light is used, the associated electric fields are very large and the induced polarisation is usually nonlinear (Figure 1.3).

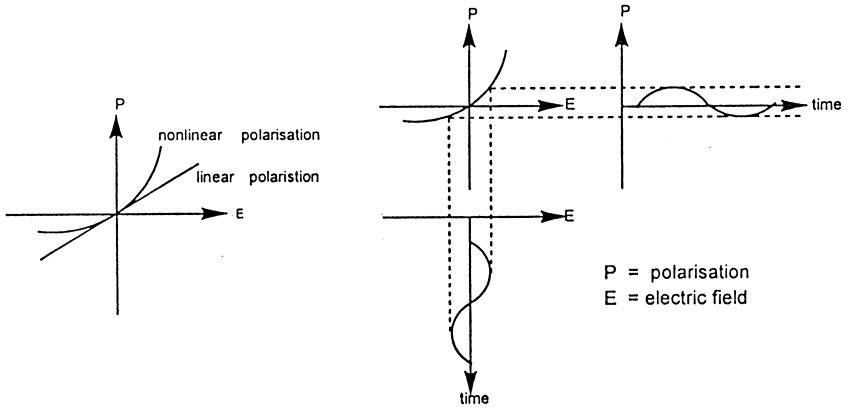

Figure 1.3 Plot of induced polarisation against applied field

In such a case, asymmetrically varying electromagnetic radiation, say a sinusoidal wave with frequency ω, can induce an unsymmetrically fluctuating polarisation in a noncentrosymmetric material. Such a periodic, but unsymmetrical function can be

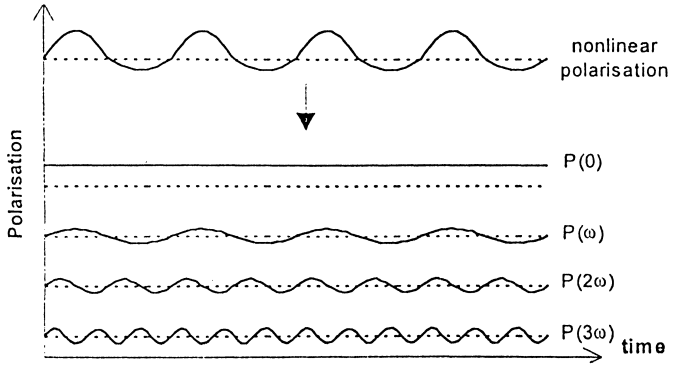

Figure 1.4 Plot of polarisation response to an incident electromagnetic field at frequency w and the Fourier components of that response

decomposed into several symmetric (sine or cosine) functions with frequencies *0*, w, $2w$, $3w$ and so on; these terms correspond to the phenomena of optical rectification, linear electro-optic effect, second harmonic generation, third harmonic generation and so on (Figure 1.4).

The total nonlinear polarisation, **P** can be related to the permanent polarisation $\mathbf{P_o}$ and the applied electric field, **E**, for the case of molecules and for bulk materials using the following equations, respectively.

$$\mathbf{P}_{\text{microscopic}} = \mathbf{P}_o + a.\mathbf{E} + b.\mathbf{E}.\mathbf{E} + g.\mathbf{E}.\mathbf{E}.\mathbf{E} + \ldots\ldots \qquad \textbf{1.1}$$

$$\mathbf{P}_{\text{macroscopic}} = \mathbf{P}_o + c^{(1)}\mathbf{E} + c^{(2)}\mathbf{E}.\mathbf{E} + c^{(3)}\mathbf{E}.\mathbf{E}.\mathbf{E} + \ldots\ldots \qquad \textbf{1.2}$$

Where, a, b and g are the molecular polarisabilty, first hyperpolarisability and second hyperpolarisability and $c^{(i)}$ is susceptibility coefficient with tensors of order (i+1); e.g., c^2 will have tensor element c_{ijk}. The largest NLO coefficient has been found for semiconductors and unsaturated extended organic molecules, which comprise of highly delocalised electrons (15). The magnitude of these tensorial nonlinear coefficients are quite small and decrease with increasing order. It is due to this reason that the nonlinearities show up only at high electric fields. The quadratic term gives rise to phenomena such as second harmonic generation (wherein two photons of frequency w give rise to one photon of frequency $2w$) and the linear electro-optic effect. The cubic term leads to effects such as third harmonic generation and the quadratic electro-optic effect.

The tensor used traditionally by theorists to characterise the second order NLO responses is $\chi^{(2)}_{ijk}$. Experimentalists use the coefficient d_{jk} to describe second order NLO effects. Usually the two are simply related by:

$$d_{ijk} = \tfrac{1}{2}\chi^{(2)}_{ijk} \qquad \textbf{1.3}$$

The first subscript refers to the resultant polarisation of the material along a defined axis and following subscripts refer to the orientations of the applied electric fields. The SHG coefficients d_{31} ($d_{31} = \chi^{(2)}_{31}/2$) and d_{33} ($d_{33} = \chi^{(2)}_{33}/2$) are deduced from the s-p and p-p configuration experiments, respectively.

Materials having a centre of inversion symmetry will have their induced polarisation exactly reversed in direction when the electric field of the electromagnetic radiation is reversed i.e. P(**-E**) = -P(**E**). The quadratic and higher even order products of **E**, which contribute to the polarisation, are unchanged by the change of direction of **E**, whereas the cubic and other odd order terms are reversed by the reversal of **E**. Hence, in centrosymmetric systems, the even order terms vanish completely and the nonlinear effects arise exclusively from cubic and higher order odd terms. On the other hand, in a noncentrosymmetric system there are no symmetry constraints which relate the polarisations in opposite directions and hence NLO effects of any order can be observed. It can be easily understood why the even order contributions to the nonlinearity disappear if centre of symmetry exists. For centrosymmetric molecules like benzene (27), the magnitude of induced dipole moments is independent of the direction (sign) of applied electric field.

$$\boldsymbol{\mu}_{ind}(+\mathbf{E}) = -\boldsymbol{\mu}_{ind}(-\mathbf{E}) \qquad \textbf{1.4}$$

By inserting +E in equation 1.4, one obtains for the induced dipole moment

$$\boldsymbol{\mu}_{ind}(+\mathbf{E}) = \alpha\mathbf{E} + \beta\,\mathbf{E}.\mathbf{E} + \gamma\,\mathbf{E}.\mathbf{E}.\mathbf{E} \ldots \qquad \textbf{1.5}$$

In the case of reverse (negative sign) field, one obtains

$$\boldsymbol{\mu}_{ind}(-\mathbf{E}) = -\alpha\mathbf{E} + \beta\,\mathbf{E}.\mathbf{E} - \gamma\,\mathbf{E}.\mathbf{E}.\mathbf{E} \ldots \qquad \textbf{1.6}$$

Owing to the fact that **E**.**E** is positive, irrespective of the sign of field **E**, equation 1.4 can only be fulfilled for centrosymmetric molecules, if either $\beta = 0$ or if the field strength E=0. For asymmetrically substituted molecules, not possessing centrosymmetry, equation 1.4 need not be fulfilled.

1.2.1 Relation between molecular and macroscopic properties

In order to obtain optically nonlinear materials with large (macroscopic) nonlinear susceptibilities, one has to know the relation between the macroscopic $\chi^{(n)}$-values and the corresponding molecular hyperpolarisabilities. The relation between second order susceptibility $\chi^{(2)}$ and the molecular β can be approximated by (28,29):

$$\chi^{(2)}_{IJK} = NF\ \beta_{ijk} \langle \cos\theta_{Ii} \cos\theta_{Jj} \cos\theta_{Kk} \rangle \qquad 1.7$$

in which N denotes the number of molecules per unit volume, and F the local field factor. Upper-case subscripts refer to the macroscopic frame; lower-case subscripts refer to the molecular frame. The cosines are projection factors, the brackets denote an averaging over molecular orientation; such averaged projection factors are polar ordering parameters.

For second-order nonlinearities no centrosymmetry is allowed. Samples containing isotropically oriented molecules do not, therefore, show any second-order effect (unallowed inversion centre present). For isotropic systems, the polar ordering parameters in equation 1.7 are equal to zero, resulting in a zero value for $\chi^{(2)}$. In order to show the desired second-order nonlinear effect, a bulk material must have some degree of polar (uniaxial) ordering; only axial ordering is not enough in this case (27).

After having obtained organic molecules with large β-values, one has to find a method for ordering the individual molecules in the macroscopic sample such that a net polar ordering results. Several methods exist for doing so, such as:

(i) Growth of noncentrosymmetric single crystals;

(ii) Deposition of highly uniaxially ordered layers by the Langmuir-Blodgett technique and

(iii) Electric field poling of polar optically nonlinear molecules, contained in suitable matrices.

1.2.2 NLO materials

Reflection, refraction, diffraction and absorption are commonly observed interactions of light with matter. During these processes the optical properties of

materials such as the refractive index and absorption coefficients remain unaffected by electromagnetic radiation. But, when light used is in the form of powerful laser beams, some materials manifest marked changes in their optical properties as a result of the interaction with the strong electromagnetic field of the radiation. This in turn effects a modification of frequency, phase or amplitude of the light transmitted through the material. Such interactions arising out of multiphoton effects are known as nonlinear optical or NLO processes and the materials in which such processes can be carried out efficiently are called NLO materials (30).

When the electronic charge in the optical material is displaced by the electric field (**E**) of the light and polarisation takes place, the total electric field (the displaced field, **D**) within the material becomes:

$$\mathbf{D} = \mathbf{E} + 4\pi\mathbf{P} \qquad \textbf{1.8}$$

Since $P = \chi.E$,

$$\mathbf{D} = (1+ 4\pi\,\mathbf{c})\,\mathbf{E} \qquad \textbf{1.9}$$

The dielectric constant $\varepsilon(\omega)$ and the refractive index $n(\omega)$ are two common bulk parameters that characterise the susceptibility of a material. The dielectric constant in a given direction is defined as the ratio of the displaced internal electric field to applied field ($\varepsilon = D/E$). Therefore, from equation 1.9,

$$\varepsilon_{ij}(\omega) = 1+ 4\pi\chi_{ij}(\omega) \qquad \textbf{1.10}$$

The frequency dependence of the dielectric constant provides insight into the mechanism of charge polarisation (see Figure 1.2).

1.2.3 Linear optical effects

1.2.3.1 Refractive index

When light travels from one medium to another its path changes. The ratio of speed of light in a vacuum, c, to that in material, v, is the refractive index, n.

$$n = c/v \qquad \textbf{1.11}$$

At optical frequencies, the dielectric constant equals the square of the refractive index:

$$\varepsilon(\omega) = n^2(\omega) \qquad \textbf{1.12}$$

$$n^2(\omega) = 1+ 4\pi\chi(\omega) \qquad \textbf{1.13}$$

Since χ (ω) is related to individual atomic or molecular polarisabilities, the equation 1.13 relates the speed of light to electron density distribution (polarisability). Therefore, structural alterations change the optical properties.

1.2.4 Nonlinear optical effects

Nonlinear polarisation leads to nonlinear optical effects as linear polarisation leads to linear optical effects. Until recently, it was assumed that the polarisation of a molecule is a linear function of the applied electric field. In reality, the individual polarisation generates an internal electric field that modifies the applied electric field and the subsequent polarisation. This inter-relationship is the origin of nonlinear polarisation. The mathematical formulation of the nonlinear polarisation is not known but a common approximation is to expand the polarisability as a Taylor series (31):

$$\mu_i = \mu^o_i + \alpha_{ij}.E_j + \beta_{ijk}/2\ E_j.E_k + \gamma_{ijkl}/6\ E_j.E_k.E_l + ... \qquad \textbf{1.14}$$

where, μ^o_i is the static dipole in the absence of an electric field.

The terms beyond αE, are not linear in E; they are referred as nonlinear polarisations and give rise to nonlinear optical effects. At small fields, the polarisations approximate a linear response, but with increasing field strength, nonlinear effects become more important. Just as α is linear polarisability β, and γ are first and second order hyperpolarisabilities.

1.2.5 Second harmonic generation (SHG)

When a material is under laser of frequency ω, the response of the material can be expressed in the form of polarisation equation. In the expression limited to the second order, the NLO effect can be clearly noted by substituting a field equation for E (32), as:

$$\mathbf{P} = P_0 + \chi^1 E_0 \cos \omega t + \mathbf{c}^2\ E_0 E_0 \cos \omega t \qquad \textbf{1.15}$$

On simplification, the above equation transforms to:

$$\mathbf{P} = P_0 + 1/2\mathbf{c}^2 E_0^2 + \chi^1\ E_0 \cos \omega t + 1/2\mathbf{c}^2 \cos 2\omega t \qquad \textbf{1.16}$$

The above equation shows the presence of newer components due to nonlinear polarisation. The second order term gives a frequency independent contribution and a frequency dependent one at 2ω. The former suggests that a DC polarisation should appear in a second order NLO material when appropriately irradiated. This phenomenon is

referred to as optical rectification. The latter term corresponds to the well-known effect in NLO, namely frequency doubling or second harmonic generation.

1.2.5.1 Frequency doubling

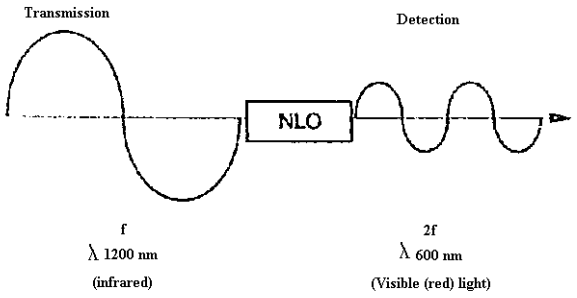

Figure 1.5 Frequency doubling effect for optical communications

The phenomenon known as frequency doubling is potentially most important. The frequency doubling effect, whereby the incident radiation is converted to radiation of double the frequency, is especially useful in data storage. In both telecommunications and optical telecommunications, the most efficient way to transmit data is by using infrared laser radiation, for example 1200 nm, produced by an In-P laser diode, along optical fibres (32). However, detection of this long wavelength radiation is inefficient. In contrast, visible radiation is much easier to detect but is an inefficient transmitter of data. Consequently, an important use of NLO materials would be to convert the infrared radiation to visible radiation by frequency doubling, thus enabling easier detection of the signals (Figure 1.5).

The second important area for frequency doubling is optical data storage. Currently, semiconductor lasers which emit in the near infrared at 780 nm are used to write and then read the information. Doubling the frequency of this infrared radiation would produce near ultraviolet radiation at 390 nm (Figure 1.6). Since the wavelength is inversely proportional to the energy of the radiation (equation 1.17), the laser radiation at 390 nm has a wavelength half that at 780 nm, thus enabling four times more information to be recorded on a given area of optical disc.

$$\mathbf{E} = hc/\lambda \qquad \textbf{1.17}$$

where, E= energy, h = Planck's constant, c = velocity of light and λ = wavelength.

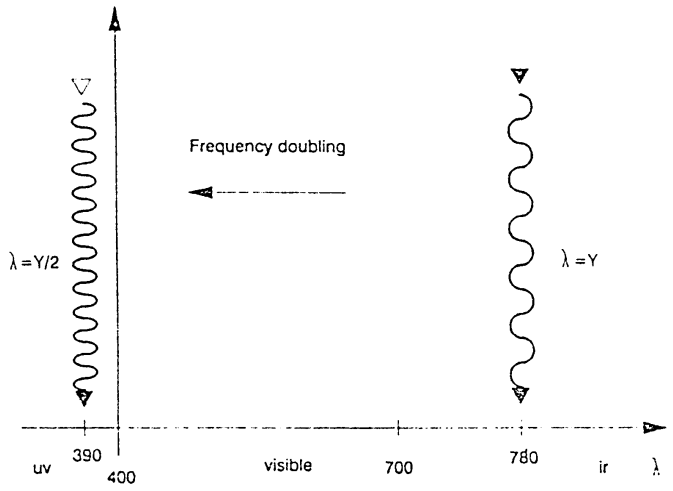

Figure 1.6 Frequency doubling effect for optical data storage

1.3 Optimisation of b

Design of second order NLO materials is now quite advanced, as over the years criteria have been discovered that are essential for the exhibition of large hyperpolarisabilities. While there is discussion on the importance and variation of these points, the basic tenets that are universally accepted are as follows (1,33-35):

1. Polarisable materials (the electrons need to be greatly perturbed from their equilibrium position);
2. Asymmetric charge distribution (incorporation of donor-acceptor units);
3. A pathway of π- conjugated electrons and
4. Accentric crystal packing

1.3.1 Donor-acceptor system

Molecules having delocalised π electronic systems and asymmetry in their response to an applied electric field tend to exhibit large values of β. The largest values are obtained when the molecules have low-lying charge-transfer (CT) resonance states which can be mixed with the ground state by an external electric field. This process, combined with substituent-induced charge asymmetry in the π electronic system, is the main requirement for large values of β. Co-operations between the donor and acceptor groups permit the electron cloud to be polarised over the entire molecule so as to enhance

the β value. Thus better values are obtained when the interaction between donor and acceptor groups are high, as seen from ortho/meta/para substituted systems in Table 1.1 (36).

Table 1.1 b Value of substituted benzene system

Molecule	b ´ 10^{30}esu
Nitro benzene	2.2
Aniline	1.1
2-Nitro aniline	10.2
3-Nitro aniline	6.0
4-Nitro aniline	34.5

1.3.2 The nature of substituents

The substituents are vital to the generation of higher β values. The force of the internal fields, which exist in polarisable electron clouds and permits the enhancement of β, is also dictated by the electron donor and acceptor groups. The strength of the internal field, which polarises the electron cloud, increases with the following donor and acceptor groups, as shown in Table 1.2 (37).

Table 1.2 Effect of donor-acceptor groups on b value

Acceptor	-CN	<	-CHO	<	$-COCH_3$	<	$-NO_2$	<	N_2^+
Donor	$-CH_3$	<	$-OCH_3$	<	NH_2	<	$N(CH_3)_2$	<	O^-

Just as length of the conjugated π systems is an important factor to produce hyper-polarisability, in addition, the appropriate functionality at the ends of the π system can enhance the required asymmetric electronic distribution in either or both the ground state and excited state configurations. Functional groups are divided into two categories based on their ability to donate electrons into or accept electrons from the π system. The common donor (D) groups are characterised by predominant p character (sp^3) bonding and often have available lone pair of electrons [as in an amine $-NR_2$ such as aniline (38)].

The common acceptor groups are characterised by more s character (sp^2 or sp) bonding, as in the nitro (NO_2) in nitrobenzene, in which nitrogen is sp^2 or nitrile (–C≡N) in benzonitrile, in which the carbon is sp hybridised. The fully charged substituent such as O^- (phenoxide) and N_2^+ (diazonium ion) are among the most potent D and A groups but have found very limited use.

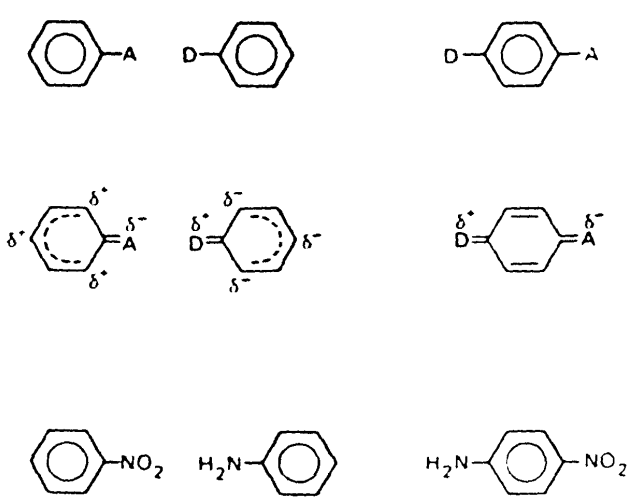

Figure 1.7 Substituent-induced electronic perturbations

Either D or A group alone on π system will perturb the electron density via resonance with the main perturbations in aromatic molecules at ortho and para positions. The most dramatic effect is found when both D and A groups interact in a mesomeric fashion (39) (Figure 1.7). The asymmetric polarisation induced in these molecules, which gives rise to the second order NLO effects, is schematically illustrated in Figure 1.8 for the case benzene substituted with donor (D) and acceptor (A) groups. The ease with which the π-electrons in these systems can be polarised leads to nonlinear reponses that are stronger and faster than that of most inorganic materials.

For D-A systems, particularly polarised aromatic systems, a variety of treatments have been successfully developed to explain the origins of large β values (40). The simplest approximation for describing β is (41):

$$\beta = \beta_{ADD} + \beta_{CT} \qquad \textbf{1.18}$$

This approximation, although quantum mechanically incorrect, has allowed the physical organic chemist to design NLO molecules. The β_{ADD} involves a substituent-

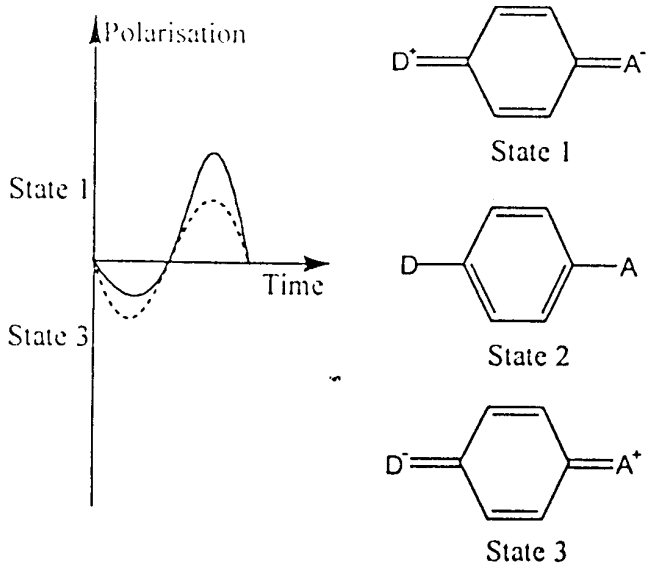

Figure 1.8 Schematic representation of the origin of asymmetric polarisation in donor-acceptor substituted benzene. (---) symmetric response; (¾) asymmetric response

induced charge asymmetry, and β_{CT} is the contribution due to charge transfer through bond or mesomerism. For the generic D-A substituted aromatic system (Figure 1.7), the relative contributions of β_{ADD} and β_{CT} are determined by the individual characteristics of the specific A and D groups, respectively, as well as by their interactive properties. For example, in the specific case of 4-nitro aniline, β_{ADD} is given by the vector sum of β contribution from nitrobenzene and aniline and β_{CT} is the predominating contribution due to charge transfer between these substituents.

1.3.3 Conjugated π systems

Different polarisable π systems are synthesised from aromatic cycles, ethylene groups, or a combination of both. A significant enhancement of polarisability has been demonstrated by extending the conjugation length between the donor and acceptor (42). This generally results from decreasing the energy gap and increasing the transition dipole moment between the relevant states. An increase in length of this system as well as the presence of double bonds increases the hyperpolarisability values, as shown below. The β value increases proportionally with the number of benzene rings. The maximum β value is obtained when the numbers of benzene rings are two or three, as shown in Table 1.3.

Table 1.3 Effect of conjugation on b value

Compound	E (eV)	f	$\beta \times 10^{30}$ esu
O_2N-Ph-NH_2	3.89	0.51	34.5
O_2N-Ph-CH=CH-Ph-NH_2	3.06	0.54	260
O_2N-Ph-CH=CH-CH=CH-Ph-NH_2	2.67	0.73	650

Ph = 1,4-disubstituted benzene ring

1.3.4 Influence of planarity

The molecules need to be planar for maximal charge transfer. This is favoured by the presence of covalent bonds and intra-molecular hydrogen bonds, which improve charge circulation between the two ends of the molecule. Sometimes steric hindrance can be used as a tool to induce planarity in the structure to attain higher β values. It is also important that the molecule has a broad transparency range. However, coloured molecules do not pose a problem provided these are macroscopically non-centrosymmetric and could be made into good films.

1.4 Second order NLO materials

Second order materials are used in optical switching (modulation), frequency conversion (SHG, wave mixing) and electro-optic applications, especially modulators (SLM). These materials are used as single crystals, thin polycrystalline films, or dispersed in polymers and oriented in strong electric field to provide an accentric environment.

1.4.1 Inorganics

The traditional materials, which have been studied for their optically non-linear properties, are inorganic single crystals such as quartz (naturally active in nonlinear optics), and lithium niobate, amongst others. Inorganics are current work-horse materials for NLO. For inorganic materials, it is mainly the ions in the crystal which are displaced under the influence of the electromagnetic field. Nonlinear optical effects can also be seen in certain semi-conductor materials such as GaAs and AlGaAs. One problem with

these materials is the difficulty and high costs involved in getting a monocrystal that is of good quality and a good size. Some of these materials are compared and contrasted in Table 1.4 (43).

Table 1.4 NLO coefficients of inorganic materials

Compound	Coefficient(s)	FOM
β-BaB_2O_4	d_{11} = 4.1	26
$Ba_2NaNb_5O_{15}$	d_{31} = 32	-
KH_2PO_4	d_{36} = 1.0	1
LiB_3O_5	d_{32} = 3.1	1
$LiNbO_3$	d_{31} = 13	-
$LiIO_3$	d_{31} = 10	50
$KTiOPO_4$	d_{31} = 15	215

a) Relative to potassium dihydrogen phosphate (KDP) as 1; b) The FOM (figure of merit), relative to KDP, is a function of the d coefficient. FOM = (d^2/n^3) $(EL/\lambda^2)(\Delta\theta^2)$.

1.4.2 Organometallic compounds

A growing number of organometallic compounds, such as metal pyridine complexes and ferrocene, have shown good SHG (44-47). The hyperpolarisability of metalloarene and other metal complexes has been demonstrated by incorporating the complex as a guest into an inclusion host to provide polar orientation and thus SHG capability (48,49) (Figure 1.9).

1.4.3 Organics

Since inorganic materials are mature, it will be difficult to displace them. However, organic molecules, due to their rich diversity and much lower dielectric constants, would soon be established for electro-optic applications. Using organic synthesis and molecular engineering techniques, molecules can be made to measure and having higher values of hyperpolarisability. It is essential, however, that the molecules do not form centrosymmetric structures.

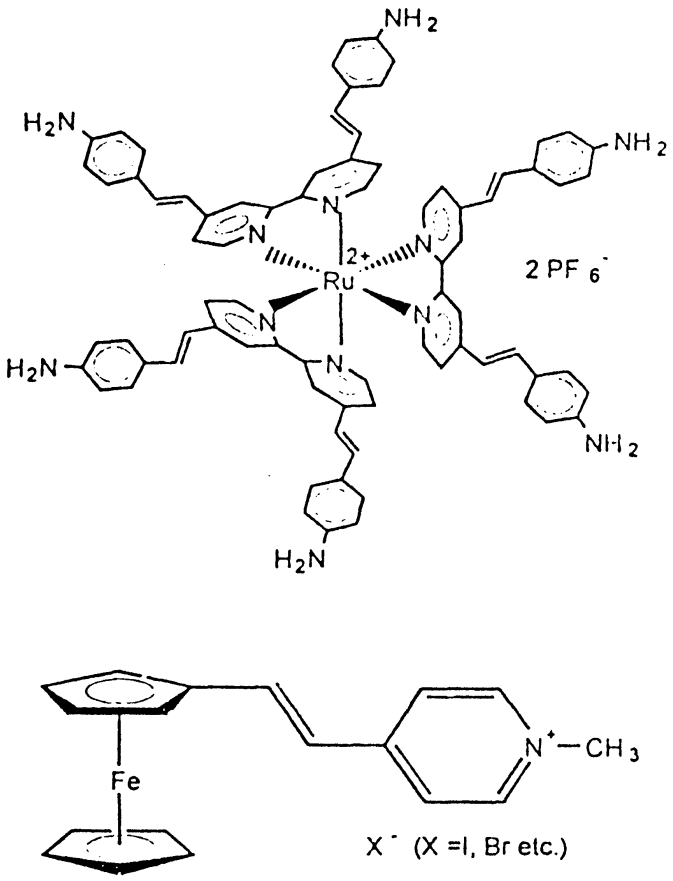

Figure 1.9 A co-ordination complex with large hyperpolarisability and an organometallic molecule which produces strong SHG

Organic single crystal and Langmuir-Blodgett films have also been used in previous studies, but they have not been as successful as polymer films, the technique used in this study (15,50).

Urea (51,52), which has a molecular β of 0.5×10^{-30} esu, is used as standard. The d_{14} of urea is 1.4 pm/V. This is useful due to high optical transparency and high damage threshold (53). Table 1.5 lists the NLO coefficients of some organic materials, and their structures are represented in Figure 1.10.

Table 1.5 NLO coefficients of organic materials

Compound	b	SHG	Coefficient(s)	FOM
BMC		10-70	$d_{13} = 90$	
COANP		50	$d_{32} = 32$; $d_{31} = 15$, $d_{33} = 14$	100
DAN	36	115	$d_{eff} = 27$	420
MAP	22	5	$d_{21} = 17$; $d_{22} = 18$; $d_{23} = 4$	
MBA-NP		25	$d_{22} = 28$	430
MMONS	18	750-1250	$d_{33} = 140$; $d_{32} = 34$; $d_{24} = 82$	850
MNA	16	22	$d_{11} = 67$	
NPP	45	50-150	$d_{21} = 84$; $d_{22} = 29$	
PNP		140	$d_{21} = 48$; $d_{22} = 17$	
POM	8.5	13	$d_{25} = 10$	

FOM (figure of merit); BMC: 4-bromo-4'-methoxychalcone; COANP: 2-N-cyclooctylamino-5-nitropyridine; DAN: 4-(N,N-dimethylamino)-3-acetamidonitrobenzene; MAP: 2,4-dinitrophenyl-(L)-alanine methylester; MBA-NP: [(-)-2-(α-methylbenzylamino)-5-nitropyridine); MMONS: 3-methyl-4-methoxy-4'-nitrostilbene; MNA: 2-methyl-4-nitroaniline; NPP: [N-(4-nitrophenyl)-(S)-prolinol]; PNP: 2-(N-(S)-prolinol)-5-nitropyridine; POM: methyl-4-nitropyridine-N-oxide

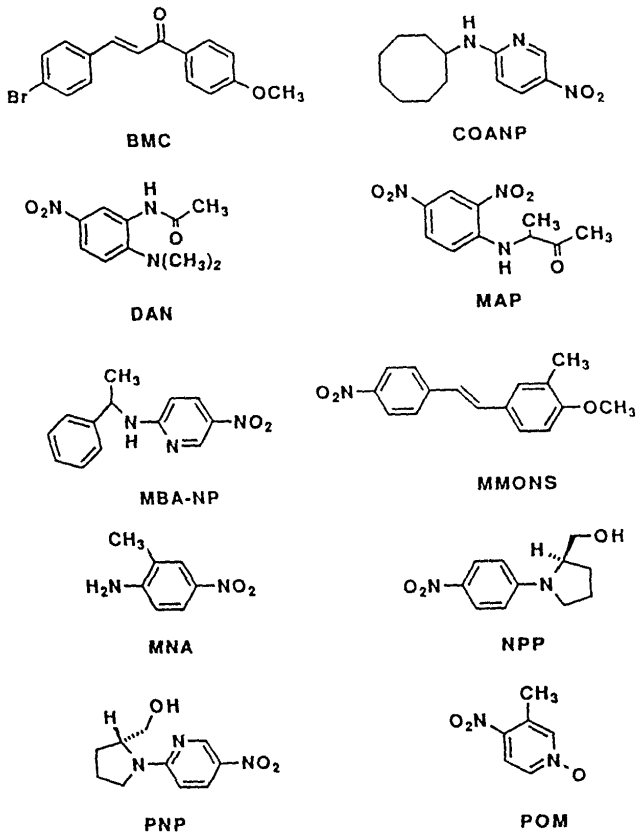

Figure 1.10 Structures of organic materials used for NLO

The largest single class of second order materials are stilbenes and diarylacetylenes (54-56). The acceptor moieties other than nitro are pyridinium ions (57), fulvenes (58), dicyano (59), tricyanovinyl groups (60), sulphones (61), enone (62), or imides (63). The donors other than amino are methoxy (64), oxazole (65), dithiafulvene (66) and dihydrapyrazole (67).

POLYMER		CRYSTAL
	General	
0	transparency	0
0	dielectric properties	0
	Fabrication	
+++	waveguide	−
−−	poling required	x
x	xtal growth required	−−
+	patterning by poling	x
+	dye molecule flexibility	−−
	Stability	
++	mechanical robustness	−−
0	optical (damage)	0
−−	nonlinear (orientational)	++
	EO	
++	level of integration	−−
++	$V_{1/2} \propto L/d$	−−
++	only d_{33} needed	−
	SHG	
−−	phase matching enhancement	++
++	waveguide enhancement	−−
−−	cavity enhancement	++
−	large off diagonal d_{ij}	++

Figure 1.11 Tradeoffs between polymer and crystal organic nonlinear optical materials. EO refers to applications for electro-optic waveguide devices such as modulators and switches. SHG refers to applications for frequency doubling of moderate and low power laser sources. + indicates favoured, -indicates disfavoured, 0 indicates neither favoured nor disfavoured, and x indicates not relevent

1.5 Polymer films

Polymer films are the best adapted so far for their nonlinear optical applications. They are easy to make and to prepare than previous methods, especially as thin films cast onto small glass plates. They give good optical properties since there are only small

losses due to absorption or diffusion and are relatively cheap to produce (68). The conjugated molecules of the system D-π-A can be introduced to a polymer either in solution in a polymer matrix or by grafting the system onto a polymer backbone during its synthesis.

Figure 1.11 shows the tradeoffs between crystal and polymer organic NLO materials for device applications. Although either type of materials could in principle be used for both applications, crystals are best for second harmonic generation, and poled polymers are best for electro-optic waveguide devices such as modulators and switches.

Organic polymers can be 'tailor made' using organic synthetic techniques. Any chromophore can be attached onto nearly any polymer backbone. The solid organic polymers are dissolved in certain organic solvents and it is this solution that is cast as a film on the glass plates by dropping a small amount onto the plate placed on a spinning head which spreads this film out using the centrifugal force generated, hence making it very thin. This method will be described later in greater detail.

The chromophore is the part of the molecule that possesses the dipole and is aligned by the d.c. field. The polymer provides a support on which the chromophores can be either directly grafted, or attached using a flexible spacer.

1.5.1 Amorphous doped or "guest-host" polymers

These polymers consist of an amorphous isotropic polymer matrix (the host), onto which the active chromophore is doped (guest, dopant). These systems have marginal optical loss due to absorption or diffusion. The fabrication is easy and reproducible. The most important work is that of Singer et al. (69) who incorporated disperse red-1 in poly(methyl methacrylate) matrix. Polystyrene, polycarbonate and polyacrylate are common host while disperse red or 4-dimethylamino-4'-nitroso stilbene are suitable as guest (70). However, their uses are limited due to marginal solubility, phase separation and plasticising effect, which depress the glass transition temperature of the polymer, resulting in the relaxation of chromophores in the poled films negating the induced order.

1.5.2 Functionalised polymers

These Polymers have the active units fixed onto the macromolecular chain either directly or through intermediate flexible spacers. The mole percent of this functional

group could be varied from 1 to 100%. However, here the segregation of the molecules and losses by relaxation in poled samples are considerably less. The flexible spacers linking the chromophores to the polymer backbone are always aliphatic and have between two and twelve carbons in their chains.

1.6 Liquid crystals

The practical applications of liquid crystals were demonstrated only in 1960 (71,72), even though these materials were discovered in 1888. Liquid crystals are stable and well defined phases that exist between the isotropic liquid state and the perfectly three-dimensionally ordered crystalline phase of some classes of molecules. They are known as the 'mesophases' and are usually formed by rod or disc shaped molecules. The hallmark of liquid crystals is their partial order which leads to simultaneous liquid and solid-like characteristics. The first molecule to be discovered possessing these properties was cholesteroyl benzoate, discovered by Reinitzer in 1888. Liquid crystals are broadly classified as thermotropic and lyotropic based on whether temperature or presence of solvent stabilises the liquid crystalline phase (73-75). The transition temperature between that of the mesophase-isotropic liquid is called the clarification temperature. Some liquid crystals have several different liquid crystalline states before they pass into the isotropic liquid phase as opposed to just one. This is known as 'Polymorphism'.

1.6.1 Classification

Thermotropic liquid crystals which are the more popular ones, may be grouped into calaminitic and discotic types based on the molecular shape (76,77). *Calaminitic liquid crystals* are those formed from rod-shaped molecules. They are further classified on the basis of the type of order present. Though a large number of different phases have been identified, the most basic types are the nematic, twisted nematic (chiral nematic or cholesteric) and smectic phases (Figure 1.12).

1.6.1.1 Nematic

The nematic phase (N) is the least ordered mesophase. It is characterised by the long axes of the molecules being oriented on an average in the same direction; this net direction is usually defined by a parameter known as the director, *n*. There is no positional ordering in the nematic phase.

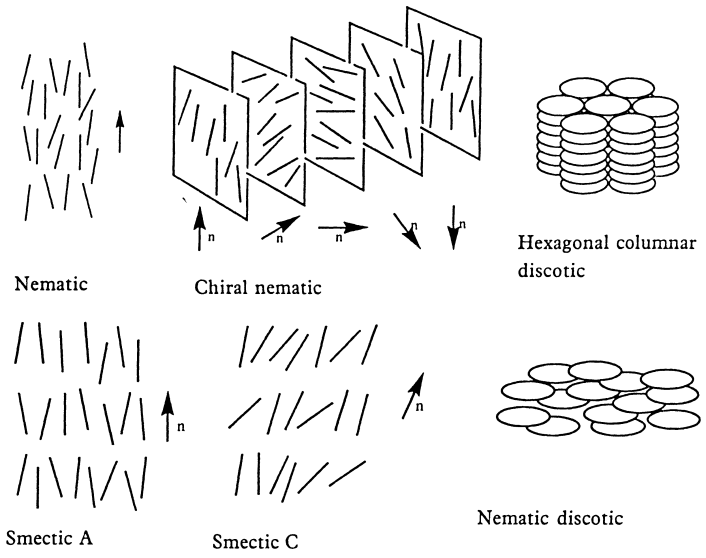

Figure 1.12 **Types of liquid crystals**

1.6.1.2 Cholesteric

When the nematic phase is made up of chiral molecules or if it is doped with chiral molecules, the director precesses through the phase describing a helix. Such phases are known as twisted nematic (N*), chiral nematic or cholesteric phases.

1.6.1.3 Smectic

When, in addition to the orientational correlation of molecules present in the nematic phase, a positional correlation of molecules into layers also occurs, the phase is known as the smectic phase. If the director is perpendicular to the layer, the phase is denoted as S_A; if the director is tilted from the normal to the layer, it is denoted as S_C. This is shown in Figure 1.12.

1.6.1.4 Chiral smectic C phase

As in the nematic, the smectic C mesophase has a chiral state designated C*. Consistent with the smectic C, the director makes a tilt angle with respect to the smectic layer. The difference is that this angle rotates from layer to layer forming a helix. In other words, the director of the smectic C* mesophase is not parallel or perpendicular to the layers, and it rotates from one layer to the next. Notice the twist of the director, represented by green arrows, in each layer in the following diagram (Figure 1.13).

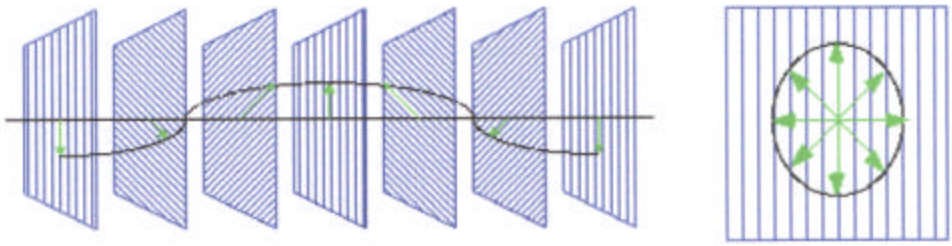

Figure 1.13 A schematic representation of a smectic C* phase (left); and a view of the same phase, but along the axis (right)

Rod-shaped molecules, mesogens, in the smectic phase show a translational order as well as orientational order. In the smectic C phase, the periodic spacing of the mesogens along one axis, we will use the z axis, causes them to form layers in the x-y plane. The director of each planar layer is tilted at an angle θ from the normal. This angle is temperature dependent if a smectic C to smectic A transition occurs with increasing temperature. When the molecule is chiral, successive smectic C layers show gradual change in the direction of tilt, such that the director precesses about the z axis from layer to layer, always lying on the surface of a hypothetical cone of angle 2θ, as illustrated in Figure 1.14. The angle around the circle of precession is known as the azimuthal angle. This creates a helical structure in the chiral smectic C (SmC*) mesophase with the pitch being the distance along the z axis needed to reach the same molecular orientation. In addition to producing this helical structure, chirality results in a spontaneous molecular polarisation, shown by the blue arrow in the Figure 1.14. This polarisation vector is perpendicular to the molecule and is contained in the layer plane. Therefore, all possible directions for the vector are tangent to the circle of intersection of the cone with the plane. A bulk S_{C*} sample, free to develop its helical structure, will not show ferroelectric behaviour since the spontaneous polarisation will average to zero over one pitch (since polarisation vectors go around an entire circle and cancel each other out). This is often referred to as the helielectric phase. Due to the helicoidal superstructure, not ferroelectricity but helielectricity occurs. Only an unwinding of this helicoidal structure

yields samples with a macroscopic spontaneous polarisation exhibiting point symmetry C_2. The polarisation P is a polar vector. For spontaneous polarisation to

$$P = (P_x, P_y, P_z)$$

exist in a given phase, we must demand that the vector P is invariant under all symmetry operations compatible with the symmetry of the phase in question. Let us now see if this requirement explains the fact that the SmC* phase is ferroelectric, whereas the achiral SmC phase is not. The x, y, z coordinate system and the arrangement of the molecules in the SmC and SmC* phases as shown in Figure 1.15.

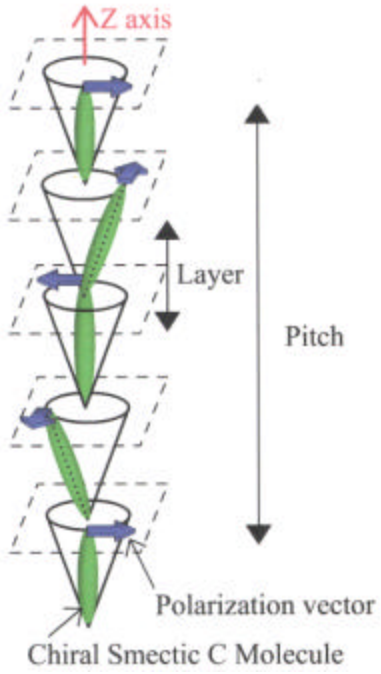

Figure 1.14 Chiral smectic C molecule

In both the SmC (symmetry C_{2h}) and SmC* (symmetry C_2) phases, a 180° rotation around the y-axis is an allowed symmetry operation.

SmC	SmC*
$\xrightarrow{C_{2y}}$ $(P_x, P_y, P_z) \Rightarrow (-P_x, P_y, -P_z)$	$\xrightarrow{C_{2y}}$ $(P_x, P_y, P_z) \Rightarrow (-P_x, P_y, -P_z)$
$\Downarrow$	$\Downarrow$
$\vec{P} = (0, P_y, 0)$	$\vec{P} = (0, P_y, 0)$

Under this transformation the polarisation vector transforms according to $(P_x, P_y, P_z) \Rightarrow (-P_x, P_y, -P_z)$. Since these two expressions must be identical, we can only allow the possibility of a spontaneous polarisation in the direction of the two-fold axis: $P=(0,P_y,0)$. In the SmC phase (but, not in the SmC* phase) the xz plane is a mirror plane.

SmC	SmC*
$\xrightarrow{m_{xz}}$ $(0, P_y, 0) \Rightarrow (0, -P_y, 0)$	Reflection not allowed due to chirality
$\Downarrow$	$\Downarrow$
$\vec{P} = (0, 0, 0)$	$\vec{P} = (0, P_y, 0)$

The existence of this mirror plane changes $(0,P_y,0)$ into $(0,-P_y,0)$ in the SmC phase. Since these two expressions must be identical, P must be zero and ferroelectricity is not allowed in the SmC phase. In the case of the SmC*, the molecules are chiral and are not any longer a mirror plane and ferroelectricity is permitted by symmetry. The spontaneous polarisation in the SmC* phase points in the direction of the y-axis. It lies in the smectic planes in a direction perpendicular to the tilt plane as stated above.

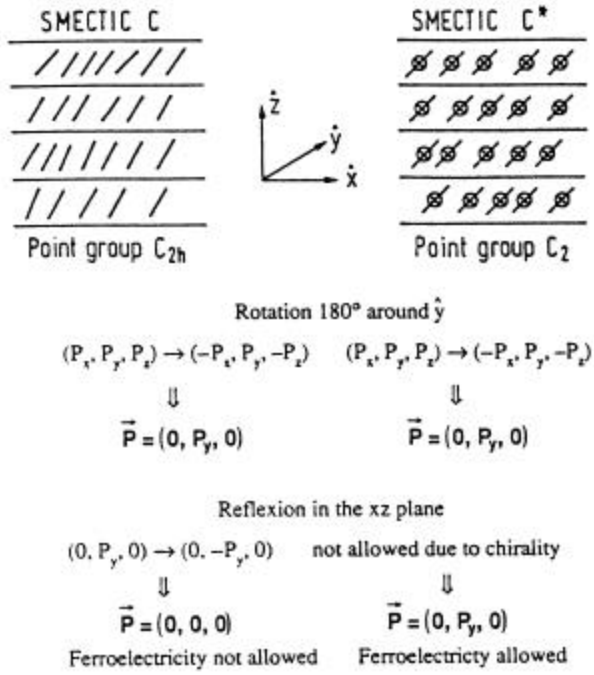

Figure 1.15 Relation between the allowed point group symmetry operations and the appearance of ferroelectricity vanishing in the tilted smectic C^* and C phases

The C_2 symmetry implies that the untwisted S_{C^*} phase can exhibit second-order nonlinear optical (NLO) properties such as the linear electro-optic effect and second harmonic generation (SHG). Furthermore, the correct phase symmetry must exist for phase-matched SHG to be observed. This has been proved for homeotropically aligned low molar mass liquid crystals (78,79).

Discotic liquid crystals are generally formed by molecules with an aromatic core unit surrounded by long alkyl chain substituents. Nematic discotics (ND) possess only orientational ordering of the molecular short axes. The more common phases are the columnar phases which are characterised by the symmetry of the side-to-side molecular arrangement and the presence or absence of order within the columns.

1.6.2 Liquid crystalline polymers

Liquid crystal polymers consist of a polymer chain which provides a 'backbone' to bond to the mesogenic liquid crystal pendant units. This double structure is good since it has the polymer properties: a glass transition, a flexible molecule, the ability to be processed into a thin film, and it also possesses the anisotropic properties of the liquid crystal (i.e. an intrinsic axial order). It has been recognised that the axial ordering present in liquid crystalline polymers can be used to enhance field-induced polar ordering by elongating the orientational distribution function along the direction of electric field.

1.6.3 Ferroelectric liquid crystals

Since the early days of ferroelectric low molar mass LC research, the exploration of the NLO properties of these substances has been a topic of interest. Unfortunately, the SHG efficiency of most ferroelectric LCs investigated so far (80-83) is orders of magnitude below that of state-of-the art inorganic crystals, such as lithium niobate.

In order to create ferroelectric LC materials with improved second-order NLO activity, implanting well-known NLO chromophores into the core of standard ferroelectric LC molecules might be considered. However, since the direction of dipolar orientation of the ferroelectric LC molecules is parallel to the C_2 axis (perpendicular to the director), these NLO active molecular groups have to be incorporated in such a fashion that the direction of maximum second-order polarisability is polarly oriented along this axis. This is expected to occur if the chromophore is coupled to the chiral centre of the molecule, because the specific nature of the chiral group is assumed to define the tilt direction and hence the direction of the polar axis. This requirement is automatically fulfilled if the chirality is part of the NLO group. If this is not the case, it seems to be advantageous to locate the two groups as close to each other as possible.

As already mentioned, NLO chromophores with large β values normally consist of donor and an acceptor group that are linked by a conjugated spacer, often in the form of aromatic rings. The direction of large second-order polarisability is then roughly along the charge-transfer axis. In view of the symmetry requirements discussed above, the NLO chromophores have to be integrated in the ferroelectric LC structure with their long axis perpendicular to the long axis of the LC molecule. It follows that liquid crystallinity can

only then be compatible with such a functionalisation if the NLO group is sufficiently compact and the rigid core of the mesogen is sufficiently long.

On the basis of this design approach, Walba et al. (84) succeeded in synthesising the 4-[(3-nitroalkyloxy-1,4-phenylene oxycarbonyl)-4'-(alkyloxy)]biphenyl exhibiting a $d_{22} = d_{23}$ value of 0.6 pm/V (d_{eff} = 0.23 pm/V).

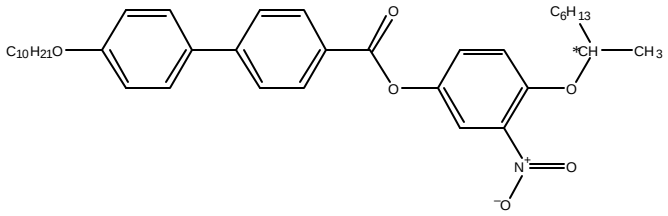

Quite recently, Schmitt et al. (85) presented highly efficient NLO ferroelectric LC materials whose SHG properties were investigated in 13 μm thin, homeotropically aligned layers.

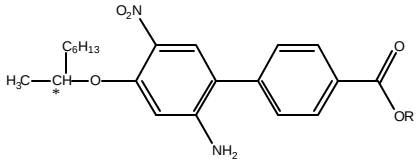

where R =

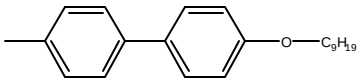

Positioning the chiral centre in the alkoxy terminal chain adjacent to the nitroaniline dipole moment strongly enhances both P_s and the SHG efficiency, leading to the largest SHG coefficients (e.g. d_{22} = 5 pm V^{-1}) reported so far for ferroelectric low molar mass LCs.

Recently, Wischerhoff et al. (86) reported the synthesis, the thermal behaviour, and the ferroelectric properties of liquid-crystalline copolysiloxanes containing chiral mesogens and NLO chromophores.

The investigators showed that in all the polymer series a noticeable amount of chromophore (up to about 30 mol%) could be incorporated without losing the chiral smectic C phase. However, approaching high chromophore contents, a tendency for the copolymers to form the ferroelectric smectic A phase could be detected. SHG measurements were performed on thin homeotropically aligned polymer films, with the

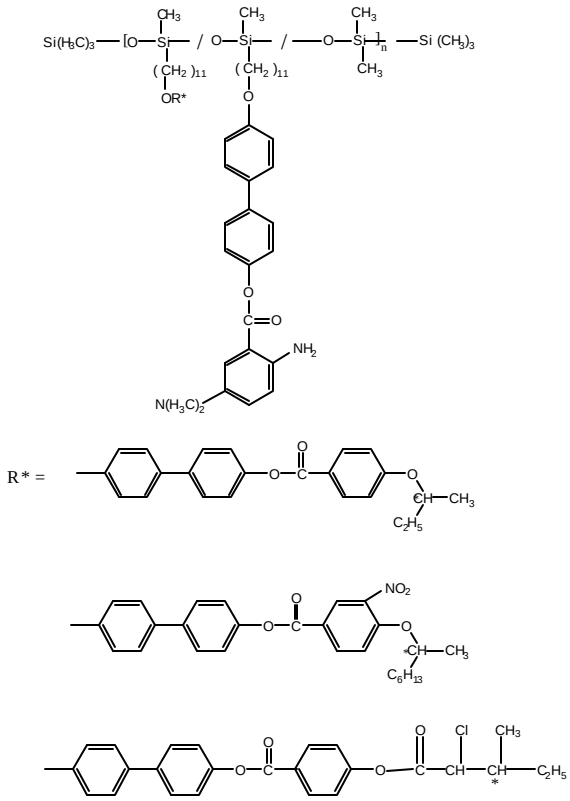

polar axis perpendicular to the incoming beam. However, in the geometry used, the applied electric field was necessarily limited and did not allow the helix to untwist completely, leading to low SHG efficiency.

1.7 Applications of NLO materials

Material research and application for NLO has progressed rapidly since the past decade to the point where several systems are available commercially. A variety of materials including inorganic and organic crystals, polymers, semiconductors, composites and metal-based systems possess NLO properties. Each material has properties that are advantageous to certain applications but also possess properties that are detrimental to other applications.

1.7.1 Optical switches

All optical applications, whether linear or nonlinear, require proper orientation of light. Optical signal carried on an optical fibre can be decoded and converted into electric signal by optical switches (70). In an optical switch, the laser beam is directed at an NLO material, which confines the light beam within the channel. When a wave-guide is connected in parallel to the first NLO material, both will out-put the light because the

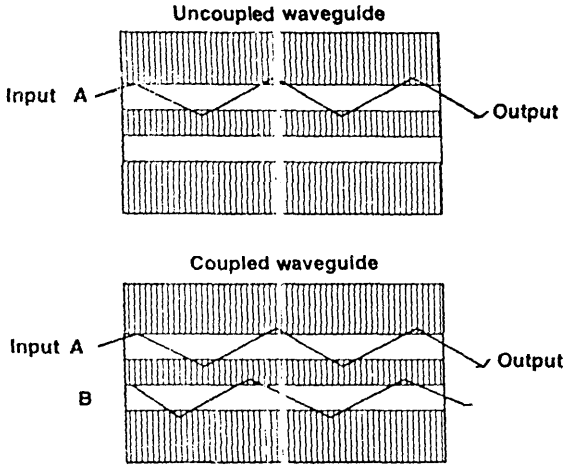

Figure 1.16 Design of an optical switch. The index of refraction within the wave-guide is higher than that of the surrounding shaded material. When two wave-guides are coupled, some of the light input at channel A spills over and is output through channel B as schematically shown.

zigzag movement of light exceeds the confinement. Thus, a light input in one-channel results in light output through another channel. Polydiacetylenes are used to control the switching speed (87,88). One example for the design of an optical switch regulated solely by fluctuations in the light beam's intensity is provided in Figure 1.16.

1.7.2 Second order devices

The ability to transform the frequency of light from one regime to other is of practical importance (89). The devices used in this area are colour-specific lasers, such as frequency doubled semiconductor or YAG (yittrium aluminium garnet) lasers, electro-optic modulators, such as SLM (spatial light modulators).

A continuous uniform light beam is not useful for information transfer. However, any of its observable properties, including intensity, frequency, phase, or polarisation, may be deliberately modified to impart an information content to the beam.

A modulator, a device that performs this function, is at the crux of any system based on optically transmitted signals. The modulator transposes coded information from an electrical, acoustic or magnetic signal onto a light beam. One popular scheme for modulating light, the Mach-Zender interferometer,consists of a wave-guide of a nonlinear material split into channels that reunite (90) (Figure 1.17).

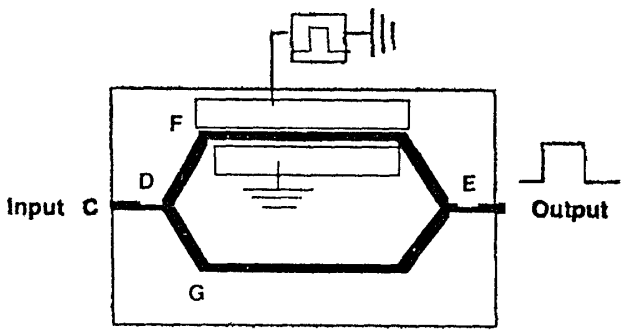

Figure 1.17 **A Mach-Zender interferometer**

1.7.3 Holographic optical element (HOE)

The HOE is a hologram designed to function as a lens. This is used to focus as well as to separate mixed frequency signals. This will also function as a wave-guide to move light into two-dimensional plane. The above functions play a critical role in fabrication of small optical devices and signal processing elements (91).

1.8 Scope of this work

Materials with a nonlinear optical (NLO) response are expected to play a major role in the development of optoelectronic and photonics technologies. Organic polymers are already involved in many optical applications (92,93), such as microlithography and electrophotography, and have shown particular promise for NLO applications (94,95). They have advantages of good processing capabilities, but in terms of performance have to compete with inorganic crystals such as lithium niobate ($LiNbO_3$), which have been around for a longer time and are still preferred over polymers in most commercial electro-optic devices, due to their higher nonlinearity and better environmental stability. In the search for better materials for photonic applications, nonlinear response, sensitivity, optical quality, mechanical strength and thermal and chemical stabilities are the major criteria. Since materials with low-cost and facility in processing are preferred in large scale device fabrication, organic polymers demonstrate particular promise. The structural flexibility of polymers, that provides them with important technological potential, has generated intensive research efforts in the development of functional and multifunctional polymers (96-98).

This study aims at investigating the nonlinear optical properties of some novel

homo and copolymers. The synthesis is aimed at the preparation of novel chromophores, which are presumably NLO active. Acceptors like nitro, cyano, aldehyde and barbiturate and donors like ether and thio groups have been investigated. The study is restricted to azo and azomethine polymers. The interconnecting group should cause the resulting compound to have a linear and consequently planar conformation. Azo (-N=N-) and azomethine (-CH=N-) are preferred as they restrict the freedom of rotation; can conjugate with phenylene rings thereby enhancing the anisotropic polarisability. Polymers with azobenzene moieties are gaining much attention due to their intriguing optical properties such as optical nonlinearities, light induced dichroism and birefringence. Azobenzene is thermally stable upto about 350^{o} C. Irradiation of azo polymer with a linearly polarised beam reorients azobenzene groups to align perpendicular to the incoming beam through trans-cis-trans isomerisation cycles (99-101). These light-induced dichroism and birefringence properties make azo polymers ideal materials for applications as erasable optical memory devices, optical sensors and holographic information storage devices (102).

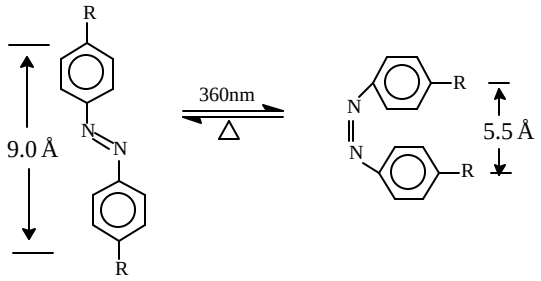

Figure 1.18 Trans-cis isomerisation in azobenzene

It is interesting to note that several long chain dipolar aromatic azomethines (more commonly called Schiff bases) are liquid crystalline (103). Most of these imines are disubstituted N-benzylidene anilines, that arrange themselves in a parallel orientation with each other in the liquid melt, giving smectic and nematic mesomorphic states before reaching the melting point. Oligomethylene spacer (2 or 3) is used to decouple the chromophore from the main chain and thus to enhance the possibility of self organisation into an anisotropic liquid crystalline mesophase. For a particular NLO active mesogen, side group and spacer, the flexibility of backbone influences the nature of the phase as well as the thermal transitions (86). The backbones used in this study are polyacrylates,

polymethacrylates, polystyrenes, polymaleimides and polyurethanes. The thermal behaviour of these polymers were investigated by differential scanning calorimetry, optical microscopy and X-ray diffraction. Thin polymeric films were spin coated and electric field poling measurements were carried out as a function of temperature. The second harmonic (SH) coefficients d_{33} and d_{31} were measured by Maker-Fringe analysis and compared with the values predicted of polymers.

Molecular asymmetry imparts chirality to LC phases, resulting in the formation of helical ordering of the constituent molecules of the phase, resulting in a reduction in the space symmetry (104), leading to some phases having unusual NLO properties. Because of the lack of a centre of symmetry, uniformly oriented substances with S_{C*} phases show nonlinear optical behaviour. Chiral Smectic LC phases have polar symmetry C_2 and possess an easily measured macroscopic polarisation once the helical structure is unwound. A number of approaches have been established to obtain the untwisted S_C* phase structure. For low mass liquid crystals and linear liquid crystal polymers, the common practice is to apply an external electrical field or to use surface forces (105-107). These methods, however, are limited to thin layers of the S_C* material, with the additional difficulty for electrically poled systems being a possible reorientation process after removing the field. For liquid crystal (LC) polymers these techniques often fail owing to their high viscosity. However, using a mechanical field by drawing fibres from the melt of uniaxial systems offers the chance to obtain well-aligned samples.

In contrast to this, liquid crystalline elastomers (LCE) can be macroscopically, uniformly oriented by mechanical deformations (108), and this orientation process is not limited to thin samples or suitable dielectric anisotropy of the material. Furthermore, for LCEs the oriented structure can be chemically locked in by cross-linking, resulting in the so-called liquid single crystal elastomers (LSCE) (109). It is well known that, with respect to the director, nematic elastomers can be macroscopically aligned by uniaxial mechanical fields. It has been shown that uniaxial mechanical fields are sufficient to get a macroscopic alignment either of the director or of the smectic layers for the uniaxial S_A-phase (110). Extending this method to a chiral smectic C elastomer, depending on the experimental set-up, either smectic layer orientation or director orientation parallel to the stress axis occurs. In order to align the director and the smectic layers a biaxial

mechanical field, consistent with the phase symmetry, has to be used to achieve a macroscopically uniform orientation of the untwisted smectic C* structure.

The question arises whether an elastomer exhibiting the biaxial smectic C phase or the helielectric chiral smectic C phase can also be uniformly aligned by a mechanical field. It has been reported that a chiral S_C* elastomer can be made to achieve the correct phase symmetry for SHG by using two uniaxial stress experiments (111). In this study, we present the synthesis of new monomers, linear polymers and elastomers. Also we present the orientation behaviour of a chiral smectic C elastomer by suitable shear fields consistent with the phase symmetry.

1.9 REFERENCES

1. Prasad, P. N. and Williams, D. J., in *Introduction to Nonlinear Optical Effects in Molecules and Polymers,* Prasad, P. N. and Williams, D. J., (eds.), Wiley: NY (1991).

2. Hegger, A. J., Orenstein, J. and Ulrich, D. R., (eds.) *Mater. Res. Soc. Symp. Proc.*, 109 (1988).

3. Hann, R. A. and Bloor, D., (eds.), *Organic Molecules for Nonlinear Optics,* Royal Soc. of Chemistry: London (1989).

4. Singer, K. D., in *Polymers for Light Wave and Integrated Optics Technology and Application,* Hornak, L. A. (ed.), Marcel Dekker: NY (1992).

5. Saleh, B. E. A. and Teich, M. C., in *Fundamentals of Photonic,* Wiley: NY (1991).

6. Franken, P. A., Hill, A. E., Peters, C. W. and Weinrich, G., *Phy. Rev. Letts*., **7**, 118 (1961).

7. Bloembergen, N., *Nonlinear Optics*, Benjamin: Reading, MA (1965).

8. Goirdamine, J. A. and Miller, R. C., *Phys. Rev. Letts.*, **14**, 973 (1965).

9. Rentzepis, P. M. and Poa, Y. H., *Appl. Phys. Letts*., **5**, 156 (1965).

10. Heilmeir, G. H., Ockman, N., Braunstein, N. and Kramer, D. A., *Appl. Phys. Lett*., *5*, 229 (1964).

11. Eaton, D. F. in *Materials for Nonlinear Optics Chemical Perspectives*, Marder, S. R., Sohn, J. E. and Stocky, G. D. (eds.), Amer. Chem. Soc., 455: Washington, DC (1991); p.128

12. Ulrich, R. and Weber, H. P., *Appl. Opt.*, **11**, 428 (1972).

13. Kurtz, S. K. and Perry, T. T., *J. Appl. Phys*. **39**, 3798 (1968).

14. Schlotter, N. E., Jakel, J. and Baker, G. L., *Appl. Phys. Lett*., **56**, 13 (1990).

15. Williams, D. J., *Angew. Chem. Int. Ed. Eng*., **23**, 690 (1984).

16. Williams, D. J., in *Nonlinear Optical Properties of Organic Materials*, Williams, D. J., (ed.), Amer. Chem. Soc., 233: Washington, DC (1983).

17. Gedanken, A., Robin, M. B. and Keubler, N., *J. Phys. Chem.*, **86**, 4096 (1982).

18. Basu, S., *Ind. Eng. Chem. Prod. Res*., **23**, 183 (1984).

19 Glass, A. M., *Science*, **226**, 657 (1984).

20. Pugh, D. and Sherwood, J. N., *Chemistry in Britain*, 544 (1988).

21. Chemla, D. S., *Physics Today*, **57** (1985).

22. Feinberg, J., *Physics Today*, **46** (1986).

23. Hecht, J., *High Technology*, **55** (1983).

24. Abu-Mostafa, Y. S., Psaltis, D. and Smith, S. D., *Sci. Amer*., **88** (1987).

25. Boyd, G. T., *J. Opt. Soc. Am. B*, **6**, 685 (1989).

26. Feynman, R. P., Leighton, R. B., Sands, M. and Auson, D. H., *The Feynman Lectures on Physics*, Vol. **1**, Addison Wesley Reading: Massachusetts (1963).

27. Möhlmann, G. R. and van der Vorst, C. P. J. M., in *Side Chain Liquid Crystal Polymers*, McArdle C. B., (ed.), Chapman and Hall: NY (1989); p.330.

28 Singer, K. D., Kuzyk, M. G. and Sohn, J. E., *J. Opt. Soc. Am. B*, **4**, 968 (1987).

29. Legrange, J. D., Kuzyk, M. G. and Singer, K. D., *Mol. Cryst. Liq. Cryst.*, **150b**, 567 (1987).

30. Radhakrishnan, T. P., *Resonance*, **3**(8), 14 (1998).

31. Stucky, G. D., Marder, S. R. and Sohn, J. E., in *Materials for Nonlinear Optics Chemical Perspectives*, Marder, S. R., Sohn, J. E. and Stocky, G. D. (eds.), Amer. Chem. Soc., 455: Washington, DC (1991); p.2.

32. Nakazumi, H., *J. Soc. Dyers Colorists*, **104**, 121 (1988).

33. Long, N. J., *Angew Chem. Int. Ed. Engl.*, **34**, 21 (1995).

34. Andraud, C., Brotin, T., Carcia, C., Pelle, F., Goldner, P., Bigot, B. and Collet, A., *J. Am. Chem. Soc.*, **116**, 2094 (1994).

35. Gangadhara, Ponrathnam, S., Noël, C., Reyx, D. and Kajzar, F., *J. Poly. Sci., Poly. Chem., Part A*, **37**, 513 (1999).

36. Zernike, F., Midwinter, J. E., *Applied Nonlinear Optics*, John Wiley: NY (1973); p.29

37. Morely, J. D., Docherty, V. J. and Pugh, D., *J. Chem. Soc. Perkin Trans., 2*, 1357 (1987).

38. Nicoud, J. F. and Twieg, R. J., in *Nonlinear Optical Properties of Organic Molecules and Crystals*, Vol. **1**, Chemla, D. S. and Zyss, J. (eds.), Academic Press: NY (1987); p.227.

39. Levine, B. F., *Chem. Phys. Lett*., **37**, 516 (1976).

40. Levine, B. F. and Bethea, C. G., *J. Chem. Phys.*, **63**, 2666 (1975).

41. Ulman, A., *J. Phys. Chem.*, **92**, 2385 (1988).

42. Dulcic, A., and Flytzanis, C., *Opt. Commun*., **25**, 402 (1978).

43. Lin, J. T. and Chen, C., *Lasers and Optronics*, **59** (1987).

44. Frazier, C. C., Harvey, M. A., Cockerham, M. P., Chauchard, E. A. and Lee, C. H., *J. Phys. Chem.*, **90**, 5703 (1986).

45. Eaton, D. F., Anderson, A. G., Tam, W. and Wang, Y., *J. Am. Chem. Soc*., **133**, 1886 (1987).

46. Tam, W. and Calaberse, J. C., *Chem. Phys. Letts*., **133**, 244, 1987.

47. Green, M. L. H., Marder, S. R., Thompson, M. E., Bandy, J. A., Bloor, D., Kolinsky, P. V. and Jones, R. J., *Nature*, **330**, 360 (1987).

48. Anderson, A. G., Calabrese, J. C., Tam, W. and Williams, I. D., *Chem. Phys. Lett*., **134**, 392 (1987).

49. Tam, W., Calabrese, J. C., Williams, I. D., Wang, Y. and Anderson, A. G., *Chem. Mat.*, **1**, 128 (1989).

50. Garito, A. F., Singer, K. D. and Teng, C. C., in *Nonlinear Optical Properties of Organic and Polymeric Materials*, Williams, D. J. (ed.), Amer. Chem. Soc., 233: Washington, DC (1983).

51. Cassidy, C., Halbout, J. M., Donaldson, W. and Tang, C. L., *Opt. Commun*., **29**, 243 (1977).

52. Ledoux, I. and Zyss, J., *J. Chem. Phys*., **73**, 203 (1982).

53. Halbout, J. M. and Tang, C. L., in *Nonlinear Optical Properties of Organic Molecules and Crystals*, Vol. **1**, Chemla, D. S. and Zyss, J. (eds.), Academic Press: NY (1987); p.385.

54. Fouqey, C., Lehn, J. M. and Malthete, J., *J. Chem. Soc. Chem. Commn*., **19**, 1424 (1987).

55. Wang, Y., Tam, W., Stevenson, S. H., Clement, R. A. and Calabrese, J. C., *Chem. Phys. Letts*., **148**, 136 (1988).

56. Tabei, H., Kurihara, T. and Kaino, T., *Appl.Phys. Lett*., **50**, 1855 (1987).

57. Meredith, G. R., in *Nonlinear Optical Properties of Organic and Polymeric Materials*, Williams, D. J. (ed.), Amer. Chem. Soc., 233: Washington, DC (1983); p.30.

58. Ikeda, H., Kawabe, Y., Sakai, T. and Kawasaki, K., *Chem. Phys. Lett*., **157**, 576 (1989).

59. Allen, S., Gordon, P., Bothwell, B. D. and Karaulov, S. A., *J. Appl. Phys*., **64**, 2583 (1988).

60. Katz, H. E., Singer, K. D., Sohn, J. E., Dirk, C. W., King, L. A. and Gordon, H. M., *J. Am. Chem. Soc*., **109**, 6561 (1987).

61. Ulman, A., *U.S. Pat.*, 4,792,208 (1989).

62. Goto, Y., *Eur. Pat.*, 262672 (1988).

63. Palazoto, M. C., *U.S. Pat.*, 4,733,109 (1988).

64. Tam, W., Guerin, B., Calabrese, J. C. and Stevenson, S. H., *Chem. Phys. Letts*., **154**, 93 (1989).

65. Kaino, T., Kurihara, T., Matsumoto, S. and Tomaru, A., *Jap. Pat.*, 6326638 (1988).

66. Nogami, T., Shirota, Y., Umegaki, S., Ueyimia, T. and Yasuda, N., *Chem. Phys. Letts*., **155**, 338 (1989).

67. Combellas, C., Gauiter, H., Simon, J., Thiebault, A., Josse, D., Ledoux, I. and Verpeaux, J. N., *J. Chem. Soc. Chem. Commn*., **3**, 203 (1988).

68. Dulmage, W. J., Light, W. A., Marino, S. J., Salzberg, C. D., Smith, D. L. and Staudenmayer, W. J., *J. Appl. Phys*., **49**, 5543 (1978).

69. Singer, K. D., Lalama, S. L., Sohn, J. E. and Small, R. D., in *Nonlinear Optical Properties of Organic Molecules and Crystals*, Vol. **1**, Chemla, D. S. and Zyss, J. (eds.), Academic Press: NY (1987); p.437.

70. Glass, A. M., *MRS Bull.*, **13**(8), 16 (1988).

71. Fergason, J., *J. Scient. Am.*, **211**, 77 (1964).

72. Henmeter, G. H., *J. Chem. Phys.*, **44**, 644 (1964).

73. Kwolek, S. L., Morgan, P. W. and Gulrich, L. W., *Macromolecules*, **10**, 1390 (1977).

74. Gonin, D., Guichard, B., Noël, C. and Kajzar, F., *Macromol. Symp*., **96**, 185 (1995).

75. Noël, C., in *Liquid Crystal Polymers: From Structures to Applications*, Collver, A. A. (ed.), Elsevier Applied Science: London (1992); p.31.

76. Noël, C., *Makromol. Chem. Macromol. Symp*., **22**, 95 (1988).

77. Noël, C. and Navard, P., *Prog. Polym. Sci.*, **16**, 55 (1991).

78. Yoshino, K., Utsumi, M., Morita, Y., Sadohara, Y. and Ozaki, M., *Liq. Cryst.*, **143**, 1021 (1993).

79. Schmitt, K., Herr, R.-P., Schadt, M., Fünfschilling, J., Buchecker, R., Chen, X. H. and Benecke, C., *Liq. Cryst.*, **14**, 1735 (1993).

80. Lui, J. Y., Robinson, M. G., Johnson, K. M. and Doroski, D., *Opt. Lett*., **15**, 267 (1990).

81. Taguchi, A., Oucji, Y., Takezoe, H. and Fukuda, A., *Jpn. J. Appl. Phys*., **28**, L-997 (1989).

82. Ozaki, M., Utsumi, M., Gotou, T., Morita, Y., Daido, K., Sadohara, Y. and Yoshino, K., *Ferroelectrics*, **121**, 259 (1991).

83. Yoshino, K., Utsumi, M., Morita, Y., Sadohara, Y., Osaki, M. *Liq. Cryst*., **143**, 1021 (1993).

84. Walba, D. M., Ros, M. B., Clark, N. A., Shao, R., Robinson, M. G., Liu, J. Y., Johnson, K. M. and Doroski, D., *J. Am. Chem. Soc*., **113**, 5471 (1991).

85. Benne, I., Semmler, K. and Finkelmann, H., *Macromol. Rapid Commun*., **15**, 295 (1994).

86. Wischerhoff, E., Zentel, R., Redmond, M., Mondain-Monval, O. and Coles, H., *Makromol. Chem. Phys.*, **195**, 1593 (1994).

87. Tamir, T., in *Integrated Optics*, Tamir, T., (ed.), Springer-Verlag: NY (1982); p.83.

88. Smith, P. W., *IEEE Circuit and Devices*, **9**, May (1987).

89. Ulrich, D. R., *Mol. Cryst. Liq. Cryst*., **160**, 1 (1988).

90. Tripathy, S., Cavicelic, C., Kumar, J. and Saikumar, R., *Chemtech*, **19**, 620 (1989).

91. Tult, L.W. and Kost A., *Nature*, **356**, 225 (1992).

92. Service, R. F., *Science*, **267**, 1918 (1995).

93. Chilton, J. A. and Goosey, M. T., *Special Polymers for Electronics and Optoelectronics*, Chapman & Hall: London (1995).

94. Zyss, J., *Molecular Nonlinear Optics Materials, Physics and Devices*, Academic Press: San Diego (1994).

95. Bosshard, C., Sutter, K. and Prêtre, P., *Organic Nonlinear Optical Materials*, Gordon and Breach Publishers: Basel (1995).

96. Burland, D. M., *Chem. Review*, **94**, 1 (1994).

97. Dalton, L. R., Harper, A. W. and Ghosn, R., *Chem. Mater*. **7**, 1060 (1995).

98. *Organic Thin Films for Photonics Applications, Proceedings of the Topical Meeting of the Optical Society of America*, September 11-14, Portland, Technical Digest, Vol. **21** (1995).

99. Kumar, G. S. and Neckers, G. N., *Chem. Rev*., **89**, 1915 (1989).

100. Zollinger, H., *Diazo Chemistry*, Verlag Chemie: Veinheim (1994).

101. Rau, H., *Photochemistry and Photophysics*, Vol. **2**, Chap. 4, CRC Press: Boca Raton, FL (1990).

102. Lytel, R., Libscomb, G. F., Stiller, M., Thackara, J. I. and Tickner, A. J., *Nonlinear Optical effects in Organic Polymers*, Kluwer: Dordrecht (1989).

103. McCulloch, I. A. and Bailey, R. T., *Mol. Cryst. Liq. Cryst*., **200**, 157 (1991).

104. Goodby, J. W., *J. Mater. Chem.*, **1**, 307 (1991).

105. Shtykov, N. M., Barnik, M. I., Beresnev, L. A. and Blinov, L. M., *Mol. Cryst. Liq. Cryst*., **124**, 379 (1985).

106. Poths, H., Schönfeld, A., Zentel, R., Kremer, F. and Siemens-meyer, K., *Adv. Mater*., **4**, 351 (1992).

107. Clark, N. A. and Lagerwall, S. T., *Appl. Phys. Lett*., **36**, 899 (1980).

108. Gleim, W. and Finkelmann, H., in *Side Chain Liquid Crystal Polymers*, McArdle, C. B. (ed.), Chapman and Hall: NY (1989); p.287.

109. Küpfer, J. and Finkelmann, H., *Makromol. Chem., Rapid Commun*., **12**, 717 (1991).

110. Freidzon, Y. S., Talroze, R. V., Baiko, N. I., Kostromin, S. G., Shibaev, V. P. and Plate, N. A., *Liq. Cryst.* **3**, 127 (1988).

111. Benné, I., Semmler, K. and Finkelmann, H., *Macromolecules,* **28**, 1854 (1995).

2

Synthesis of MONOMERS

2 Synthesis of monomers

2.1 Azomethines

2.1.1 General synthesis of substituted azomethine

Aliphatic and aromatic aldehydes condense with aliphatic and aromatic primary amines to form N-substituted imines. Reaction conditions vary widely, such as passing a gaseous amine through a melt of a solid ketone (1,2); reaction of amine with aldehydes without solvent and catalyst (3); azeotropic removal of water in a low-boiling solvent in the preparation of some aldimines (4); treatment of aldehydes with amines in solvents such as ether, tetrahydrofuran, or benzene in the presence of a molecular sieve (5-9); reaction of aqueous amines with ketones (10); reactions catalysed by potassium or sodium hydroxide solutions at low temperatures (4,11-13); reactions in the presence of base under heat and pressure (4); dehydrations in the presence of acidic reagents such as *p*-toluene sulphonic acid (14,15); methane sulphonic acid (4), or titanium tetrachloride (4).

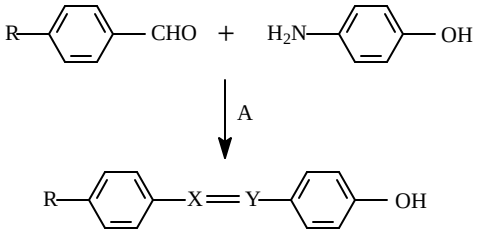

R = CN, NO_2, CHO

A = ethanol (dry), CH_3COOH (cat), reflux

X=Y: CH=N or N=CH

Scheme 2.1: Synthesis of azomethine

2.1.1.1 General procedure for synthesis of azomethine bases

4-Nitro benzaldehyde, 4-cyano benzaldehyde, terephthaldicarboxaldehyde, 4-nitro aniline, 4-hydroxy benzaldehyde and 4-amino phenol were procured from Aldrich Chemical Co. U.S.A., and recrystallised according to established standard procedures. Ethanol, glacial acetic acid were obtained from S.D. Fine Chemicals, Mumbai, India.

5.0 g (0.046 mol) of 4-amino phenol and 6.1 g (0.046 mol) of 4-cyano benzaldehyde in dry ethanol (50 mL) were refluxed for 24 hours with glacial acetic acid as catalyst (2 mL) to give 4-hydroxy-N-(4'-cyanobenzylidene)aniline. The other azomethine bases synthesised comprised of nitro and aldehyde as electron withdrawing groups. Yield: 75-90%. Three equivalents of terephthaldicarboxaldehyde was used for the synthesis of 4-hydroxy-N-(4'-formylbenzylidene)aniline. Three equivalents of phenylenediamine was used for the synthesis of 4-amino-N-(4'-cyanobenzylidene)aniline for condensation with 4-cyano benzaldehyde and 4-nitro benzaldehyde respectively. Characterisation of these compounds is given below:

2.1.1.1.1 4-Hydroxy-N-(4'-cyano benzylidene)aniline (I1)

Structure

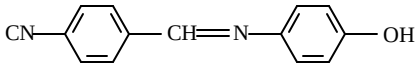

Formula	$C_{14}H_{10}N_2O$
Melting Point	170^{o} C
UV (l_{max})	391 nm
IR (cm^{-1})	3000 (CH_2), 2230 (CN), 1675 (CH=N), 1510 (C=C)
^{1}H NMR (d)	8.7 (s, 1H), 8.1 (d, 2H), 7.9 (d, 2H), 7.3 (d, 2H), 6.9 (d, 2H)
Mass	M^+ 222 (90%), 129 (10%), 120 (65%), 93 (55%)

2.1.1.1.2 4-Hydroxy-N-(4'-nitro benzylidene)aniline (I2)

Structure

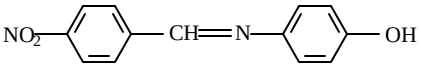

Formula	$C_{13}H_{10}N_2O_3$
Melting Point	165^{o} C
UV (l_{max})	333 nm
IR (cm^{-1})	3000 (CH_2), 1675 (CH=N), 1510 (C=C), 1340 (NO_2)
^{1}H NMR (d)	8.8 (s, 1H), 8.4 (d, 2H), 8.2 (d, 2H), 7.3 (d, 2H), 6.9 (d, 2H)

Mass M^+ 242 (80%), 149 (15%), 120 (60%), 93 (60%)

2.1.1.1.3 4-Hydroxy-N-(4'-formyl benzylidene)aniline (I3)

Structure

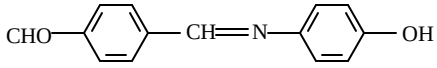

Formula $C_{14}H_{11}NO_2$

UV (l_{max}) 391 nm

IR (cm^{-1}) 3000 (CH_2), 1690 (CHO), 1675 (CH=N), 1510 (C=C)

^{1}H NMR (d) 10.1 (s, 1H), 8.6 (s, 1H), 8.2 (d, 2H), 8.0 (d, 2H), 7.2 (d, 2H), 6.8 (d, 2H)

Mass M^+ 225 (100%), 196 (10%), 132 (5%), 120 (30%), 105 (5%), 93 (10%)

2.1.1.1.4 4-Nitro-N-(4'-hydroxy benzylidene)aniline (I4)

Structure

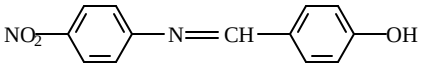

Formula $C_{13}H_{10}N_2O_3$

Melting Point 89^o C

UV (l_{max}) 335 nm

IR (cm^{-1}) 3000 (CH_2), 1675 (CH=N), 1510 (C=C), 1340 (NO_2)

^{1}H NMR (d) 8.7 (s, 1H), 8.4 (d, 2H), 8.1 (d, 2H), 7.4 (d, 2H), 6.8 (d, 2H)

Mass M^+ 242 (55%), 149 (5%), 136 (10%), 93 (25%), 77 (25%)

2.1.1.1.5 4-Amino-N-(4'-nitro benzylidene)aniline (I5)

Structure

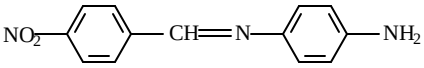

Formula $C_{13}H_{11}N_3O_2$

UV (l_{max}) 277 nm

IR (cm^{-1}) 1675 (CH=N), 1510 (C=C), 1340 (NO_2)

^{1}H NMR (d) 8.8 (s, 1H), 8.5 (d, 2H), 8.2 (d, 2H), 7.3 (d, 2H), 6.7 (d, 2H)

Mass M^+ 330 (85%), 135 (20%), 120 (65%), 101 (90%)

2.1.1.1.6 4-Amino-N-(4'-cyano benzylidene)aniline (I6)

Structure

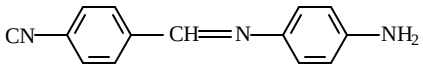

Formula $C_{14}H_{11}N_3$

UV (l_{max}) 267 nm

IR (cm^{-1}) 2230 (CN), 1675 (CH=N), 1510 (C=C)

^{1}H NMR (d) 8.6 (s, 1H), 8.0 (d, 2H), 7.8 (d, 2H), 7.2 (d, 2H), 6.8 (d, 2H)

Mass M^+ 310 (72%), 120 (50%), 115 (30%), 101 (95%)

2.2 Azomethines with spacer

The spacer was attached to azomethines as shown in Scheme 2.2:

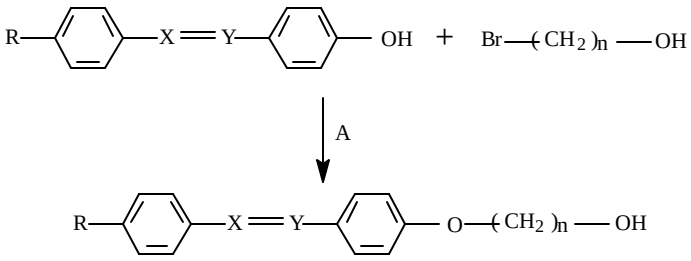

R = CN, NO_2, CHO

A = K_2CO_3, dry dimethylformamide, 80^o C

X=Y: CH=N or N=CH

n = 2 and 6

Scheme 2.2: Alkylation of azomethine

2.2.1 General procedure for alkylation

2-Bromo ethan-1-ol and 6-chloro hexan-1-ol were obtained from Aldrich Chemical Co., U.S.A. and used as received. Potassium carbonate was dried by usual procedure. Dimethylformamide obtained from S.D. Fine Chemicals, Mumbai was dried using standard method.

4-Hydroxy-N-(4'-cyano benzylidene)aniline (5.0 g, 0.026 mol), anhydrous potassium carbonate (10.8 g, 0.078 mol) and 2-bromo ethan-1-ol (4.2 g, 0.039 mol) were dissolved in 25 mL of dry dimethylformamide under nitrogen. The reaction mixture was heated in a oil bath at 80^{o} C for 16 hours under nitrogen and the reaction was monitored by thin layer chromatography (TLC). The resulting solution was cooled to room temperature, diluted with 100 mL of water, stirred and filtered. The precipitate obtained was washed with 100 mL of water. The crude product was recrystallised from ethanol. Yield: 71%. The characterisation of the products synthesised are summarised below:

2.2.1.1 4-(2-Hydroxyethyloxy)-N-(4'-cyano benzylidene)aniline (I7)

Structure

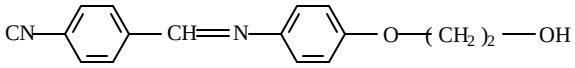

Formula $C_{16}H_{14}N_2O_2$

Melting Point 116^{o} C

UV (λ_{max}) 391 nm

IR (cm^{-1}) 3000 (CH_2), 2230 (CN), 1675 (CH=N), 1510 (C=C), 1260 (O-CH_2)

^{1}H NMR (d) 8.6 (s, 1H), 8.1 (d, 2H), 7.7 (d, 2H), 7.4 (d, 2H), 7.0 (d, 2H), 4.2 (t, 2H), 4.0 (t, 2H)

Mass M^+ 266 (67%), 221 (91%), 128 (15%), 120 (50%), 93 (30%)

2.2.1.2 4-(2-Hydroxyethyloxy)-N-(4'-nitro benzylidene)aniline (I8)

Structure

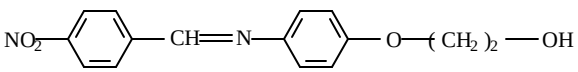

Formula $C_{15}H_{14}N_2O_4$

Melting Point 120^{o} C

UV (λ_{max}) 375 nm

IR (cm^{-1}) 3000 (CH_2), 1675 (CH=N), 1510 (C=C), 1340 (NO_2), 1260 (O-CH_2)

^{1}H NMR (d) 8.8 (s, 1H), 8.4 (d, 2H), 8.2 (d, 2H), 7.4 (d, 2H), 7.0 (d, 2H), 4.1 (t, 2H), 3.9 (t, 2H)

Mass M^+ 286 (100%), 241 (90%), 149 (10%), 120 (15%)

2.2.1.3 4-(2-Hydroxyethyloxy)-N-(4'-formyl benzylidene)aniline (I9)

Structure

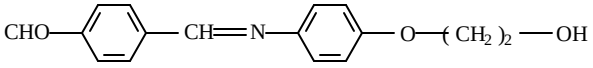

Formula $C_{16}H_{15}NO_3$

UV (λ_{max}) 390 nm

IR (cm^{-1}) 3000 (CH_2), 2230 (CN), 1690 (CHO), 1675 (CH=N), 1510 (C=C), 1260 (O-CH_2)

^{1}H NMR (d) 10.0 (s, 1H), 8.5 (s, 1H), 7.9-7.7 (m, 4H), 7.2 (d, 2H), 6.8 (d, 2H), 4.1 (t, 2H), 3.9 (t, 2H).

Mass M^+ 269 (50%), 224 (85%), 196 (10%), 119 (25%), 93 (10%)

2.2.1.4 4-Nitro-N-[4'-(2-hydroxyethyloxy) benzylidene]aniline (I10)

Structure

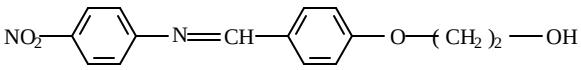

Formula $C_{15}H_{14}N_2O_4$

UV (λ_{max}) 337 nm

IR (cm^{-1}) 3000 (CH_2), 1675 (CH=N), 1510 (C=C), 1340 (NO_2), 1260 (O-CH_2)

^{1}H NMR (d) 8.6 (s, 1H), 7.7 (d, 2H), 7.6 (d, 2H), 6.9 (d, 2H), 6.5 (d, 2H), 4.0 (t, 2H), 3.8 (t, 2H)

Mass M^+ 286 (91%), 241 (85%), 148 (5%), 76 (30%)

2.2.1.5 **4-(6-Hydroxyhex-1-yloxy)-N-(4'-nitro benzylidene)aniline (I11)**

Structure

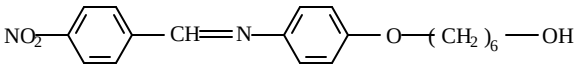

Formula $C_{19}H_{22}N_2O_4$

UV (λ_{max}) 333 nm

IR (cm^{-1}) 3000 (CH_2), 1675 (CH=N), 1510 (C=C), 1340 (NO_2), 1260 (O-CH_2)

^{1}H NMR (d) 8.6 (s, 1H), 8.4 (d, 2H), 8.2 (d, 2H), 7.4 (d, 2H), 7.0 (d, 2H), 4.0 (t, 2H), 3.8 (t, 2H), 1.6 (m, 8H)

Mass M^+ 241 (75%), 135 (20%), 119 (50%), 106 (25%),

2.2.1.6 **4-(6-Hydroxyhex-1yloxy)-N-(4'-cyano benzylidene)aniline (I12)**

Structure

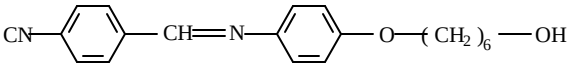

Formula $C_{20}H_{22}N_2O_2$

Melting Point 97^o C

UV (λ_{max}) 391 nm

IR (cm^{-1}) 3000 (CH_2), 2230 (CN), 1675 (CH=N), 1510 (C=C), 1260 (O-CH_2)

^{1}H NMR (d) 8.5 (s, 1H), 7.9 (d, 2H), 7.7 (d, 2H), 7.3 (d, 2H), 6.9 (d, 2H), 4.1 (t, 2H), 3.8 (t, 2H), 1.6 (m, 8H)

Mass M^+ 221 (65%), 119 (50%), 115 (20%), 106 (30%)

2.3 4-(2-Methacryloyloxyethyloxy)-N-(4'-formyl/methinebarbiturate benzylidene) aniline

Because of their excellent optical properties, a variety of polymethacrylates with pendant NLO-chromophores have been prepared by different research groups. All methacrylate monomers were synthesised by the esterification of alkylated chromophore with methacryloyl chloride. The monomers were synthesised as shown in Scheme 2.3:

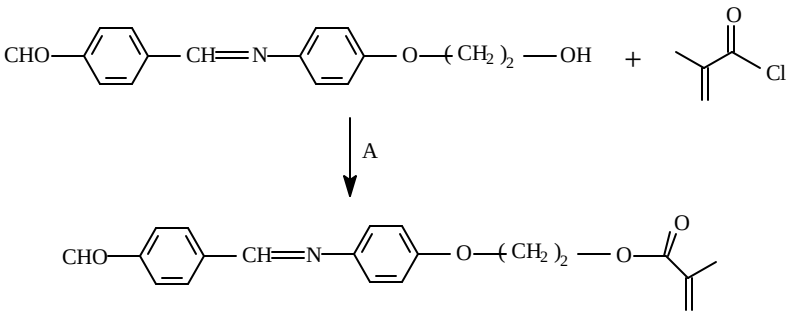

A = Et_3N, dichloromethane (dry), room temperature, stir

Scheme 2.3: Synthesis of 4-(2-methacryloyloxy ethyloxy)-N-(4'-formyl benzylidene) aniline

2.3.1 Preparation of methacryloyl chloride

Methacrylic acid and hydroquinone were obtained from Aldrich Chemical Co., U.S.A. and used as received. Thionyl chloride was obtained from S.D. Fine Chemicals, Mumbai and distilled before use.

In a 100 mL round bottom flask, 24 mL of methacrylic acid (0.3 mol), 3.0 g of hydroquinone, and few drops of dimethylformamide were placed. To this 23 mL of thionyl chloride (0.32 mol) was added drop-wise over 1 hour at room temperature. The reaction mixture was heated at 60^o C for 6 hours. This was then allowed to cool and left overnight at room temperature. Hydroquinone (1.0 g) was added to reaction mixture and acid chloride was distilled off. Yield: 72%.

2.3.2 Synthesis of 4-(2-methacryloyloxy ethyloxy)-N-(4'-formyl benzylidene) aniline

Triethyl amine was obtained from S.D. Fine Chemicals, Mumbai. This was kept in potassium hydroxide overnight and distilled under vacuum. Chloroform (analytical reagent grade) obtained from S.D. Fine Chemicals was purified by shaking sequentially with portions of concentrated sulphuric acid, water, 5% sodium bicarbonate solution and water, dried in anhydrous sodium sulphate and distilled under nitrogen atmosphere.

4-(2-Hydroxyethyloxy)-N-(4'-formyl benzylidene)aniline 1.0 g (0.004 mol) was dissolved in dry chloroform (25 mL) and 0.25 mL of triethyl amine was added and stirred under nitrogen for 30 minutes. Methacryloyl chloride 1.04 g (2.5 mole equivalents) was then added and stirred for three hours at room temperature and then the reaction was

monitored by thin layer chromatography. After the reaction was complete, the reaction mixture was poured into cold water, extracted with chloroform, washed with dilute hydrochloric acid, several times with water, brine and dried over anhydrous sodium sulphate. The solvent was evaporated under reduced pressure and the crude product was purified by column chromatography (4% acetone-petroleum ether combination was used). The characterisation of monomers is given below.

2.3.2.1 4-(2-Methacryloyloxyethyloxy)-N-(4'-formyl benzylidene)aniline (M1)

Structure

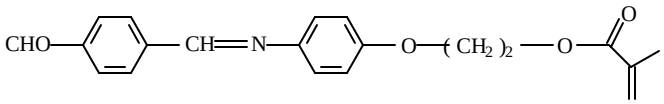

Formula $C_{20}H_{19}NO_4$

UV (l_{max}) 346 nm

IR (cm^{-1}) 3000 (CH_2), 1710 (C=0), 1690 (CHO), 1675 (CH=N), 1510 (C=C)

^{1}H NMR (d) 10.1 (s, 1H), 8.2-7.8 (m, 7H), 7.5 (d, 2H), 6.1 (s, 1H), 5.7 (s, 1H), 4.2 (t, 2H), 4.0 (t, 2H), 2.0 (s, 3H)

Mass M^+ 337 (15%), 308 (25%), 268 (90%), 253 (5%), 224 (20%), 105 (10%)

2.3.3 Synthesis of 4-(2-methacryloyloxyethyloxy)-N-(4'-methinebarbiturate benzylidene)aniline

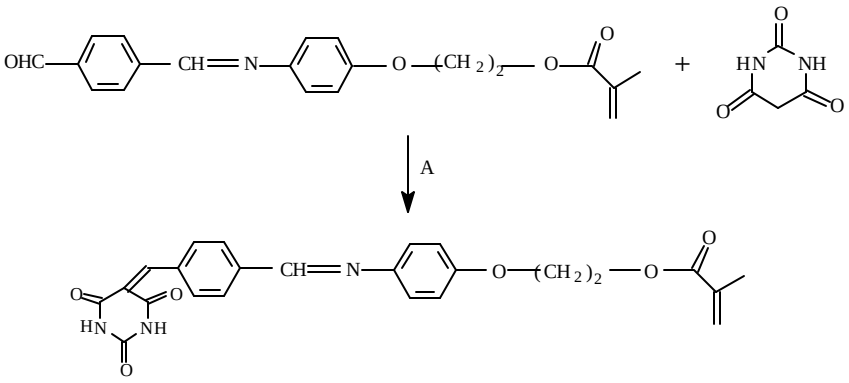

A = ethanol, ambient temperature, stir

Scheme 2.4: Coupling of 4-(2-methacryloyloxyethyloxy)-N-(4'-formyl benzylidene)aniline with barbituric acid

4-(2-Methacryloyloxy ethyloxy)-N-(4'-formyl benzylidene)aniline 1.0 g (0.003 mol) was taken in dry ethanol. To this reaction mixture was added 0.46 g (0.0035 mol) of

barbituric acid and was allowed to stir at room temperature for 3 hours. Product precipitating out was filtered, washed with ethanol and dried. Yield: 40%. Characterisation is given below.

2.3.3.1 4-(2-Methacryloyloxy ethyloxy)-N-(4'-methinebarbiturate benzylidene)aniline (M2)

Structure

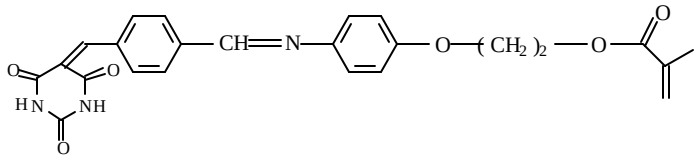

Formula $C_{24}H_{21}N_3O_6$

UV (l_{max}) 346 nm

IR (cm^{-1}) 3350, 3500 (-NH-), 1725 (-NH-C=O), 1675 (CH=N), 1510 (C=C), 1260 (O-CH_2)

^{1}H NMR (d) 11.2 (s, 1H), 11.1 (s, 1H), 8.4 (s, 1H), 8.2-7.8 (m, 7H), 7.0 (d, 2H), 6.1 (s, 1H), 5.6 (s, 1H), 4.4 (t, 2H), 4.2 (t, 2H), 1.9 (s, 1H)

Mass M^+ 447 (10%), 378 (80%), 318 (20%), 129 (10%), 69 (5%)

2.4 4-(2-Acryloyloxy ethyloxy)-N-(4'-formyl/methinebarbiturate benzylidene) aniline

All monomers were synthesised by a procedure involving the esterification of alcohol with acryloyl chloride. The acrylate monomer was synthesised as shown in Scheme 2.5:

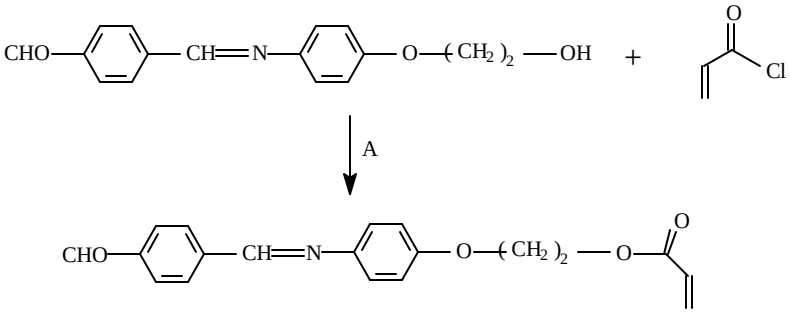

A = ethanol, ambient temperature, stir

Scheme 2.5: Synthesis of 4-(2-acryloyloxy ethyloxy)-N-(4'-formyl benzylidene) aniline

2.4.1 Preparation of acryloyl chloride

Acrylic acid and hydroquinone were obtained from Aldrich Chemical Co., U.S.A. and used as received. Thionyl chloride was obtained from S.D. Fine Chemicals, Mumbai and distilled before use.

In a 100 mL round bottom flask, 24 mL of acrylic acid (0.3 mol), 3.0 g of hydroquinone, and few drops of dimethylformamide were placed. To this 23 mL of thionyl chloride (0.32 mol) was added drop-wise over 1 hour at room temperature. The reaction mixture was heated at 60^{o} C for 6 hours. This was then allowed to cool and left overnight at room temperature. Hydroquinone (1 g) was added to reaction mixture and acid chloride was distilled off. Yield: 63%.

2.4.2 Synthesis of 4-(2-acryloyloxy ethyloxy)-N-(4'-formyl benzylidene) aniline

Triethyl amine was obtained from S.D. Fine Chemicals, Mumbai, India. This was kept in potassium hydroxide overnight and distilled under vacuum. Analytical reagent grade chloroform, obtained from S.D. Fine Chemicals was purified by reported procedure.

The 4-(2-hydroxyethyloxy)-N-(4'-formyl benzylidene)aniline, 1.0 g (0.004 mol) was dissolved in dry chloroform (25 mL) and 0.25 mL of triethyl amine were added to a reaction vessel and stirred under nitrogen for 30 minutes. Acryloyl chloride 0.86 g (2.5 equivalents) was then added and stirred for 3 hours at room temperature. The reaction was monitored by thin layer chromatography. After reaction was complete the reaction mixture was poured into cold water, extracted with chloroform, washed with dilute hydrochloric acid, several times with water, brine and dried over anhydrous sodium sulphate. The solvent was evaporated under reduced pressure and the crude product was purified by column chromatography (4% acetone in petroleum ether combination was used). Monomer characterisation is given below. Yield: 60%.

2.4.2.1 4-(2-Acryloyloxyethyloxy)-N-(4'-formyl benzylidene)aniline (M3)

Structure

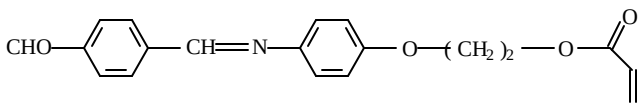

Formula $C_{19}H_{17}NO_4$

UV (l_{max}) 346 nm

IR (cm^{-1}) 3000 (CH_2), 1710 (C=O), 1690 (CHO), 1675 (CH=N), 1510 (C=C)

^{1}H NMR (d) 10.1 (s, 1H), 8.1 (s, 1H), 7.5 (m, 6H), 6.9 (d, 2H), 6.3 (m, 1H), 6.2 (m, 1H), 5.7 (d, 1H), 4.5 (d, 1H), 4.1 (d, 2H)

Mass M^+ 323 (20%), 294 (10%), 268 (80%), 115 (25%), 55 (5%)

2.4.3 Synthesis of 4-(2-acryloyloxy ethyloxy)-N-(4'-methinebarbiturate benzylidene) aniline

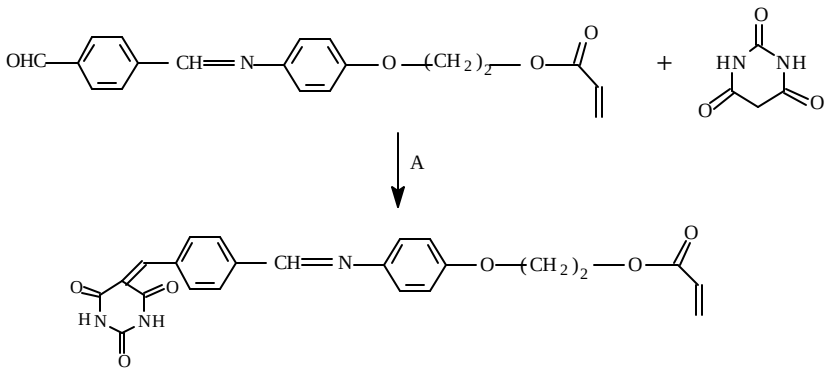

A = ethanol, ambient temperature, stir

Scheme 2.6: Coupling of 4-(2-acryloyloxyethyloxy)-N-(4'-formyl benzylidene)aniline with barbituric acid

4-(β-Acryloyloxyethyloxy)-N-(4'-formyl benzylidene)aniline 1.0 g (0.003 mol) was taken in dry ethanol and to it 0.46 g (0.0035 mol) of barbituric acid was added. The reaction mixture was stirred at room temperature for 3 hours. Product precipitated was filtered, washed with ethanol and dried. Characterisation is given below. Yield: 74%.

2.4.3.1 4-(2-Acryloyloxyethyloxy)-N-(4'-methinebarbiturate benzylidene)aniline (M4)

Structure

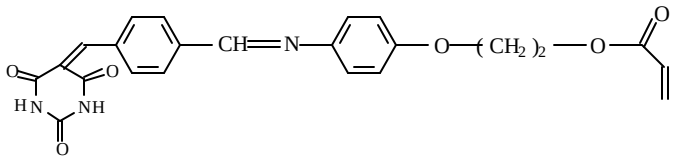

Formula $C_{23}H_{19}N_3O_6$

UV (l_{max}) 346 nm

IR (cm^{-1}) 3350, 3500 (-NH-), 1725 (-NH-C=O), 1675 (CH=N), 1510 (C=C), 1260 (O-CH_2)

^{1}H NMR (d) 11.3 (s, 1H), 11.1 (s, 1H), 8.6 (s, 1H), 8.3-7.9 (m, 9H), 7.5 (m, 1H), 7.1 (d, 1H), 6.8 (d, 1H), 4.2 (d, 2H), 4.0 (d, 2H)

Mass M^+ 433 (20%), 378 (70%), 318 (30%), 115 (20%), 55 (5%)

2.5 4-[2-(4-Vinylbenzyl oxy) ethyloxy]-N-(4'-cyano/nitro/formyl/methine barbiturate benzylidene) aniline

4-Vinylbenzyl ethers (styrenes) were prepared by the phase-transfer catalysed Williamson etherification of the corresponding alcohol with 4-chloromethylstyrene in THF at room temperature (16-18). The synthesis methodology is shown in Scheme 2.7.

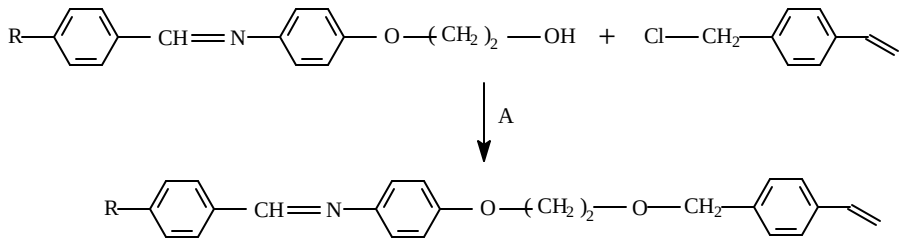

R = CN, NO_2, CHO

A = KOH, K_2CO_3, KI, TBAB, tetrahydrofuran, room temperature, stir

Scheme 2.7: Synthesis of 4-[2-(4-vinylbenzyloxy) ethyloxy]-N-(4'-cyano/nitro/formyl benzylidene) aniline

2.5.1 Synthesis of 4-[2-(4-vinylbenzyloxy) ethyloxy]-N-(4'-cyano/nitro/formyl benzylidene) aniline

4-Chloromethyl styrene was obtained from Polysciences Inc., U.S.A. Potassium hydroxide, potassium carbonate, potassium iodide, tertrabutylammonium bromide and tetrahydrofuran were obtained from S.D. Fine Chemicals, Mumbai, India.

4-(2-Hydroxy ethyloxy)-N-(4'-cyano benzylidene)aniline 1.0 g (0.0036 mol) was dissolved in tetrahydrofuran (50 mL) and 1.5 equivalents of potassium hydroxide, 1 equivalent of potassium carbonate, catalytic amount of tetrabutylammonium bromide (TBAB) and potassium iodide were added and stirred at room temperature for 1 hour. 4-Chloromethyl styrene 1.09 g (2 equivalents) was injected into the reaction mixture drop-wise over half an hour and stirred at room temperature for 48 hours. The reaction was monitored by thin layer chromatography. After the completion of reaction, the reaction mixture was filtered and tetrahydrofuran was evaporated. The residue was extracted with dichloromethane and washed with dilute hydrochloric acid, bicarbonate solution, water and brine. The dichloromethane layer was kept over anhydrous sodium sulphate and the solvent was evaporated under reduced pressure. The crude product was purified by

column chromatography (8% acetone in petroleum ether). Yield: 65%. The characterisation of purified monomers are presented below:

2.5.1.1 4-[2-(4-Vinylbenzyloxy) ethyloxy]-N-(4'-cyano benzylidene)aniline (M5)

Structure

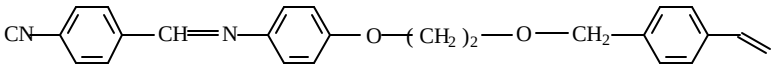

Formula $C_{25}H_{22}N_2O_2$

UV (l_{max}) 346 nm

IR (cm^{-1}) 3000 (CH_2), 2230 (CN), 1675 (CH=N), 1510 (C=C), 1260 (O-CH_2)

^{1}H NMR (d) 7.8-7.2 (m, 13H), 6.7 (q, 1H), 5.7 (d, 1H), 5.2 (d, 1H), 4.6 (s, 2H), 4.1 (t, 2H), 3.8 (t, 2H)

Mass M^+ 382 (35%), 265 (20%), 221 (25%), 129 (5%), 117 (100%), 92 (10%)

2.5.1.2 4-[2-(4-Vinylbenzyloxy) ethyloxy]-N-(4'-nitro benzylidene)aniline (M6)

Structure

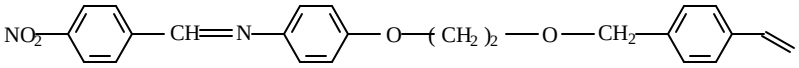

Formula $C_{24}H_{22}N_2O_4$

UV (l_{max}) 345 nm

IR (cm^{-1}) 3000 (CH_2), 1675 (CH=N), 1510 (C=C), 1340 (NO_2), 1260 (O-CH_2)

^{1}H NMR (d) 8.5 (s, 1H), 7.8-7.4 (m, 13H), 6.8 (q, 1H), 5.7 (d, 1H), 5.2 (d, 1H), 4.6 (s, 2H), 4.1 (t, 2H), 3.8 (t, 2H)

Mass M^+ 402 (20%), 358 (15%), 285 (30%), 117 (95%), 92 (10%)

2.5.1.3 4-[2-(4-Vinylbenzyloxy) ethyloxy]-N-(4'-formyl benzylidene)aniline (M7)

Structure

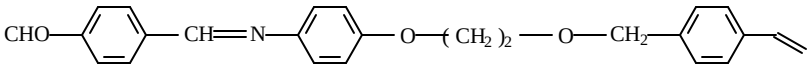

Formula $C_{25}H_{23}NO_3$

UV (l_{max}) 346 nm

IR (cm^{-1}) 3000 (CH_2), 1690 (CHO), 1675 (CH=N), 1510 (C=C), 1260 (O-CH_2)

^{1}H NMR (d) 10.1 (s, 1H), 8.0-6.9 (m, 13H), 5.7 (d, 1H), 5.2 (d, 1H), 4.6 (s, 2H), 3.9 (t, 2H)

Mass M^+ 385 (35%), 356 (5%), 341 (10%), 268 (25%), 117 (100%),

2.5.2 Synthesis of 4-[2-(4-vinylbenzyloxy)ethyloxy]-N-(4'-methinebarbiturate benzylidene)aniline

Barbituric acid was coupled to the styrene monomer as shown in Scheme 2.8 below:

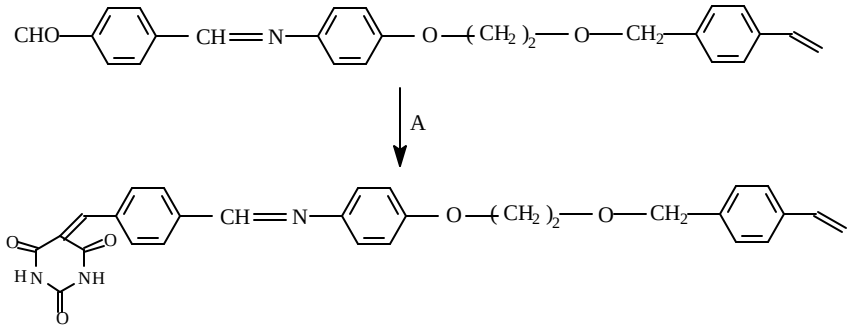

A = barbituric acid, ethanol, room temperature, stir

Scheme 2.8: Coupling of 4-[2-(4-vinylbenzyloxy) ethyloxy]-N-(4'-formyl benzylidene)aniline with barbituric acid

4-[2-(4-Vinylbenzyloxy) ethyloxy]-N-(4'-formyl benzylidene)aniline 1.0 g (0.003 mol) was taken in dry ethanol and to it 0.46 g (0.0035 mol) of barbituric acid was added. The reaction mixture was stirred at room temperature for 3 hours. Product precipitated was filtered, washed with ethanol and dried. Yield: 75%. The characterisation is presented below:

2.5.2.1 4-[2-(4-Vinylbenzyloxy)ethyloxy]-N-(4'-methinebarbiturate benzylidene)aniline (M8)

Structure

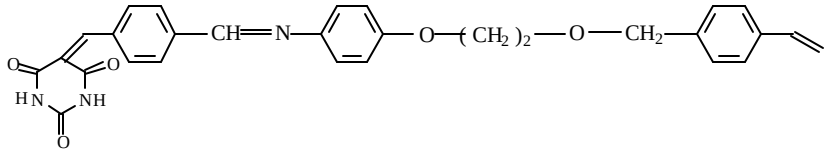

Formula $C_{29}H_{25}N_3O_5$

UV (λ_{max}) 300 nm

IR (cm^{-1}) 3350, 3500 (-NH-), 1725 (NH-C=O), 1675 (CH=N), 1640, 1610 (C=C)

^{1}H NMR (d)	11.3 (s, 1H), 11.1 (s, 1H), 8.1-7.0 (m, 13H), 5.7 (d, 1H), 5.1 (d, 1H), 4.5 (s, 2H), 4.1 (t, 2H), 3.8 (t, 2H)
Mass	M^+ 495 (20%), 378 (40%), 334 (20%), 126 (5%), 117 (80%)

2.6 4-[2/6-(N-Maleimido)eth-1-yloxy/hex-1-yloxy)-N-(4'-cyano/nitro benzylidene)] aniline

The maleimide monomers are synthesised by a procedure involving the Mitsunobu reaction between the alkylated chromophore and maleimide. The Mitsunobu reaction between the maleimide and the alkylated chromophore results in intermolecular dehydration on treatment with triphenyl phosphine (Ph_3P) and diethylazodicarboxylate (DEAD) (19). In order to minimise the formation of ylide adduct between Ph_3P and maleimide (Michael addition on maleimide double bond) the following experimental procedure given below in Section 2.6.1 was adopted. The maleimide monomers were synthesised as shown in Scheme 2.9 below:

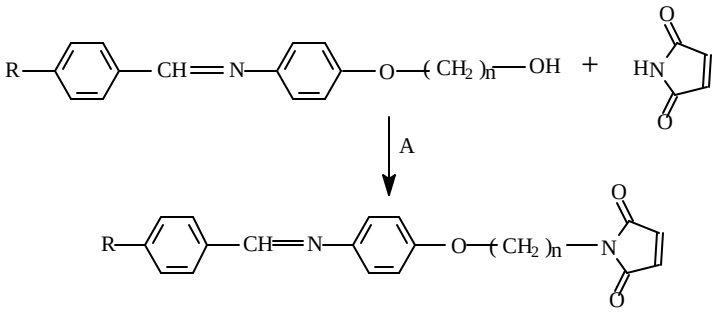

A = PPh_3, DEAD, tetrahydrofuran (dry), rt, stir

n = 2 and 6, R = CN / NO_2

Scheme 2.9: Synthesis of 4-[2/6-(N-maleimido)eth-1-yloxy/hex-1-yloxy)-N-(4'-cyano/nitro benzylidene)] aniline

2.6.1 Synthesis of 4-[2/6-(N-maleimido) eth-1-yloxy/ hex-1-yloxy)-N-(4'-cyano/ nitro benzylidene)]aniline

Maleimide, triphenyl phosphine and diethylazodicarboxylate (DEAD) were obtained from Aldrich Chemical Co., U.S.A. Tetrahydrofuran was obtained from S.D. Fine Chemicals, Mumbai and was dried according to standard procedure.

4-(2-Hydroxy ethyloxy)-N-(4'-cyano benzylidene)aniline 1.0 g (0.0035 mol), maleimide (1.1 molar equivalent) and triphenyl phosphine (1.1 molar equivalent) were

powdered and dried under vacuum to remove even slight traces of moisture. To this mixture, anhydrous tetrahydrofuran (5 mL) was added drop-wise under nitrogen atmosphere and at 0-5^{o} C. This was stirred for 20 minutes and then diethylazodicarboxylate (1.1 equivalents) was added drop-wise. The reaction mixture was slowly brought to room temperature and stirred for 56 hours. The reaction was monitored by thin layer chromatography. After the reaction was complete, the reaction mixture was quenched by the addition of 50 mL of brine. The layers were separated and the aqueous layer was washed 3 times with 25 mL portions of chloroform and the combined organic fraction was washed with water, bicarbonate and brine. The organic fractions were collected together, dried in anhydrous sodium sulphate and concentrated under vacuum. The crude product was purified by column chromatography (15% acetone in petroleum ether) followed by recrystallisation in ethanol. Yield: 82%. Characterisation of monomers is presented below:

2.6.1.1 4-[2-(N-Maleimido)eth-1-yloxy)-N-(4'-cyano benzylidene)]aniline (M9)

Structure

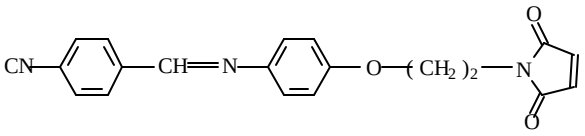

Formula $C_{20}H_{15}N_3O_3$

Melting Point 124^{o} C

UV (l_{max}) 349 nm

IR (cm^{-1}) 2960, 2850 (CH_2), 2230 (CN), 1740 (C=O), 1675 (CH=N), 1615 (C=C)

^{1}H NMR (d) 8.5 (s, 1H), 7.9 (d, 2H), 7.7 (d, 2H), 7.3 (d, 2H), 6.9 (d, 2H), 6.7 (s, 2H), 4.2 (t, 2H), 3.9 (t, 2H)

Mass M^+ 345 (20%), 221 (30%), 195 (15%), 124 (90%)

2.6.1.2 4-[2-(N-Maleimido)eth-1-yloxy)-N-(4-nitro benzylidene)]aniline (M10)

Structure

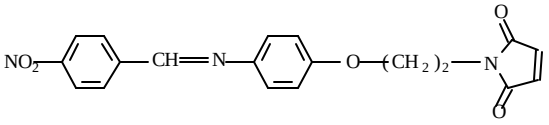

Formula $C_{19}H_{15}N_3O_5$

Melting Point 140^{o} C

UV (l_{max}) 366 nm

IR (cm^{-1}) 2960, 2850 (CH_2), 1740 (C=O), 1675 (CH=N), 1615 (C=C), 1340 (NO_2)

^{1}H NMR (d) 8.6 (s, 1H), 8.3 (d, 2H), 8.1 (d, 2H), 7.3 (d, 2H), 6.9 (d, 2H), 6.7 (s, 2H), 4.2 (t, 2H), 3.9 (t, 2H)

Mass M^+ 365 (20%), 241 (20%), 213 (5%), 195 (20%), 124 (100%)

2.6.1.3 4-[6-(N-Maleimido)hex-1-yloxy)-N-(4-cyano benzylidene)]aniline (M11)

Structure

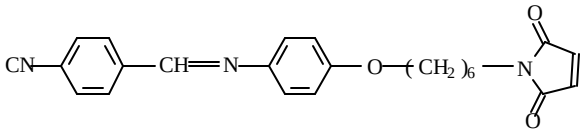

Formula $C_{24}H_{23}N_3O_3$

Melting Point 94^{o} C

UV (l_{max}) 332 nm

IR (cm^{-1}) 2960, 2850 (CH_2), 2230 (CN), 1740 (C=O), 1675 (CH=N), 1615 (C=C)

^{1}H NMR (d) 8.5 (s, 1H), 7.9 (d, 2H), 7.7 (d, 2H), 7.3 (d, 2H), 6.9 (d, 2H), 6.7 (s, 2H), 4.2 (t, 2H), 3.9 (t, 2H), 1.6 (m, 8H)

Mass M^+ 399 (30%), 303 (10%), 219 (95%), 203 (5%), 96 (20%)

2.6.1.4 4-[6-(N-Maleimido)hex-1-yloxy)-N-(4'-nitro benzylidene)]aniline (M12)

Structure

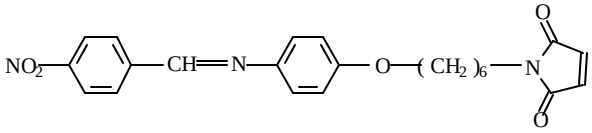

Formula $C_{23}H_{23}N_3O_5$

UV (l_{max}) 336 nm

IR (cm^{-1}) 2960, 2850 (CH_2), 1740 (C=O), 1675 (CH=N), 1615 (C=C), 1340 (NO_2)

^{1}H NMR (d) 8.5 (s, 1H), 8.3 (d, 2H), 8.0 (d, 2H), 7.3 (d, 2H), 6.9 (d, 2H), 6.7 (s, 2H), 4.1 (t, 2H), 3.9 (t, 2H), 1.6 (m, 8H)

Mass M^+ 419 (25%), 239 (80%), 223 (10%), 96 (25%)

2.7 Azobenzenes

2.7.1 General synthesis of substituted azobenzene

The best known method of preparing aromatic azo compounds involves the coupling of diazonium salts with sufficiently reactive compounds such as phenols, aromatic amines, phenyl ethers, related naphthalene compounds and even sufficiently reactive aromatic hydrocarbons (20). Generally, the coupling must be carried out in neutral or slightly basic media or that are buffered in the appropriate pH range. The general reaction of diazotisation is given below. The coupling reaction requires deprotonation of the corresponding phenol or naphthol derivative, so that a base must be added during development.

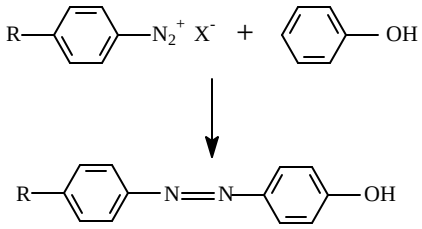

Scheme 2.10: Diazotisation methodology

2.7.2 Diazotisation with phenol

4-Amino benzaldehyde was procured from Fluka and recrystallised according to established standard procedures. Phenol, sodium hydroxide, sodium nitrite and concentrated hydrochloric acid were obtained from S.D. Fine Chemicals, Mumbai, India.

4-Amino benzaldehyde 5.0 g (0.041 mol) was dissolved in a warm mixture of 13 mL concentrated hydrochloric acid in a 250 mL beaker. The beaker was placed in an ice-salt bath and cooled to 0-5^o C with vigorous stirring. To this, 4.2 g (0.062 mol) sodium nitrite in minimum amount of cold water was added slowly with stirring. The end-point was noted with potassium iodide-starch paper. The temperature of the solution was kept below 8^o C throughout the addition. Phenol 3.8 g (0.041 mol) was dissolved in a solution of 8.2 g (0.205 mol) sodium hydroxide in 25 mL water and cooled in ice. The diazotised solution was slowly added to this alkaline phenolic solution with stirring. The bright

orange solid obtained was filtered with gentle suction, dried on a filter paper in air. Yield: 50%.

2.7.2.1 4'-Formyl-4-hydroxy azobenzene (I13)

Structure

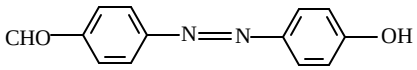

Formula	$C_{13}H_{10}N_2O_2$
Melting Point	70^oC
UV (l_{max})	361 nm
IR (cm^{-1})	1695 (C=O), 1590 (N=N), 1510 (C=C)
^1H NMR (d)	10.1 (s, 1H), 7.5-7.9 (m, 6H), 6.7 (d, 2H)
Mass	M^+ 226 (25%), 197 (100%), 91 (100%)

2.8 Azo compounds with spacer

The spacer was attached to the azo phenols as shown in Scheme 2.11 below:

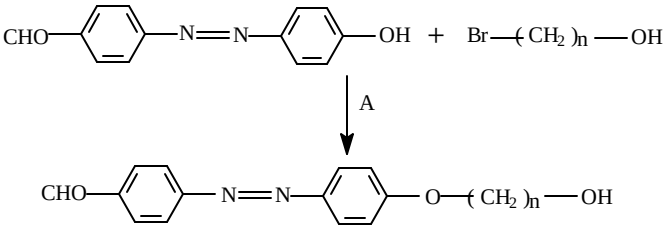

A = K_2CO_3, acetonitrile, reflux

n = 2 or 3

Scheme 2.11: Alkylation of azo phenol

2.8.1 General procedure for alkylation

2-Bromoethan-1-ol and 3-bromopropan-1-ol were obtained from Aldrich Chemical Co. and used as received. Potassium carbonate was dried by usual procedure. Acetonitrile was obtained from S.D. Fine Chemicals, Mumbai and was dried using standard method.

4'-Formyl-4-hydroxy azobenzene 2.0 g (0.009 mol) was dissolved in dry acetonitrile (30 mL). To this solution, anhydrous potassium carbonate (7 equivalents) and a catalytic amount of tetrabutylammonium bromide were added and stirred for one hour. Then 2-bromo ethan-1-ol (1.7 g, 1.5 equivalents) was taken in acetonitrile and injected to this slowly over half an hour. This was refluxed for 8 hours and the reaction was monitored by thin layer chromatography (TLC). After the reaction was complete, acetonitrile was distilled off under vacuum and the residue was mixed with chloroform and poured into cold water. This was washed several times with dilute hydrochloric acid, sodium bicarbonate and brine solutions. The organic layer was separated and dried in anhydrous sodium sulphate and concentrated. The crude product was purified by column chromatography. 15% Acetone in petroleum ether was used to elute the pure product. Yield: 82%.

2.8.1.1 4-(2-Hydroxy ethyloxy)-4'-formyl azobenzene (I14)

Structure

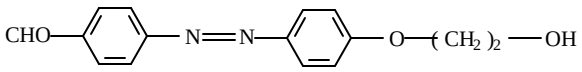

Formula	$C_{15}H_{14}N_2O_3$
Melting Point	129° C
UV (λ_{max})	365 nm
IR (cm^{-1})	3300 (OH), 1680 (C=0), 1590 (N=N), 1510 (C=C)
^{1}H NMR (d)	10.1 (s, 1H), 8.2-7.8 (m, 6H), 7.1 (d, 2H), 4.2 (t, 2H), 4.0 (t, 2H)
Mass	M^+ 270 (30%), 241 (65%), 137 (20%), 133 (15%)

2.9 4-(2-Methacryloyloxy ethyloxy)-4'-formyl/methinebarbiturate azobenzene

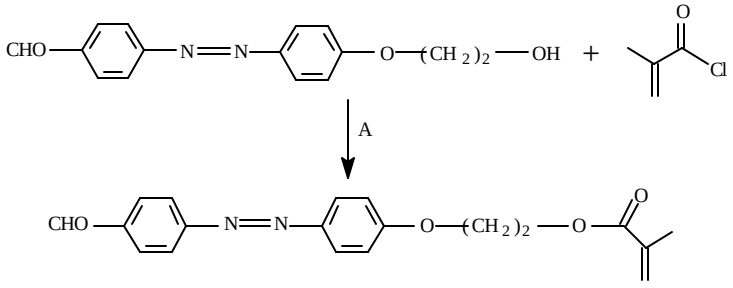

A = Et_3N, chloroform (dry), room temperature, stir

Scheme 2.12: Synthesis of 4-(2-methacryloyloxyethyloxy)-4'-formyl azobenzene

2.9.1 Synthesis of 4-(2-methacryloyloxy ethyloxy)-4'-formyl azobenzene

Triethyl amine was obtained from S.D. Fine Chemicals, Mumbai, India. This was kept in potassium hydroxide overnight and distilled under vacuum. Chloroform (analytical reagent grade) obtained from S.D. Fine Chemicals was purified by the following procedure. Chloroform was shaken with portions of concentrated sulphuric acid, then with water, 5% sodium bicarbonate solution and then with water, dried in anhydrous sodium sulphate and distilled under nitrogen atmosphere.

4-(2-Hydroxyethyloxy)-4'-formyl azobenzene 1.0 g (0.004 mol) was dissolved in dry chloroform (25 mL) and 0.25 mL of triethyl amine was added and stirred under nitrogen for 30 minutes. Methacryloyl chloride 1.04 g (2.5 mole equivalents) was then added and stirred for three hours at room temperature and then the reaction was monitored by thin layer chromatography. After the reaction was complete, the reaction mixture was poured into cold water, extracted with chloroform, washed with dilute hydrochloric acid, several times with water, brine and dried over anhydrous sodium sulphate. The solvent was evaporated under reduced pressure and the crude product was purified by column chromatography (4% acetone-petroleum ether combination was used). Yield: 72%.

2.9.1.1 4-(2-Methacryloyloxyethyloxy)-4'-formyl azobenzene (M13)

Structure

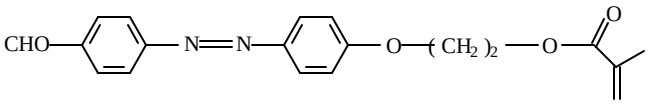

Formula	$C_{19}H_{18}N_2O_4$
UV (λ_{max})	359 nm
IR (cm^{-1})	3000 (CH_2), 1710 (C=O), 1590 (N=N), 1510 (C=C)
^{1}H NMR (d)	10.1 (s, 1H), 8.1-7.8 (m, 6H), 7.0 (d, 2H), 6.1 (s, 1H), 5.3 (s, 1H), 4.2 (t, 2H), 4.0 (t, 2H), 1.95 (s, 3H)
Mass	M^+ 338 (20%), 269 (10%), 209 (5%), 129 (100%), 69 (25%)

2.9.2 Synthesis of 4-(2-methacryloyloxyethyloxy)-4'-methinebarbiturate azobenzene

Barbituric acid was coupled to the methacrylate monomer as shown in Scheme 2.13 below:

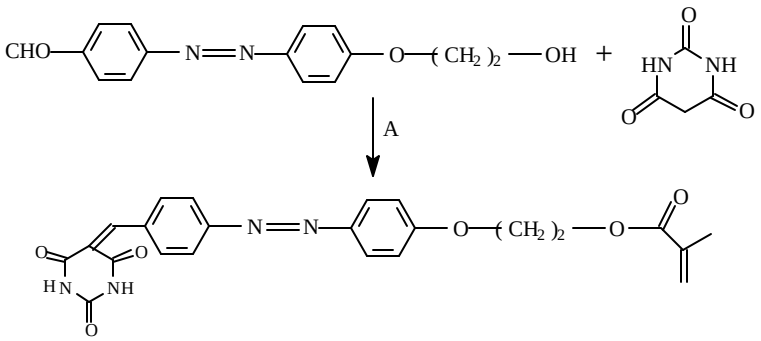

A = ethanol, room temperature, stir

Scheme 2.13: Coupling of 4-(2-methacryloyloxyethyloxy)-4'-formyl azobenzene with barbituric acid

4-(2-Methacryloyloxyethyloxy)-4'-formyl azobenzene 1.0 g (0.003 mol) was taken in dry ethanol. To this reaction mixture was added 0.46 g (0.0035 mol) of barbituric acid. The reaction mixture was stirred at room temperature for 3 hours. Product precipitated out. It was filtered, washed with ethanol and dried. Yield: 40%.

2.9.2.1 4-(2-Methacryloyloxyethyloxy)-4'-methinebarbiturate azobenzene (M14)

Structure

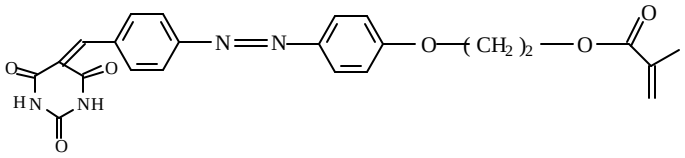

Formula $C_{23}H_{20}N_4O_6$

Melting Point 210° C

UV (l_{max}) 346 nm

IR (cm^{-1}) 3500, 3350 (-NH-), 1725 (-NH-C=O), 1710 (C=O), 1615 (C=C), 1490 (N=N)

^{1}H NMR (d) 11.5 (s, 1H), 11.3 (s, 1H), 8.4 (s, 1H), 8.3 (d, 2H), 7.9 (m, 4H), 7.1 (d, 2H), 6.1 (s, 1H), 5.6 (s, 1H), 4.1 (t, 2H), 3.9 (t, 2H)

Mass M^+ 448 (20%), 233 (5%), 215 (15%), 113 (100%), 69 (20%)

2.10 4-(2-Acryloyloxyethyloxy)-4'-formyl/methinebarbiturate azobenzene

The acrylate monomer was synthesised as shown in Scheme 2.14 below:

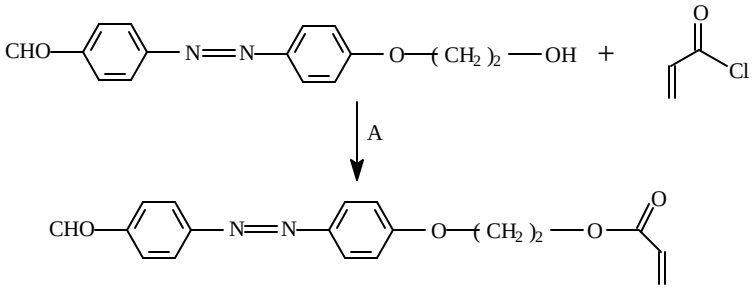

A = Et_3N, chloroform (dry), room temperature, stir

Scheme 2.14: Synthesis of 4-(2-acryloyloxyethyloxy)-4'-formyl azobenzene

2.10.1 Synthesis of 4-(2-acryloyloxyethyloxy)-4'-formyl azobenzene

Triethyl amine was obtained from S.D. Fine Chemicals, Mumbai, India. This was kept in potassium hydroxide overnight and distilled under vacuum. Analytical reagent grade chloroform, obtained from S.D. Fine Chemicals was purified by standard procedure.

4-(2-Hydroxyethyloxy)-4'-formyl azobenzene, 1.0 g (0.0038 mol) was dissolved in dry chloroform (25 mL) and 0.25 mL of triethyl amine were added to a reaction vessel and stirred under nitrogen for 30 minutes. Acryloyl chloride 0.86 g (2.5 equivalents) was then added and stirred for 3 hours at room temperature. The reaction was monitored by thin layer chromatography. After reaction was complete the reaction mixture was poured into cold water, extracted with chloroform, washed with dilute hydrochloric acid, several times with water, brine and dried over anhydrous sodium sulphate. The solvent was evaporated under reduced pressure and the crude product was purified by column chromatography (4% acetone in petroleum ether combination was used). Yield: 60%.

2.10.1.1 4-(2-Acryloyloxyethyloxy)-4'-formyl azobenzene (M15)

Structure

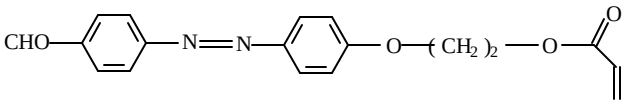

Formula $C_{18}H_{16}N_2O_4$

Melting Point 104° C

UV (l_{max}) 361 nm

IR (cm^{-1}) 2960, 2850 (CH), 1710, 1680 (C=O), 1640, 1615 (C=C), 1490 (N=N)

^{1}H NMR (d) 10.0 (s, 1H), 8.0 (m, 6H), 7.0 (d, 2H), 6.5 (d, 1H), 6.1 (dd, 1H), 5.8 (d, 1H), 4.5 (t, 2H), 4.3 (t, 2H)

Mass M^+ 324 (30%), 269 (10%), 209 (5%), 115 (100%), 55 (20%)

2.10.2 Synthesis of 4-(2-acryloyloxyethyloxy)-4'-methinebarbiturate azobenzene

Barbituric acid was coupled to the acrylate monomer as shown in Scheme 2.15 below:

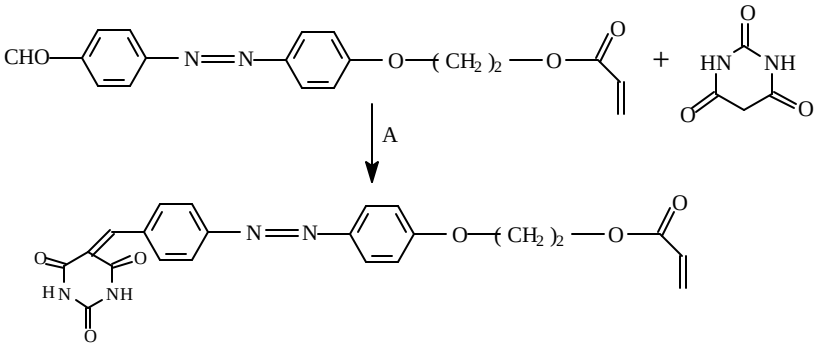

A = ethanol, room temperature, stir

Scheme 2.15: Coupling of 4-(2-acryloyloxyethyloxy)-4'-formyl azobenzene with barbituric acid

4-(2-Acryloyloxyethyloxy)-4'-formyl azobenzene 1.0 g (0.003 mol) was taken in dry ethanol and to it 0.46 g (0.0035 mol) of barbituric acid was added. The reaction mixture was stirred at room temperature for 3 hours. Product precipitated was filtered, washed with ethanol and dried. Yield: 55%.

2.10.2.1 4-(2-Acryloyloxyethyloxy)-4'-methinebarbiturate azobenzene (M16)

Structure

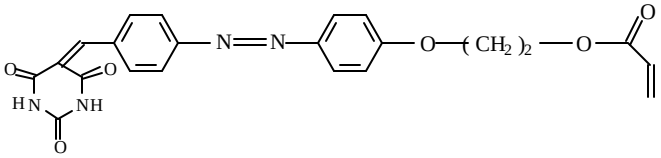

Formula $C_{22}H_{18}N_4O_6$

Melting Point 170° C

UV (l_{max})	346 nm
IR (cm^{-1})	3500-3350 (-NH-), 1725 (-NH-C=O), 1640, 1610 (C=C), 1490 (N=N)
^{1}H NMR (d)	11.5 (s, 1H), 11.3 (s, 1H), 8.4 (s, 1H), 7.9 (d, 2H), 7.8 (d, 2H), 7.3 (d, 2H), 7.1 (d, 2H), 6.5 (d, 1H), 6.2 (d, 1H), 5.9 (d, 1H), 4.4 (t, 2H), 4.2 (t, 2H)
Mass	M^+ 434 (20%), 201 (5%), 128 (100%)

2.11 4-[2-(3/4-Vinylbenzyloxy)ethyloxy]-4'-formyl/methinebarbiturate azobenzene

The styrene monomers are synthesised as shown in Scheme 2.16 below:

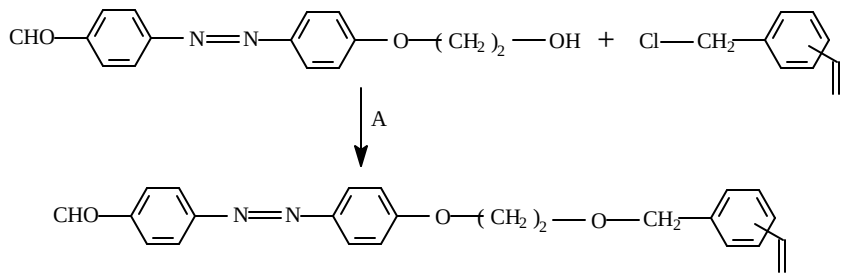

A = KOH, K_2CO_3, KI, TBAB, tetrahydrofuran, room temperature, stir

Scheme 2.16: Synthesis of 4-[2-(3/4-vinylbenzyloxy)ethyloxy]-4'-formyl azobenzene

2.11.1 Synthesis of 4-[2-(3/4-vinylbenzyloxy)ethyloxy]-4'-formyl azobenzene

Mixture of 3/4-chloromethyl styrene was obtained from Aldrich Chemical Co., U.S.A. Potassium hydroxide, potassium carbonate, potassium iodide, and tetrahydrofuran were obtained from S.D. Fine chemicals, Mumbai, India.

4-(2-Hydroxyethyloxy)-4'-formyl azobenzene 1.0 g (0.0038 mol) was dissolved in tetrahydrofuran (50 mL) and 1.5 equivalents of potassium hydroxide, 1 equivalent of potassium carbonate, catalytic amount of tetrabutylammonium bromide (TBAB) and potassium iodide were added and stirred at room temperature for 1 hour. A mixture of 3/4 chloromethyl styrene (1.5 equivalents) was injected to the reaction mixture drop-wise over half an hour and stirred at room temperature for 24 hours. The reaction was monitored by thin layer chromatography (TLC). After the completion, contents were filtered and tetrahydrofuran was evaporated. The residue was extracted with chloroform and washed with dilute hydrochloric acid, bicarbonate solution, water and brine. The

chloroform layer was kept over sodium sulphate and the solvent was evaporated under reduced pressure. The crude product was purified by column chromatography (8% acetone in petroleum ether). Yield: 61%.

2.11.1.1 4-[2-(3/4-Vinylbenzyloxy) ethyloxy]-4'-formyl azobenzene (M17)

Structure

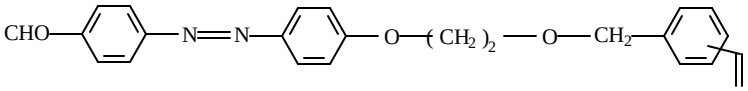

Formula $C_{24}H_{22}N_2O_3$

UV (l_{max}) 342 nm

IR (cm^{-1}) 2960, 2850 (CH_2), 1680 (C=O), 1645, 1615 (C=C), 1490 (N=N)

^{1}H NMR (d) 7.9 (m, 10H), 7.0 (d, 2H), 6.7 (q, 1H), 5.7 (d, 1H), 5.3 (d, 1H), 4.7 (s, 1H), 4.1 (t, 2H), 3.8 (t, 2H)

Mass M^+ 386 (50%), 269 (10%), 253 (60%), 209 (100%), 117 (90%)

2.11.2 Synthesis of 4-[2-(3/4-vinylbenzyloxy)ethyloxy]-4'-methinebarbiturate azobenzene

Barbituric acid was coupled to the styrene monomer as shown in Scheme 2.17 below:

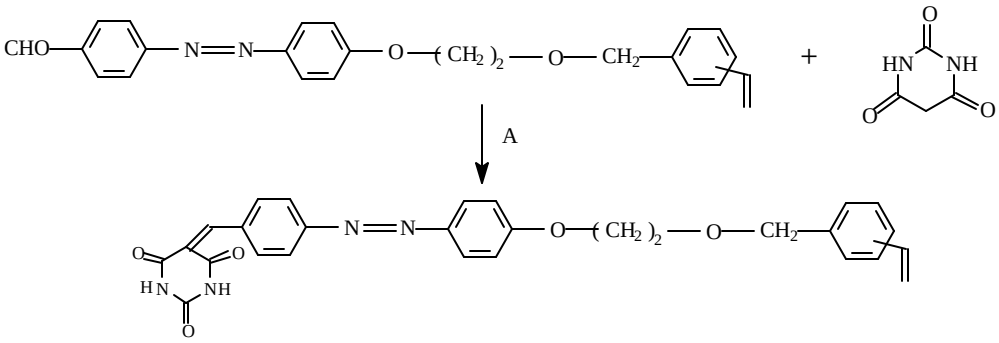

A = ethanol, room temperature, stir

Scheme 2.17: Coupling of 4-[2-(3/4-vinylbenzyloxy) ethyloxy]-4'-formyl azobenzene with barbituric acid

4-[2-(3/4-Vinylbenzyloxy) ethyloxy]-4'-formyl azobenzene 1.0 g (0.004 mol) was taken in dry ethanol and 0.614 g (0.005 mol) of barbituric acid was added. The reaction mixture was stirred at room temperature for 4 hours. Product precipitated was filtered, washed with ethanol and dried. Yield: 76%.

2.11.2.1 4-[2-(3/4-Vinylbenzyloxy)ethyloxy]-4'-methinebarbiturate azobenzene (M18)

Structure

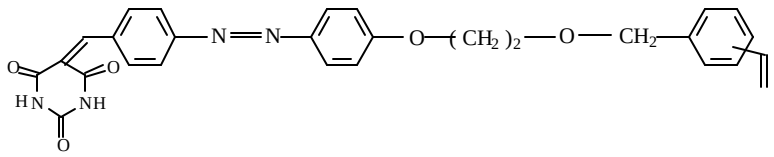

Formula $C_{28}H_{24}N_4O_5$

UV (λ_{max}) 346 nm

IR (cm^{-1}) 3350, 3500 (-NH-), 1725 (-NH-C=O), 1640, 1610 (C=C), 1490 (N=N)

^{1}H NMR (d) 11.3-11.1 (s, 2H), 8.1 (s, 1H), 7.8-6.9 (m, 12H), 6.7 (m, 1H), 5.7 (d, 1H), 5.2 (d, 1H), 4.6 (s, 2H), 4.1 (t, 2H), 3.9 (t, 2H)

Mass M^+ 386 (50%), 269 (20%), 254 (60%), 239 (5%), 149 (100%), 117 (85%)

2.12 4-[2-(N-Maleimido) ethyloxy]-4'-formyl azobenzene

The maleimide monomer was synthesised as shown in Scheme 2.18 below:

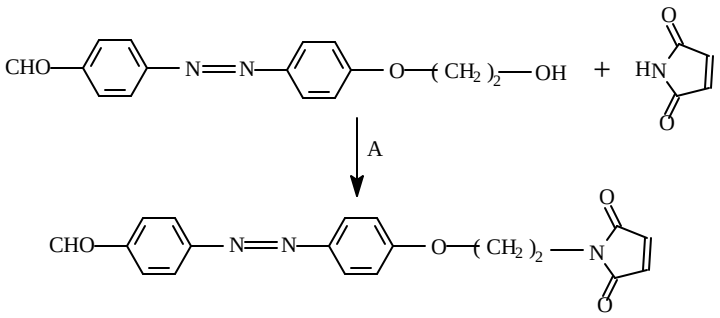

A = PPh_3, DEAD, tetrahydrofuran (dry), room temperature, stir

Scheme 2.18: Synthesis of 4-[2-(N-maleimido)ethyloxy]-4'-formyl azobenzene

2.12.1 Synthesis of 4-[2-(N-maleimido)ethyloxy]-4'-formyl azobenzene

Maleimide, triphenyl phosphine and diethylazodicarboxylate (DEAD) were obtained from Aldrich Chemical Co., U.S.A. Tetrahydrofuran was obtained from S.D. Fine Chemicals, Mumbai and dried according to standard procedure.

4-(2-Hydroxyethyloxy)-4'-formyl azobenzene 1.0 g (0.004 mol), maleimide (1.1 molar equivalent) and triphenyl phosphine (1.1 molar equivalent) were powdered and dried under vacuum to remove even slight traces of moisture. To this mixture, anhydrous

tetrahydrofuran (5 mL) was added drop-wise under nitrogen atmosphere and at 0-5^{o} C. This was stirred for 20 minutes and then diethylazodicarboxylate (1.1 equivalents) was added drop-wise. The reaction mixture was slowly brought to room temperature and stirred for 56 hours. The reaction was monitored by thin layer chromatography. After the reaction was complete, the reaction mixture was quenched by the addition of 50 mL of brine. The layers were separated and the aqueous layer was washed 3 times with 25 mL portions of chloroform and the combined organic fraction was washed with water, bicarbonate and brine. The organic fractions were collected together, dried in anhydrous sodium sulphate and concentrated under vacuum. The crude product was purified by column chromatography (15% acetone in petroleum ether) followed by recrystallisation in ethanol. Yield: 70%.

2.12.1.1 4-[2-(N-Maleimido)ethyloxy]-4'-formyl azobenzene (M19)

Structure

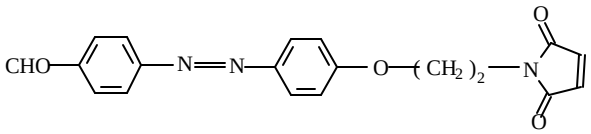

Formula $C_{19}H_{15}N_3O_4$

UV (l_{max}) 346 nm

IR (cm^{-1}) 2960, 2850 (CH_2), 1740 (C=O), 1680 (CHO), 1615 (C=C), 1490 (N=N)

^{1}H NMR (d) 10.0 (s, 1H), 7.9 (d, 2H), 7.5 (d, 2H), 7.3 (d, 2H), 7.0 (d, 2H), 6.7 (s, 2H), 4.2 (t, 2H), 3.9 (t, 2H)

Mass M^+ 349 (25%), 225 (50%), 197 (10%), 124 (100%)

2.13 Heterocycles as chromophores

The carbazole monomers were synthesised as shown in Scheme 2.19:

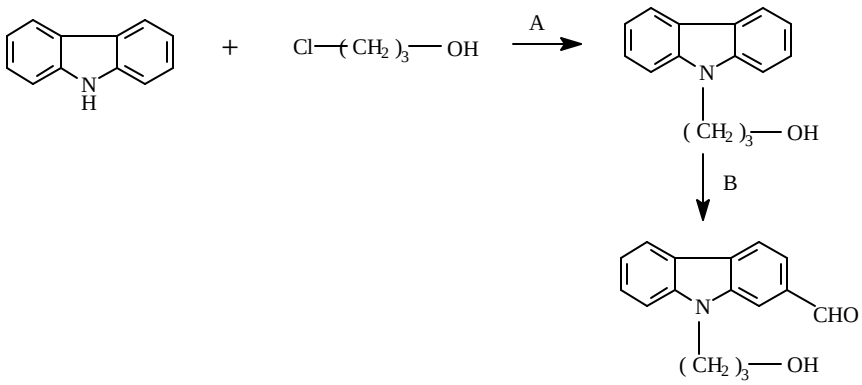

A = dimethylformamide (dry), 80° C

B = $POCl_3$, dimethylformamide, 90° C

Scheme 2.19: Alkylation followed by formylation of carbazole

2.13.1 Synthesis of N-(3-hydroxypropyl)carbazole

3-Chloro propan-1-ol, 4-amino benzonitrile, 4-nitro aniline, 3/4-chloromethyl styrene were procured from Aldrich Chemical Co., U.S.A. and were used as such. Potassium hydroxide, potassium iodide, potassium carbonate, tetrabutylammonium bromide, tetrahydrofuran, dimethylformamide, phosphorus oxychloride ($POCl_3$), ethanol, acetic acid were obtained from S. D. Fine chemicals, Mumbai, India.

Carbazole (5.0 g, 0.026 mol), anhydrous potassium carbonate (10.8 g, 0.078 mol) and 3-chloro propan-1-ol (4.2 g, 0.039 mol) were dissolved in 25 mL dry dimethylformamide under nitrogen. The reaction mixture was heated in a oil bath at 80° C for 16 hours under nitrogen and the reaction was monitored by thin layer chromatography (TLC). The resulting solution was cooled to room temperature, diluted with 100 mL of water, stirred, filtered and the obtained white product was washed with 100 mL of water. The crude product recrystallised from ethanol yielded 3.0 g. (46% yield).

2.13.1.1 N-(3-Hydroxypropyl)carbazole (I15)

Structure

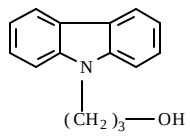

Formula $C_{15}H_{15}NO$

UV (λ_{max}) 333 nm

IR (cm^{-1}) 3000 (CH_2), 1510 (C=C), 1260 (O-CH_2)

^{1}H NMR (d) 8.0 (d, 2H), 7.4-7.1 (m, 6H), 4.4 (t, 2H), 3.6 (t, 2H), 2.1 (m, 2H)

Mass M^+ 225 (15%), 208 (10%), 180 (30%), 166 (100%), 159 (10%)

2.13.2 Synthesis of 2-formyl-N-(3-hydroxypropyl)carbazole

To dimethylformamide at 0° C, $POCl_3$ (1:1 equivalent) was added drop-wise. The solution was allowed to warm to room temperature. To this, N-(3-hydroxypropyl) carbazole in 1,2-dichloroethane was added. Reaction mixture was heated to 90° C and kept at this temperature for 24 hours. It was poured into water, extracted with chloroform, washed with water. All extracts were mixed, kept on anhydrous sodium sulphate and concentrated. Yield: 40%.

2.13.2.1 2-Formyl-N-(3-hydroxypropyl)carbazole (I16)

Structure

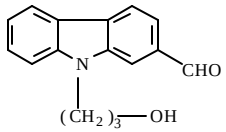

Formula $C_{16}H_{15}NO_2$

UV (λ_{max}) 346 nm

IR (cm^{-1}) 3000 (CH_2), 1690 (CHO), 1510 (C=C), 1260 (O-CH_2)

^{1}H NMR (d) 10.1 (s, 1H), 8.5 (s, 1H), 7.9 (m, 2H), 7.4 (m, 4H), 4.4 (t, 2H), 3.5 (t, 2H), 2.2 (m, 2H)

Mass M^+ 253 (20%), 194 (100%), 165 (50%), 59 (10%)

2.13.3 2-Formyl-N-[3-(3/4-vinylbenzyloxy)propyl]carbazole

The styrene monomer was synthesised as shown in Scheme 2.20 below:

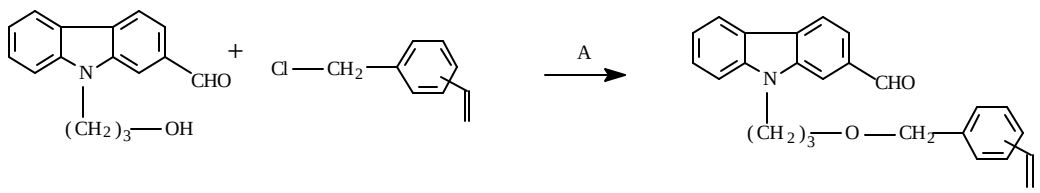

A = KOH, K_2CO_3, KI, TBAB, tetrahydrofuran, room temperature, stir

Scheme 2.20: Synthesis of 2-formyl-N-[3-(3/4-vinylbenzyloxy)propyl]carbazole

2.13.3.1 Synthesis of 2-formyl-N-[3-(3/4-vinylbenzyloxy)propyl]carbazole

2-Formyl-N-(3-hydroxypropyl)carbazole 1.0 g (0.0038 mol) was dissolved in tetrahydrofuran (50 mL) and 1.5 equivalents of potassium hydroxide, 1 equivalent of potassium carbonate, catalytic amount of tetrabutylammonium bromide (TBAB) and potassium iodide were added and stirred at room temperature for 1 hour. A mixture of 3/4 chloromethyl styrene (1.5 equivalents) was injected to the reaction mixture drop-wise over half an hour and stirred at room temperature for 24 hours. The reaction was monitored by thin layer chromatography. After completion, the contents were filtered and tetrahydrofuran was evaporated. The residue was extracted with chloroform and washed with dilute hydrochloric acid, bicarbonate solution, water and brine. The chloroform layer was kept over sodium sulphate and the solvent was evaporated under reduced pressure. The crude product was purified by column chromatography (8% acetone in petroleum ether). Yield: 66%.

2.13.3.1.1 2-Formyl-N-[3-(3/4-vinylbenzyloxy)propyl]carbazole (M20)

Structure

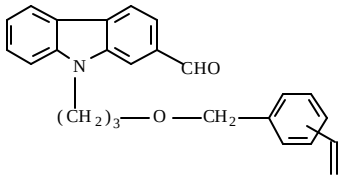

Formula	$C_{25}H_{23}NO_2$
UV (λ_{max})	340 nm
IR (cm^{-1})	3000 (CH_2), 1690 (CHO),1510 (C=C), 1260 (-OCH_2)
^{1}H NMR (d)	10.1 (s, 1H), 8.5 (s, 1H), 8.0 (d, 2H), 7.5-7.3 (m, 8H), 6.7 (m, 1H), 5.7 (d, 1H), 5.5 (s, 1H), 5.2 (d, 1H), 4.5 (t, 2H), 3.5 (t, 2H), 2.4 (m, 2H)
Mass	M^+ 369 (20%), 252 (20%), 236 (10%), 117 (100%)

2.13.4 2-(4-Cyano/nitro phenylene-1-azomethine)-N-(3-hydroxypropyl) carbazole

Acid catalysed condensation to form Schiff's bases is shown in Scheme 2.21.

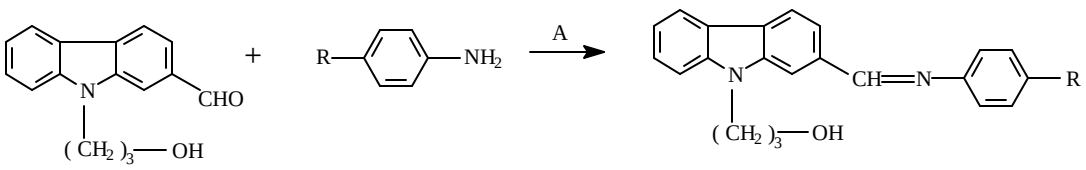

A = ethanol (dry), CH_3COOH

R = CN / NO_2

Scheme 2.21: Condensation of 2-formyl-N-(3-hydroxypropyl)carbazole with substituted aniline

2.13.4.1 Synthesis of 2-(4-cyano/ nitro phenylene-1-azomethine)-N-(3-hydroxy propyl) carbazole

2-Formyl-N-(3-hydroxypropyl) carbazole 5.0 g (0.046 mol) and 5.4 g (0.046 mol) of 4-aminobenzonitrile in dry ethanol (50 mL) were refluxed for 24 hours with glacial acetic acid as catalyst (2 mL) to 2-(4-cyano phenylene-1-azomethine)-N-(3-hydroxypropyl) carbazole. Yield: 72%.

2.13.4.1.1 2-(4-Cyano phenylene-1-azomethine)-N-(3-hydroxypropyl) carbazole (I17)

Structure

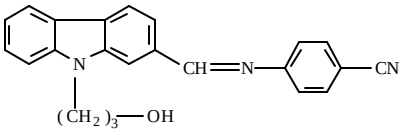

Formula $C_{23}H_{19}N_3O$

UV (l_{max}) 335 nm

IR (cm^{-1}) 3000 (CH_2), 2230 (CN), 1675 (CH=N), 1510 (C=C), 1260 (O-CH_2)

^{1}H NMR (d) 8.6 (s, 1H), 8.1 (m, 4H), 7.4 (d, 2H), 7.3 (m, 5H), 4.6 (t, 2H), 3.6 (t, 2H), 2.4 (m, 2H)

Mass M^+ 353 (30%), 294 (70%), 224 (10%), 129 (30%)

2.13.4.1.2 2-(4-Nitro phenylene-1-azomethine)-N-(3-hydroxypropyl) carbazole (I18)

Structure

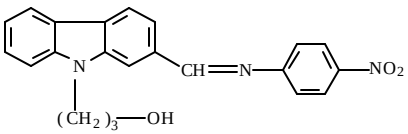

Formula $C_{22}H_{19}N_3O_3$

UV (l_{max})	337 nm
IR (cm^{-1})	3000 (CH_2), 1675 (CH=N), 1510 (C=C), 1340 (NO_2), 1260 (O-CH_2)
^{1}H NMR (d)	8.5 (s, 1H), 8.0 (d, 4H), 7.4-7.0 (m, 7H), 4.5 (t, 2H), 3.5 (t, 2H), 2.3 (m, 2H)
Mass	M^+ 373 (10%), 327 (20%), 314 (80%), 224 (10%), 149 (20%)

2.13.5 2-(4-Cyano/nitro phenylene-1-azomethine)-N-[3-(3/4-vinylbenzyloxy) propyl] carbazole

Acid catalysed condensation to form Schiff's bases is shown in Scheme 2.22.

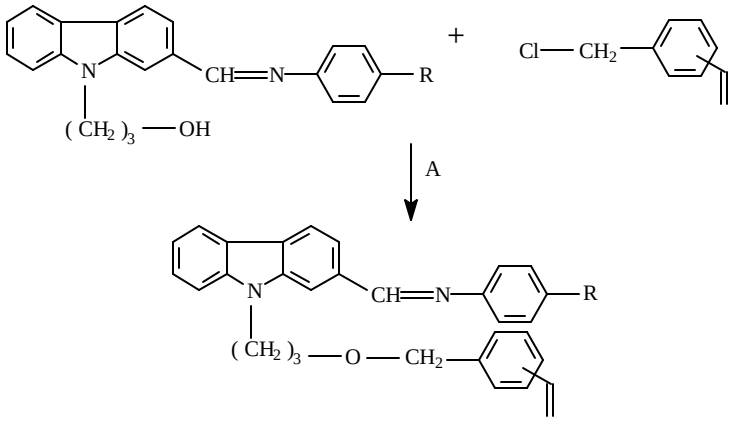

A = KOH, K_2CO_3, KI, TBAB, tetrahydrofuran, room temperature, stir

R = CN / NO_2

Scheme 2.22: Synthesis of 2-(4-cyano/nitro phenylene-1-azomethine)-N-[3-(3/4-vinylbenzyloxy) propyl] carbazole

2.13.5.1 Synthesis of 2-(4-cyano/nitro phenylene-1-azomethine)-N-[3-(3/4-vinyl benzyloxy)propyl] carbazole

2-(4-Cyano phenylene-1-azomethine)-N-(3-hydroxypropyl) carbazole 1.0 g (0.003 mol) was dissolved in tetrahydrofuran (50 mL) and 1.5 equivalents of potassium hydroxide, 1 equivalent of potassium carbonate, catalytic amount of tetrabutylammonium bromide (TBAB) and potassium iodide were added and stirred at room temperature for 1 hour. A mixture of 3/4-chloromethyl styrene (1.5 equivalents) was injected to the reaction mixture drop-wise over half an hour and stirred at room temperature for 24 hours. The reaction was monitored by thin layer chromatography. After completion, the contents were filtered and tetrahydrofuran was evaporated. The residue was extracted with

chloroform and washed with dilute hydrochloric acid, bicarbonate solution, water and brine. The chloroform layer was kept over sodium sulphate and the solvent was evaporated under reduced pressure. The crude product was purified by column chromatography (8% acetone in petroleum ether). Yield: 62%.

2.13.5.1.1 2-(4-Cyano phenylene-1-azomethine)-N-[3-(3/4-vinylbenzyloxy) propyl] carbazole (M21)

Structure

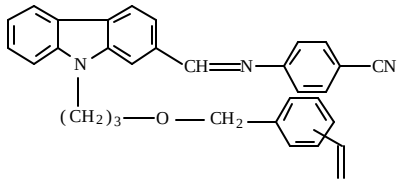

Formula $C_{32}H_{27}N_3O$

UV (l_{max}) 346 nm

IR (cm^{-1}) 3000 (CH_2), 2230 (CN), 1675 (CH=N), 1510 (C=C), 1260 (O-CH_2)

^{1}H NMR (d) 8.6 (s, 1H), 8.1 (s, 1H), 8.0 (d, 2H), 7.6 (d, 2H), 7.4-7.1 (m, 8H), 6.7 (m, 1H), 6.6 (d, 2H), 5.8 (d, 1H), 5.3 (d, 1H), 4.7 (s, 2H), 4.3 (d, 2H), 3.5 (d, 2H), 2.3 (m, 2H)

Mass M^+ 469 (30%), 352 (55%), 340 (20%), 129 (10%), 117 (100%)

2.13.5.1.2 2-(4-Nitro phenylene-1-azomethine)-N-[3-(3/4-vinylbenzyloxy) propyl] carbazole (M22)

Structure

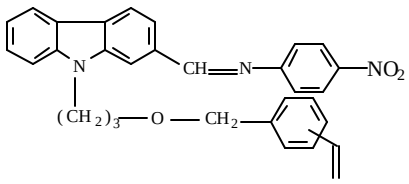

Formula $C_{31}H_{27}N_3O_3$

UV (l_{max}) 388 nm

IR (cm^{-1}) 3000 (CH_2), 1675 (CH=N), 1510 (C=C), 1340 (NO_2), 1260 (O-CH_2)

^{1}H NMR (d) 8.5 (s, 1H), 8.0 (d, 3H), 7.4-7.0 (m, 10H), 6.7 (m, 2H), 6.6 (d, 2H), 5.8 (d, 1H), 5.3 (d, 1H), 4.4 (s, 2H), 3.7 (t, 2H), 3.4 (t, 2H), 2.3 (m, 2H)

Mass M^+ 489 (40%), 372 (60%), 340 (30%), 149 (10%), 117 (100%)

2.14 Synthesis of monomers from 5-amino-1,3,4-thiadiazole-2-thiol

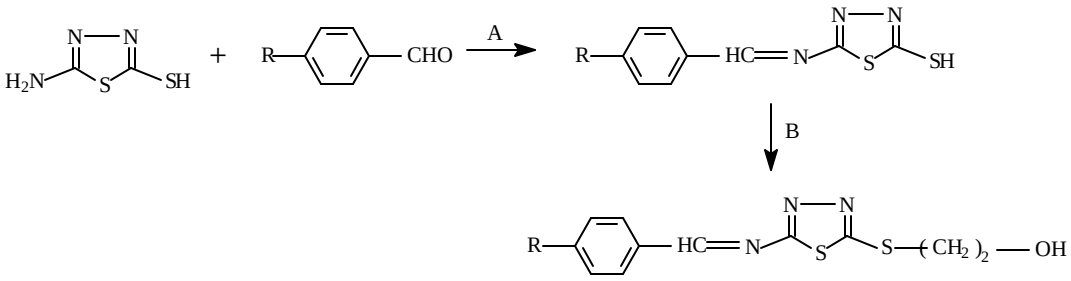

A = ethanol (dry), CH_3COOH (catalyst), reflux

B = Br-$(CH_2)_2$-OH, dimethyformamide, 80° C

R = CN / NO_2

Scheme 2.23: Condensation followed by alkylation of 5-amino-1,3,4-thiadiazole-2-thiol

2.14.1 Synthesis of 5-[N-(4'-cyano/nitro benzylidene)amine]-1,3,4-thiadiazole-2-thiol

4-Nitro benzaldehyde, 4-cyano benzaldehyde, 5-amino-1,3,4-thiadiazole-2-thiol, 2-bromo ethan-1-ol, 3/4-chloromethylstyrene were obtained from Aldrich Chemical Co., U.S.A. and used as received. Ethanol, dimethylformamide, tetrahydrofuran, potassium carbonate, potassium hydroxide, potassium iodide, tetrabutylammonium bromide were obtained from S. D. Fine Chemicals, Mumbai, India.

5.0 g (0.046 mol) of 5-amino-1,3,4-thiadiazole-2-thiol and 6.1 g (0.046 mol) of 4-cyano benzaldehyde in dry ethanol (50 mL) were refluxed for 24 hours with glacial acetic acid as catalyst (2 mL) to give the product. The other azomethine base synthesised comprised of nitro as the electron withdrawing group. Yield: 80%.

2.14.1.1 5-[N-(4'-Cyano benzylidene)amine]-1,3,4-thiadiazole-2-thiol (I19)

Structure

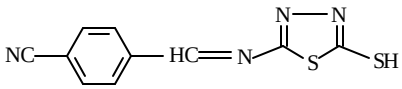

Formula $C_{10}H_6N_4S_2$

UV (l_{max}) 331 nm

IR (cm^{-1}) 2500 (S-H stretching), 2230 (CN), 1675 (CH=N)

^{1}H NMR (d) 8.0 (s, 1H), 7.9 (d, 2H), 7.7 (d, 2H)

Mass M^+ 266 (100%), 220 (20%), 135 (10%), 131 (20%), 89 (45%)

2.14.1.2 5-[N-(4'-Nitro benzylidene)amine]-1,3,4-thiadiazole-2-thiol (I20)

Structure

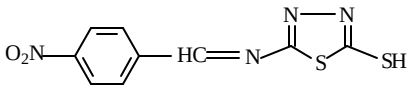

Formula $C_9H_6N_4S_2O_2$

UV (l_{max}) 332 nm

IR (cm^{-1}) 2500 (S-H stretching), 1675 (CH=N), 1340 (NO_2)

^{1}H NMR (d) 8.2 (d, 2H), 8.0 (s, 1H), 7.6 (d, 2H)

Mass M^+ 246 (80%), 220 (30%), 131 (10%), 115 (20%), 89 (40%)

2.14.2 Synthesis of 5-[N-(4'- cyano/nitro benzylidene)amine]-2-(2-hydroxyethyl thio)-1,3,4-thiadiazole

5-[N-(4'-Cyano benzylidene)amine]-1,3,4-thiadiazole-2-thiol (5.0 g, 0.02 mol), anhydrous potassium carbonate (10.8 g, 0.078 mol) and 2-bromo ethan-1-ol (4.2 g, 0.039 mol) were dissolved in 25 mL dry dimethylformamide under nitrogen. The reaction mixture was heated in a oil bath at 80^o C for 16 hours under nitrogen and the reaction was monitored by thin layer chromatography (TLC). The resulting solution was cooled to room temperature, diluted with 100 mL of water, and extracted with chloroform. The chloroform extracts were kept on anhydrous sodium sulphate and later concentrated under reduced pressure. Yield: 54%.

2.14.2.1 5-[N-(4'-Cyano benzylidene)amine]-2-(2-hydroxyethylthio)-1,3,4-thiadiazole (I21)

Structure

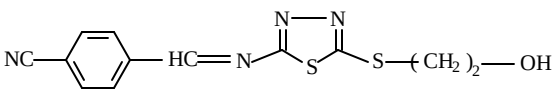

Formula $C_{12}H_{10}N_4S_2O$

UV (l_{max}) 335 nm

IR (cm^{-1}) 3000 (CH_2), 2230 (CN), 1675 (CH=N), 1260 (O-CH_2), 600 (C-S stretching)

^{1}H NMR (d) 8.0 (s, 1H), 7.6-7.5 (m, 4H), 4.2 (t, 2H), 3.9 (t, 2H)

Mass M^+ 290 (20%), 245 (30%), 129 (100%), 77 (35%)

2.14.2.2 5-[N-(4'-Nitro benzylidene)amine]-2-(2-hydroxyethylthio)-1,3,4-thiadiazole (I22)

Structure

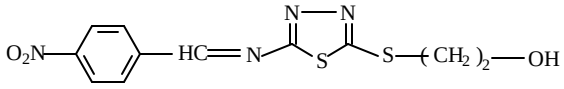

Formula $C_{11}H_{10}N_4S_2O_3$

UV (l_{max}) 337 nm

IR (cm^{-1}) 3000 (CH_2), 1675 (CH=N), 1340 (NO_2), 1260 (O-CH_2), 600 (C-S stretching)

^{1}H NMR (d) 8.3 (d, 2H), 8.0 (s, 2H), 7.6 (d, 2H), 4.1 (t, 2H), 3.2 (t, 2H)

Mass M^+ 310 (10%), 265 (20%), 161 (60%), 149 (100%), 77 (40%)

2.14.3 5-[N-(4'-Cyano/nitro benzylidene)amine]-2-(2-methacryloyloxyethylthio)-1,3,4-thiadiazole

The methacrylate monomers were synthesised as shown in Scheme 2.24 below:

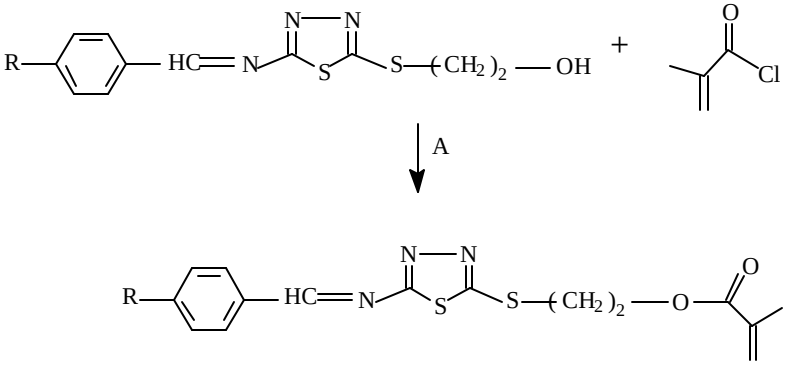

A = Et_3N, chloroform (dry), room temperature, stir

Scheme 2.24: Synthesis of 5-[N-(4'-cyano/nitro benzylidene)amine]-2-(2-methacryloyloxyethylthio)-1,3,4-thiadiazole

2.14.3.1 Synthesis of 5-[N-(4'-cyano/nitro benzylidene)amine]-2-(2-methacryloyl oxyethylthio)-1,3,4-thiadiazole

Triethyl amine was obtained from S.D. Fine Chemicals, Mumbai. This was kept in potassium hydroxide overnight and distilled under vacuum. Chloroform (analytical reagent grade) obtained from S.D. Fine Chemicals was purified by the following procedure. Chloroform was shaken with portions of concentrated sulphuric acid, then thoroughly washed with water, finally dried over anhydrous calcium chloride and distilled.

5-[N-(4'-Cyano benzylidene)amine]-2-(2-hydroxyethylthio)-1,3,4-thiadiazole 1.0 g (0.003 mol) was dissolved in dry chloroform (25 mL) and 0.25 mL of triethyl amine was added and stirred under nitrogen for 30 minutes. Methacryloyl chloride 1.04 g (2.5 mole equivalents) was then added and stirred for three hours at room temperature and then the reaction was monitored by thin layer chromatography. After the reaction was complete, the reaction mixture was poured into cold water, extracted with chloroform, washed with dilute hydrochloric acid, several times with water, brine and dried over anhydrous sodium sulphate. The solvent was evaporated under reduced pressure and the crude product was purified by column chromatography. (4% acetone-petroleum ether combination was used). Yield: 49%.

2.14.3.1.1 5-[N-(4'-Cyano benzylidene) amine]-2-(2-methacryloyloxy ethylthio)-1,3,4-thiadiazole (M23)

Structure

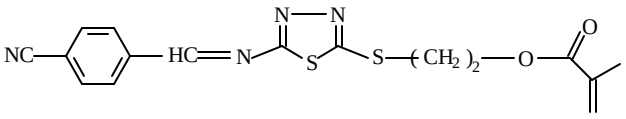

Formula $C_{16}H_{14}N_4O_2S_2$

UV (l_{max}) 335 nm

IR (cm^{-1}) 3000 (CH_2), 2230 (CN), 1710 (C=O), 1675 (CH=N), 600 (C-S stretching)

^{1}H NMR (d) 8.0 (s, 1H), 7.6-7.5 (m, 4H), 6.1 (d, 1H), 5.6 (d, 1H), 4.1 (t, 2H), 3.9 (t, 2H), 1.9 (s, 3H)

Mass M^+ 358 (20%), 289 (20%), 215 (10%), 145 (30%), 69 (100%)

2.14.3.1.2 5-[N-(4'-Nitro benzylidene) amine]-2-(2-methacryloyloxy ethylthio)-1,3,4-thiadiazole (M24)

Structure

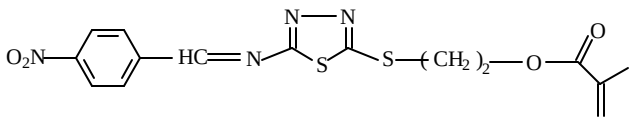

Formula $C_{15}H_{14}N_4O_4S_2$

UV (l_{max}) 337 nm

IR (cm^{-1}) 3000 (CH_2), 1710 (C=O), 1675 (CH=N), 1340 (NO_2), 600 (C-S stretching)

^{1}H NMR (d) 7.9 (d, 3H), 7.4 (d, 2H), 6.1 (d, 1H), 5.6 (d, 1H), 4.3 (t, 2H), 3.9 (t, 2H), 1.9 (s, 3H)

Mass M^+ 378 (20%), 309 (30%), 233 (20%), 145 (10%), 69 (100%)

2.14.4 5-[N-(4'-Nitro benzylidene) amine]-2-(2-acryloyloxy ethylthio)-1,3,4-thiadiazole

The acrylate monomer was synthesised as shown in Scheme 2.25 below:

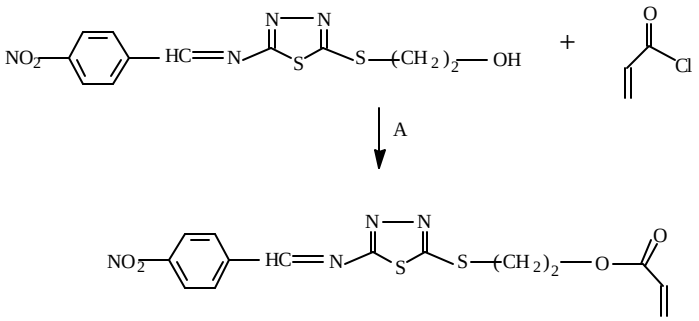

A = Et_3N, chloroform (dry), room temperature, stir

Scheme 2.25: Synthesis of 5-[N-(4'-nitro benzylidene)amine]-2-(2-acryloyloxy ethylthio)-1,3,4-thiadiazole

2.14.4.1 Synthesis of 5-[N-(4'-nitro benzylidene) amine]-2-(2-acryloyloxyethyl thio)-1,3,4-thiadiazole

Triethyl amine was obtained from S.D. Fine Chemicals, Mumbai. This was kept in potassium hydroxide overnight and distilled under vacuum. Analytical reagent grade chloroform, obtained from S.D. Fine Chemicals was purified by standard procedure.

4-[N-(4'-Nitro benzylidene)amine]-2-(2-hydroxyethylthio)-1,3,4-thiadiazole 1.0 g (0.0038 mol) dissolved in dry chloroform (25 mL) and 0.25 mL of triethyl amine were

added to a reaction vessel and stirred under nitrogen for 30 minutes. Acryloyl chloride 0.86 g (2.5 equivalents) was then added and stirring continued for 3 hours at room temperature. The reaction was monitored by thin layer chromatography. After reaction was complete the reaction mixture was poured into cold water, extracted with chloroform, washed with dilute hydrochloric acid, several times with water, brine and dried over anhydrous sodium sulphate. The solvent was evaporated under reduced pressure and the crude product was purified by column chromatography (4% acetone in petroleum ether was used). Yield: 52%.

2.14.4.1.1 5-[N-(4'-Nitro benzylidene) amine]-2-(2-acryloyloxy ethylthio)-1,3,4-thiadiazole (M25)

Structure

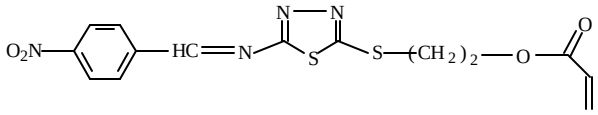

Formula $C_{14}H_{12}N_4O_4S_2$

UV (l_{max}) 337 nm

IR (cm^{-1}) 3000 (CH_2), 1710 (C=O), 1675 (CH=N), 1340 (NO_2), 600 (C-S stretching)

^{1}H NMR (d) 8.2 (d, 3H), 6.8 (d, 2H), 6.4 (s, 1H), 6.1 (d, 1H), 5.9 (d, 1H), 4.2 (t, 2H), 3.7 (t, 2H)

Mass M^+ 364 (30%), 309 (45%), 233 (20%), 131 (10%), 55 (70%)

2.14.5 5-[N-(4'-Cyano/nitro benzylidene)amine]-2-[2-(3/4-vinylbenzyloxy)ethyl thio]-1,3,4-thiadiazole

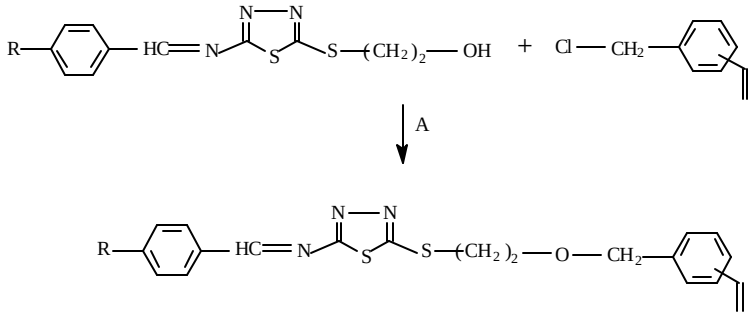

A = KOH, K_2CO_3, KI, TBAB, tetrahydrofuran, room temperature, stir

R = NO_2 / CN

Scheme 2.26: Synthesis of 5-[N-(4'-cyano/nitro benzylidene)amine]-2-[2-(3/4-vinylbenzyloxy) ethylthio]-1,3,4-thiadiazole

2.14.5.1 Synthesis of 5-[N-(4'-cyano/nitro benzylidene)amine]-2-[2-(3/4-vinyl benzyloxy) ethylthio]-1,3,4-thiadiazole

3/4-Chloromethyl styrene was procured from Aldrich Chemical Co., U.S.A. and was used as such. Potassium hydroxide, potassium iodide, potassium carbonate, tetrabutylammonium bromide, tetrahydrofuran were obtained from S. D. Fine Chemicals, Mumbai, India.

5-[N-(4'-Cyano benzylidene)amine]-2-(2-hydroxyethylthio)-1,3,4-thiadiazole 1.0 g (0.0038 mol) was dissolved in tetrahydrofuran (50 mL) and 1.5 equivalents of potassium hydroxide, 1 equivalent of potassium carbonate, catalytic amount of tetrabutylammonium bromide (TBAB) and potassium iodide were added and stirred at room temperature for 1 hour. Mixed 3/4 chloromethyl styrene (1.5 equivalents) is injected to the reaction mixture drop-wise over half an hour and stirred at room temperature for 24 hours. The reaction was monitored by thin layer chromatography. After completion, the contents were filtered and tetrahydrofuran was evaporated. The residue was extracted with chloroform and washed with dilute hydrochloric acid, bicarbonate solution, water and brine. The chloroform layer was kept over sodium sulphate and the solvent was evaporated under reduced pressure. The crude product was purified by column chromatography (8% acetone in petroleum ether). Yield: 64%.

2.14.5.1.1 5-[N-(4'-Cyano benzylidene) amine]-2-[2-(3/4-vinylbenzyloxy) ethylthio]-1,3,4-thiadiazole (M26)

Structure

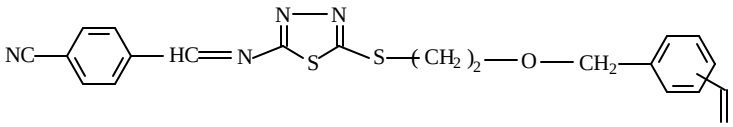

Formula $C_{21}H_{18}N_4S_2O$

UV (l_{max}) 335 nm

IR (cm^{-1}) 3000 (CH_2), 2230 (CN), 1675 (CH=N), 1260 (O-CH_2), 600 (C-S stretching)

^{1}H NMR (d) 7.6 (m, 3H), 7.3 (m, 6H), 6.7 (m, 1H), 5.8 (d, 1H), 5.3 (d, 1H), 4.6 (s, 1H), 4.0-3.7 (m, 4H)

Mass M^+ 406 (20%), 289 (35%), 245 (15%), 117 (100%)

2.14.5.1.2 **5-[N-(4'-Nitro benzylidene) amine]-2-[2-(3/4-vinylbenzyloxy) ethylthio]-1,3,4-thiadiazole (M27)**

Structure

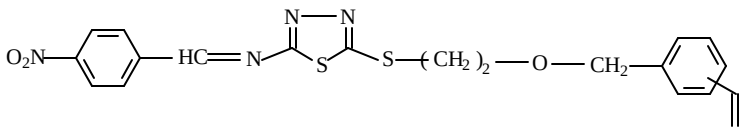

Formula $C_{20}H_{18}N_4S_2O_3$

UV (l_{max}) 331 nm

IR (cm^{-1}) 3000 (CH_2), 1675 (CH=N), 1340 (NO_2), 1260 (O-CH_2), 600 (C-S stretching)

^{1}H NMR (d) 8.3 (d, 2H), 7.7 (d, 2H), 7.3 (m, 5H), 6.7 (m, 1H), 5.7 (d, 1H), 5.3 (d, 1H), 4.4 (s, 2H), 3.7 (t, 2H), 3.5 (t, 2H)

Mass M^+ 426 (30%), 309 (10%), 265 (5%), 117 (100%)

2.15 4-[g-(2,3-Dihydroxypropaneoxy) propyloxy]-4'-nitro/cyano azobenzene *and* N-(4'-nitro/cyano benzylidene)-4-[g-(2,3-dihydroxypropaneoxy) ethyloxy] aniline

N,*N*-Dimethylformamide (DMF) (S.D. Fine Chemicals, Mumbai, India) was purified by vacuum distillation over phosphorus pentoxide and dried further on 4 Å molecular sieves. 2,4-Tolylene diisocyanate (BASF, Germany) was purified by distillation under reduced pressure and methylene-4,4'-bis(phenyl isocyanate) (BASF, Germany) was used as received. All other reagents like potassium hydroxide, potassium carbonate, potassium iodide, tetrabutylammonium bromide, epichlorohydrin, dimethylsulphoxide, tetrahydrofuran were obtained from S. D. Fine Chemicals, India and used as received.

The monomers were synthesised as shown in Scheme 2.27.

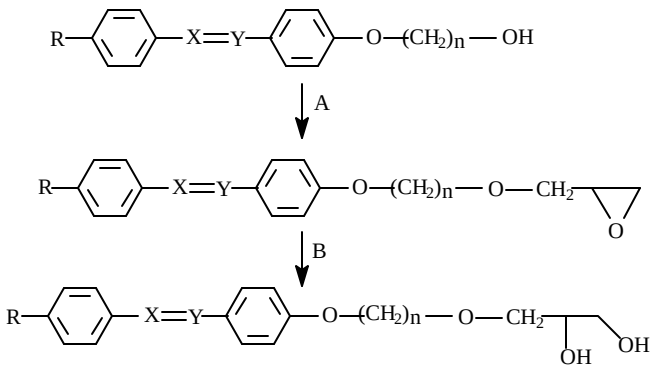

A = epichlorohydrin, K_2CO_3, KOH, KI, TBAB, room temperature, stir

B = 0.3 N KOH, DMSO-H_2O (85-15), 100^o C

R = CN / NO_2; X=Y} N=N and CH=N

Scheme 2.27: Epoxide formation and ring opening by base catalysed hydrolysis

2.15.1 Synthesis of 4-[g-(2,3-epoxypropaneoxy) propyloxy]-4'-nitro/cyano azobenzene *and* N-(4'-nitro/cyano benzylidene)-4-[b-(2,3-epoxypropane oxy) ethyloxy]aniline

4-(3-Hydroxypropyloxy)-4'-nitro azobenzene (1.0 g; 0.0033 mol) was dissolved in 50 mL tetrahydrofuran and 8 equivalents of potassium hydroxide, 3 equivalents of potassium carbonate, catalytic amount of tetrabutylammonium bromide were added and stirred at room temperature for 1 hour. The colour of the solution changed to dark and then chloro epoxypropane 1.214 g (4 equivalents) was injected to this drop-wise over half an hour and stirred at room temperature for 36 hours. The reaction was monitored by thin layer chromatography and after the completion, the reaction mixture was filtered and tetrahydrofuran was evaporated. The residue was extracted with dichloromethane and washed with dilute hydrochloric acid, bicarbonate solution, water and brine. The dichloromethane layer was kept over sodium sulphate and the solvent was evaporated under reduced pressure. The crude product was purified by column chromatography using acetone-petroleum ether 6/94 v/v solvent mixture. Yield: 76%.

2.15.1.1 4-[g-(2,3-epoxypropaneoxy) propyloxy]-4'-nitro azobenzene (I23)

Structure

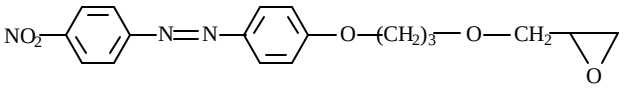

Formula $C_{18}H_{19}N_3O_5$

UV (l_{max}) 375 nm

IR (cm^{-1}) 2960, 2850 (CH_2), 1615 (C=C), 1598, 1504 (ArCH), 1515, 1340 (NO_2), 1490 (N=N), 1250 (C-O)

^{1}H NMR (d) 8.4 (d, 2H), 8.0 (dd, 4H), 7.1 (d, 2H), 4.2 (t, 2H), 3.8 (m, 2H), 3.4 (m, 1H), 3.3 (m, 2H), 2.7 (m, 1H), 2.6 (m, 1H), 2.2 (m, 2H)

Mass M^+ 357 (20%), 284 (25%), 242 (5%), 115 (20%), 73 (50%), 57 (100%)

2.15.1.2 **4-[g-(2,3-epoxypropaneoxy) propyloxy]-4'-cyano azobenzene (I24)**

Structure

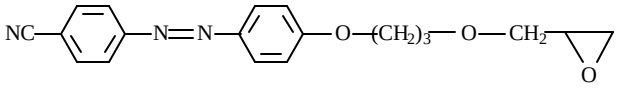

Formula $C_{19}H_{19}N_3O_3$

UV (λ_{max}) 378 nm

IR (cm^{-1}) 2960, 2850 (CH_2), 2200 (CN), 1615 (C=C), 1598, 1504 (ArCH), 1490 (N=N), 1250 (C-O)

^{1}H NMR 8.0 (d, 4H), 7.8 (d, 2H), 7.0 (d, 2H), 4.2 (t, 2H), 3.8 (m, 2H), 3.4 (m, 1H), 3.2 (m, 2H), 2.8 (m, 1H), 2.6 (m, 1H), 2.2 (m, 2H)

Mass M^+ 337 (20%), 242 (10%), 115 (15%), 73 (75%), 57 (10%)

2.15.1.3 **N-(4'-nitro benzylidene)-4-[b-(2,3-epoxy propaneoxy) ethyloxy]aniline (I25)**

Structure

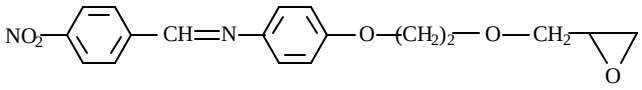

Formula $C_{18}H_{18}N_2O_5$

UV (λ_{max}) 343 nm

IR (cm^{-1}) 2960, 2850 (CH_2), 1675 (CH=N), 1615 (C=C), 1598, 1504 (ArCH), 1515, 1340 (NO_2), 1250 (C-O)

^{1}H NMR 8.6 (s, 1H), 8.3 (d, 2H), 8.0 (d, 2H), 7.3 (d, 2H), 7.0 (d, 2H), 4.2 (t, 2H), 3.8 (m, 2H), 3.4 (m, 1H), 3.2 (m, 2H), 2.8 (m, 1H), 2.6 (m, 1H)

Mass M^+ 330 (15%), 273 (30%), 215 (10%), 115 (25%), 73 (60%), 57(100%)

2.15.1.4 **N-(4'-cyano benzylidene)-4-[b-(2,3-epoxy propaneoxy) ethyloxy]aniline (I26)**

Structure

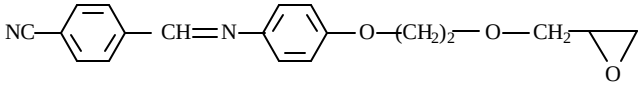

Formula $C_{19}H_{18}N_2O_3$

UV (λ_{max}) 345 nm

IR (cm^{-1}) 2960, 2850 (CH_2), 2200 (CN), 1675 (CH=N), 1615 (C=C), 1598, 1504 (ArCH), 1250 (C-O)

^{1}H NMR 8.5 (s, 1H), 7.9 (d, 2H), 7.7 (d, 2H), 7.3 (d, 2H), 7.0 (d, 2H), 4.2 (t, 2H), 3.9 (m, 2H), 3.5 (m, 1H), 3.2 (m, 2H), 2.8 (m, 1H), 2.6 (m, 1H)

Mass M^+ 310 (10%), 253 (20%), 195 (25%), 73 (50%), 57 (100%)

2.15.2 Synthesis of 4-[g-(2,3-dihydroxypropaneoxy) propyloxy]-4'-nitro/cyano azobenzene *and* N-(4'-nitro/cyano benzylidene)-4-[g-(2,3-dihydroxypropaneoxy) ethyloxy]aniline

To a 100 mL round bottom flask containing 4-[γ-(2,3-epoxypropaneoxy) propyloxy]-4'-nitro azobenzene (1.0 g, 0.003 mol) was added 0.3N KOH / 85% DMSO-H_2O (20 mL). The reaction mixture was kept at 100^o C for 6 hours. The reaction was monitored by thin layer chromatography (TLC). After completion, the contents were poured in water, extracted with chloroform. All extracts were collected, kept on anhydrous sodium sulphate and concentrated. Yield: 57%.

2.15.2.1 4-[g-(2,3-Dihydroxypropaneoxy) propyloxy]-4'-nitro azobenzene (M28)

Structure

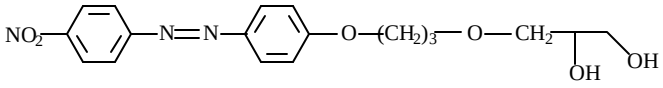

Formula $C_{18}H_{21}N_3O_6$

UV (λ_{max}) 383 nm

IR (cm^{-1}) 3600-3100 (OH), 2960, 2850 (CH_2), 1615 (C=C), 1598, 1504 (ArCH), 1515, 1340 (NO_2), 1490 (N=N), 1250 (C-O)

^{1}H NMR (d) 8.38 (d, 2H), 7.96 (d, 2H), 7.83 (d, 2H), 6.97 (d, 2H), 4.1 (t, 2H), 3.8 (m, 4H), 3.69 (m, 1H), 3.54 (m, 2H), 2.06 (m, 2H)

Mass M^+ 375 (20%), 357 (85%), 300 (50%), 57 (20%)

2.15.2.2 4-[g-(2,3-Dihydroxypropaneoxy) propyloxy]-4'-cyano azobenzene (M29)

Structure

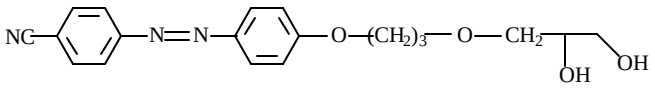

Formula $C_{19}H_{21}N_3O_4$

UV (λ_{max}) 363 nm

IR (cm^{-1}) 3100-3600 (OH), 2960, 2850 (CH_2), 2200 (CN), 1615 (C=C), 1598, 1504 (ArCH), 1490 (N=N), 1250 (C-O)

^{1}H NMR (d) 8.1-7.8 (m, 6H), 7.1 (d, 2H), 4.1 (t, 2H), 3.8 (m, 4H), 3.69 (m, 1H), 3.5 (m, 2H), 2.1 (m, 2H)

Mass M^+ 355 (40%), 337 (75%), 280 (30%), 57 (10%)

2.15.2.3 **4-[g-(2,3-Dihydroxypropaneoxy) ethyloxy]-N-(4'-nitro benzylidene)aniline (M30)**

Structure

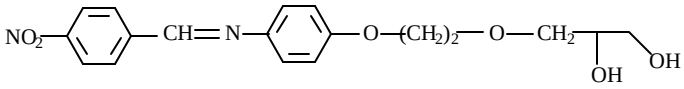

Formula $C_{18}H_{20}N_2O_6$

UV (l_{max}) 333 nm

IR (cm^{-1}) 3600-3100 (OH), 2960, 2850 (CH_2), 1675 (CH=N), 1615 (C=C), 1598, 1504 (ArCH), 1515, 1340 (NO_2), 1250 (C-O)

^{1}H NMR (d) 8.5 (s, 1H), 8.38 (d, 2H), 7.96 (d, 2H), 6.9 (d, 2H), 6.5 (d, 2H), 4.1-3.5 (m, 7H), 2.06 (m, 2H)

Mass M^+ 357 (10%), 348 (30%), 330 (80%), 273 (20%), 57 (30%)

2.15.2.4 **4-[g-(2,3-Dihydroxypropaneoxy) ethyloxy]-N-(4'-cyano benzylidene)aniline (M31)**

Structure

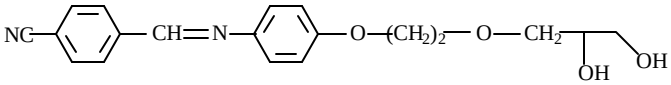

Formula $C_{19}H_{20}N_2O_4$

UV (l_{max}) 338 nm

IR (cm^{-1}) 3600-3100 (OH), 2960, 2850 (CH_2), 2200 (CN), 1675 (CH=N), 1615 (C=C), 1598, 1504 (ArCH), 1250 (C-O)

^{1}H NMR (d) 8.5 (s, 1H), 7.8-8.0 (d, 2H), 7.1-6.7 (m, 6H), 4.1-3.5 (m, 7H), 2.1 (m, 2H)

Mass M^+ 328 (50%), 310 (70%), 253 (40%), 57 (10%)

2.16 2-[3-(4-Nitro/cyano azobenzene-4'-oxy) propyl]-1,3-propanediol

N,*N*-Dimethylformamide (DMF) (S. D. Fine Chemicals, Mumbai, India) was purified by vacuum distillation over phosphorus pentoxide and dried further on 4 Å molecular sieves. 2,4-Tolylene diisocyanate (BASF, Germany) was purified by distillation under reduced pressure and methylene-4,4'-bis(phenyl isocyanate) (BASF,

Germany) was used as received. Phosphorus tribromide, diethylmalonate, sodium methoxide, sodium borohydride were obtained from Aldrich Chemical Co., U.S.A., and used as received. All solvents like tetrahydrofuran, methanol and dichloromethane were obtained from S.D. Fine Chemicals, India and purified and dried following standard procedures.

The monomer was synthesised as shown in Scheme 2.28.

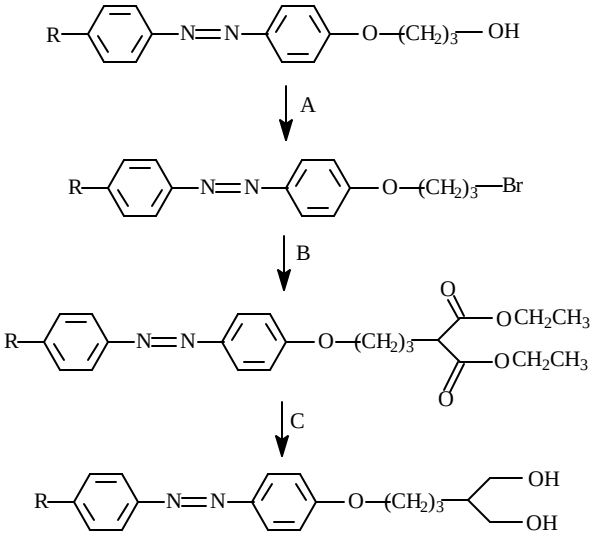

A = PBr_3, dichloromethane, room temperature, stir

B = diethyl malonate, NaOMe, tetrahydrofuran (dry)

C = $NaBH_4$, methanol (dry), tetrahydrofuran, reflux

R = CN / NO_2

Scheme 2.28: Synthesis of diester followed by hydrolysis

2.16.1 Synthesis of 4-(3-bromopropyloxy)-4'-nitro/cyano azobenzene

In a dry vessel, dry dichloromethane solution of 4-cyano-4'-(3-hydroxypropyloxy) azobenzene was cooled in an ice bath. To this cold solution was added phosphorus tribromide drop-wise. After the addition was complete, the reaction mixture was allowed to come to room temperature and stirred at this temperature for 8 hours. The reaction was monitored by thin layer chromatography (TLC). After the reaction was complete, the reaction mixture was poured in water and extracted in chloroform. The extracts were washed 4 to 5 times with water. All extracts were mixed and kept on anhydrous sodium sulphate and later

concentrated. The crude product was purified by silica gel column chromatography. Yield: 80%.

2.16.1.1 4-(3-Bromo propyloxy)-4'-cyano azobenzene (I27)

Structure

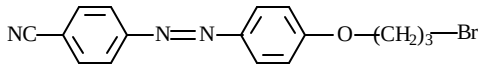

Formula $C_{16}H_{14}N_3OBr$

UV (λ_{max}) 367 nm

IR (cm^{-1}) 3000 (CH_2), 2230 (CN), 1590 (N=N), 1510 (C=C)

^{1}H NMR (d) 8.3 (d, 2H), 7.9 (d, 2H), 7.7 (d, 2H), 6.9 (d, 2H), 4.1 (t, 2H), 3.6 (t, 2H), 2.3 (m, 2H)

Mass M^+ 281 (40%), 201 (80%), 143 (40%), 138 (20%)

2.16.1.2 4-(3-Bromo propyloxy)-4'-nitro azobenzene (I28)

Structure

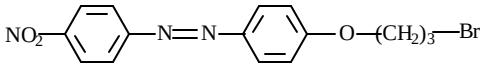

Formula $C_{15}H_{14}N_3O_3Br$

UV (λ_{max}) 373 nm

IR (cm^{-1}) 3000 (CH_2), 1590 (N=N), 1510 (C=C), 1340 (NO_2)

^{1}H NMR (d) 8.4 (d, 2H), 8.0 (dd, 4H), 7.1 (d, 2H), 4.2 (t, 2H), 3.9 (t, 2H), 2.2 (m, 2H)

Mass M^+ 301 (30%), 221 (75%), 163 (20%), 138 (50%)

2.16.2 Synthesis of 2-[3-(4-nitro/cyano azobenzene-4'-oxy)propyl] diethylmalonate

In a dry vessel, dry tetrahydrofuran solution of diethylmalonate 0.32 g (0.002 mol) and sodium methoxide 0.2 g (0.003 mol) were refluxed for 30 minutes. A dry tetrahydrofuran solution of 4-(3-bromo propyloxy)-4'-cyano azobenzene 0.85 g (0.002 mol) was added to the reaction mixture and were refluxed for 24 hours. The reaction was monitored by thin layer chromatography. After maximum conversion to malonate diester, the reaction mixture was poured into water and extracted with chloroform. The extracts were washed 4 to 5 times with water. All extracts were mixed and kept on anhydrous sodium sulphate and later

concentrated. The crude product was purified by silica gel column chromatography. Yield: 75%.

2.16.2.1 **2-[3-(4-Cyano azobenzene-4'-oxy)propyl]diethylmalonate (I29)**

Structure

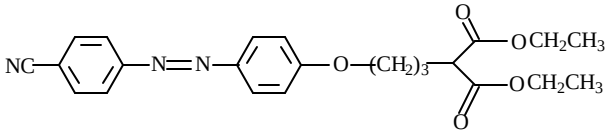

Formula $C_{23}H_{25}N_3O_5$

UV (l_{max}) 378 nm

IR (cm^{-1}) 2960, 2850 (CH_2), 2200 (CN), 1745 (-O-C=O), 1615 (C=C), 1598, 1504 (ArCH), 1490 (N=N)

^{1}H NMR (d) 8.0-7.7 (m, 4H), 7.8 (d, 2H), 7.1 (d, 2H), 4.3 (m, 6H), 3.4 (t, 1H), 2.1 (m, 2H), 1.8 (q, 2H), 1.3 (t, 6H)

Mass M^+ 423 (30%), 264 (70%), 206 (10%), 159 (30%)

2.16.2.2 **2-[3-(4-Nitro azobenzene-4'-oxy)propyl]diethylmalonate (I30)**

Structure

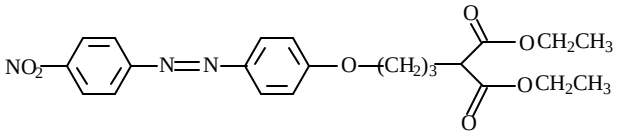

Formula $C_{22}H_{25}N_3O_7$

UV (l_{max}) 375 nm

IR (cm^{-1}) 2960, 2850 (CH_2), 1745 (-O-C=O), 1615 (C=C), 1598, 1504 (ArCH), 1490 (N=N), 1340 (NO_2)

^{1}H NMR (d) 8.4 (d, 2H), 8.1-7.9 (m, 4H), 7.1 (d, 2H), 4.1 (m, 6H), 3.4 (t, 1H), 2.2 (m, 2H), 1.9 (q, 2H), 1.3 (t, 6H)

Mass M^+ 443 (20%), 284 (80%), 226 (30%), 159 (20%)

2.16.3 Synthesis of 2-[3-(4-nitro/cyano azobenzene-4'-oxy) propyl]-1,3-propanediol

In an atmosphere of nitrogen, a tetrahydrofuran solution of 2-[3-(4-cyano azobenzene-4'-oxy)propyl]diethylmalonate and sodium borohydride were refluxed for 30 minutes. To this, dry methanol was added drop-wise over one hour. Then the reaction mixture was refluxed for 6 hours. The reaction was monitored by thin layer chromatography.

After completion, the reaction mixture was poured into water and extracted with chloroform. The extracts were washed 4 to 5 times with water. All extracts were mixed and kept on anhydrous sodium sulphate and later concentrated. The crude product was purified by silica gel column chromatography. Yield: 59%.

2.16.3.1 2-[3-(4-Cyano azobenzene-4'-oxy)propyl]-1,3-propanediol (M32)

Structure

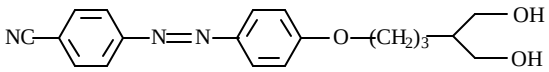

Formula $C_{19}H_{21}N_3O_3$

UV (l_{max}) 373 nm

IR (cm^{-1}) 3600-3100 (OH), 2960, 2850 (CH_2), 2200 (CN), 1615 (C=C), 1598, 1504 (ArCH), 1490 (N=N)

^{1}H NMR (d) 8.0 (d, 2H), 7.8 (d, 2H), 7.1 (d, 2H), 6.8 (d, 2H), 4.2 (t, 2H), 3.4 (d, 4H), 2.9 (q, 2H), 2.8 (m, 2H), 1.6 (m, 1H)

Mass M^+ 339 (30%), 264 (50%), 206 (15%), 75 (20%)

2.16.3.2 2-[3-(4-Nitro azobenzene-4'-oxy)propyl]-1,3-propanediol (M33)

Structure

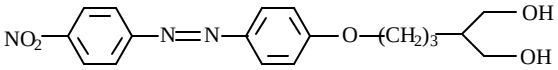

Formula $C_{18}H_{21}N_3O_5$

UV (l_{max}) 376 nm

IR (cm^{-1}) 3600-3100 (OH), 2960, 2850 (CH_2), 1615 (C=C), 1598, 1504 (ArCH), 1490 (N=N), 1340 (NO_2)

^{1}H NMR 8.4 (d, 2H), 7.9 (d, 4H), 7.0 (d, 2H), 4.1 (t, 2H), 3.5 (d, 4H), 2.9 (q, 2H), 2.7 (m, 2H), 1.9 (m, 1H)

Mass M^+ 359 (40%), 284 (80%), 226 (10%), 75 (30%)

2.17 4-[(S-1-Methylheptyl oxy)-3-nitro-1,4-phenylene carbonyloxy]-4'-(undec-10-enoxy) biphenyl (M34)

All the solvents and reagents were of analytical grade quality, purchased commercially from Aldrich Chemical Co., U.S.A. and used as received, unless otherwise stated.

Monomer **M34** was synthesised as shown in Scheme 2.29 below:

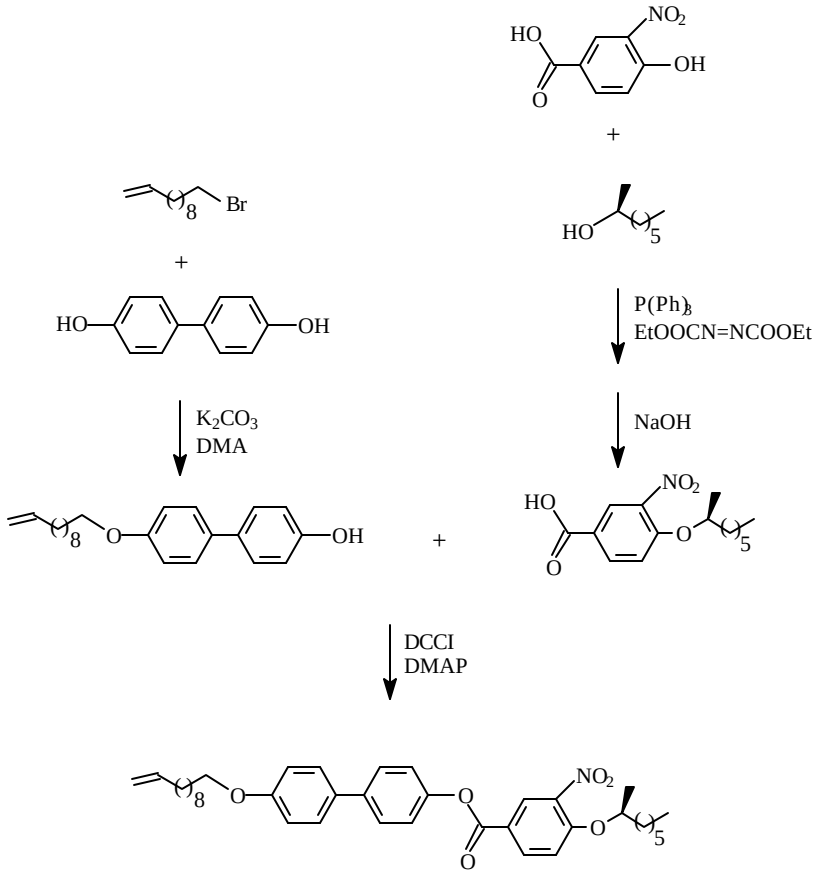

Scheme 2.29: Synthesis of 4-[(S-1-methylheptyl oxy)-3-nitro-1,4-phenylene carbonyloxy]-4'-(undec-10-enoxy) biphenyl (M34)

2.17.1 Synthesis of 4-hydroxy-4'-(undec-10-enoxy) biphenyl

4,4'-Dihydroxybiphenyl 79.79 g (427 mmol) was dissolved in N,N-dimethylacetamide (DMA) (300 mL) and saturated with nitrogen. To this was added potssium carbonate (100 g), potassium iodide (a pinch) and the reaction mixture was stirred at 80^{o} C under nitrogen atmosphere. After a while 1-bromo-10-undecene taken in 30 mL of DMA was added drop-wise to the reaction mixture. The reaction mixture was allowed to stir further at 80^{o} C for 5 hours and then overnight at room temperature. Reaction was monitored by TLC. The crude product was purified using flash-chromatography at 60^{o} C using toluene as eluant. Yield: 58%.

2.17.1.1 4-Hydroxy-4'-(undec-10-enoxy) biphenyl (I31)

Structure

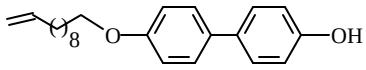

Formula $C_{23}H_{30}O_2$

Melting Point 133° C

IR (cm^{-1}) 3360 (OH), 3060, 980, 900 (=C-H), 2910, 2840, 1440, 1290, 720 (-CH_2-), 1630 (C=C), 1590 (C=C arom.), 1260 (Ar-OH)

^{1}H NMR (d) 7.4 (m, 4H), 6.9 (m, 4H), 5.8 (m, 1H), 5.0 (m, 2H), 3.9 (t, 2H), 1.96 (q, 2H), 1.7 (m, 2H), 1.3 (m, 12H)

Elemental Analysis

Calculated:	**C**	81.66%	**H**	8.88%	**O**	9.47%
Found:	**C**	82.01%	**H**	9.10%	**O**	8.89%

2.17.2 Synthesis of 4-(S-1-methylheptyloxy)-3-nitro benzoic acid

A solution of 57.8 g (220 mmol) triphenylphosphine, 4-hydroxy-3-nitro ethyl benzoate 32.4 g (154 mmol) and S(+) octanol 20.0 g (144 mmol) in tetrahydrofuran (300 mL) under nitrogen atmosphere was cooled to –20° C using CO_2/isopropanol bath. This was followed by drop-wise addition of diethylazodicarboxylate solution in 100 mL THF over a period of one hour, still maintaining the temperature at –20° C. After complete addition, the resulting solution was allowed to warm to room temperature and stirred overnight. The reaction was monitored by TLC. After completion of reaction, the solvent was removed in vacuo. Ether was added to the residue to precipitate triphenyl phosphine oxide and diethylazodicarboxylate which was removed by filtration. The filtrate (ether phase) was concentrated on rotavapor. To this was added 7.5 g sodium hydroxide in 40 mL water/100 mL ethanol and the reaction mixture was refluxed for 2 hours. Ethanol was then removed on rotavapor. The remaining solution was treated with 300 mL water and extracted with diethyl ether (3 times). The aqueous phase was acidified with concentrated hydrochloric acid. The product precipitated out and was filtered and dried on vacuum pump. Yield: 49%.

2.17.2.1 4-(S-1-Methylheptyloxy)-3-nitro benzoic acid (I32)

Structure

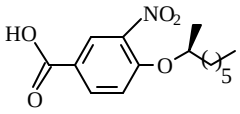

Formula $C_{15}H_{21}O_5N$

Melting Point 58° C

IR (cm^{-1}) 3200 (-OH), 2920, 2840, 1680 (C=O), 1600 (C=C) arom.), 1520, 1340 (NO_2), 1420 (C-H), 1270 (C-OH), 1230 (Aryl-O), 1020 (Alkyl-O)

^{1}H NMR (d) 8.8 (s, 1H), 8.4 (d, 1H), 7.3 (d, 1H), 4.8 (q, 1H), 1.6 (m, 2H), 1.4-1.3 (m, 11H), 0.96 (t, 3H)

Elemental Analysis

Calculated:	**C**	64.52%	**H**	7.53%	**O**	22.94%	**N**	5.02%
Found:	**C**	64.13%	**H**	7.83%	**O**	23.43%	**N**	5.32%

2.17.3 Synthesis of 4-[(S-1-methylheptyloxy)-3-nitro-1,4-phenylene carbonyloxy]-4'-(undec-10-enoxy) biphenyl (M34)

11.25 g (38.1 mmol) 4-(S-1-methylheptyloxy)-3-nitro benzoic acid, 12.96 g (38.1 mmol) 4-hydroxy-4'-(undec-10-enoxy) biphenyl and 0.46 g (3.8 mmol) 4-N,N-dimethylaminopyridine were dissolved in 650 mL of dry dichloromethane. To this solution 8.15 g (39.5 mmol) 1,3-dicyclohexylcarbodiimide (DCCI) was added and the resulting solution was allowed to stir at room temperature for 24 hours. The reaction was monitored by thin layer chromatography. After the reaction was complete, the resulting solution was filtered and the filtrate was dried on the rotavapor. The crude product obtained was purified by flash-chromatography on silica gel 60 using petroleum ether:ethyl acetate (5:1) as eluant. Yield: 44%.

2.17.3.1 4-[(S-1-Methylheptyloxy)-3-nitro-1,4-phenylene carbonyloxy]-4'-(undec-10-enoxy) biphenyl (M34)

Structure

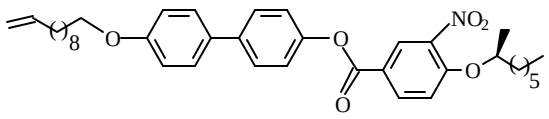

Formula $C_{38}H_{49}O_6N$

Melting Point 62° C

IR (cm^{-1}) 2920, 2840, 1420 (-C-H), 1680 (C=O), 1600 (C=C arom.), 1520, 1340 (NO_2), 1230 (Aryl-O), 1020 (Alkyl-O)

^{1}H NMR (d)	8.6 (s, 1H), 8.2 (d, 1H), 7.1 (d, 1H), 6.9 (d, 2H), 6.7 (d, 2H), 5.7 (m, 1H), 4.9 (m, 2H), 4.5 (m, 1H), 3.8 (m, 2H), 1.3-2.0 (m, 29H), 0.96 (m, 3H)							
Elemental Analysis	Calculated:	**C**	74.15%	**H**	7.97%	**O**	15.61%	**N** 2.28%
	Found:	**C**	74.15%	**H**	8.18%	**O**	15.30%	**N** 2.37%

2.18 1-[(S-2-Methylbutyl)oxycarbonyl-1,4-phenylene oxycarbonyl]-4-(hex-5-enoxy) phenylene (M35)

The synthetic scheme is given in Scheme 2.30.

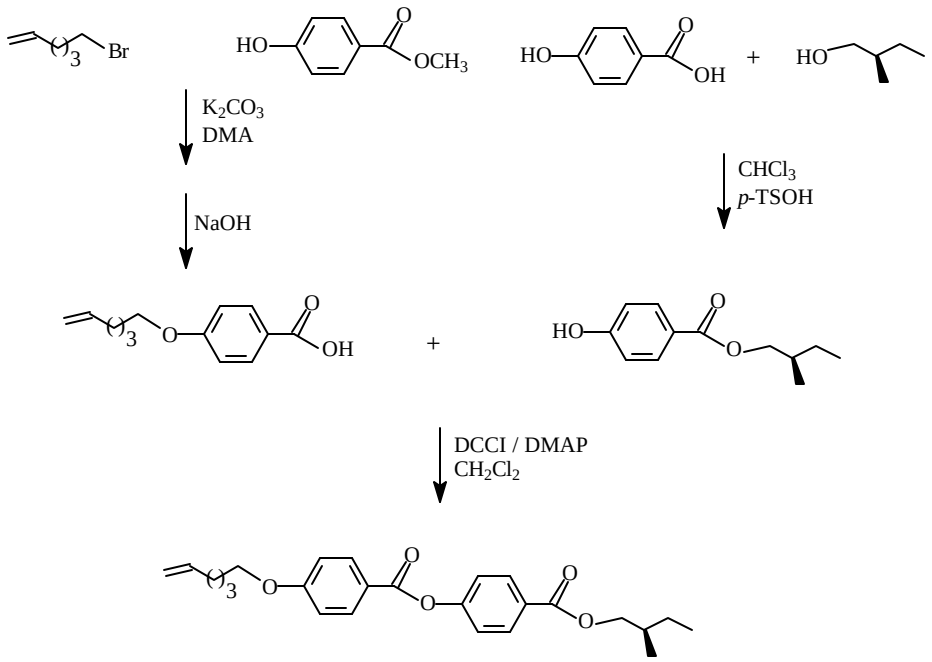

Scheme 2.30: Synthesis of 1-[(S-2-methylbutyl) oxycarbonyl-1,4-phenylene oxycarbonyl]-4-(hex-5-enoxy) phenylene (M35)

2.18.1 Synthesis of 4-(hex-5-enoxy) benzoic acid

4-(Hex-5-enoxy) benzoic acid was synthesised by following the procedure given in Section 2.17.1. The crude product was purified by recrystallisation from methanol. Yield: 82%.

2.18.1.1 4-(Hex-5-en-oxy) benzoic acid (I33)

Structure

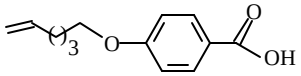

Formula	$C_{13}H_{16}O_3$						
Melting Point	101.9° C						
IR (cm^{-1})	3060, 980, 900 (=C-H), 2910, 2840 (CH_2), 1645 (C=O), 1630 (C=C), 1590 (C=C arom.)						
^{1}H NMR (d)	11.2 (s, 1H), 8.0 (d, 2H), 6.9 (d, 2H), 6.2-5.6 (m, 1H), 5.2-4.9 (m, 2H), 4.1 (t, 2H), 2.8-2.3 (m, 6H)						
Elemental Analysis	Calculated:	**C**	70.91%	**H**	7.27%	**O**	21.82%
	Found:	**C**	71.11%	**H**	7.87%	**O**	21.64%

2.18.2 Synthesis of 4-(S-2-methylbutyl oxycarbonyl) phenol

A mixture of 42.9 g (480 mmol) S-2-methylbutan-1-ol, 62.2 g 4-hydroxy benzoic acid and 2.5 g of p-toluenesulphonic acid in 200 mL of chloroform was refluxed for 60 h in a Dean-Stark apparatus. For the last 24 h of the reaction, molecular sieves 4 Å were added to the Dean-Stark apparatus as drying agent for the refluxed solvent. Then the solvent was evaporated in vacuum. The residue was dissolved in 30 mL ether. The organic solution was washed three times with 2N sodium hydroxide solution. Organic phase was dried over anhydrous sodium sulphate and ether was evaporated. The product obtained was dried under vacuum. The product was a highly viscous yellow oil. Yield: 68%.

2.18.2.1 4-(S-2-Methylbutyl oxycarbonyl) phenol (I34)

Structure

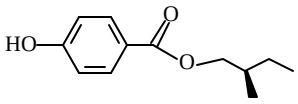

Formula	$C_{12}H_{16}O_3$						
IR (cm^{-1})	3400 (OH), 1750 (C=O)						
^{1}H NMR (d)	7.2 (d, 2H), 4.1 (m, 2H), 2.1-0.6 (m, 9H)						
Elemental Analysis	Calculated:	**C**	67.35%	**H**	8.16%	**O**	24.49%
	Found:	**C**	67.05%	**H**	8.32%	**O**	24.97%

2.18.3 Synthesis of 1-[(S-2-methylbutyl) oxycarbonyl-1,4-phenylene oxycarbonyl]-4-(hex-5-enoxy) phenylene (M35)

The synthesis of 1-[(S-2-methylbutyl) oxycarbonyl-1,4-phenylene oxycarbonyl]-4-(hex-5-enoxy) phenylene (**M35**) follows the same procedure as given in Section 2.17.3. Yield: 60%.

2.18.3.1 1-[(S-2-Methylbutyl) oxycarbonyl-1,4-phenylene oxycarbonyl]-4-(hex-5-en-oxy) phenylene (M35)

Structure

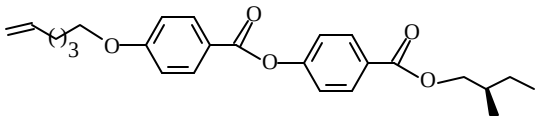

Formula $C_{25}H_{30}O_5$

Melting Point 45.7° C

IR (cm^{-1}) 3040 (C-H, arom.); 2940-2860 (alkyl C-H); 1710 (C=O)

^{1}H NMR (d) 8.2-8.0 (m, 4H), 7.4 (d, 2H), 7.1 (d, 2H), 5.9 (m, 1H), 5.1 (m, 2H), 4.3-4.1 (m, 2H), 2.3-1.0 (m, 15H)

Elemental Analysis

Calculated:	**C**	73.2%	**H**	7.3%	**O**	19.5%
Found:	**C**	72.9%	**H**	7.4%	**O**	19.7%

2.19 1-[(S-1-Methylheptyloxy)-3-nitro-1,4-phenylene carbonyloxy]-4-(undec-10-enoxy) phenylene (M36)

Monomer (**M36)** was synthesised as shown in Scheme 2.31 below:

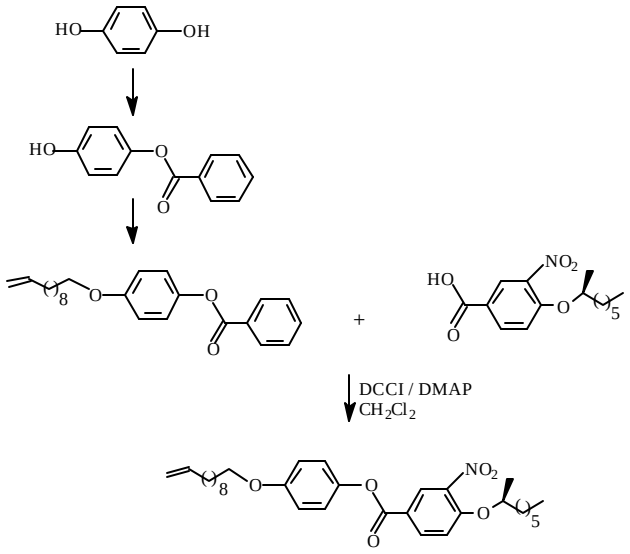

Scheme 2.31: Synthesis of 1-[(S-1-methylheptyloxy)-3-nitro-1,4-phenylene carbonyloxy]-4-(undec-10-enoxy) phenylene (M36)

2.19.1 Synthesis of 4-(undec-10-enoxy) phenol

46.3 g 1-[(phenylene carbonyloxy)-4-(undec-10-enoxy)] phenylene and 10.1 g sodium hydroxide were dissolved in a mixture of ethanol /water (175/75 mL) and stirred over night. The reaction is monitored by TLC. After completion of reaction, ethanol was evaporated and the rest was taken up in 600 mL 2M sodium hydroxide and extracted seven times with 300 mL ether. The organic phase was dried over magnesium sulphate and the solvent was evaporated to dryness. The crude product was purified by column chromatography. Yield: 62%.

2.19.1.1 4-(Undec-10-enoxy) phenol (I35)

Structure

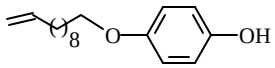

Formula $C_{17}H_{26}O_2$

Melting Point 65° C

IR (cm^{-1}) 3435 (OH), 2919, 2851 (CH_2), 1630 (C=C), 1608, 1516 (C=C arom.)

^{1}H NMR (d) 6.8 (m, 4H), 5.8 (m, 1H), 5.0 (m, 2H), 3.9 (t, 2H), 1.9 (q, 2H), 1.7 (m, 2H), 1.2-1.4 (m, 12H)

Elemental Analysis

Calculated:	**C**	77.86%	**H**	9.92%	**O**	12.21%
Found:	**C**	77.64%	**H**	10.23%	**O**	11.91%

2.19.2 Synthesis of 1[(S-1-methylheptyloxy)-3-nitro-1,4-phenylene carbonyloxy]-4-(undec-10-enoxy) phenylene (M36)

The synthesis of monomer **M36** follows the procedure given in Section 2.17.3. Pentafluorophenol (a pinch) was added to increase the yield of the reaction. Yield: 40%.

2.19.2.1 1[(S-1-Methylheptyloxy)-3-nitro-1,4-phenylene carbonyloxy]-4-(undec-10-enoxy) phenylene (M36)

Structure

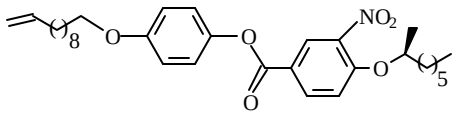

Formula $C_{32}H_{45}O_6N$

IR (cm^{-1}) 2920, 2840, 1420 (-C-H), 1680 (C=O), 1600 (C=C arom.), 1520, 1340 (NO_2), 1230 (Aryl-O), 1020 (Alkyl-O)

^{1}H NMR (d)	8.6 (s, 1H), 8.2 (d, 1H), 7.1 (d, 1H), 6.9 (d, 2H), 6.7 (d, 2H), 5.7 (m, 1H), 4.9 (m, 2H), 4.5 (m, 1H), 3.8 (m, 2H), 2.0-1.3 (m, 29H), 0.96 (m, 3H)

Elemental Analysis								
Calculated:	**C**	71.24%	**H**	7.35%	**O**	17.81%	**N**	2.60%
Found:	**C**	71.42%	**H**	7.95%	**O**	17.63%	**N**	3.11%

2.20 4-Nitro/cyano-4'-(undec-10-enoxy) azobenzene (M37)/ (M39) *and* 2,5-dimethyl-4-nitro-4'-(undec-10-enoxy) azobenzene (M38)

Monomers **M37**, **M38** and **M39** were synthesised as shown in Scheme 2.32.

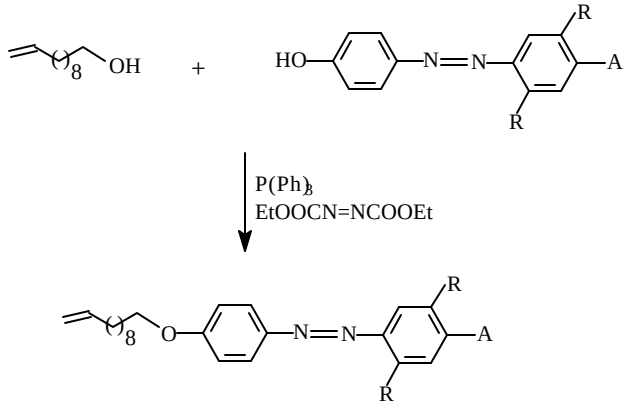

A = NO_2 / CN and R = H /CH_3

Scheme 2.32: Synthesis of 4-nitro/cyano-4'-(undec-10-enoxy) azobenzene (M37)/ (M39) *and* 2,5-dimethyl-4-nitro-4'-(undec-10-enoxy) azobenzene (M38)

2.20.1 Synthesis of 4-nitro/cyano-4'-(undec-10-enoxy) azobenzene (M37)/ (M39)/ and 2,5-dimethyl-4-nitro-4'-(undec-10-enoxy) azobenzene (M38)

4-Hydroxy-4'-nitroazobenzene **(I36)** was prepared by standard diazotisation procedure (20). Mitsunobu condensation reaction was used for the synthesis of monomer **M37** as given in Section 2.17.2. The crude product was purified by flash-chromatography (P.E/EE). Yield: 52%.

2.20.1.1 4-Nitro-4'-(undec-10-enoxy) azobenzene (M37)

Structure

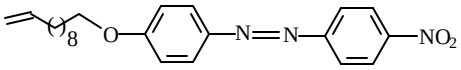

Formula	$C_{23}H_{29}O_3N_3$
Melting Point	87° C
IR (cm^{-1})	2920, 2840, 1680 (C=O), 1600 (C=C arom.), 1520, 1490 (N=N), 1420 (C-H), 1340 (NO_2), 1230 (Aryl-O), 1020 (Alkyl-O)

^{1}H NMR (d)	7.4 (m, 4H), 6.9 (m, 4H), 5.8 (m, 1H), 5.0 (m, 2H), 3.9 (t, 2H), 3.9 (t, 2H), 1.96 (q, 2H), 1.7 (m, 2H), 1.3 (m, 12H)								
Elemental Analysis	Calculated:	**C**	69.87%	**H**	7.34%	**O**	12.15%	**N**	10.63%
	Found:	**C**	69.58%	**H**	7.82%	**O**	11.90%	**N**	10.26%

2,5-Dimethyl-4-hydroxy-4'-nitro azobenzene **(I37)** and 4-hydroxy-4'-cyano azobenzene **(I38)** were prepared by standard diazotisation procedure (20). Mitsunobu condensation reaction was used for the synthesis of monomers 2,5-dimethyl-4'-nitro-4-(undec-10-enoxy) azobenzene **(M38)** and 4'-cyano-4-(undec-10-enoxy) azobenzene **(M39)** as presented in Section 2.17.2. The crude product was purified by flash-chromatography (petroleum ether/ethyl acetate).

2.21 1-{[(S-2-Chloro-4-methyl) pent-1-yloxy]-1,4-phenylene carbonyloxy}-4-(undec-10-enoxy) phenylene (M40)

Monomer **M40** was synthesised as shown in Scheme 2.33.

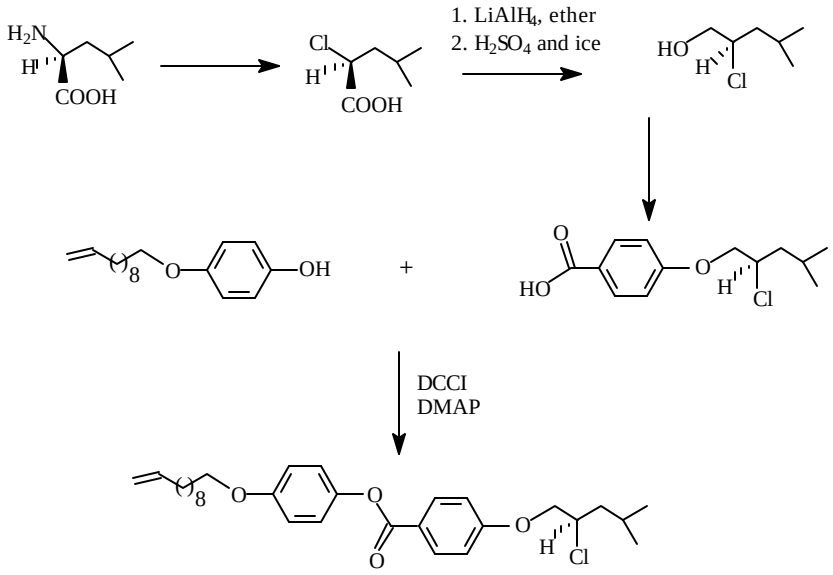

Scheme 2.33: Synthesis of 1-{[(S-2-chloro-4-methyl)pent-1-yloxy]-1,4-phenylene carbonyloxy}-4-(undec-10-enoxy) phenylene (M40)

2.21.1 Synthesis of S-2-chloro-4-methylpentan-1-oic acid

A partially soluble solution of L-Leucine was prepared by taking 100 g of it in 1 L of dilute hydrochloric acid. To this a cold solution of aqueous sodium nitrite was added dropwise. The reaction mixture was stirred for 3 days after which fresh nitrogen was

bubbled through the reaction mixture to remove the dissolved nitrogen. To this solution sodium bicarbonate was added to make the solution pH 3 and extracted thrice with ether. The ether extracts were dried over anhydrous magnesium sulphate and the solvent was evaporated under reduced pressure. The crude product was purified by fractional distillation. Yield: 72%.

2.21.1.1 S-2-Chloro-4-methylpentan-1-oic acid (I39)

Structure

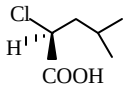

Formula $C_6H_{11}O_2Cl$

Melting Point 90^o C (1 mbar)

IR (cm^{-1}) 3100 (OH), 2960, 2870 (CH_2), 1715 (C=O)

^{1}H NMR (d) 10.3 (s, 1H), 4.3 (t, 1H), 1.85 (m, 3H), 0.95 (d, 6H)

Elemental Analysis

Calculated:	**C**	47.84%	**H**	7.31%	**O**	21.26%
Found:	**C**	48.14%	**H**	7.82%	**O**	21.07%

2.21.2 Synthesis of S-2-chloro-4-methylpentan-1-ol

79.2 g S-2-Chloro-4-methylpentan-1-oic acid was added drop-wise to a suspension of lithium aluminium hydride $LiAlH_4$ in ether (KOH dried) pre-cooled to –20 to -10^o C (using an isopropanol/dry ice bath). After the addition was complete, the reaction mixture was stirred for 4 hours at 0^o C. The contents were again cooled to -10^o C and ethyl acetate (99 mL) was added drop-wise. The ester was hydrolysed by addition of a mixture of sulphuric acid and ice, maintaining the reaction temperature at -10^o C. The organic phase was then separated from the aqueous phase. The aqueous phase was extracted with ether (2 times). The organic phase was dried over anhydrous magnesium sulphate and evaporated to dryness under reduced pressure. The pure product was obtained as a colourless liquid by fractional distillation. Yield: 80%.

2.21.2.1 S-2-Chloro-4-methylpentan-1-ol (I40)

Structure

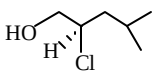

Formula	$C_6H_{12}OCl$						
Melting Point	39° C (0.15 mbar)						
IR (cm^{-1})	3360 (OH), 2960, 2930 (CH_2)						
^{1}H NMR (d)	3.95 (m, 1H), 3.55 (d, 2H), 2.55 (s, 1H), 1.7 (m, 1H), 1.45 (d, 2H), 0.8 (d, 6H)						
Elemental Analysis	Calculated:	**C**	53.14%	**H**	8.86%	**O**	11.81%
	Found:	**C**	52.94%	**H**	9.06%	**O**	12.11%

2.21.3 Synthesis of 4-(S-2-chloro-4-methylpent-1-yloxy) benzoic acid

4-(S-2-Chloro-4-methylpent-1-yloxy) benzoic acid was prepared following the procedure given in Section 2.17.2. Yield: 55%.

2.21.3.1 4-(S-2-Chloro-4-methyl pent-1-yloxy) benzoic acid (I41)

Structure

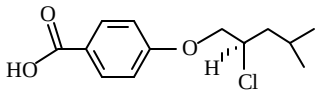

Formula	$C_{13}H_{17}O_3Cl$						
Melting Point	110° C						
IR (cm^{-1})	2940 (CH_2), 1600 (C=C arom.), 1230 (Aryl-O), 1020 (Alkyl-O)						
^{1}H NMR (d)	8.0 (d, 2H), 6.9 (d, 2H), 4.1 (m, 3H), 1.9 (m, 1H), 0.9 (m, 6H)						
Elemental Analysis	Calculated:	**C**	60.82%	**H**	6.63%	**O**	18.71%
	Found:	**C**	60.53%	**H**	6.84%	**O**	18.33%

2.21.4 Synthesis of 1-{[(S-2-chloro-4-methyl)pent-1-yloxy]-1,4-phenylene carbonyl oxy}-4-(undec-10-enoxy) phenylene (M40)

1-{[(S-2-Chloro-4-methyl) pent-1-yloxy]-1,4-phenylene carbonyloxy}-4-(undec-10-enoxy) phenylene (**M40**) was prepared according to the procedure given in Section 2.17.3. The crude product was recrystallised from ethanol. Yield: 77%.

2.21.4.1 1-{[(S-2-Chloro-4-methyl) pent-1-yloxy]-1,4-phenylene carbonyloxy}-4-(undec-10-enoxy) phenylene (M40)

Structure

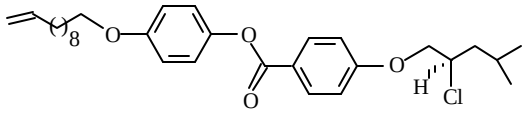

Formula $C_{30}H_{41}O_4Cl$

Melting Point 55° C

IR (cm^{-1}) 3071, 980, 900 (=C-H), 2920, 2852 (CH_2), 1736 (C=O), 1630 (C=C), 1590 (C=C arom.)

^{1}H NMR (d) 8.1 (d, 2H), 7.0 (d, 2H), 6.9 (d, 2H), 6.85 (d, 2H), 5.75 (m, 1H), 4.85 (m, 2H), 4.1 (m, 3H), 3.85 (t, 2H), 1.95 (q, 2H), 1.85 (m, 1H), 1.65 (m, 4H), 1.25 (m, 12H), 0.9 (m, 6H)

Elemental Analysis

Calculated:	**C**	71.93%	**H**	8.19%	**O**	12.79%
Found:	**C**	71.74%	**H**	8.55%	**O**	12.56%

2.22 1,4-Bis(undec-10-enoxy) phenylene (M41)

The cross-linker **(M41)** was synthesised as shown in Scheme 2.34.

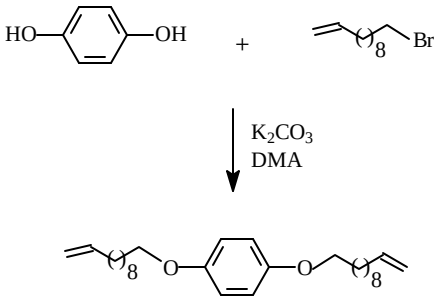

Scheme 2.34: Synthesis of 1,4-bis(undec-10-enoxy) phenylene (M41)

The cross-linker (**M41**) was prepared by the procedure given in Section 2.17.1. The crude product was purified by flash-chromatography using petroleum ether:ethyl acetate (5:1) as eluant. The compound was further purified by recrystallisation from methanol. Yield: 68%.

2.22.1 1,4-Bis(undec-10-enoxy) phenylene (M41)

Structure

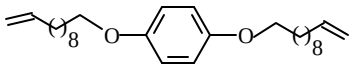

Formula $C_{28}H_{46}O_2$

Melting Point 60° C

IR (cm^{-1})	3071, 980, 900 (=C-H), 1630 (C=C), 2919, 2851 (CH_2), 1608, 1500 (C=C arom.)						
^{1}H NMR (d)	6.8 (m, 4H), 6.1-5.6 (m, 2H), 5.1-4.8 (m, 4H), 3.9 (t, 4H), 2.2-1.2 (m, 32H)						
Elemental Analysis	Calculated:	**C**	81.16%	**H**	11.11%	**O**	7.73%
	Found:	**C**	81.65%	**H**	10.71%	**O**	7.51%

2.23 Physico-chemical characterisation of synthesised materials

The following characterisation techniques were used to analyse the synthesised monomers and polymers.

Melting points were determined on a MEL-TEMP II capillary melting point apparatus (Laboratory Devices, USA). Elemental analyses (C, H, N, O) were determined on Carlo Erba CHNSO elemental analyser EA 1108, using helium as the carrier gas. Halogens were estimated by Waters 432 ion chromatography using thermal conductivity detector. The column was HR 4.6 x 75 mm. The mobile phase was sodium borate gluconate of pH 8.5.

Infra-red spectra of polymers in potassium bromide pellets were recorded on Shimadzu IR-470 unit calibrated with standard polystyrene film. Analytical reagent grade potassium bromide was dried under vacuum at 100^o C and stored in the vacuum dessicator. 100 mg of KBr and 1 mg of the sample were used to prepare the pellet. The infra-red data were collected at 2 cm^{-1} resolutions with a minimum of 128 scans between 4000 and 400 cm^{-1}wave number.

Nuclear magnetic resonance (NMR) spectroscopy (^{1}H) was carried out on a Brucker NMR spectrometer, operating at static magnetic field strength of 4.7 MHz. 200 and 300 MHz MAS/cross polarisation (CP) techniques were used at speeds of 3.5 KHz. Spectra were acquired at room temperature in deutrated chloroform or dimethyl sulphoxide. Proton and carbon spectra were collected with a spectral width of 4000 and 20,000 Hz respectively. All samples were prepared by dissolving 5 mg in 0.2 mL deuterated solvent. The data were obtained with a pulse width of 15 μsec (90°), gain time of 0.819 sec and 1-sec interval between pulses. Proton carbon bond connectivities were obtained by 2D spectra. Both the HETCOR and LRHETCOR experiments were carried out with an F1 spectral width of 2493 Hz and F2 spectral width of 1650 Hz. The data gained over an acquisition period of 9.062 sec was digitised by 2048 points in F2. A total of 128 increments were acquired in F2 utilising 32 scans for HETCOR experiments and

238 scans for the LRHETCOR. An one band coupling of 140 Hz was used to earn the HETCOR experiments while 7.5 Hz was selected for the long variant. Sine ball weighing was applied in both dimensions prior to zero filling, 2048 V 256 and Fourier transformation. All chemical shifts were expressed in ppm downfield from internal standard tetramethyl silane. Coupling constant (J) is in Hz.

Differential Scanning Calorimetry were recorded with 10 ± 2 mg specimen on Mettler TA 4000 with the TC 11 processor and 30 S DSC cell at a heating/cooling rate of 10^o C/min with nitrogen flow of 30 cm^3/min. The DSC unit was calibrated for temperature and enthalpy with indium. The lag between sample and pan holder temperature was also taken into account and computed through indium crystallisation tests. The samples were taken in standard aluminium pans with gold nickel thermoelement sensor. The data processing unit allowed automatic subtraction of the base line and normalisation of the thermogram for the sample weight. The thermal transitions were determined. The glass transition temperature, T_g, was taken as the middle point of the heat capacity change.

Thermogravimetric analysis (TGA) was performed on Seiko Instruments SSC 5100 model coupled with TG/DTA 32. Experiments were conducted with a sample size of 5 $\pm$ 2 mg, heated at 10^o C/min under/air at a flow rate of 50 cm^3/min. Samples were taken in platinum pan and calibrated with calcium oxalate, indium and zinc.

Mass spectra were recorded on Finnigon Mat 1020 B unit with solid probe, from ambient to 300^o C. The probe temperature was maintained at each step until a significant decrease occurred in the total ion current. This treatment effectively reduced the amount of volatile material for the next higher temperature run. Both 70 eV and 20 eV (electron volt) energies were used. The former for higher sensitivity and the latter with reduced fragmentation for information on molecular weight. The emission current was 100 mA at 10^{-4} Torr. Molecular weights of soluble polymers were determined using Knauer vapour pressure osmometer at 30^o C in chloroform or in DMSO at 80^o C using benzil as standard. 0.5 wt % sample solutions with four different concentrations were used. The molecular weights were calculated using the following formula:

$$K_{sample} = [\Delta T/C]_{C=O}$$

$M_n = K_{std} / K_{sample} = X$ g/mol where X = molecular weight of sample.

2.24 REFERENCES

1. Hauser, C. R. and Lednicer, D., *J. Org. Chem.*, **24**, 46 (1959).
2. Ehrhardt, R. L., Gopalkrishnan, G. and Hogg, J. L., *J. Org. Chem.*, **48**, 1586 (1983).
3. Bigelow, L. A. and Eatough, H., *Org. Syn. Coll. Vol.* **1**, 80 (1941).
4. Weingarten, H., Chupp, J. P. and White, W., *J. Org. Chem.*, **32**, 3246 (1967).
5. Brady, W. T. and Shieh, C. H., *J. Org. Chem.*, **48**, 2499 (1983).
6. Kajimoto, T. and Tsuji, J., *J. Org. Chem.*, **48**, 1685 (1983).
7. Demailly, G. and Solladie, G., *J. Org. Chem.*, **46**, 3102 (1981).
8. Dinizo, S. E. and Watt, D. S., *J. Amer. Chem. Soc*., **97**, 6900 (1975).
9. Babler, J. H. and Invergo, B. J., *J. Org. Chem.*, **46**, 1937 (1981).
10. Sommers, A. H. and Aaland, S. E., *J. Org. Chem.*, **21**, 484 (1956).
11. Campbell, K. N., Sommers, A. H. and Campbell, B. K., *J. Amer. Chem. Soc*., **66**, 82 (1944).
12. Mosher, W. A. and Piesch, S., *J. Org. Chem.*, **35**, 1026 (1970).
13. Sawhney, K. N. and Lemke, T. M., *J. Org. Chem.*, **48**, 4326 (1983).
14. Hutchins, R. O., Su, W. –Y., Cistone, F. and Stercho, Y. P., *J. Org. Chem.*, **48**, 3412 (1983).
15. Sannicolo, F., *J. Org. Chem.*, **48**, 2924 (1983).
16. Pugh, C. and Percec, V., *Polym. Bull*., **16**, 521 (1986).
17. Pugh, C. and Percec, V., *Polym. Bull*., **16**, 513 (1986).
18. Rodriguez-Parada, J. M. and Percec, V., *J. Poly. Sci. Polym. Chem. ed*., **24**, 1363 (1986).
19. Mitsunobu, O., *Synthesis*, **1** (1981).
20. Zollinger, H., *Diazo Chemistry*, Verlag Chemie: Veinheim (1994).

3

Synthesis of POLYMERS

3 Synthesis of polymers

3.1 Introduction

A major virtue of radical polymerisation is that it can typically be carried out under relatively undemanding conditions. The reaction also exhibits a tolerance to trace impurities. Staudinger (1) was the first to propose the concept of a chain polymerisation and define the basic structure of polymer molecules produced by such mechanisms. He proposed that the monomer residue [Figure 3.1(a)] were connected, head to tail, by covalent linkages in large cyclic structures [Figure 3.1(b)]. The basic mechanism of free-radical polymerisation as we know it today (2) (Scheme 3.1), was laid out in the 1940s and 50s (3,4).

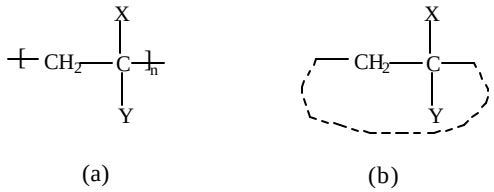

(a) (b)

Figure 3.1 Staudinger formula

The essential features of this mechanism are initiation and propagation steps which involve radical addition to the less substituted end of the double bond ("tail addition"), and a termination step, which involves disproportionation or combination between two growing chains. Polymers formed by radical polymerisation came to be represented by and their physical properties and chemistry interpreted in terms of the simple formula [Figure 3.1 (a)] proposed by Staudinger (1). However, this formula has serious limitations when it comes to understanding the detailed chemistry of polymeric materials.

3.2 Free radical polymerisation

The radical reaction is dependent on reaction conditions (such as temperature, solvent etc.). Radical additions to double bonds are in general, exothermic processes and rates increase with increasing temperature. Rates of propagation in radical polymerisation and reactivity ratios in copolymerisation can show marked variation according to the solvent employed (5-9). The simple initiation process does not proceed according to the

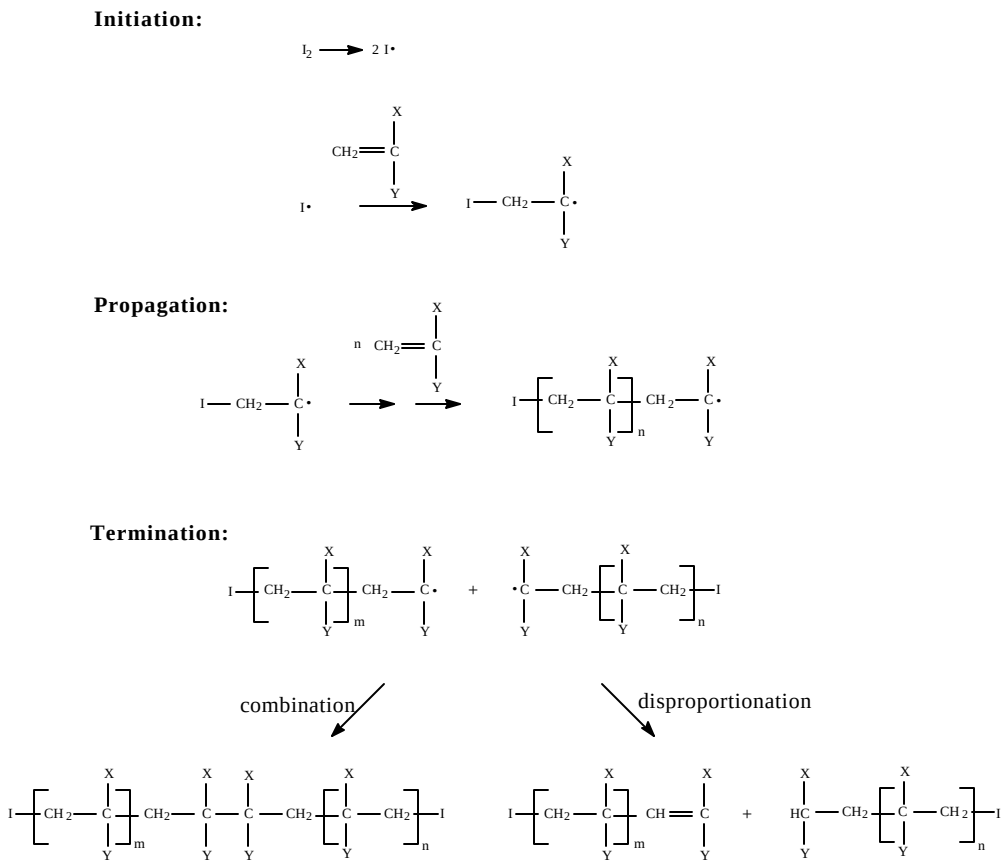

Scheme 3.1: Mechanism of free radical polymerisation

rule, as the yield of the primary radicals is usually not 100%. This is due to the rearrangement or fragmentation of primary radicals to form new species other than monomer. The commonly used initiators are azobisisobutyronitrile (AIBN), dibenzoyl peroxide (BPO) and di-*t*-butylperoxide (DBPOX). The primary radicals formed from these initiators are shown in Scheme 3.1. The propagation step of radical polymerisation comprises sequence of radical additions to carbon-carbon double bonds. In order to produce high molar mass polymers, a propagating radical must show a high degree of specificity in its reactions with unsaturated systems. Termination is a diffusion-controlled process. The rate of reaction is dependent on how fast the radical centres of the propagating chains come together.

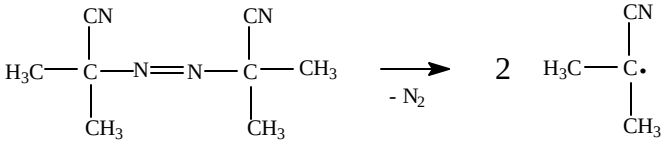

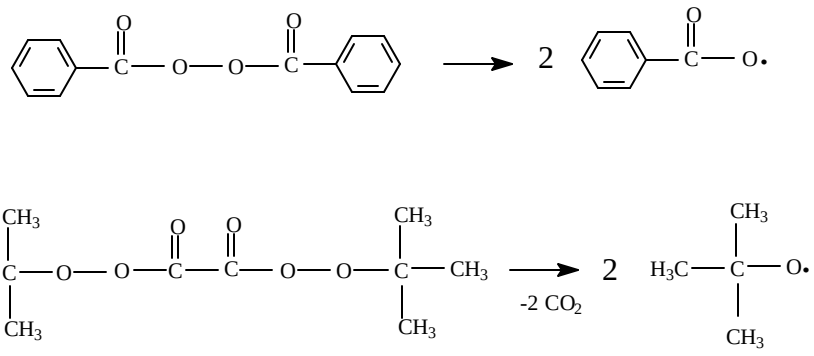

Scheme 3.2: Primary radicals formed from initiators

3.3 Synthesis of polymethacrylates

2,2'-Azobisisobutyronitrile (AIBN) (S.D. Fine Chemicals, Mumbai, India) was recrystallised twice from methanol before use. Dimethylsulphoxide (DMSO) (S.D. Fine Chemicals, Mumbai, India) was dried over activated alumina overnight, then stirred over calcium hydride for 4-5 hours and decanted. It was then purified by vacuum distillation and stored over 4Å molecular sieves.

A representative radical polymerisation procedure is as follows: In the presence of nitrogen atmosphere, the monomer, initiator azobisisobutyronitrile (2 mol% of monomer) were taken in dimethylsulphoxide. The resulting solution was degassed and sealed under vacuum. The polymerisation was carried out at 70^{o} C. After polymerisation was complete (24 to 48 hours), the solution was poured in excess methanol and stirred for 1 hour. The precipitated polymer was filtered and washed with methanol. Thus, the obtained polymer was dried under vacuum below T_g.

The methacrylate monomers were synthesised as described in Sections 2.3, 2.9 and 2.14.3. The polymerisation proceeded as shown in Scheme 3.3. The following polymers were synthesised in the polymethacrylate series. The characterisation data is presented in Section 3.3.1. The ^{1}H NMR spectra taken in $CDCl_3$ or *d*-DMSO, depending on the solubility of the polymer, are presented in Appendix II. The number-average molecular weight (M_n), determined by vapour pressure osmometric measurements (using either chloroform at 40^{o} C or dimethylsulphoxide at 80^{o} C as solvent, depending on the solubility of the polymer), were in the range 5,600 to 7,200. The thermal properties (T_g)

of polymers were determined by DSC. These showed a wide temperature range from 20 to 117^{o} C.

No.	Polymer	Code
1	Poly{[N-(4'-formyl benzylidene)aniline-4-oxyethyl] methacrylate}	**V 1**
2	Poly{[N-(4'-methinebarbiturate benzylidene)aniline-4-oxyethyl] methacrylate}	**V 2**
3	Poly[(4'-methinebarbiturate azobenzene-4-oxyethyl) methacrylate]	**V 3**
4	Poly{[5-[N-(4'-cyano benzylidene) amine]-1,3,4-thiadiazole-2-thioethyl] methacrylate}	**V 4**
5	Poly{[5-[N-(4'-nitro benzylidene) amine]-1,3,4-thiadiazole-2-thioethyl] methacrylate}	**V 5**

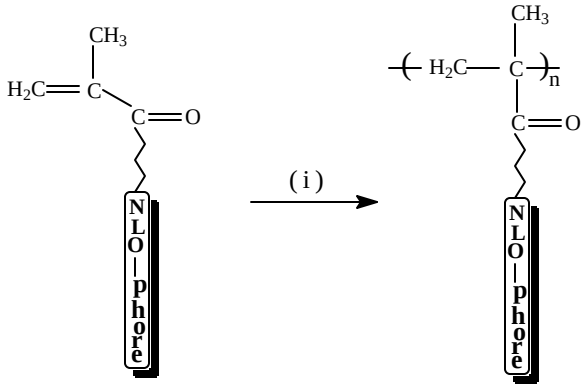

(i) = AIBN, dimethylsulphoxide (dry), 70^{o} C

Scheme 3.3: Polymerisation of methacrylates

3.3.1 Characterisation of polymethacrylates

3.3.1.1 Poly{[N-(4'-formyl benzylidene)aniline-4-oxyethyl] methacrylate} (V 1)

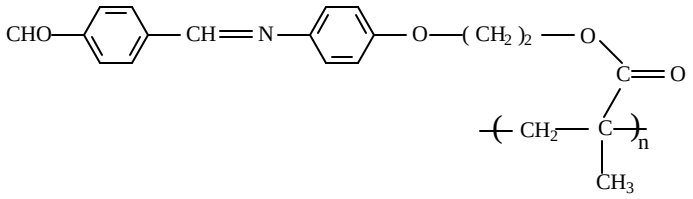

Yield	45%
T_g	117^{o} C
UV (λ_{max})	346 nm
IR (cm^{-1})	1740, 1710, 1675, 1615, 1500
^{1}H NMR (d)	10.1 (1H), 8.4 (1H), 8.0 (6H), 6.8 (2H), 4.4 (4H), 1.8 (2H), 1.1 (3H)
M_n (VPO)	5,900

3.3.1.2 Poly{[N-(4'-methinebarbiturate benzylidene)aniline-4-oxyethyl]methacrylate} (V 2)

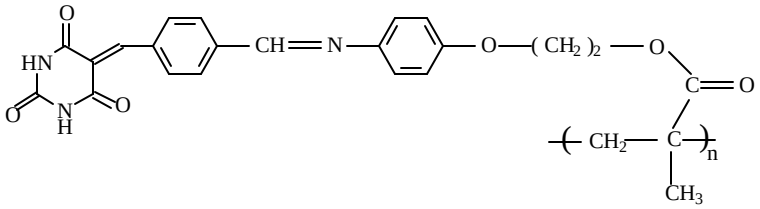

Yield	52%
UV (λ_{max})	346 nm
IR (cm^{-1})	3500-3350, 1725, 1710, 1675, 1615, 1500
^{1}H NMR (d)	11.5 (2H), 8.5 (2H), 7.9 (6H), 6.9 (2H), 4.2 (4H), 1.8 (2H), 1.1 (3H)
M_n (VPO)	5,600

3.3.1.3 Poly[(4'-methinebarbiturate azobenzene-4-oxyethyl) methacrylate] (V 3)

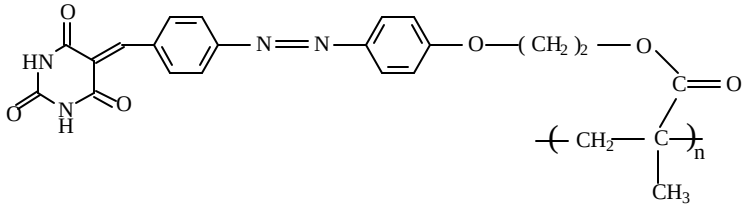

Yield	81%
T_g	76^o C
UV (λ_{max})	346 nm
IR (cm^{-1})	3500-3350, 1725, 1710, 1585, 1490
^{1}H NMR (d)	11.5 (2H), 8.4 (1H), 7.9-7.6 (6H), 7.0 (2H), 4.4-4.2 (4H), 1.8 (2H), 1.1 (3H)
M_n (VPO)	6,000

3.3.1.4 Poly{[5-[N-(4'-cyanobenzylidene)amine]-1,3,4-thiadiazole-2-thioethyl] methacrylate} (V 4)

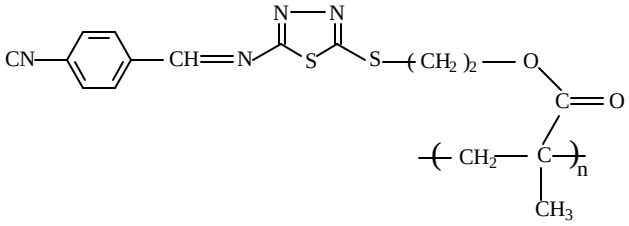

Yield	61%
T_g	57^o C
UV (λ_{max})	335 nm
IR (cm^{-1})	3800, 1700, 1585, 1490, 1340
^{1}H NMR (d)	7.9-7.6 (4H), 4.4 (2H), 3.8 (2H), 2.0 (2H), 1.1 (3H)
M_n (VPO)	7,200

3.3.1.5 Poly{[5-[N-(4'-nitrobenzylidene)amine]-1,3,4-thiadiazole-2-thioethyl] methacrylate} (V 5)

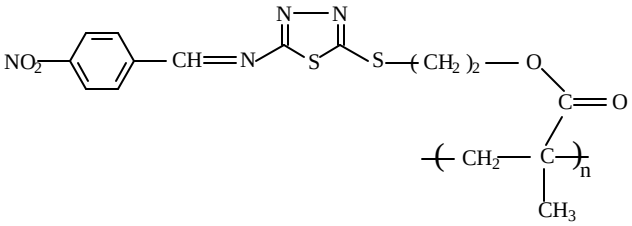

Yield	52%
UV (λ_{max})	337 nm
IR (cm^{-1})	3800, 1700, 1585, 1490, 1340
^{1}H NMR (d)	7.9-7.6 (4H), 4.3 (2H), 3.8 (2H), 2.0 (2H), 1.1 (3H)
M_n (VPO)	5,600

3.4 Synthesis of polyacrylates

The acrylate monomers were synthesised as described in Sections 2.4, 2.10 and 2.14.4. The polyacrylates were synthesised according to the procedures reported in Section 3.3 and represented in Scheme 3.4. The following polymers were synthesised in the acrylate series. The characterisation data is presented in Section 3.4.1.

No.	Polymer	Code
1	Poly{[N-(4'-formyl benzylidene)aniline-4-oxyethyl] acrylate}	**V 6**
2	Poly{[N-(4'-methinebarbiturate benzylidene)aniline-4-oxyethyl] acrylate}	**V 7**
3	Poly[(4'-methinebarbiturate azobenzene-4-oxyethyl) acrylate]	**V 8**

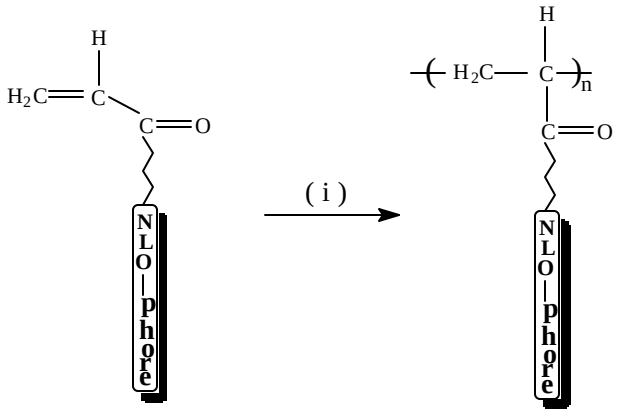

(i) = AIBN, dimethylsulphoxide (dry), 70° C

Scheme 3.4: Polymerisation of acrylates

3.4.1 Characterisation of polyacrylates

The ^{1}H NMR spectra taken in $CDCl_3$ or *d*-DMSO, depending on the solubility of the polymer, are presented in Appendix II. The number-average molecular weight (M_n), determined from vapour pressure osmometric measurements (using either chloroform at 40^o C or dimethylsulphoxide at 80^o C as solvent, depending on the solubility of the polymer), were in the range 2,710 to 3,200. The polyacrylate synthesised in this study were characterised for thermal properties using differential scanning calorimetry (DSC). These were much lower than the analogous polymethacrylates and were in the 20-25^o C range. The data for the polyacrylates synthesised in this study is presented below.

3.4.1.1 Poly{[N-(4'-formyl benzylidene)aniline-4-oxyethyl] acrylate} (V 6)

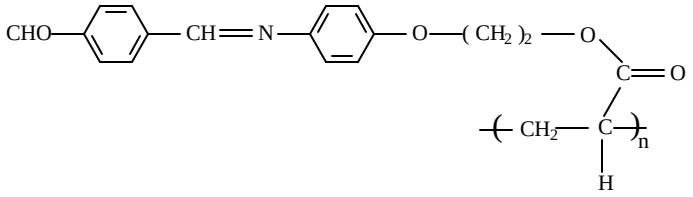

Yield	41%
UV (λ_{max})	346 nm
IR (cm^{-1})	1710, 1690, 1675, 1590, 1500
^{1}H NMR (d)	10.1 (1H), 8.5 (1H), 8.1 (6H), 6.8 (2H), 4.2 (4H), 1.8 (1H), 1.4 (2H)
M_n (VPO)	3,200

3.4.1.2 Poly{[N-(4'-methinebarbiturate benzylidene)aniline-4-oxyethyl] acrylate} (V 7)

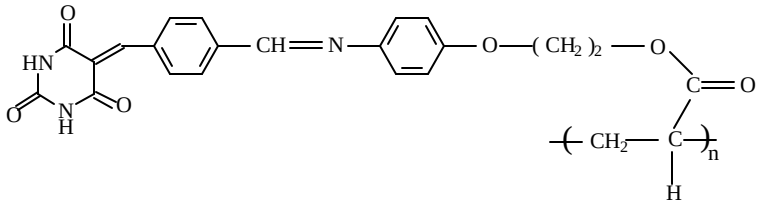

Yield	39%
T_g	20^o C
UV (λ_{max})	346 nm
IR (cm^{-1})	3500-3350, 1725, 1675, 1615, 1500
^{1}H NMR (d)	11.3 (2H), 8.5 (2H), 8.1 (6H), 6.8 (2H), 4.2 (4H), 1.8 (1H), 1.4 (2H)
M_n (VPO)	3,000

3.4.1.3 Poly[(4'-methinebarbiturate azobenzene-4-oxyethyl) acrylate] (V 8)

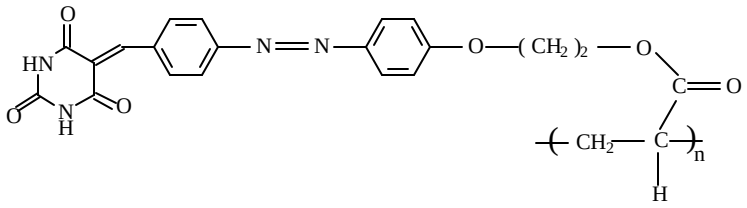

Yield	76%
T_g	-3° C
UV (l_{max})	346 nm
IR (cm^{-1})	1725, 1715, 1566, 1498
^{1}H NMR (d)	11.5 (2H), 8.4 (1H), 8.0-7.6 (6H), 7.1-6.9 (2H), 4.1 (4H), 1.8 (1H), 1.4 (2H),
M_n (VPO)	2,710

3.5 Synthesis of polystyrenes

The styrene monomers were synthesised as described in Sections 2.5, 2.11, 2.13.3, 2.13.5 and 2.14.5. The polymerisation proceeded as shown in Scheme 3.5 according to the procedure reported in Section 3.3.

No.	Polymer	Code
1	Poly[4-(4'-formyl benzylidene aniline-4-oxyethyloxy methylene) styrene]	**V 9**
2	Poly[4-(4'-nitro benzylidene aniline-4-oxyethyloxy methylene) styrene]	**V 10**
3	Poly[4-(4'-nitro aniline benzylidene-4-oxyethyloxy methylene) styrene]	**V 11**
4	Poly[4-(4'-cyano benzylidene aniline-4-oxyethyloxy methylene) styrene]	**V 12**
5	Poly[4-(4'-methinebarbiturate azobenzene-4-oxyethyloxy methylene) styrene]	**V 13**
6	Poly[4-(4'-methinebarbiturate benzylidene aniline-4-oxyethyloxy methylene) styrene]	**V 14**
7	Poly[4-(4'-nitro benzylidene amine-1,3,4-thiadiazole-2-thioethyloxy methylene)styrene]	**V 15**
8	Poly[4-(4'-cyano benzylidene amine-1,3,4-thiadiazole-2-thioethyloxy methylene)styrene]	**V 16**
9	Poly{4-[2-(4-nitrophenylene-1-azomethine)carbazolyl-N-(propyloxy methylene)]styrene}	**V 17**
10	Poly{4-[2-(4-cyanophenylene-1-azomethine)carbazolyl-N-(propyloxy methylene)]styrene}	**V 18**
11	Poly[4-(2-formyl carbazolyl-N-propyloxy methylene)styrene]	**V 19**

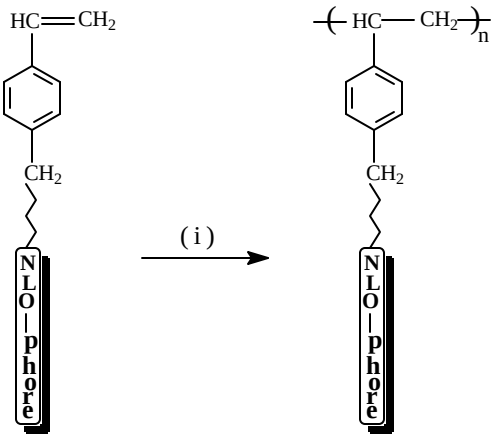

(i) = AIBN, dimethylsulphoxide (dry), 70° C

Scheme 3.5: Polymerisation of styrenes

3.5.1 Characterisation of polystyrenes

The ^{1}H NMR spectra taken in $CDCl_3$ or *d*-DMSO, depending on the solubility of the polymer, are presented in Appendix II. The number-average molecular weight (M_n), determined from vapour pressure osmometric measurements (using either chloroform at 40° C or dimethylsulphoxide at 80° C as solvent, depending on the solubility of the polymer), were in 4,750 to 11,050 range. The T_g of these polymers ranged from 30-115°C. The data for the polystyrenes synthesised in this study is presented below.

3.5.1.1 Poly[4-(4'-formyl benzylidene aniline-4-oxyethyloxy methylene) styrene] (V 9)

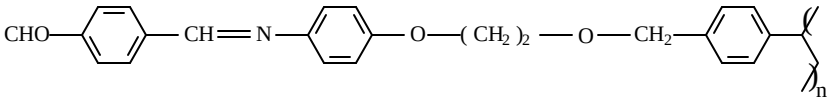

Yield	60%
T_g	112° C
UV (λ_{max})	345 nm
IR (cm^{-1})	3000, 1690, 1675, 1510, 1260
^{1}H NMR (d)	10.0 (1H), 8.5 (1H), 8.4-7.6 (7H), 7.4 (4H), 6.9 (2H), 4.6 (2H), 4.1 (2H), 3.8 (2H), 2.1 (1H), 1.35 (2H)
M_n (VPO)	8,600

3.5.1.2 Poly[4-(4'-nitro benzylidene aniline-4-oxyethyloxy methylene) styrene] (V 10)

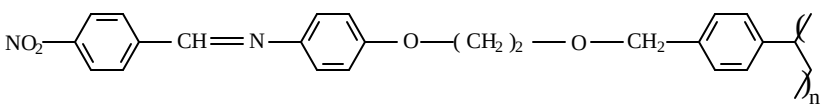

Yield	72%

T_g	25° C
UV (l_{max})	345 nm
IR (cm^{-1})	3000, 1675, 1510, 1340, 1260
^{1}H NMR (d)	8.2 (3H), 7.6-7.0 (8H), 6.8 (2H), 4.5 (2H), 4.2-3.8 (4H), 2.0 (1H), 1.4 (2H)
M_n (VPO)	6,990

3.5.1.3 Poly[4-(4'-nitro aniline benzylidene-4-oxyethyloxy methylene) styrene] (V 11)

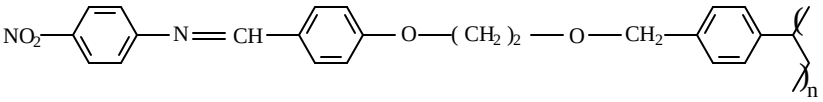

Yield	61%
T_g	70° C
UV (l_{max})	390 nm
IR (cm^{-1})	3000, 1675, 1510, 1340, 1260
^{1}H NMR (d)	8.0 (3H), 7.6-6.9 (8H), 6.6 (2H), 4.6 (2H), 3.8-3.6 (4H), 2.3 (1H), 1.6 (2H)
M_n (VPO)	4,800

3.5.1.4 Poly[4-(4'-cyano benzylidene aniline-4-oxyethyloxy methylene) styrene] (V 12)

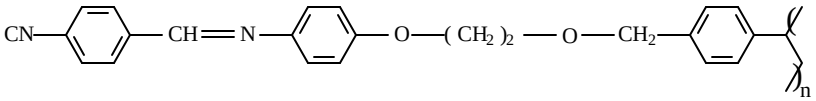

Yield	80%
T_g	30° C
UV (l_{max})	346 nm
IR (cm^{-1})	3000, 2230, 1675, 1510, 1260
^{1}H NMR (d)	8.2 (3H), 7.8 (4H), 7.4-7.2 (4H), 6.8 (2H), 4.7 (2H), 4.2-3.8 (4H), 2.1 (1H), 1.35 (2H)
M_n (VPO)	11,050

3.5.1.5 Poly[4-(4'-methinebarbiturate azobenzene-4-oxyethyloxy methylene)styrene] (V 13)

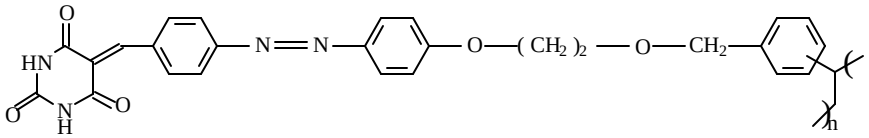

Yield	87%
T_g	20° C
UV (l_{max})	345 nm
IR (cm^{-1})	1725, 1615, 1580, 1495
^{1}H NMR (d)	11.5 (2H), 8.4 (1H), 8.1-7.8 (6H), 7.2 (4H), 6.9 (2H), 4.7 (2H), 4.1-3.8 (4H), 1.8 (1H), 1.4 (2H)
M_n (VPO)	5,100

3.5.1.6 **Poly[4-(4'-methinebarbiturate benzylideneaniline-4-oxyethyloxymethylene)styrene] (V 14)**

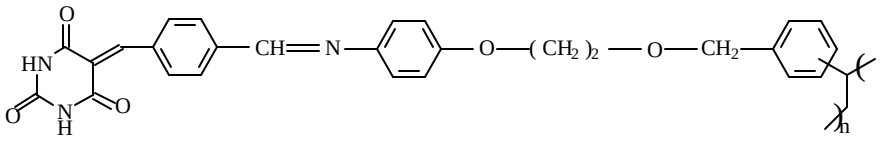

Yield	54%
T_g	25^o C
UV (l_{max})	301 nm
IR (cm^{-1})	3500, 3350, 1725, 1675, 1510, 1260
^{1}H NMR (d)	11.5-11.0 (2H), 8.5 (1H), 8.4-7.6 (7H), 7.4 (4H), 6.9 (2H), 4.6 (2H), 4.1 (2H), 3.8 (2H), 1.6 (1H), 1.35 (2H)
M_n (VPO)	4,750

3.5.1.7 **Poly[4-(4'-nitro benzylideneamine-1,3,4-thiadiazole-2-thioethyloxymethylene) styrene] (V 15)**

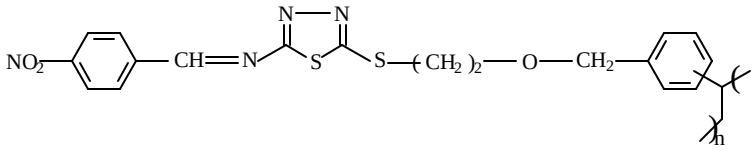

Yield	51%
UV (l_{max})	331 nm
IR (cm^{-1})	3500, 1585, 1490, 1340
^{1}H NMR (d)	7.9-7.2 (9H), 4.4 (2H), 3.8-3.6 (4H), 1.6 (1H), 1.3 (2H)
M_n (VPO)	7,000

3.5.1.8 **Poly[4-(4'-cyanobenzylideneamine-1,3,4-thiadiazole-2-thioethyloxymethylene) styrene] (V 16)**

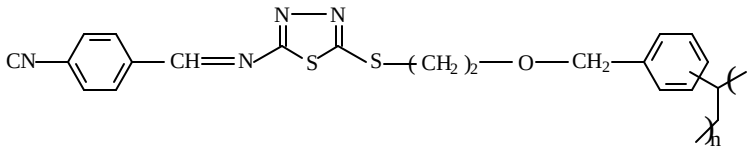

Yield	40%
T_g	100^o C
UV (l_{max})	340 nm
IR (cm^{-1})	3500, 2320, 1585, 1490
^{1}H NMR (d)	7.9-7.2 (9H), 4.4 (2H), 3.8-3.6 (4H), 1.6 (1H), 1.3 (2H)
M_n (VPO)	9,000

3.5.1.9 **Poly{4-[2-(4-nitrophenylene-1-azomethine)carbazolyl-N-(propyloxymethylene)] styrene} (V 17)**

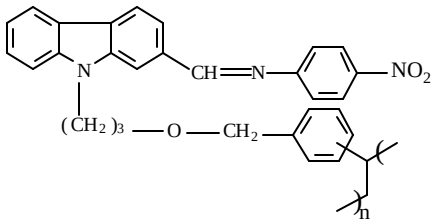

Yield	39%
UV (λ_{max})	389 nm
IR (cm^{-1})	3350, 2920, 1650, 1600, 1490, 1340
^{1}H NMR (d)	8.2-7.6 (7H), 7.5-6.8 (7H), 6.6 (2H), 4.6-3.7 (6H), 2.0-1.6 (3H), 1.3 (2H)
M_n (VPO)	7,200

3.5.1.10 **Poly{4-[2-(4-cyanophenylene-1-azomethine)carbazolyl-N-(propyloxymethylene)] styrene} (V 18)**

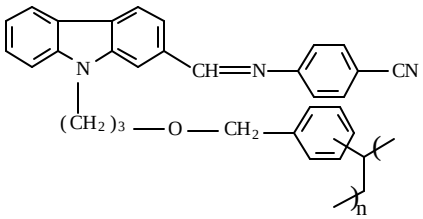

Yield	42%
UV (λ_{max})	305 nm
IR (cm^{-1})	3350, 2920, 2320, 1650, 1600, 1490
^{1}H NMR (d)	8.2-7.6 (6H), 7.5-6.8 (7H), 6.6 (2H), 4.6-3.7 (6H), 2.0-1.6 (4H), 1.3 (2H)
M_n (VPO)	8,100

3.5.1.11 **Poly[4-(2-formyl carbazolyl-N-propyloxy methylene)styrene] (V 19)**

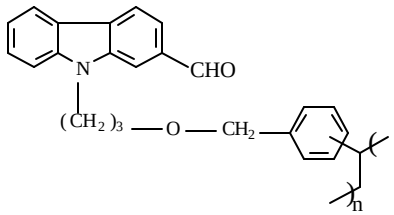

Yield	61%
T_g	59^o C
UV (λ_{max})	343 nm
IR (cm^{-1})	3500, 2920, 1680, 1600, 1490, 1460
^{1}H NMR (d)	10.0 (1H), 8.4-7.6 (4H), 7.5-6.6 (7H), 5.0 (2H), 3.7-3.5 (4H), 2.5 (1H), 1.7 (2H), 1.3 (2H)
M_n (VPO)	8,540

3.6 Synthesis of polymaleimides

The maleimide monomers were synthesised as described in Sections 2.6 and 2.12. The polymaleimides were synthesised as per the procedure given in Section 3.3 and represented in Scheme 3.6. The following polymaleimides were synthesised:

No.	Polymer	Code
1	Poly{N-[2-(4-nitro benzylidene aniline-4'-oxy)ethyl]maleimide}	**V 20**
2	Poly{N-[2-(4-cyano benzylidene aniline-4'-oxy)ethyl]maleimide}	**V 21**
3	Poly{N-[2-(4-formyl azobenzene-4'-oxy)ethyl]maleimide}	**V 22**
4	Poly{N-[6-(4-cyanobenzylidene aniline-4'-oxy)hexyl]maleimide}	**V 23**

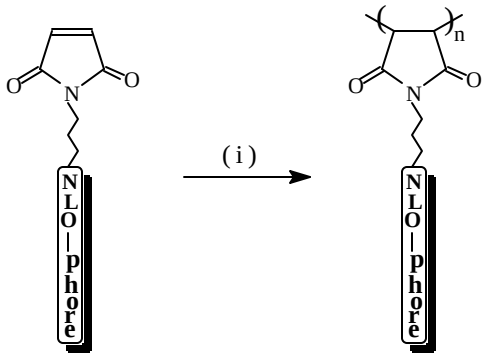

(i) = AIBN, dimethylsulphoxide (dry), 70° C

Scheme 3.6: Polymerisation of maleimides

3.6.1. Characterisation of polymaleimides

The ^{1}H NMR spectra taken in $CDCl_3$ or *d*-DMSO, depending on the solubility of the polymer, are presented in Appendix II. The number-average molecular weight (M_n), determined from vapour pressure osmometric measurements (using either chloroform at 40° C or dimethylsulphoxide at 80° C as solvent, depending on the solubility of the polymer), ranged between 6,700 to 11,250. The T_g in this series were approximately similar to the analogous polymethacrylates, polystyrenes and were better than that of corresponding polyacrylates. The data is presented below:

3.6.1.1 Poly{N-[2-(4-nitro benzylidene aniline–4'-oxy)ethyl]maleimide} (V 20)

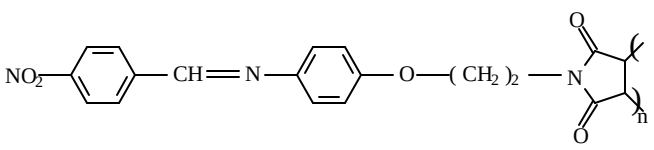

Yield	80%
T_g	60^o C
UV (l_{max})	378 nm
IR (cm^{-1})	1710, 1675, 1595, 1340
^{1}H NMR (d)	8.5 (1H), 8.0 (2H), 7.6 (2H), 7.1 (2H), 6.8 (2H),4.2-3.8 (4H), 3.8-3.2 (2H)
M_n (VPO)	6,700

3.6.1.2 Poly{N-[2-(4-cyano benzylidene aniline–4'-oxy)ethyl]maleimide} (V 21)

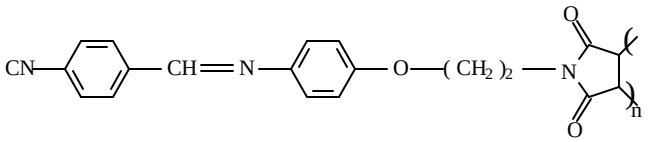

Yield	72%
T_g	105^o C
UV (l_{max})	304 nm
IR (cm^{-1})	2230, 1710, 1675, 1595
^{1}H NMR (d)	8.4 (1H), 7.9 (2H), 7.5 (2H), 7.1 (2H), 6.8 (2H), 4.2-3.8 (4H), 3.8-3.2 (2H)
M_n (VPO)	11,250

3.6.1.3 Poly{N-[2-(4-formyl azobenzene-4'-oxy)ethyl]maleimide} (V 22)

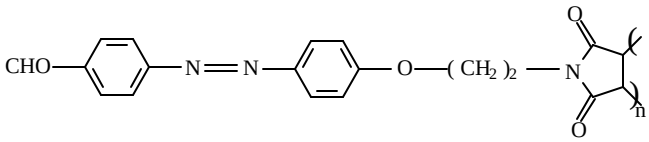

Yield	61%
T_g	40^o C
UV (l_{max})	359 nm
IR (cm^{-1})	1710, 1690, 1675, 1595
^{1}H NMR (d)	10.0 (1H), 8.0-7.6 (4H), 7.2 (2H), 6.8 (2H), 4.2-3.8 (4H), 3.8-3.2 (2H)
M_n (VPO)	8,100

3.6.1.4 Poly{N-[6-(4-cyano benzylidene aniline-4'-oxy)hexyl]maleimide} (V 23)

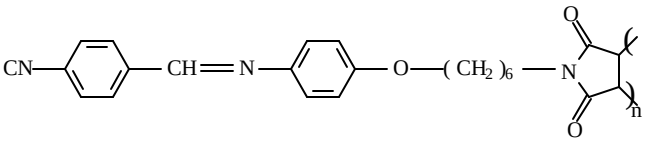

Yield	90%
T_g	30^o C
UV (l_{max})	376 nm
IR (cm^{-1})	2230, 1710, 1675, 1595
^{1}H NMR (d)	8.5 (1H), 7.9 (2H), 7.7 (2H), 7.2 (2H), 6.8 (2H), 4.2-3.8 (4H), 3.8-3.2 (2H), 2.0-1.4 (8H)
M_n (VPO)	10,100

3.7 Synthesis of copolymers of N-substituted maleimide with styrene and N-vinyl carbazole

The substituted maleimide monomers were synthesised as described in Section 2.6. The copolymers were synthesised as shown in Scheme 3.7. Styrene (Merck) was distilled under vacuum. N-vinylcarbazole (Aldrich) was used as received. 2,2-Azobisisobutyronitrile (AIBN) (S.D. Fine Chemicals, India) was recrystallised twice from methanol. 1,4-Dioxane was dried over potassium hydroxide and sodium and purified by vacuum distillation and stored over 4Å molecular sieves.

Copolymerisation was carried out by dissolution of the two monomers 4-[6-(N-maleimido)hex-1-yloxy]-N-(4'-cyano/nitro benzylidene)aniline : styrene (1:1) and monomers 4-[6-(N-maleimido)hex-1-yloxy]-N-(4'-cyano/nitro benzylidene)aniline : N-vinylcarbazole (1:1) in 1,4-dioxane using AIBN (~1 mol%) as initiator at 70^{o} C for 24 hours under nitrogen atmosphere. The polymers were precipitated in 50 mL methanol and purified by reprecipitation.

No.	Polymer	Code
1	Poly[{N-[6-(4-cyano benzylidene aniline-4'-oxy)hexyl]maleimide}-co-styrene]	**V 24**
2	Poly[{N-[6-(4-nitro benzylidene aniline-4'-oxy)hexyl]maleimide}-co-styrene]	**V 25**
3	Poly[{N-[6-(4-cyano benzylidene aniline-4'-oxy)hexyl]maleimide}-co-N-vinylcarbazole]	**V 26**
4	Poly[{N-[6-(4-nitro benzylidene aniline-4'-oxy)hexyl]maleimide}-co-N-vinylcarbazole]	**V 27**

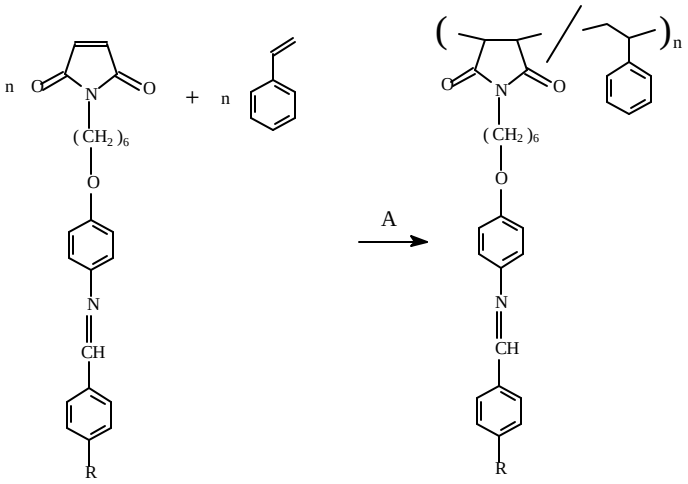

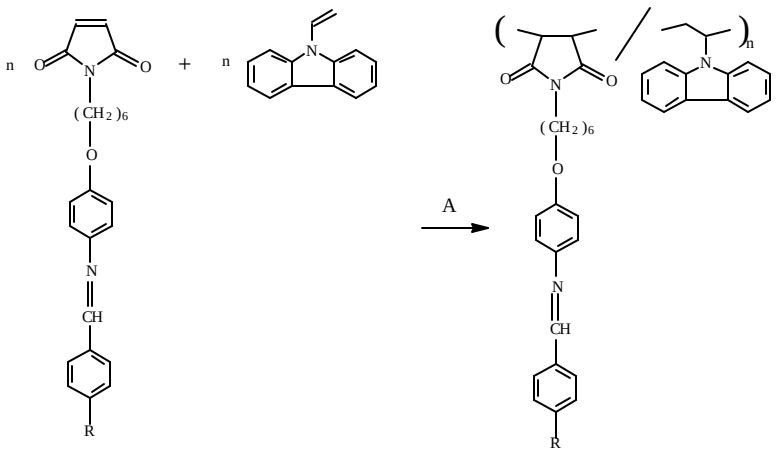

A = AIBN, 1,4-dioxane (dry), 70° C
R = NO_2, CN

Scheme 3.7: Synthesis of copolymers

3.7.1 Characterisation of copolymers of N-substituted maleimide with styrene and N-vinyl carbazole

The ^{1}H NMR spectra taken in $CDCl_3$ or *d*-DMSO depending on the solubility of the copolymer are presented in Appendix II. The number-average molecular weight (M_n), determined from vapour pressure osmometric measurements (using either chloroform at 40° C or dimethylsulphoxide at 80° C as solvent, depending on the solubility of the polymer), were between 4,255 and 7,100. The T_g in these series ranged from 60-70° C.

3.7.1.1 Poly[{N-[6-(4-cyano benzylidene aniline-4'-oxy)hexyl] maleimide}-co-styrene] (V 24)

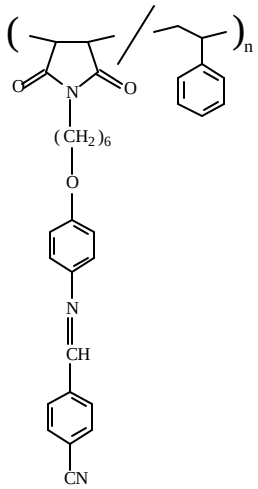

Yield	71%
T_g	74° C
UV (λ_{max})	363 nm
IR (cm^{-1})	3000, 2230, 1715, 1675, 1650

^{1}H NMR (d)	8.1 (3H), 7.9 (2H), 7.5-6.8 (9H), 4.5-4.1 (4H), 4.0-2.0 (2H, overlapped with the signals of solvent), 2.0-1.5 (11H)
M_n (VPO)	5,100

3.7.1.2 Poly[{N-[6-(4-nitro benzylidene aniline-4'-oxy)hexyl] maleimide}-co-styrene] (V 25)

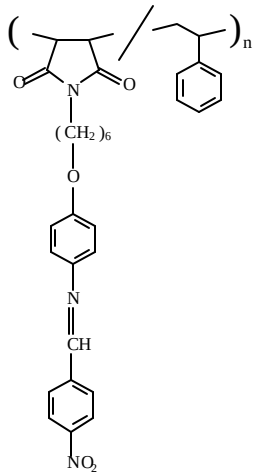

Yield	65%
T_g	66^o C
UV (l_{max})	384 nm
IR (cm^{-1})	3000, 1715, 1675, 1650, 1340
^{1}H NMR (d)	8.1 (3H), 7.9 (2H), 7.5-6.8 (9H), 4.5-4.1 (4H), 4.0-2.0 (2H, overlapped with the signals of solvent), 2.0-1.5 (11H)
M_n (VPO)	4,255

3.7.1.3 Poly[{N-[6-(4-cyano benzylidene aniline-4'-oxy)hexyl] maleimide}-co-N-vinyl carbazole] (V 26)

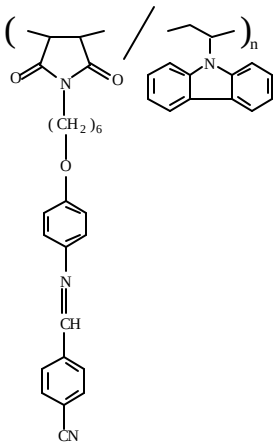

Yield	61%
T_g	63^o C
UV (l_{max})	384 nm
IR (cm^{-1})	3000, 1715, 1675, 1650, 1340
^{1}H NMR (d)	8.5 (1H), 8.0 (4H), 7.6 (4H), 7.5-7.1 (4H), 6.8 (4H), 4.0-3.6 (4H), 3.5-2.4 (4H, overlapped with signals of solvent), 2.3 (1H), 2.0-1.5 (8H)

M_n (VPO) 7,100

3.7.1.4 **Poly[{N-[6-(4-nitro benzylidene aniline-4'-oxy)hexyl] maleimide}-co-N-vinyl carbazole] (V 27)**

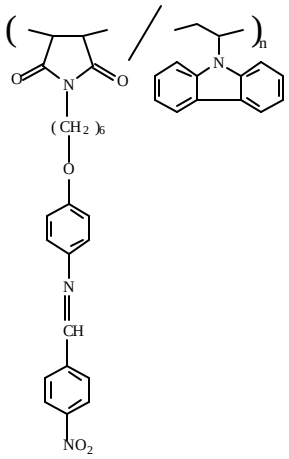

Yield 70%

T_g 71^o C

UV (l_{max}) 364 nm

IR (cm^{-1}) 3000, 2230, 1715, 1675, 1650

^{1}H NMR (d) 8.5 (1H), 8.0 (4H), 7.6 (4H), 7.5-7.1 (4H), 6.8 (4H), 4.0-3.6 (4H), 3.5-2.4 (4H, overlapped with signals of solvent), 2.3 (1H), 2.0-1.5 (8H)

M_n (VPO) 6,000

3.8 Synthesis of polyurethanes

The diols were synthesised as described in Sections 2.15 and 2.16. The polyurethanes were synthesised by reaction of diol with diisocyanates and this is represented in Schemes 3.8 and 3.9.

3.8.1 *Synthesis of polyurethanes using 2,4-tolylene diisocyanate (TDI)*

A 100-mL two-neck, round bottom flask containing 0.5 g (0.0013 mol) of 4-[γ-(2,3-dihydroxy propaneoxy)propyloxy]-4'-nitro azobenzene (**M28**) was connected to a condenser and purged with nitrogen for 20 minutes to remove the atmospheric moisture. To the flask, 1 mL of dry dimethylformamide and 1 equivalent (0.23 g, 0.0013 mol) of 2,4-tolylene diisocyanate were added. The reaction mixture was heated to 110^o C and kept at this temperature for 12 h. After the solution was allowed to cool to ambient temperature, it was poured into cold water and filtered. Poly{iminocarbonyloxy(2-[4-methyleneoxypropyloxy-4'-nitro azobenzene] ethane) oxycarbonylimino(4-methyl-1,3-phenylene)} **V 32** obtained was washed with water and methanol several times. After

drying it under vacuum at room temperature for 1 hour, the crude product was stirred in hot methanol to remove monomer, low molecular weight dimer, trimer and so on. The polymer was then filtered and dried in a vacuum desiccator. The other polymers **V 28**, **V 30**, **V 36**, **V 38**, **V 34** were prepared by reaction of respective diols with 2,4-tolylene diisocyanate (TDI).

3.8.2 *Synthesis of polyurethanes using methylene-4,4'-bis(phenyl isocyanate) (MDI)*

A 100 mL two-neck round bottom flask containing a mixture of 4-[γ-(2,3-dihydroxy propaneoxy)propyloxy]-4'-nitro azobenzene (**M28**) (0.5 g, 0.0013 mol) and 0.33 g (0.0013 mol) of methylene-4,4'-bis(phenyl isocyanate)was purged with nitrogen gas. Poly{iminocarbonyloxy(2-[4-methylene oxypropyloxy-4'-nitro azobenzene] ethane) oxycarbonylimino(1,4-phenylene)methylene(1',4'-phenylene)} **V 33** was synthesised by following the same procedure in Section 3.8.1. The polymers **V 29**, **V 31**, **V 33**, **V 35**, **V 37**, **V 39** were synthesised following procedure given in Section 3.8.1 from respective diols and methylene-4,4'-bis(phenyl isocyanate) (MDI).

No.	Polymer	Code
1	Poly{iminocarbonyloxy(2-[(4-methyleneoxyethyloxy)-N-(4'-nitro benzylidene)aniline]ethane)oxycarbonylimino(4-methyl-1,3-phenylene)}	**V 28**
2	Poly{iminocarbonyloxy(2-[(4-methyleneoxyethyloxy)-N-(4'-nitro benzylidene)aniline]ethane)oxycarbonylimino(1,4-phenylene)methylene(1',4'-phenylene)}	**V 29**
3	Poly{iminocarbonyloxy(2-[(4-methyleneoxyethyloxy)-N-(4'-cyano benzylidene)aniline]ethane)oxycarbonylimino(4-methyl-1,3-phenylene)}	**V 30**
4	Poly{iminocarbonyloxy(2-[(4-methyleneoxyethyloxy)-N-(4'-cyano benzylidene)aniline]ethane)oxycarbonylimino(1,4-phenylene)methylene(1',4'-phenylene)}	**V 31**
5	Poly{iminocarbonyloxy(2-[4-methyleneoxypropyloxy-4'-nitro azobenzene]ethane)oxycarbonylimino(4-methyl-1,3-phenylene)}	**V 32**
6	Poly{iminocarbonyloxy(2-[4-methyleneoxypropyloxy-4'-nitro azobenzene]ethane)oxycarbonylimino(1,4-phenylene)methylene(1',4'-phenylene)}	**V 33**
7	Poly{iminocarbonyloxy(2-[4-methyleneoxypropyloxy-4'-cyano azobenzene]ethane)oxycarbonylimino(4-methyl-1,3-phenylene)}	**V 34**
8	Poly{iminocarbonyloxy(2-[4-methyleneoxypropyloxy-4'-cyano azobenzene]ethane)oxycarbonylimino(1,4-phenylene)methylene(1',4'-phenylene)}	**V 35**
9	Poly{iminocarbonyloxy(2-[4'-propyloxy-4-nitro azobenzene]propane)oxycarbonylimino(4-methyl-1,3-phenylene)}	**V 36**

10	Poly{iminocarbonyloxy(2-[4'-propyloxy-4-nitro azobenzene]propane)oxycarbonylimino(1,4-phenylene)methylene(1',4'-phenylene)}	**V 37**
11	Poly{iminocarbonyloxy(2-[4'-propyloxy-4-cyano azobenzene]propane)oxycarbonylimino(4-methyl-1,3-phenylene)}	**V 38**
12	Poly{iminocarbonyloxy(2-[4'-propyloxy-4-cyano azobenzene]propane)oxycarbonylimino(1,4-phenylene)methylene(1',4'-phenylene)}	**V 39**

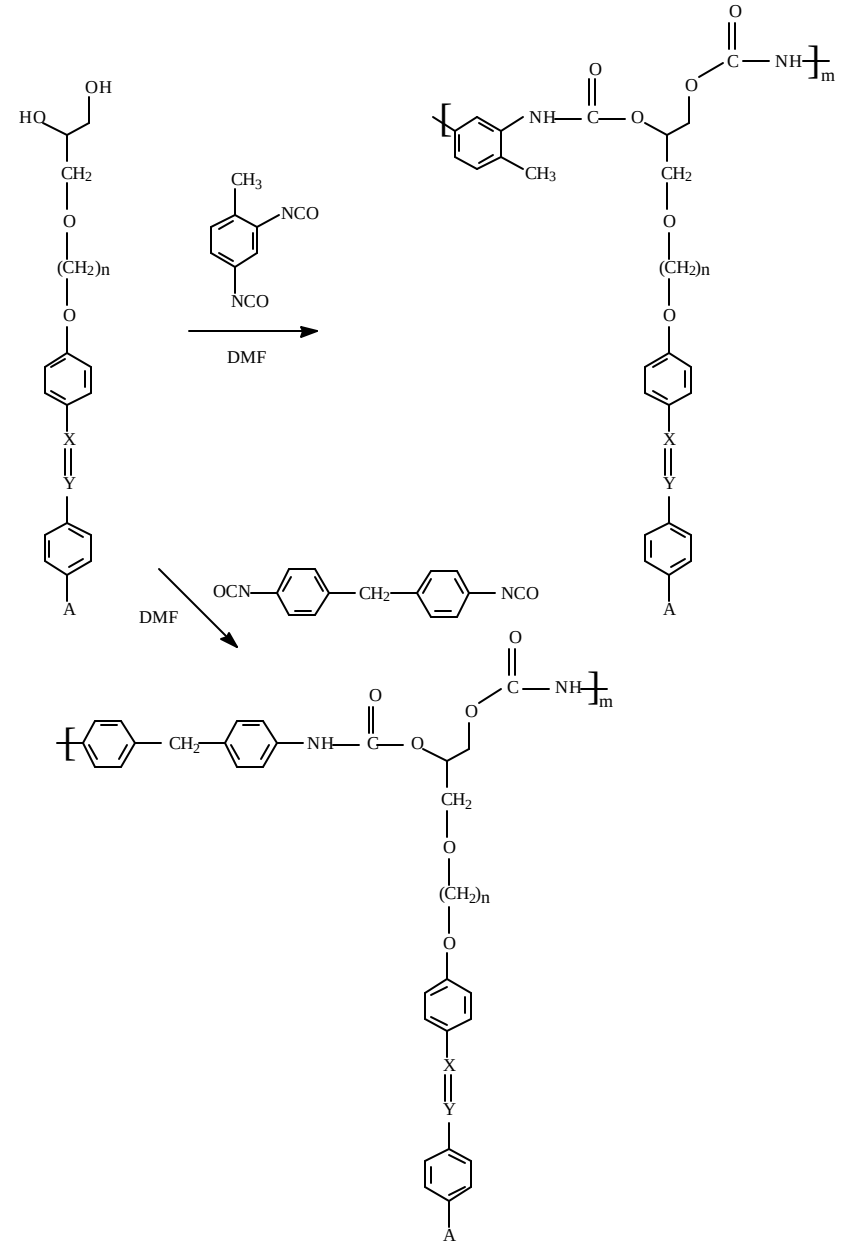

Scheme 3.8: Synthesis of polyurethanes from unsymmetrical diols

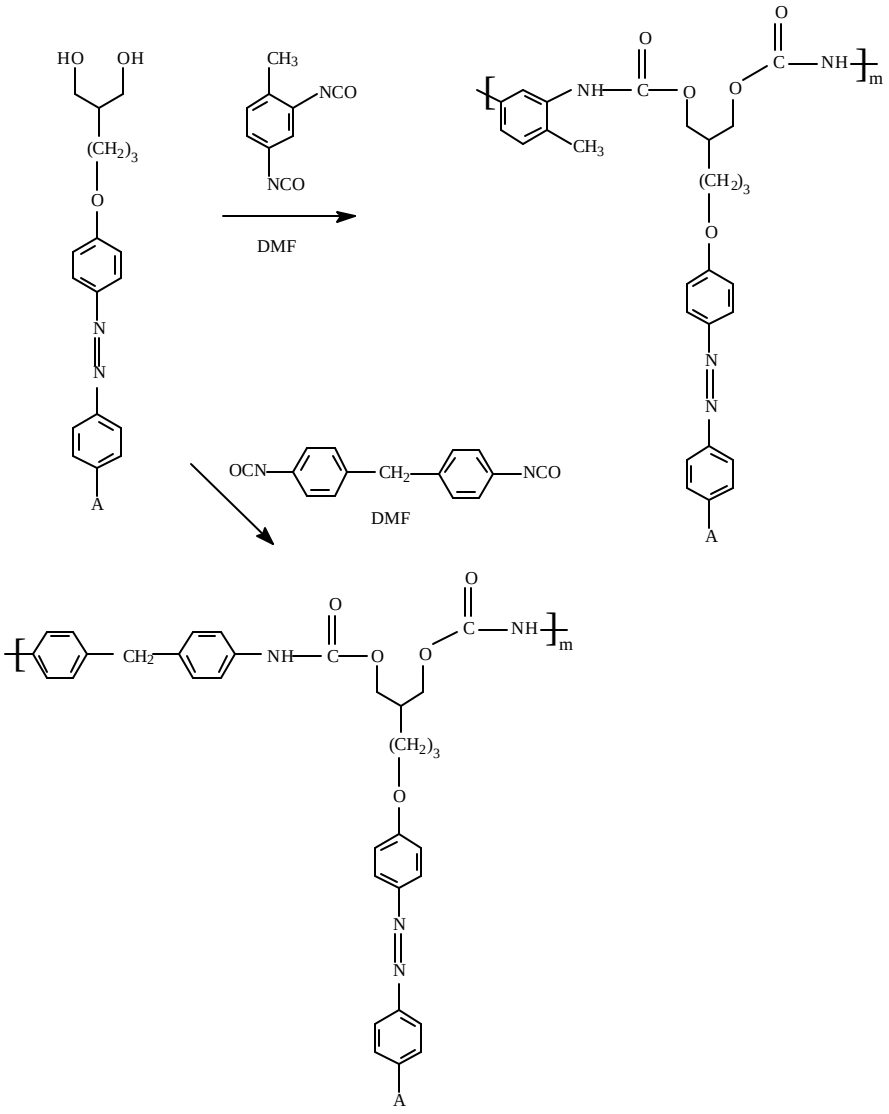

A = NO_2 / CN

Scheme 3.9: Synthesis of polyurethanes from symmetrical diols

3.8.3 Characterisation of polyurethanes

The ^{1}H NMR spectra taken in $CDCl_3$ or *d*-DMSO, depending on the solubility of the polyurethane, are presented in Appendix II. The number-average molecular weight (M_n), determined from vapour pressure osmometric measurements (in dimethylsulphoxide at 80^o C), ranged between 7,100 to 16,200. The T_g of polymers in this series were determined by DSC. The T_g values obtained ranged from 60-150^o C.

3.8.3.1 Poly{iminocarbonyloxy(2-[(4-methyleneoxyethyloxy)-N-(4'-nitro benzylidene)aniline]ethane)oxycarbonylimino(4-methyl-1,3-phenylene)} (V 28)

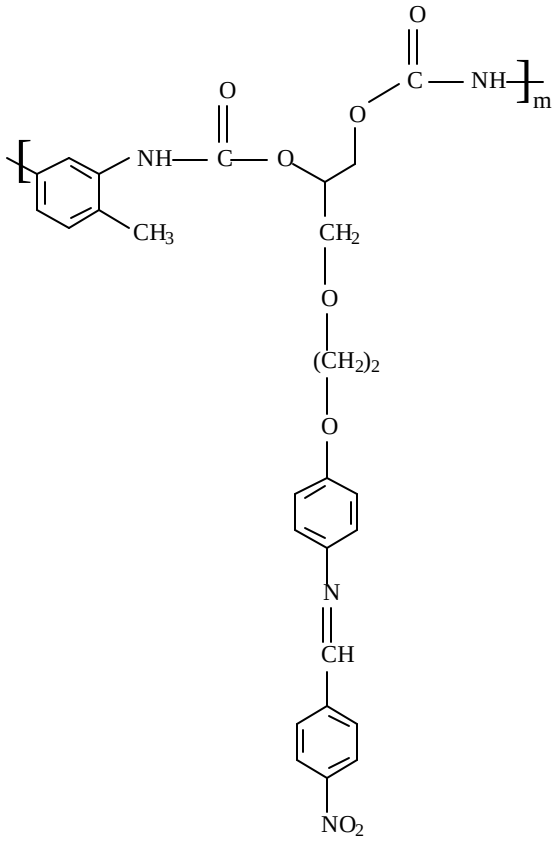

Yield	69%
UV (λ_{max})	370 nm
IR (cm^{-1})	3500-3100, 1720, 1675, 1598, 1340
^1H NMR (δ)	9.5 (1H), 8.9 (1H), 8.5 (1H), 8.2-7.7 (9H), 7.0 (2H), 4.1-3.4 (9H), 2.16 (3H)
M_n (VPO)	13,600

3.8.3.2 Poly{iminocarbonyloxy(2-[(4-methylene oxyethyloxy)-N-(4'-nitro benzylidene)aniline]ethane)oxycarbonylimino(1,4-phenylene) methylene(1',4'-phenylene)} (V 29)

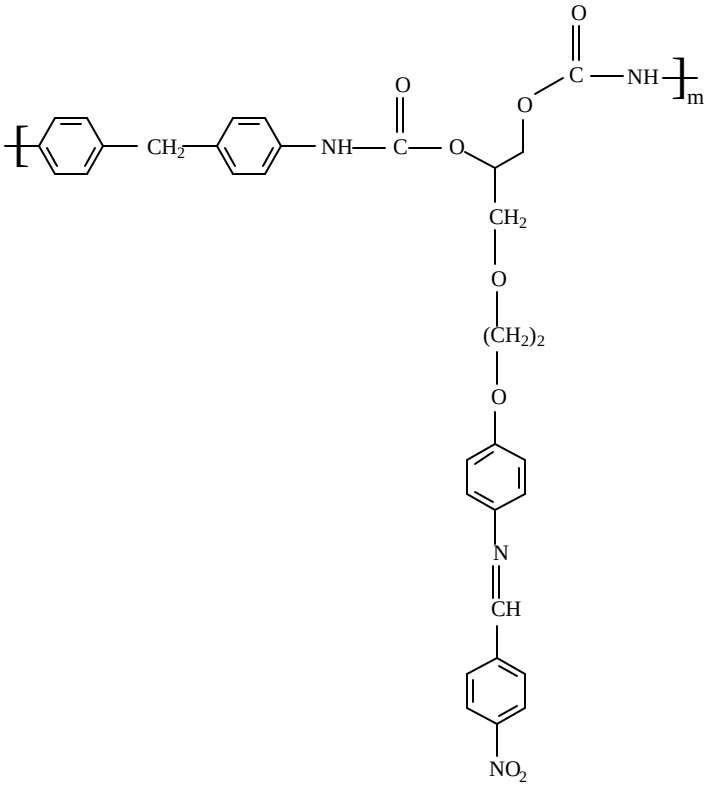

Yield	59%
T_g	101° C
UV (l_{max})	380 nm
IR (cm^{-1})	3500-3100, 1720, 1675, 1598, 1340
^{1}H NMR (d)	9.5 (1H), 8.9 (1H), 8.5 (1H), 8.2-7.86 (9H), 7.04 (2H), 4.1-3.4 (11H)
M_n (VPO)	14,015

3.8.3.3 Poly{iminocarbonyloxy(2-[(4-methyleneoxy ethyloxy)-N-(4'-cyano benzylidene)aniline]ethane)oxycarbonylimino(4-methyl-1,3-phenylene)} (V 30)

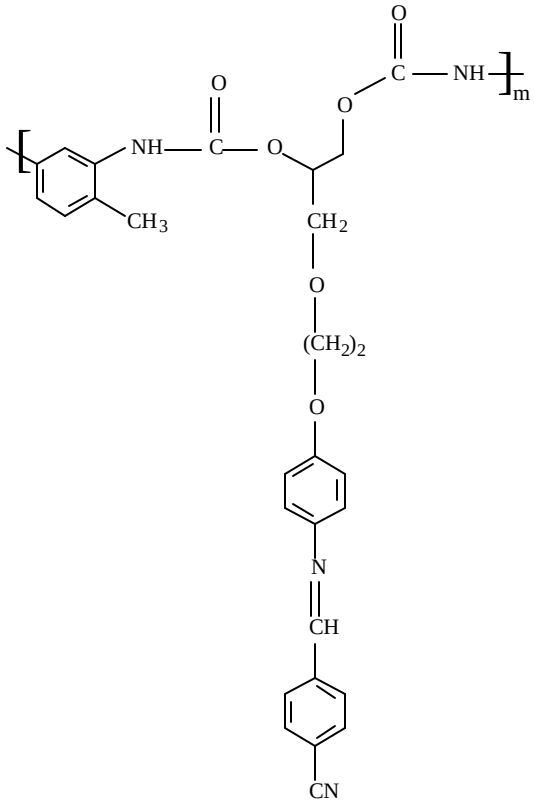

Yield	74%
T_g	151^{o} C
UV (l_{max})	360 nm
IR (cm^{-1})	3500-3100, 2200, 1720, 1675, 1598
^{1}H NMR (d)	9.5 (1H), 8.9 (1H), 8.5 (1H), 8.2-7.7 (9H), 7.0 (2H), 4.1-3.4 (9H), 2.16 (3H)
M_n (VPO)	15,000

3.8.3.4 Poly{iminocarbonyloxy(2-[(4-methyleneoxyethyloxy)-N-(4'-cyano benzylidene)aniline]ethane)oxycarbonylimino(1,4-phenylene) methylene(1',4'-phenylene)} (V 31)

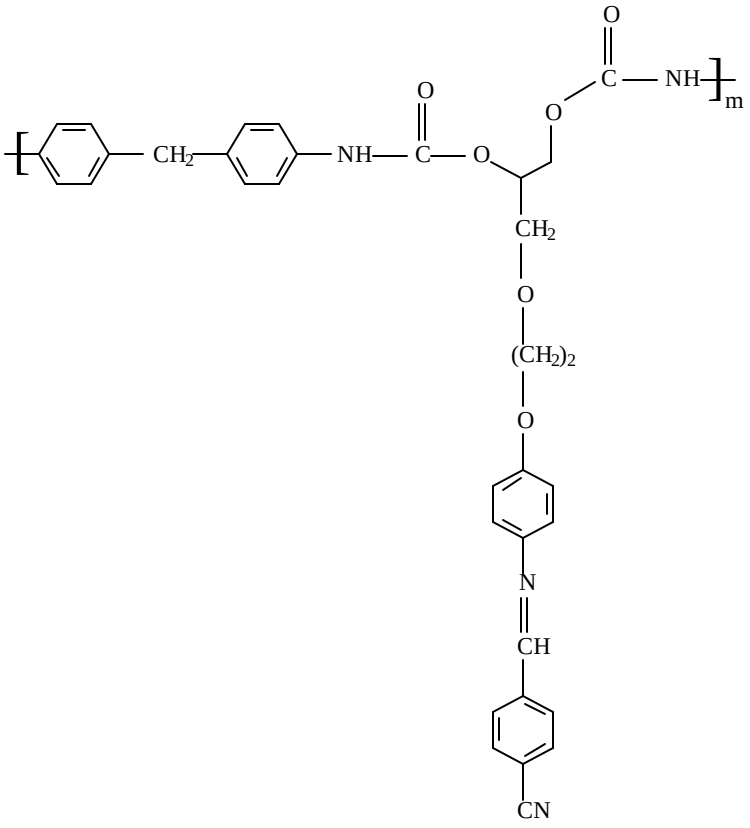

Yield	81%
T_g	53^{o} C
UV (l_{max})	363 nm
IR (cm^{-1})	3500-3100, 2230, 1720, 1675, 1598
^{1}H NMR (d)	9.5 (1H), 8.9 (1H), 8.5 (1H), 8.2-7.86 (9H), 7.04 (2H), 4.1-3.4 (11H)
M_n (VPO)	16,200

3.8.3.5 Poly{iminocarbonyloxy(2-[4-methyleneoxypropyloxy-4'-nitro azobenzene] ethane)oxycarbonyimino(4-methyl-1,3-phenylene)} (V 32)

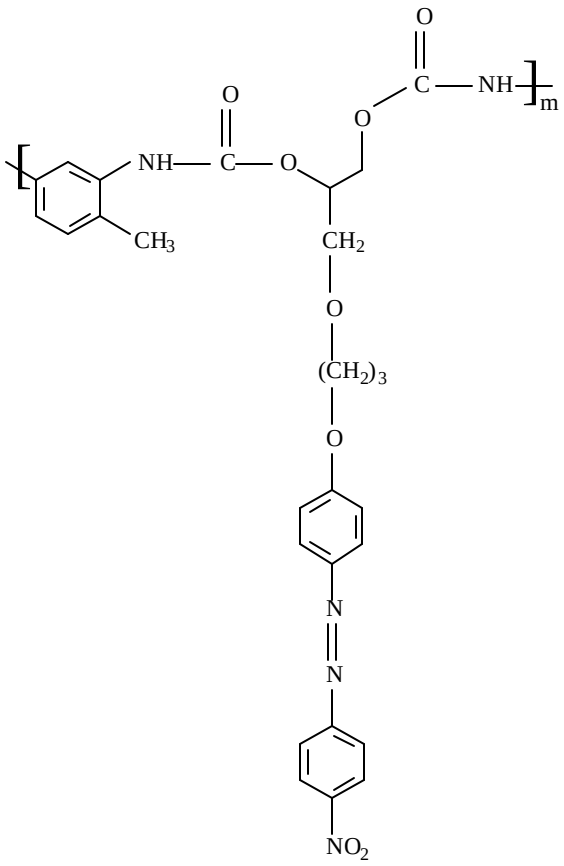

Yield	77%
T_g	68° C
UV (l_{max})	369 nm
IR (cm^{-1})	3500-3100, 1720,1598, 1490, 1340
^{1}H NMR (d)	9.5 (1H), 8.9 (1H), 8.0-7.8 (9H), 7.1 (2H), 4.1 (2H), 3.8-3.4 (7H), 2.2-2.16 (5H)
M_n (VPO)	10,080

3.8.3.6 Poly{iminocarbonyloxy(2-[4-methyleneoxypropyloxy-4'-nitro azobenzene] ethane) oxycarbonylimino(1,4-phenylene)methylene(1',4'-phenylene)} (V 33)

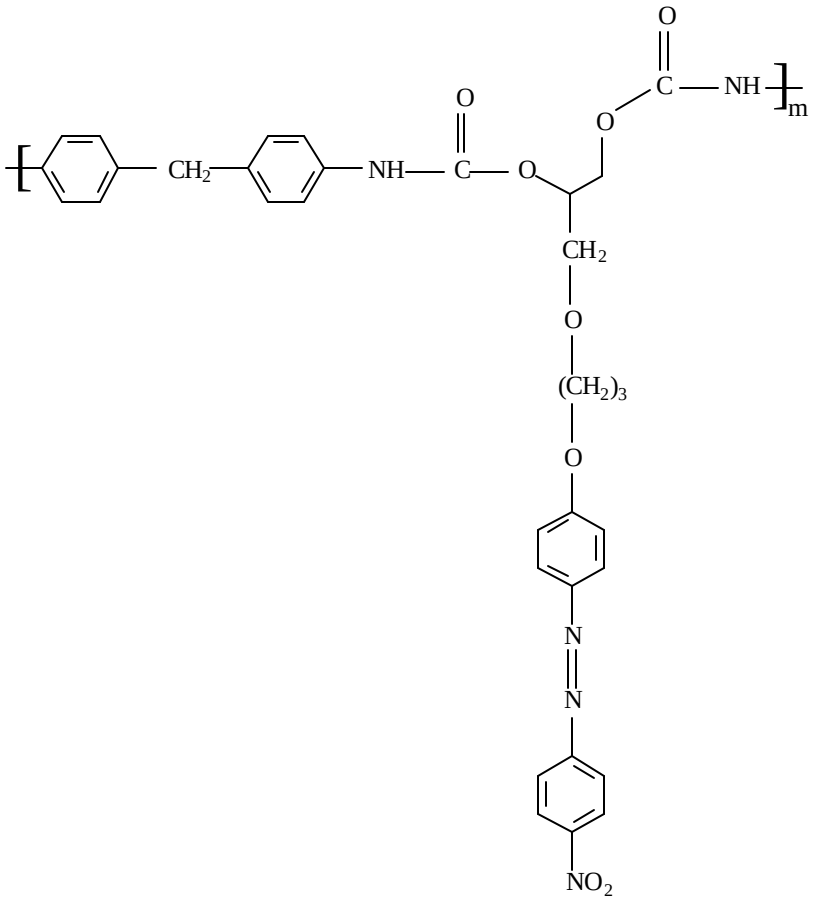

Yield	63%
UV (λ_{max})	381 nm
IR (cm^{-1})	3500-3100, 1720, 1675, 1598, 1340
^1H NMR (d)	9.5 (1H), 8.9 (1H), 7.8 (7H), 7.2 (2H), 6.8 (2H), 4.1 (2H), 3.8-3.4 (9H), 2.2 (2H)
M_n (VPO)	9,970

3.8.3.7 Poly{iminocarbonyloxy(2-[4-methyleneoxypropyloxy-4'-cyano azobenzene]ethane)oxycarbonylimino(4-methyl-1,3-phenylene)} (V 34)

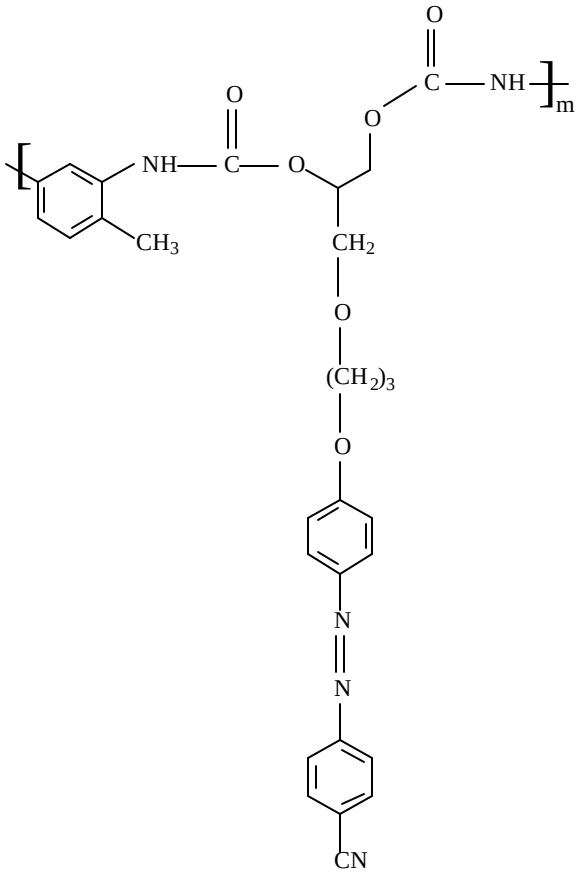

Yield	52%
T_g	69° C
UV (l_{max})	362 nm
IR (cm^{-1})	3500-3100, 2200, 1720, 1598, 1490
^{1}H NMR (d)	9.5 (1H), 8.9 (1H), 8.0-7.8 (9H), 7.1 (2H), 4.1 (2H), 3.8-3.4 (7H), 2.2-2.16 (5H)
M_n (VPO)	11,050

3.8.3.8 Poly{iminocarbonyloxy(2-[4-methyleneoxypropyloxy-4'-cyano azobenzene]ethane)oxycarbonylimino(1,4-phenylene)methylene(1',4'-phenylene)} (V 35)

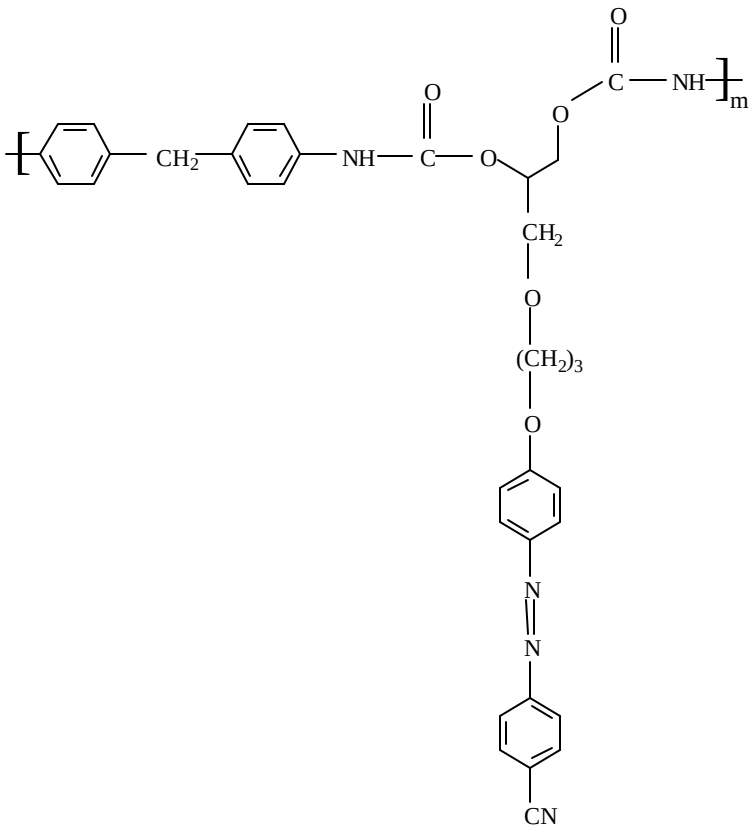

Yield	82%
T_g	115° C
UV (λ_{max})	363 nm
IR (cm^{-1})	3500-3100, 2200, 1720, 1675, 1598
^{1}H NMR (d)	9.5 (1H), 8.9 (1H), 7.8 (7H), 7.2 (2H), 6.8 (2H), 4.1 (2H), 3.8-3.4 (9H), 2.2 (2H)
M_n (VPO)	12,500

3.8.3.9 Poly{iminocarbonyloxy(2-[4'-propyloxy-4-nitro azobenzene] propane) oxycarbonyl imino (4-methyl-1,3-phenylene)} (V 36)

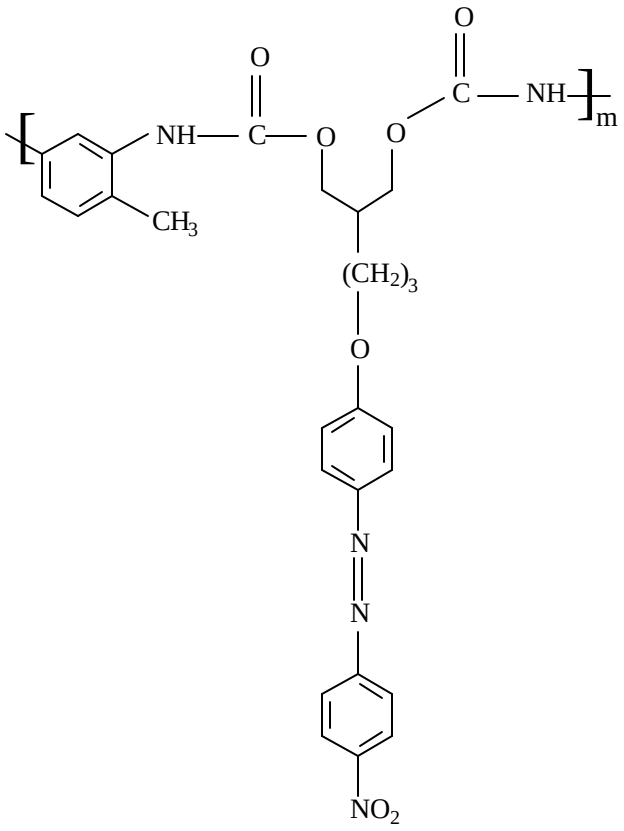

Yield	71%
T_g	57^{o} C
UV (l_{max})	363 nm
IR (cm^{-1})	3500-3100, 1720, 1598, 1490, 1340
^{1}H NMR (d)	9.5 (2H), 8.0-7.7 (7H), 7.1 (2H), 6.8 (2H), 4.2 (2H), 3.4 (4H), 2.9-2.8 (4H), 1.6 (1H)
M_n (VPO)	8,500

3.8.3.10 Poly{iminocarbonyloxy(2-[4'-propyloxy-4-nitro azobenzene] propane) oxycarbonyl imino (1,4-phenylene)methylene(1',4'-phenylene)} (V 37)

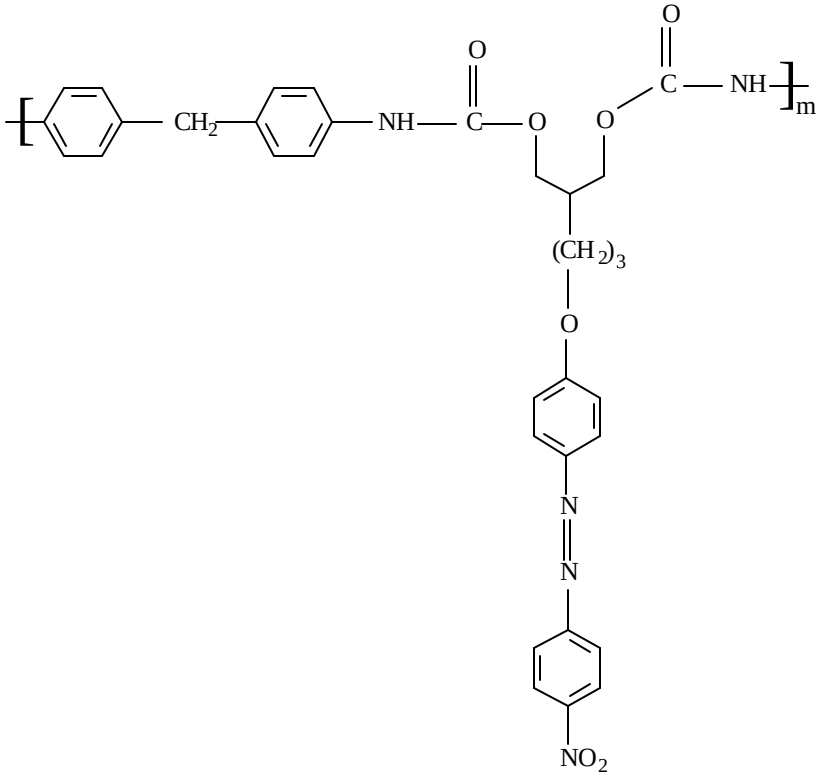

Yield	60%
T_g	81° C
UV (l_{max})	365 nm
IR (cm^{-1})	3500-3100, 1720,1598, 1490, 1340
^{1}H NMR (d)	9.5 (2H), 8.0-7.5 (8H), 7.1-6.8 (8H), 4.2 (2H), 3.8 (2H), 3.4 (4H), 2.9-2.8 (4H), 1.6 (1H)
M_n (VPO)	7,100

3.8.3.11 Poly{iminocarbonyloxy(2-[4'-propyloxy-4-cyano azobenzene]propane) oxycarbonyl imino (4-methyl-1,3-phenylene)} (V 38)

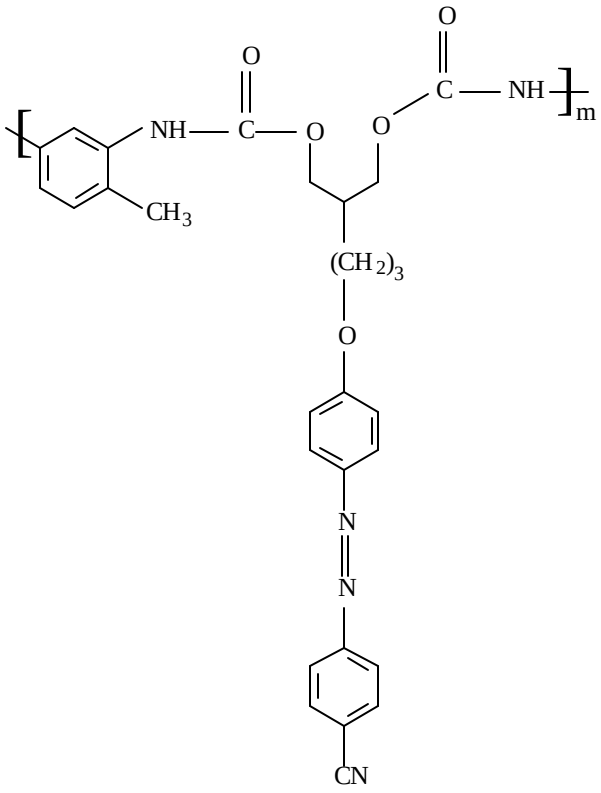

Yield	58%
UV (λ_{max})	365 nm
IR (cm^{-1})	3500-3100, 2200, 1720, 1598, 1490
^1H NMR (d)	9.5 (2H), 8.0-7.7 (7H), 7.1 (2H), 6.8 (2H), 4.2 (2H), 3.4 (4H), 2.9-2.8 (4H), 1.6 (1H)
M_n (VPO)	10,675

3.8.3.12 Poly{iminocarbonyloxy(2-[4'-propyloxy-4-cyano azobenzene]propane) oxycarbonyl imino (1,4-phenylene)methylene(1',4'-phenylene)} (V 39)

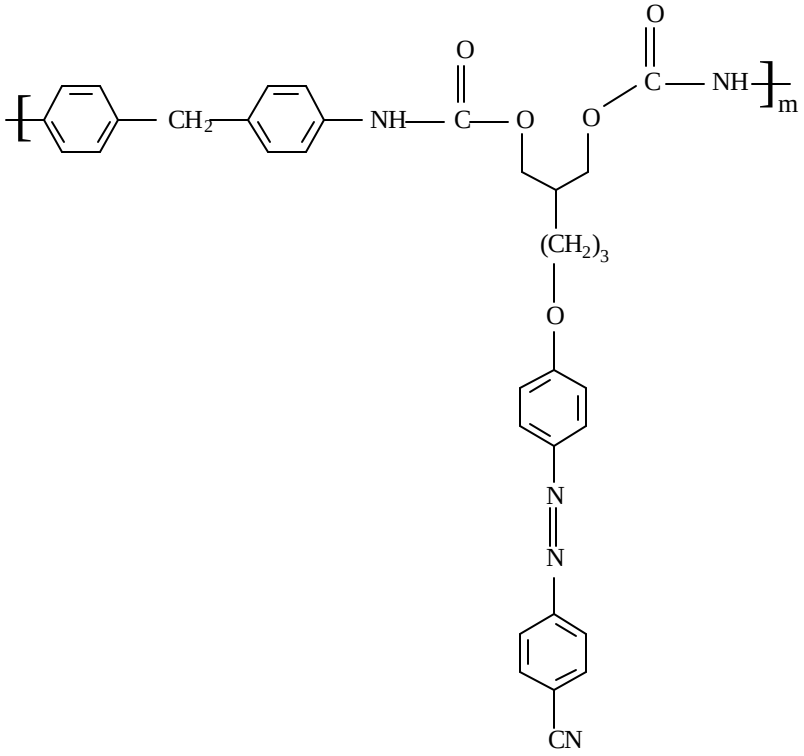

Yield	68%
T_g	64° C
UV (l_{max})	367 nm
IR (cm^{-1})	3500-3100, 2200, 1720, 1598, 1490
^{1}H NMR (d)	9.5 (2H), 8.0-7.8 (4H), 7.2-6.8 (12H), 4.2 (2H), 3.8 (2H), 3.4 (4H), 2.9 (4H), 1.6 (1H)
M_n (VPO)	14,650

3.9 Synthesis of epoxy resins

The amine-terminated NLO chromophores 4-amino-N-(4'-cyano benzylidene)aniline and 4-amino-N-(4'-nitro benzylidene)aniline were polymerised with diglycidyl ether bisphenol A monomer to give polymers poly{[N-(4-nitro benzylidene) aniline]imino(2-hydroxypropane)oxy(1,4-phenylene)-1,1-dimethyl methylene(1',4'-phenylene) oxy(2-hydroxypropane) (**V 40**) and poly{[N-(4-cyano benzylidene) aniline] imino(2-hydroxypropane) oxy (1,4-phenylene)-1,1-dimethylmethylene(1',4'-phenylene) oxy(2-hydroxypropane) (**V 41)**. Diglycidyl ether bisphenol A monomer was synthesised using reported procedure (10). These polymers were soluble in most polar solvents such as N,N-dimethylformamide (DMF), dimethylsuphoxide (DMSO), etc. This synthesis is represented in Scheme 3.10 below.

4-Amino-N-(4'-cyano benzylidene)aniline (0.3 g, 0.002 mol) and equivalent diglycidyl ether bisphenol A (0.5 g, 0.002 mol) were added into a 50 mL round-bottomed flask containing 10 mL of N,N-dimethylsulphoxide. The reaction mixture was heated at 110^{o} C for 12 hours to give a viscous solution. The solution was poured to excess of cold methanol to give a dark-brownish solid. The resulting solid poly{[N-(4-cyano benzylidene) aniline] imino (2-hydroxypropane)oxy (1,4-phenylene) 1,1-dimethyl methylene(1',4'-phenylene)oxy(2-hydroxypropane) (**V 41**) was purified by soxhlet extraction to remove low-molecular weight portions.

No.	Polymer	Code
1	Poly{[N-(4-nitro benzylidene)aniline]imino(2-hydroxypropane) oxy(1,4-phenylene)1,1-dimethylmethylene(1',4'-phenylene)oxy(2-hydroxypropane)}	**V 40**
2	Poly{[N-(4-cyano benzylidene)aniline]imino(2-hydroxypropane)oxy(1,4-phenylene)1,1-dimethylmethylene(1',4'-phenylene)oxy(2-hydroxy propane)}	**V 41**

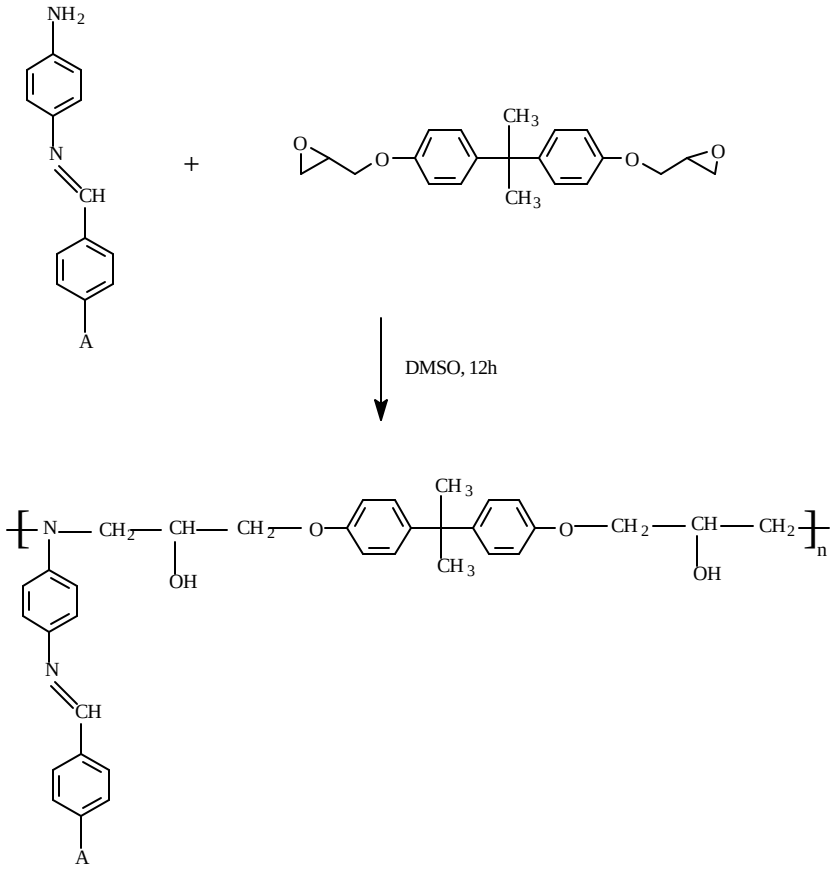

$A = NO_2 / CN$

Scheme 3.10: Synthesis of epoxy resins

3.9.1 Characterisation of epoxy resins

3.9.1.1 Poly{[N-(4-nitro benzylidene)aniline]imino(2-hydroxypropane)oxy(1,4-phenylene)-1,1-dimethylmethylene(1',4'-phenylene)oxy(2-hydroxypropane)} (V 40)

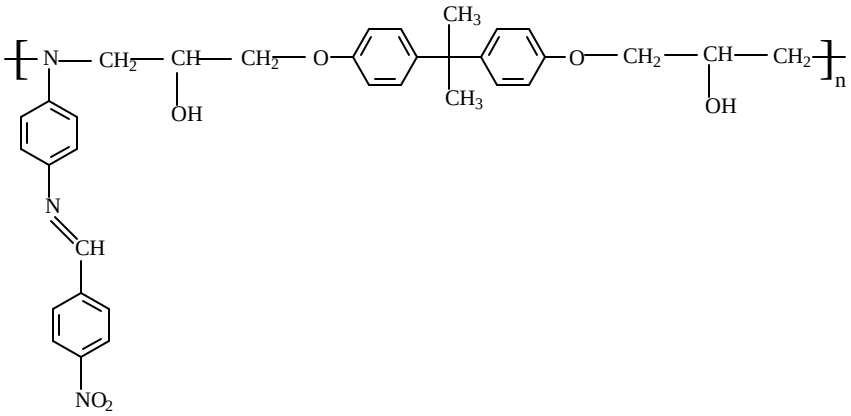

Yield	75%
T_g	89° C
UV (l_{max})	271 nm
IR (cm^{-1})	3600-3100, 2960, 2850, 1510, 1321, 1235
NMR (d)	8.5 (1H), 8.2-6.5 (16H), 4.2-3.5 (10H), 1.6 (6H)

3.9.1.2 Poly{[N-(4-cyano benzylidene)aniline]imino(2-hydroxypropane)oxy(1,4-phenylene) -1,1-dimethylmethylene (1',4'-phenylene)oxy(2-hydroxypropane)} (V 41)

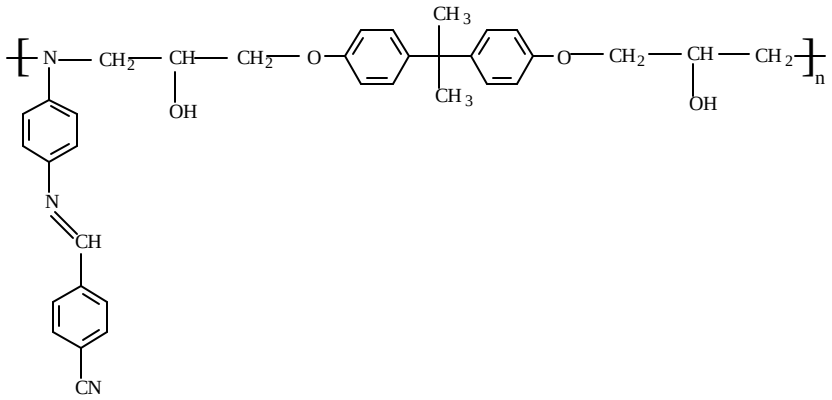

Yield	82%
T_g	58° C
UV (l_{max})	268 nm
IR (cm^{-1})	3600-3100, 2960, 2850, 2230, 1510, 1235
NMR (d)	8.6 (1H), 8.0-6.5 (16H), 4.2-3.6 (10H), 1.6 (6H)

3.10 Synthesis of siloxane polymers

Catalyst SLM86003 (Wacker Chemie, Germany) was used as received. Toluene (Merck, Germany) was made thiophene-free by shaking with concentrated sulphuric acid until the acid layer was colourless. It was then washed twice with water, once with 10% sodium carbonate solution and finally dried with anhydrous calcium chloride. For use, this toluene was then left in the presence of Type 5Å grade molecular sieve.

A representative polymerisation procedure is as follows: Linear polymers were synthesised by dissolving in thiophene-free toluene and heating to 60° C. The progress of reaction was monitored by IR spectrum. After complete disappearance of the Si-H bond at 1262 cm^{-1}, the reaction mixture was poured into methanol (20 times by volume). The precipitated polymer was filtered and dried in vacuum. Polymer was purified by reprecipitation of toluene solution with methanol. The various components, their weights

and time required for each polymer are given below. The siloxane polymers were synthesised as shown in Scheme 3.11.

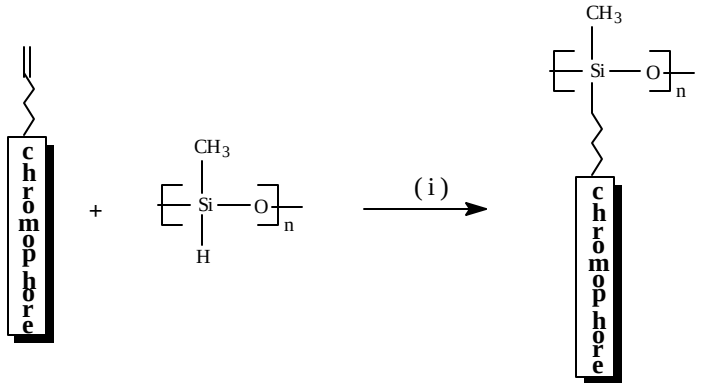

Scheme 3.11: Synthesis of siloxane polymers

3.10.1 Poly{1-methyl-1-[4-(S-1-methylheptyl oxy)-3-nitro-1,4-phenylene carbonyloxy-4'-(undecamethyleneoxy)biphenyl]siloxane} (V 42)

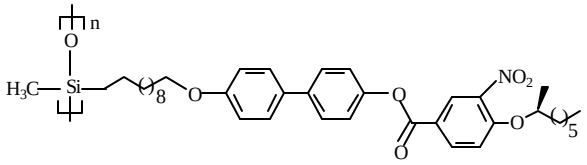

4-[(S-1-Methylheptyl oxy)-3-nitro-1,4-phenylene carbonyloxy]-4'-(undec-10-enoxy) biphenyl **(M34)**	1.13 mmol	442.8 mg	M = 615 g/mol
Poly(hydromethylsiloxane)	1.0 mmol	60 mg	M = 60 g/mol SiH
Catalyst SLM86003 (Wacker Chemie)	3 µL		
Toluene (thiophene free)	2.0 mL		
Reaction time	9 h		

3.10.2 Poly{1-methyl-1-[1-(S-2-methylbutyl oxycarbonyl-1,4-phenylene oxycarbonyl)-4-(hexamethyleneoxy)phenylene]siloxane} (V 43)

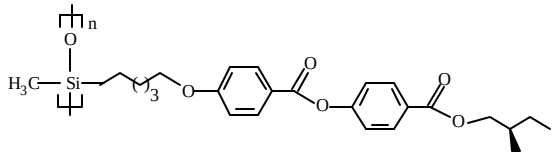

1-[(S-2-Methylbutyl) oxycarbonyl-1,4-phenylene oxycarbonyl]-4-(hex-5-enoxy) phenylene **(M35)**	0.46 mmol	250 mg	M = 410 g/mol
Poly(hydromethylsiloxane)	0.4 mmol	24 mg	M= 60 g/mol SiH
Catalyst SLM86003 (Wacker Chemie)	2 µL		
Toluene (thiophene free)	1.0 mL		
Reaction time	2 h		

3.10.3 Poly{1-methyl-1-[1-(S-1-methylheptyloxy)-3-nitro-1,4-phenylene carbonyloxy-4-(undecamethyleneoxy)biphenyl]siloxane} (V 44)

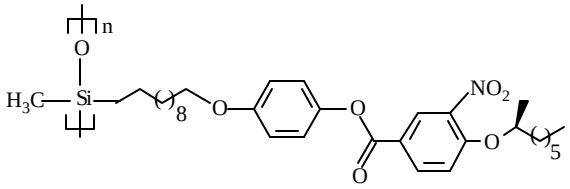

1-[(S-1-Methylheptyloxy)-3-nitro-1,4-phenylene-1-carbonyloxy]-4'-(undec-10-enoxy)phenylene (**M36**)	0.46 mmol	250 mg	M = 539 g/mol
Poly(hydromethylsiloxane)	0.4 mmol	24 mg	M= 60 g/mol SiH
Catalyst SLM86003 (Wacker Chemie)	2 µL		
Toluene (thiophene free)	1.5 mL		
Reaction time	2 h		

3.11 Synthesis of siloxane elastomers

A representative procedure for elastomer synthesis is as follows: The crosslinker, mesogens were dissolved in thiophene free toluene. To this solution, Pt-catalyst (hydrogen hexachloro-platinate(IV)hydrate) was added and the solution was filtered using a 0.5 µm millipore filter into a centrifuge with a diameter of 5 cm and a height of 2 cm, thus excluding dust particles. To avoid tack, the inner wall of the cell was covered with polytetrafluoroethylene (PTFE) film. The reaction was carried out under centrifugation (4500 rpm) at 90^{o} C for 2 hours. Thereafter the entire cell was cooled to room temperature and the swollen elastomer was carefully removed from the cell. The transparent gel was divided into two equal sections with the help of a scalpel. The gel was pulled from the PTFE foil with the help of temperature-steady tape and fastened to the metal bars. For orientation, the sample was gradually loaded with weights. The composition details of each elastomer are given below:

3.11.1 Elastomer E1

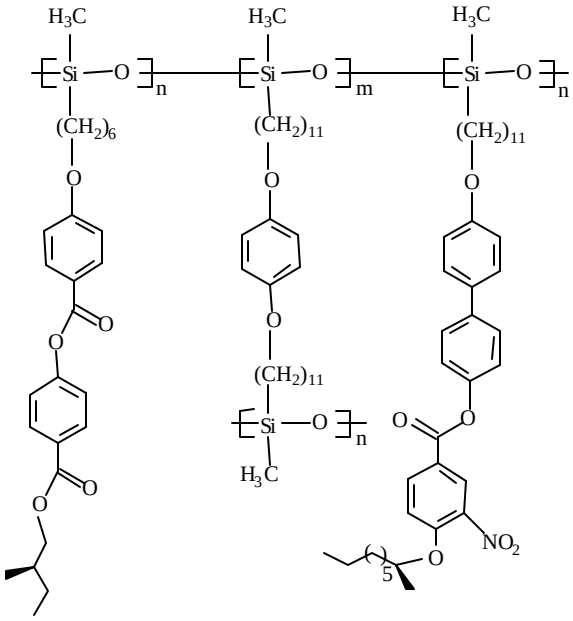

4-[(S-1-Methylheptyl oxy)-3-nitro-1,4-phenylene carbonyloxy]-4'-(undec-10-enoxy) biphenyl **(M34)**	0.72 mmol	442.8 mg	M = 615 g/mol
1-[(S-2-Methylbutyl) oxycarbonyl-1,4-phenylene oxycarbonyl]-4-(hex-5-enoxy) phenylene **(M35)**	0.72 mmol	295.2 mg	M = 410 g/mol
1,4-Bis(undec-10-enoxy) phenylene **(M41)**	0.20 mmol	82.9 mg	M=414.7 g/mol
Poly(hydromethylsiloxane)	2.0 mmol	120 mg	M=60 g/mol SiH
Catalyst SLM86003 (Wacker Chemie)	20 µL		
Toluene (thiophene free)	2.0 mL		
Reaction time	2 h		

3.11.2 Elastomer E2

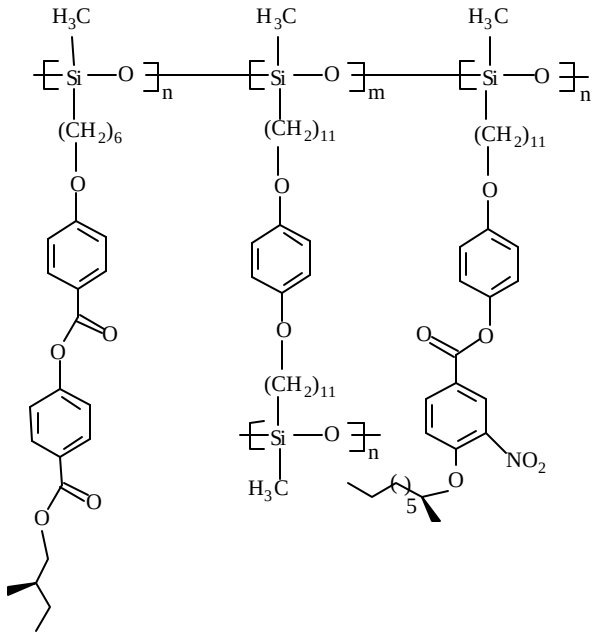

1-[(S-1-Methylheptyloxy)-3-nitro-1,4-phenylene carbonyloxy]-4-(undec-10-enoxy) phenylene **(M36)**	0.32 mmol	196.8 mg	M = 539 g/mol
1-[(S-2-Methylbutyl) oxycarbonyl-1,4-phenylene oxycarbonyl]-4-(hex-5-enoxy) phenylene **(M35)**	0.32 mmol	172.5 mg	M = 410 g/mol
1,4-Bis(undec-10-enoxy) phenylene **(M41)**	0.10 mmol	41.47 mg	M = 414.7 g/mol
Poly(hydromethylsiloxane)	1.0 mmol	120 mg	M=60 g/mol SiH
Catalyst SLM86003 (Wacker Chemie)	15 µL		
Toluene (thiophene free)	1.0 mL		
Reaction time	2 h		

3.11.3 Elastomer E3

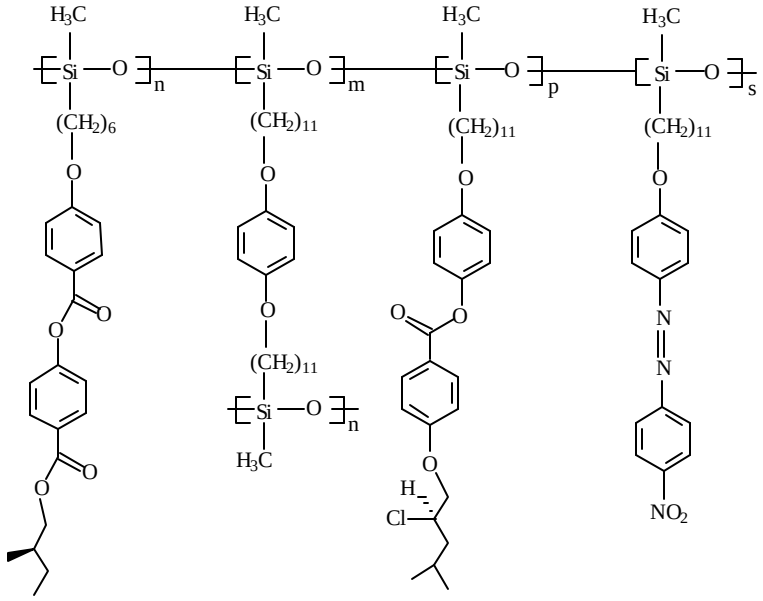

1-{[(S-2-Chloro-4-methyl) pent-1-yloxy)-1,4-phenylene carbonyloxy}-4-(undec-10-enoxy) phenylene **(M40)**	0.98 mmol	502.3 mg	M = 501 g/mol
1-[(S-2-Methylbutyl) oxycarbonyl-1,4-phenylene oxycarbonyl]-4-(hex-5-enoxy) phenylene **(M35)**	0.14 mmol	57.4 mg	M = 410 g/mol
4'-Nitro-4-(undec-10-enoxy) azobenzene **(M37)**	0.48 mmol	189.6 mg	M = 395 g/mol
1,4-Bis(undec-10-enoxy) phenylene **(M41)**	0.20 mmol	82.9 mg	M = 414.7 g/mol
Poly(hydromethylsiloxane)	2 mmol	120 mg	M=60 g/mol SiH
Catalyst SLM86003 (Wacker Chemie)	30 µL		
Toluene (thiophene free)	2 mL		
Reaction time	2 h		

3.11.4 Elastomer E4

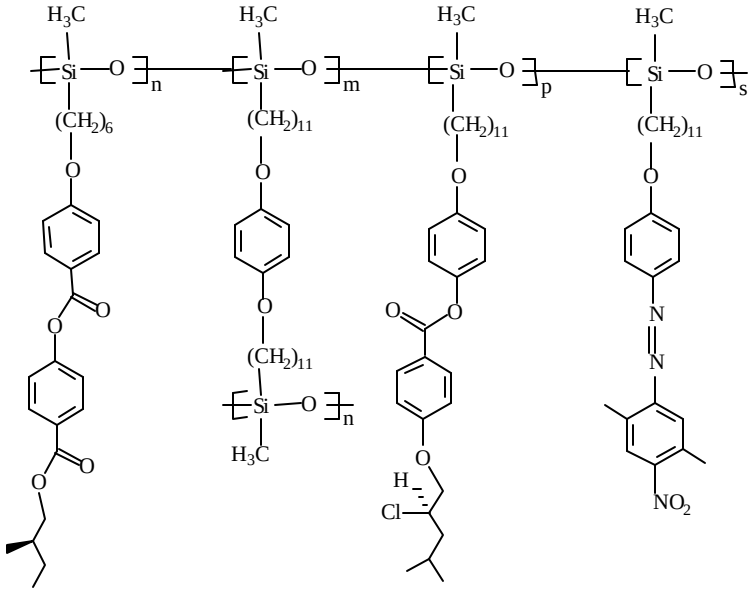

1-{[(S-2-Chloro-4-methyl) pent-1-yloxy)-1,4-phenylene carbonyloxy}-4-(undec-10-enoxy) phenylene **(M40)**	0.740 mmol	286 mg	M = 501 g/mol
1-[(S-2-Methylbutyl) oxycarbonyl-1,4-phenylene oxycarbonyl]-4-(hex-5-enoxy) phenylene **(M35)**	0.190 mmol	76.3 mg	M = 410 g/mol
2,5-Dimethyl-4'-nitro-4-(undec-10-enoxy) azobenzene **(M38)**	0.056 mmol	23.7 mg	M = 423 g/mol
1,4-Bis(undec-10-enoxy) phenylene **(M41)**	0.050 mmol	41.5 mg	M=414.7 g/mol
Poly(hydromethylsiloxane)	1.00 mmol	60.0 mg	M=60 g/mol SiH
Catalyst SLM86003 (Wacker Chemie)	15 µL		
Toluene (thiophene free)	1 mL		
Reaction time	2 h		

3.11.5 Elastomer E5

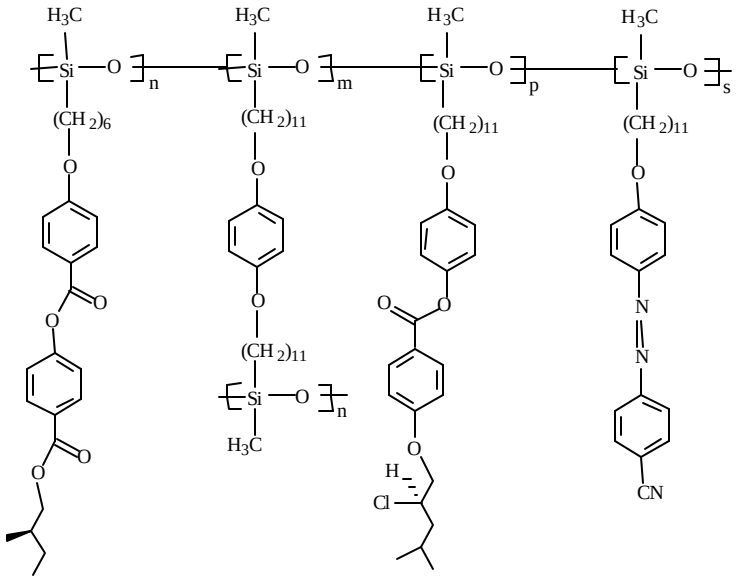

1-{[(S-2-chloro-4-methyl) pentyl-1-oxy)-1,4-phenylene carbonyloxy}-4-(undec-10-en-oxy) phenylene **(M40)**	0.63 mmol	322.8 mg	M = 501 g/mol
1-[(2-Methylbutyl) oxycarbonyl-1,4-phenylene oxycarbonyl]-4-(hex-5-en-oxy) phenylene **(M35)**	0.09 mmol	36.9 mg	M = 410 g/mol
4'-cyano-4-(undec-10-en-oxy) azobenzene **(M39)**	0.08 mmol	24.4 mg	M = 375 g/mol
1,4-Bis(undec-10-en-oxy) phenylene **(M41)**	0.10 mmol	41.5 mg	M = 414.7 g/mol
Poly(hydromethylsiloxane)	1.00 mmol	60.0 mg	M=60 g/mol SiH
Catalyst SLM86003 (Wacker Chemie)	15 µL		
Toluene (thiophene free)	1 mL		
Reaction time	2 h		

3.12 REFERENCES

1. Staudinger, H., *Chem. Ber*., **53**, 1073 (1920).

2. Bevington, J. C., in *'Comprehensive Polymer Science'*, Eastmond, G. C., Ledwith, A., Russo, S. and Sigwalt, P. (eds.), Pergamon: London, Vol **3** (1989); p.65.

3. Flory, P. J., in *Principles of Polymer Chemistry*, Cornell University Press: Ithaca, NY (1953); p.106.

4. Walling, C., *Free Radicals in Solution*, Wiley: NY (1957); p.592.

5. Spirin, Y. L., *Russ. Chem. Rev. (Engl. Transl.)*, **38**, 529 (1969).

6. Kamachi, M., *Adv. Polym. Sci.*, **38**, 55 (1981).

7. Gromov, V. F. and Khomiskovskii, P. M., *Russ. Chem. Rev. (Engl. Transl.)*, **48**, 1040 (1979).

8. Huyser, E. S., *Adv. Free Radical Chem.*, **1**, 77 (1965).

9. Martin, J. C., in '*Free Radicals*', Kochi, J. K. (ed.), Wiley: NY, Vol. **2** (1973); p.493.

10. (a) Herweh, J. E., *J. Hetrocycl. Chem.*, **5**, 687 (1968). (b) Union Carbide Corp., *US Pat.*, 2880225 (1955).

4

Results & Discussion

4 Results and Discussion

4.1 Free-radical Polymerisation

In the previous chapter, the synthesis of polymers by free-radical polymerisation was described. To summarise, polymerisation of unsaturated monomers by chain polymerisation is initiated by a reactive species R* produced from some compound I termed as initiator. The reactive species (here a free radical) adds to a monomer molecule by opening the π-bond. The process is repeated as many more monomer molecules are successively added so as to continuously propagate the reactive centre. Polymer growth is terminated at some point by the destruction of the reactive centre by an appropriate reaction.

4.1.1 Azo initiator

The most common of initiators for radical polymerisation are compounds which acts as thermal source of radicals. Usually, this is an azo or peroxy initiator. A particular initiator will have a convenient decomposition rate over a relatively narrow temperature range. Two classes of azo compounds are used as initiators: (1) diallyl diazines and (2) hyponitrites. Aliphatic cis-azo compounds have at best a transient existence under typical reaction conditions. Thus, the rate of photoisomerisation approximates the rate of initiator's disappearance. The efficiency for generation of 'useful' radicals from azo compound initiators is low, typically 50-70%. The rest of radicals are lost as recombination products (1).

4.1.1.1 2,2'-Azobis(2-methylpropanenitrile) [AIBN]

The decomposition mechanism and behaviour as a polymerisation initiator are largely understood for AIBN [azobisisobutyronitrile] (Scheme 4.1).

The nitrogen loss is sufficiently rapid so that diazenyl radical will not be in a position to initiate polymerisation. Thus, all observed reactions are attributable to the cyanoisopropyl radical (2). Studies show that they possess some electrophilic character. Cyanoisopropyl radicals generally show a high degree of specificity in reactions with unsaturated substrates. They react with most monomers (eg. Styrene, MMA) exclusively

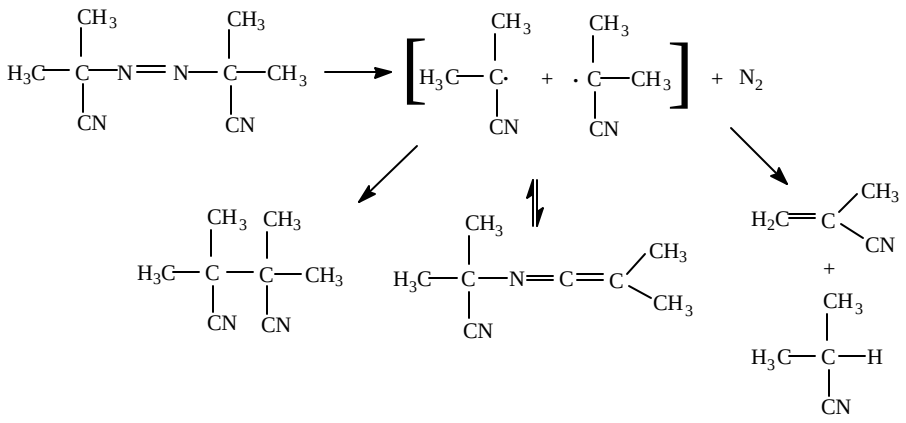

Scheme 4.1: Decomposition mechanism of AIBN

by tail addition. α-Cyanoalkyl radicals show relatively little tendency to abstract hydrogen from monomer, solvent, or polymer even in relation to other alkyl radicals (3). However, these radicals, like other carbon-centred radicals (4), react with oxygen at diffusion controlled rates. For polymerisations carried out in poorly degassed media, it has been proposed (2,5) that abstraction products, peroxide linkages and other defect structures may arise through the intermediacy of a alkylperoxy radical (Scheme 4.2).

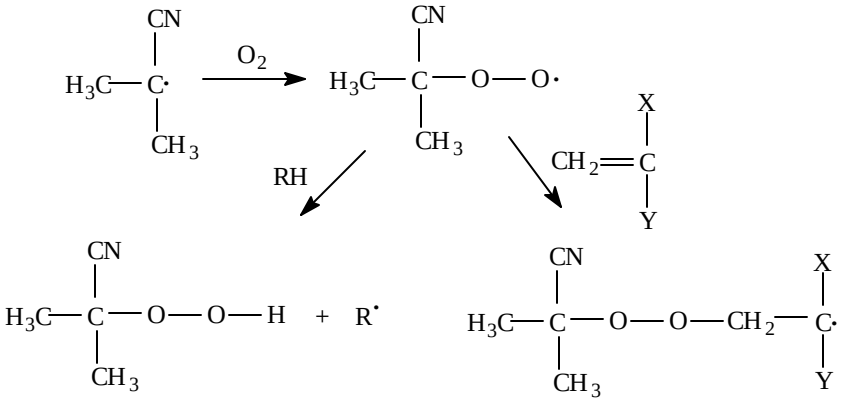

Scheme 4.2: Formation of peroxide linkages

4.1.2 Reactivity of monomers towards radical

A knowledge of the reactivity of radicals towards monomer is vital to understanding the polymerisation. A series of rules by Tedder (6) predicts the relative rate of radical addition to monomers. He has indicated that the stability of incipient radical

may be of consideration when the substituent has π orbital capable of delocalising the free spin [eg. Ph, -CH=CH_2, etc.].

As expected, the stabilised radicals show lower reactivity. There is, therefore an inverse relation between the reactivities of monomers and their derived radicals, the most reactive monomers give the least reactive radicals and vice-versa. Monomer reactivities vary with the substituent X in CH_2=CHX in the sequence Ph > CH_2=CH- > MeCO- > CN- > COOR- > Cl > -CH_2* > $MeCO_2$- > -OR (7). This sequence was interpreted as corresponding to decreasing resonance stabilisation of derived radicals of type –CH_2-CH-X. However, the NLO-chromophores which are usually large conjugated molecules with an electron donor and an electron acceptor substituent, often comprise of a number of functional groups like nitro or azo groups. These may act as retarders or inhibitors in free-radical polymerisation. So in many cases the yields are not quantitative and the molecular weights are quite low.

4.2 NLO Chromophores

In general, a typical NLO chromophore useful for poled polymer applications consists of a dipolar molecule having one or more electron donating and electron attracting substituents connected by an electron transmitting bridge (8-11). The bridges are usually π unsaturated moieties such as aromatic or hetero aromatic rings, double bond, etc. It has been shown that static hyperpolarisability is correlated with the ground state polarisation which is in turn reflected by bond length alternation (BLA). Optimal β values predicted for BLA in some chromophores have been approached by selecting appropriate combinations of donor and acceptor groups in order to tune the balance between the neutral and charge separated limiting resonance forms (12). Recent theoretical studies suggest that proper matching of donors and acceptor systems with the electron transmitting bridges are necessary to maximise the molecular hyperpolarisability (13,14). This hypothesis has been supported by experimental results. A large number of NLO chromophores have been studied in a variety of polymer hosts. Table 4.1 lists some linear and nonlinear properties of a number of typical NLO guest structures. Some of these materials are commercially available dyes, a feature which is partly responsible for their earlier popularity. The values of μβ, the product of dipole moment and the quadratic

molecular hyperpolarisability β, is a pertinent quantity for poled polymer applications, since the dipole moment determines the extent of chromophore alignment in a poling field while β is a measure of the molecular nonlinearity. The μβ terms reported in the literature for chromophores are usually derived from electric field induced second harmonic generation (EFISH) studies performed in solution (15-17).

Table 4.1 Linear and nonlinear properties of typical nonlinear optical chromophores as measured by EFISH

Guest	λ (nm)	Solvent	$\mu\beta \times 10^{30}$ (cm^5D/esu)	λ_{max} (nm)
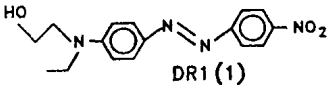 DR1 (1)	1.907	p-dioxane	343	455
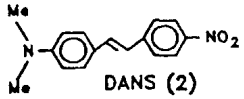 DANS (2)	1.907	$CHCl_3$	482	427
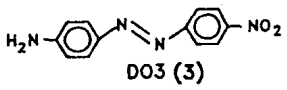 DO3 (3)	1.907	$CHCl_3$	229	410
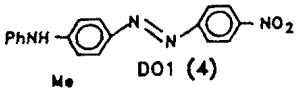 DO1 (4)	1.907	$CHCl_3$	289	452
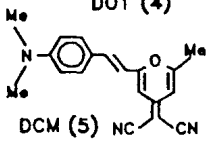 DCM (5)	1.907	$CHCl_3$	705	474
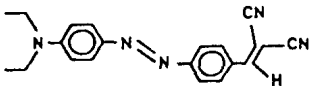 ADCVAB (6)	1.356	$CHCl_3$	2650	—
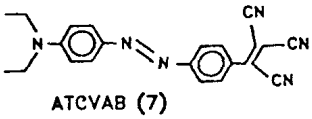 ATCVAB (7)	1.580	DMSO	4095	587
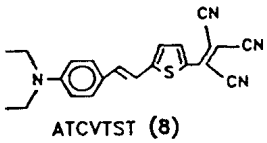 ATCVTST (8)	1.907	p-dioxane	6200	640

4.2.1 Azo chromophores

Conjugated aromatic molecules such as stilbenes or azobenzenes with electron donor and acceptor substituents are frequently used as NLO active groups. Attractive chromophores often include some nitrogen, sulphur and oxygen containing functional

groups (17). The larger d values for azo dyes compared to the stilbene dyes are attributed to the higher $\mu\beta$ product for the azo dye.

The extensively studied polar aromatic dyes are 4-dimethylamino-4'-nitrostilbene (DANS), disperse red (DR-1) and other unsymmetrically nitro, amino substituted azobenzenes and azomethines (18). However, these chromophores suffer from oxidative instabilities at the donor (amino) group, which leads to a drop in second harmonic generation (SHG) with time. Given the excellent polymeric and optical properties of polymethacrylates, it is not surprising that they have been extensively investigated. They can be easily processed into high quality thin films. Several of the reported copolymethacrylates do not show significant decay in their nonlinear optical response even after several weeks at room temperature (19). Some of the easiest types of NLO side-chain methacrylate polymers to be studied were copolymers derived from methacryloyl derivative of the azo dye DR-1 and methyl methacrylate. Films of this copolymer poled by corona discharge yielded d_{33} value of 43 pm/V (20). A large range of d_{33} values of azo methacrylates from 5.2 to 68 pm/V has been reported (20). The azo derivatives of phenol are reported to show smectic phases through hydrogen bonding under suitable conditions (21). An absence of extensive study in azo derivatives of phenol, its stability and the possibility to synthesise variety of polymers with azo chromophore with NLO properties were additional reasons to select azophenoxy chromophores for the synthesis of NLO homopolymers.

One of the first studies of NLO poled polymers is provided by the work of Meredith et al. (17). These workers studied the poling of DANS in a thermotropic liquid crystalline side chain acrylate polymer. Also much of the earlier work centred on the commercial dye DR1 incorporated in poly(methyl methacrylate) (17,22-24). Singer et al. (25) have demonstrated the efficiency of di and tri cyanovinyl acceptor groups for improving the nonlinearities of extended chromophoric system.

The novel chromophores discussed here carry acceptors like aldehyde and barbiturates in different backbones. The potential gain in aromaticity upon charge separation (Figure 4.1**)** would lead to a substantial charge transfer and reduced bond length alternation in the ground state. Thus, molecules containing acceptors whose

topology dictates that aromaticity is gained upon charge separation such as barbituric acid and its derivatives (13a) would have more nearly the correct degree of bond length alternation needed to optimise β and could thus give rise to extremely large optical nonlinearities compared to conventional molecules of similar strength.

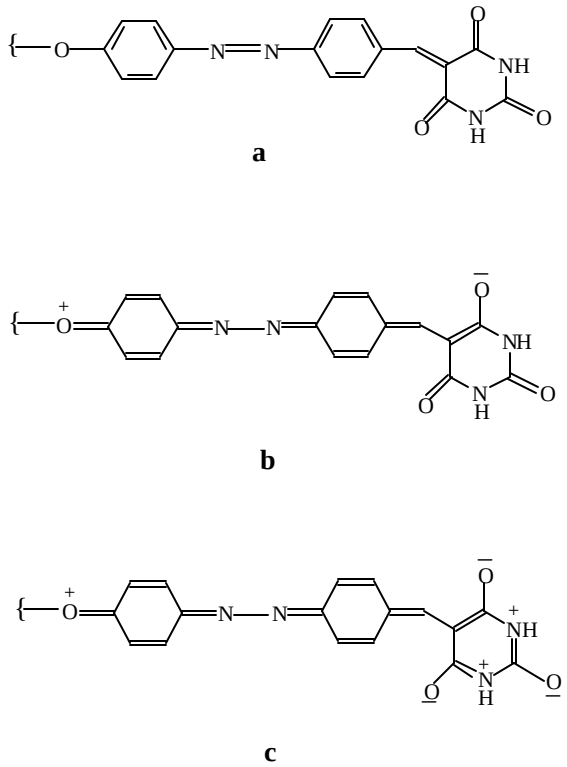

a: neutral resonance form;
b: one of the charge separated resonance forms;
c: a charge separated resonance form in which the acceptor ring has aromatic character.

Figure 4.1 Potential gain in aromaticity upon charge separation

In a simple two-level model, β is proportional to change in dipole moment ($\Delta\mu$) between ground and first electronic state. In the electric field dependence of the NLO properties of D-π-A molecules, the combination of amino and dicyanovinyl groups has larger value than amino and aldehyde groups, which in turn is better than methoxy and nitro groups (26). Given the importance of the gain in aromaticity in the zwitterionic limiting form of these D-π-A systems, it is not surprising that barbituric acid and its derivatives are powerful acceptor groups (12b,27-30). The bond length alteration of the

bridge upon polarisation is reduced in chromophores that are coupled to acceptors that simultaneously gain aromaticity when the connective segments (bridge) lose their aromaticity. This results in a significant enhancement in $\mu\beta$. Examples of such acceptors include 3-phenyl-5-isooxazolone and thiobarbituric acid derivatives (13a).

4.2.2 Azomethine chromophores

The centrosymmetry in macroscopic polymeric materials is usually broken by electric-field poling. In this, the polymer film is heated above its glass transition temperature in the presence of static electric field. The electric field orients the dipolar chromophores. The temperature is lowered to freeze in the non-centrosymmetric orientation of the NLO chromophores, and then the electric field is removed. This non-centrosymmetric arrangement of the electric dipoles in the polymer matrix can be expressed by an order parameter ϕ (31,32) within the rigid oriented gas model (33) considering that only the dipolar orientation effect is present. When ϕ is zero, the second harmonic (SH) intensity is also zero. Therefore, to maximise the SH intensity, large values of ϕ are desirable. It has been recognised that the axial ordering present in liquid crystalline polymers can be used to enhance field-induced polar ordering by elongating the orientational distribution function along the direction of electric field (34). An important factor in the synthesis of new liquid crystalline compounds is the ease and simplicity of the actual chemistry involved. For this reason derivatives of aromatic anils (benzylideneanilines) of general structure [**1**], wherein A and D are acceptor and donor groups, have received considerable attention since the final synthetic step involves an acid catalysed condensation reaction (35).

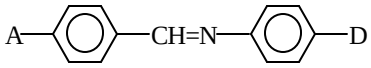

[1]

In azomethines, there is a twist angle of about 60^{o}. The twist angle between the two phenyl rings reduces efficiently the length of π electron conjugation thus leading to materials which are transparent in the near UV spectral range and therefore suitable for blue application (36). The azomethine conjugated polymers are particularly attractive due to mechanical strength, thermal stability and also fibre forming properties (37).

4.2.3 Heterocycles in NLO

Carbazoles are well known to exhibit good hole transporting properties and their photocarrier generation efficiency can be sensitised by formation of charge-transfer (CT) complexes (38). Acceptor introduced carbazoles appear to be very promising for second order (NLO) chromophores. Also structural modification is easier in carbazole. Besides 3 position, N-substituted (9-position) offers a variety of chemical modifications to introduce functional groups. E.g., Solubilisation of substituted carbazoles by alkylation. In the conjugated systems we can expect better molecular level controls of size, shape, surface chemistry, topology and flexibility than in point-like molecules.

We have synthesised novel polystyrenes containing electron-withdrawing groups like nitro, cyano, aldehyde, etc. which is linked through a π-CH=N- bridge to carbazole moiety. This in turn enhances the chromophoric content.

4.3 Side chain NLO polymers

In spite of the impressive gains and increasing database established for host-guest polymeric systems, there remains serious drawbacks to such an approach. Incompatibility of the guest with the host polymer leading to chromophore pairing, microaggregation and even phase separation is often a limiting feature. This often requires a compromise between achieving the highest possible bulk nonlinearity, which is directly related to the chromophore density, and maintaining acceptable optical properties for the polymer. Furthermore current wisdom dictates that a fully integrated optical device will operate at elevated temperatures and see brief temperature excursions to 250^{o} C or more during fabrication, requiring both thermal stability of the composite as well as stability of the induced polar order. For this reason, any sublimation and /or decomposition of the NLO chromophore is unacceptable. Finally, the strong plasticisation effects of most NLO guest chromophores on the host polymer usually lower the glass temperature which adversely affects the stability of the polar order.

Many of these problems are ameliorated by incorporation of the NLO chromophore into the polymer by chemical bonding. Higher concentrations can be tolerated without apparent phase separation problems when the chromophore is attached to the polymer as either a pendant side chain or incorporated into the main chain. It

seems, therefore, that the potential advantages of chemically bonded systems outweigh the disadvantages which include both increased synthetic and processing complexities.

For a side chain system, entire chromophore is pendant to the backbone. For such a system, the overall polymer morphology is often described as comb-like. This arrangement is depicted schematically in Figure 4.2.

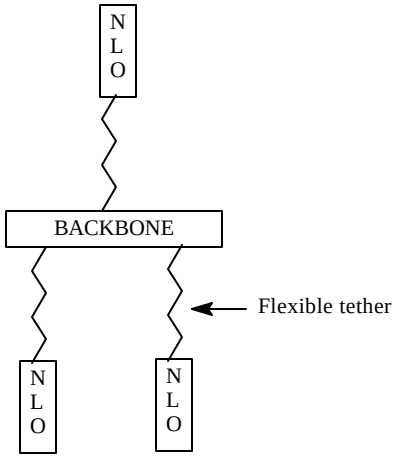

Figure 4.2 A schematic representation of an amorphous side chain substituted NLO polymer

As drawn, a side chain NLO polymer is usually composed of three basic parts: the polymer backbone, a spacer group and the NLO chromophore itself. A flexible spacer between the backbone and chromophore facilitates chromophore motion leading to more facile and efficient poling. The down side is that the relaxation of the polar order is also often faster, since the motion of the chromophore is at least partially decoupled from that of the polymer backbone. A possible consequence of this motional decoupling is that sub T_g poling (T_g and poling are described in detail in Sections 4.5.1 and 4.10 respectively) and relaxation are sometimes observed (39-41).

The polymer properties of the side chain polymer, depicted schematically in Figure 4.2, will depend on the nature of individual constituents and their interactions. For example, if the side chain component (tether + chromophore) is short and stiff, the T_g of the polymer will be higher than if it is long and flexible. To some degree, the intrinsic properties of the polymeric backbone will also be significantly modified by the side chains. The effect of the flexible tether length on the T_g of a variety of side chain

polymers, including some NLO substituted polymethacrylates and polystyrenes, has been studied, leading to the conclusion that the polymer T_g drops with increasing tether length and flexibility (42-44). For practical purposes, a tether length of greater than six carbon atoms plays no useful role and often complicates the synthesis and purification of the monomer. The most common spacer lengths therefore range between two and six carbon atoms. Although, in principle, any stable synthetically accessible flexible unit (e.g, polydialkylsiloxy, polyethyleneoxy, etc) could be used, the most common spacer groups are normally n-alkyl chain functionalised at the terminus. We have restricted our study to the use of two, three or six methylene units as spacer groups.

By virtue of the ready accessibility and excellent optical properties of polyacrylates, majority of the side chain polymers investigated to date have been of these types.

For the preparation of functionalised polymethacrylates and polystyrenes, two primary synthetic approaches have been utilised, as summarised in Scheme 4.3.

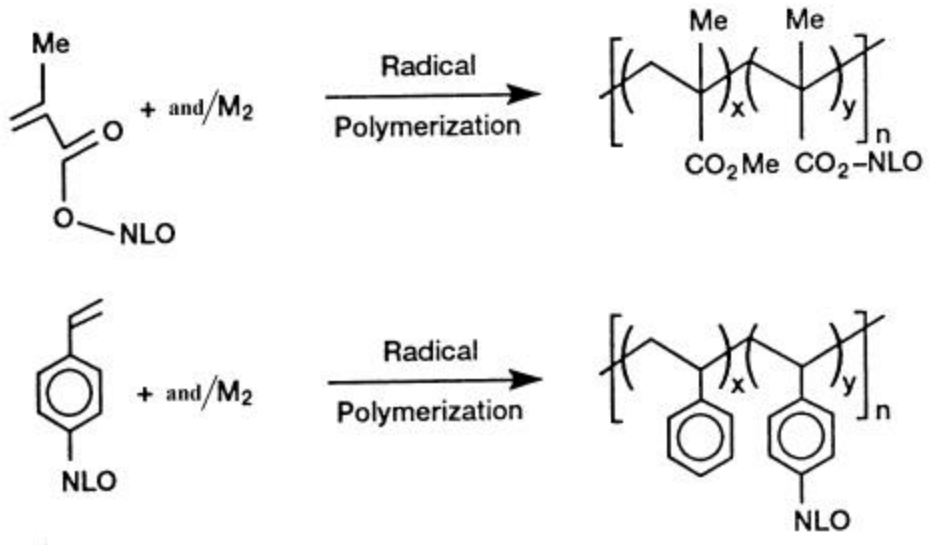

(a)

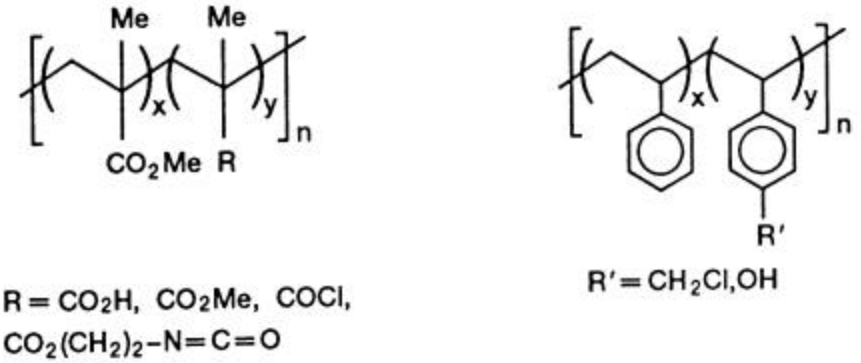

(b)

Scheme 4.3: Generalised procedures for the preparation of side chain NLO functionalised methacrylate and styrene polymers/copolymers by: (a) vinyl polymerisation of functionalised monomers and (b) polymer analogous reactions

The first (a) involves the synthesis of a polymerisable monomer containing a chemically bound NLO chromophore. This material is then polymerised or copolymerised, usually with a closely related monomer M_2 (e.g. methyl methacrylate for methacrylate substituted monomers or styrene for styrene substituted derivatives). In this study, more focus is given for the synthesis of homopolymers. The idea is to increase the d_{33} values by increasing the chromophore density. This also gives space to tailor the desired polymeric materials.

A truly impressive number of NLO side chain methacrylate and acrylate homo and copolymers have been prepared by free radical polymerisation of the respective functionalised monomers. The donor substituents of the incorporated chromophores are usually nitrogen or oxygen while the acceptor groups include nitro, sulphone, cyano, dicyanovinyl, pyridinium, etc. The electron transmitting bridges includes substituted aromatics, stilbenes, tolanes and a variety of azo derivatives.

Although NLO substituted methacrylate polymers have received the bulk of the attention, functionalised styrene homo and copolymers have not been neglected. While the polymerisation of these by polymerisation of a prefunctionalised monomer is much less common than in the case of the methacrylates, a number of examples have been described (45-47). The T_g values for the functionalised polystyrenes ranged from 94-182^oC. As expected, those polymers with short, relatively stiff pendant substituents had

higher glass temperatures than those materials with longer more flexible side chains. NLO functionalised polystyrene derivatives can also be produced from preformed and reactively functionalised polymers as in case of polymethacrylates and polyacrylates.

Recently, attention has been focused on processable NLO thermoplastic polymers with high glass transition temperatures (20). It is well known that high dipole moment of the maleimide unit is at right angle to the backbone and that its cyclic structure imparts great stiffness to the polymer chain, thus resulting in high T_g. Functionalised polymaleimides display reduced mobility and high T_gs desired to maintain the induced polar order in poled systems. It should be noted, however, that rigid polymers of high T_g for thermal stability of induced polar order usually have difficulties in processing. High concentrations of NLO chromophores for high NLO activity also have adverse effects on processability. These conflicting properties can be optimised by utilising copolymers. There have been three main approaches to the synthesis of NLO copolymers of N-substituted maleimides: (1) The reaction of reactive precursor poly(maleic anhydride-alt-styrene) with aminoalkyl functionalised azo dye (48,49). The polyamic acid first formed is cyclised by activation with acetic anhydride at 120^o C; (2) The synthesis of alternating copolymers of N-substituted maleimide and vinylisocyanate to which functionalised chromophores are attached via reaction with the polymeric isocyanate group (50); and (3) Radical copolymerisation of N-substituted maleimides, bearing pendant chromophores, with vinyl monomers namely styrene (51-53), methylmethacrylate (51) and 4-vinylpyridine (53).

Polyurethane derivatives (54,55) constitute another interesting class of polymers. These are produced by reaction of aromatic diisocyanates with functionalised aromatic diamines. For the polyurethane **PU** (Figure 4.3) (R=H), a χ^2_{333} = 3.3 pm/V (1.064 μm) has been measured in a poled sample.

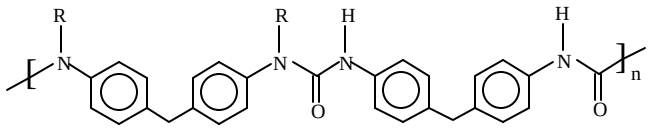

Figure 4.3 **Structure of polyurethane PU**

The nonlinearity is stable indefinitely at room temperature after an initial decay of a few percent. Such materials can contain additional pendant NLO functionality (e.g., p-nitroaniline or any other NLO chromophore). These materials are thermally stable, can be poled at elevated temperatures (>100^o C) and are significantly nonlinear (d_{33} up to 8.3 pm/V at 1.06 μm). Substituents can be used both to modify the nonlinearity and to control the absorption spectra. For the polymer in Figure 4.3, when R=Ph, T_g was found to be 123^o C and it was thermally stable up to 290^o C, having a cutoff of 307 nm. This material, when solution cast, can be poled at 130^o C and remarkably nonlinear considering the structure (d_{33} = 5.4 pm/V at 1.064 μm). This nonlinearity is four times that of urea and no decay of the second harmonic signal of the poled polymer was noticeable over several hours at room temperature. It seems that the polyurethanes constitute an interesting class of thermally stable polymers where the nonlinearity and transparency can be effectively tailored by the choice of substituent.

Backbones used in the present study include polymethacrylates, -acrylates, -styrenes, -maleimides and polyurethanes.

4.4 IR and NMR of polymers

^{1}H NMR spectra of monomers and polymers synthesised in this study are presented in Appendix-I and Appendix-II, respectively.

4.4.1 *Polymethacrylates*

The ^{1}H NMR spectra of polymethacrylates [**V 1** to **V 5**] show no peaks between 5.0 δ - 6.0 δ, indicating absence of vinylic protons. Additional peaks at 1.8 (due to –CH) and 2.0 (due to –CH_2) also indicate vinyl-type polymerisation. The olefinic methyl peak at 1.95 δ in the monomer is shifted upfield to 1.1 δ, also indicating absence of vinylic linkage. The presence of peak at 1730 cm^{-1} in the IR spectrum is indicative of carbonyl group without conjugation adjacent to it (56).

4.4.2 *Polyacrylates*

The ^{1}H NMR of these polymers [**V 6** to **V 8**] indicate the absence of vinylic protons. Additional peak at 1.8-2.0 δ was observed indicating that the polymerisation is exclusively of vinyl-type. Broadening of peaks was also observed, which could be due to aggregation (57).

IR spectra also indicated the occurrence of vinyl-type polymerisation / or absence of vinylic grouping as the presence of peak at 1725-1730 cm^{-1} in all polyacrylates is indicative of carbonyl grouping without conjugation adjacent to it (37,58).

4.4.3 *Polystyrenes*

The ^1H NMR of all polymers [**V 9** to **V 19**] showed two additional peaks at 1.3-1.4 δ (2H, -$\underline{CH_2}$-CH<) and 1.6-1.8 δ (-CH_2-$\underline{CH}$<). Peaks due to vinylic protons were absent, indicating that the radical polymerisation proceeded cleanly via vinyl type polymerisation. IR spectra of these polymers showed peaks corresponding to the functional groups present in them, some being CN at 2230, nitro at 1340 and carbonyl between 1730-1710 cm^{-1}.

4.4.4 *Polymaleimides*

The ^1H NMR of all polymaleimides [**V 20** to **V 23**] cleanly indicate the absence of olefinic protons of maleimide at 6.9 δ and appearance of broad peaks at 1.9 to 2.3 δ. The IR spectra shows peak at 1710 cm^{-1} which is of carbonyl in the maleimide ring.

4.4.5 *Copolymers of N-substituted maleimide with styrene and N-vinyl carbazole*

^1H NMR spectra of all copolymers indicated that radical polymerisation proceeds cleanly via vinyl-type. The ^1H NMR spectra of styrene-maleimide copolymer [**V 24** and **V 25**] indicate loss of vinylic protons of both styrene and maleimide units. Additional peaks were also observed at 1.4 δ (due to -$\underline{CH_2}$-CH<) and at 1.8 δ (due to -CH_2-$\underline{CH}$<) for the styrene moiety and at 3.1 δ due to the maleimide unit. These peaks are seen to merge with peaks of the solvent in the spectra. IR spectra showed peaks corresponding to the functional groups present in the proposed polymer structures.

4.4.6 *Polyurethanes*

^1H NMR spectra of all polymers [**V 28** to **V 35**] showed an inclination to broadening due to polymerisation. The chemical shifts are consistent with proposed polymer structures. Also broad peaks at 8.9 and 9.5 δ, which are due to (–NH-) protons of the isocyanate group, indicate that coupling has occurred.

The IR spectra of polyurethanes is given in Appendix III. The typical IR spectra of polyurethanes synthesised reveal absorption bands at 3390 cm^{-1} (N-H stretching), 1710-1720 cm^{-1} (>C=O stretching), 1540 cm^{-1} (C-N-H bending) and 1280 cm^{-1} (N-C-O

stretching) attributed to the urethane group. Based on the N-H band in the region 3200-3500 cm^{-1}, the polyurethane appears to be primarily hydrogen bonded since the bonded N-H peak at 3390 cm^{-1} predominates. The free (non-hydrogen bonded) N-H peak at 3470 cm^{-1} is also detected but only as a small shoulder. In the carbonyl region between 1650-1750 cm^{-1}, the peak due to bonded C=O stretching centred at 1700 cm^{-1} predominates and that due to free C=O stretching appears as a shoulder at 1730 cm^{-1}. If it is presumed that the extinction co-efficients of free and bonded C=O are similar, the dominance of the bonded C=O peak indicates that a large fraction of hard segments are hydrogen-bonded. In the IR spectra, the characteristic difference between the monomer and polymers show up in the large differences in the intensity of the strong peak between 1700-1720 cm^{-1}, which is attributed to the vibration of the carbonyl group in the urethane linkage. The IR spectra of polymers with TDI and polymers with MDI are nearly identical, except the small differences in the fingerprint region, which may easily be anticipated from their structural similarities.

4.5 Thermal Properties

4.5.1 *Glass Transition (T_g)*

The glass transition is by far the most important one among many transitions observed in amorphous polymers. When an amorphous polymer undergoes the glass transition, almost all of its properties related to processing and/ or performance change dramatically. At a relatively simple-minded practical and operational level of treatment, we can define T_g as the temperature at which the forces holding the distinct components (segments) of an amorphous solid together are overcome, so that these components are able to undergo large scale viscous flow (segmental motion), limited mainly by the inherent resistance of each component to such flow, i.e. above T_g there is enough freedom of motion for chain segments of up to several "statistical chain segments" in length to be able to execute co-operative motions (59).

The "intrachain" effect of stiffness of individual chain segments is generally somewhat of greater importance than interchain effect of the cohesive (attractive) forces between different chains in determining the values of T_g. For eg., a pendant hydroxyl group has relatively little effect on chain stiffness but can increase the cohesive forces

very significantly by hydrogen bonding. On the other hand, the chain stiffness and the interchain cohesive forces are not completely independent of each other. For example, phenyl rings are much more rigid than cyclohexyl rings and therefore result in greater chain stiffness. Phenyl rings are also much more dense than cyclohexyl rings and result in much higher cohesive energy densities. Therefore, most theories of T_g describe this phenomenon in terms of key physical ingredients whose values strongly depend on the chain stiffness and/or cohesive forces.

The factors determining the measured T_g values of polymers are summarised below:

1. *The rate of measurement*. Faster the rate of dynamic measurement, higher will be the perceived temperature.
2. *Structural and compositional factors*, the most fundamental of which are chain stiffness and interchain cohesive forces.
3. *Conformational factors*: The most important one being the tacticity of vinyl-type polymers.
4. *Cross-linking:* T_g increases with increasing crosslink density.
5. *The average molecular weight of polymer chains:* T_g increases asymptotically, with increasing average molecular weight.
6. The presence of *additives, unreacted monomers or impurities or undesirable by-products* generally decreases T_g.

In our study, the DSC trace is characterised by T_g. Above T_g, an endotherm is noted for some polymers. But careful observation under crossed polarised light did not reveal any textures. There is no real evidence for liquid crystallinity in the resulting polymers, which resemble typical amorphous isotropic polymers. Side chain polymers with azo and azomethine units did not reveal any liquid crystallinity, although the corresponding alcohol (with CH=N bridge, CN as acceptor) was found to show texture (Figure 4.4). It should be pointed out now that, except in a few cases (34), polymers with mesogenic group attached directly or with short spacers (up to three methylene units) to the backbones give only glasses with an anisotropy of structure that is lost at the glass transition (60). Coupled with the steric interaction between the side groups, the tendency

towards a statistical distribution of chain conformation hinders the ordered arrangement of the pendant groups and liquid crystallinity is suppressed.

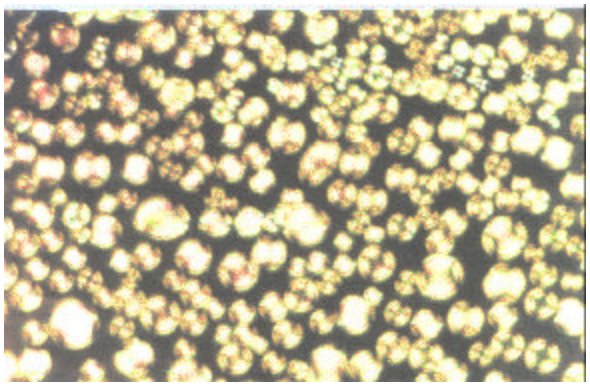

Figure 4.4 Optical texture of alkylated chromophore 4-(2-hydroxy ethyl oxy)-N-(4'-cyano benzylidene) aniline at 112^{o} C

4.5.1.1 *Polymethacrylates*

Polymethacrylates [**V 1, V 2, V 3, V 4** and **V 5**] have T_g over a wide temperature range, from 15-117^{o} C. Better values are expected as T_g of PMMA is 105^{o} C. The T_g's are comparable with the other reported homopolymers (36). The maximum T_g value of 117^{o} C was obtained for **V 1**. This increase could be related to interchain hydrogen bonding between chain segments.

4.5.1.2 *Polyacrylates*

Polyacrylates [**V 6**, **V 7** and **V 8**] have very low T_g, in the range of 20-25^{o} C. This is to be expected since the T_g of poly(methyl acrylate) is only 10^{o} C. The low average molecular weight must have decreased the T_g in **V 8** to as low as –3^{o} C. Also, conformational factors and side products with similar solubilities could be the reason for lesser T_g. In comparison, a slightly higher T_g value of 20^{o} C for **V 7** may be due to the cohesive forces of hydrogen bonding.

4.5.1.3 *Polystyrenes*

Polymerisation of a pre-functional styrene derivative has been much less common than in case of methacrylates. The T_g values of styrene polymers ranged from 30-115^{o} C. Comparitively lower T_g values were obtained for polystyrenes with barbiturate as an electron-accepting moiety. This could be due to the conformational factors (like tacticity of vinyl type polymers). The maximum value of 112^{o} C for **V 9** may be due to inter-chain

H-bonding, which restricts the mobility and hence results in higher T_g. Also an interesting difference in T_g is observed for polymers **V 10** (25^o C) and **V 11** (70^o C). This may be due to conformational factors which allows better packing between side chains, thus increasing T_g. In polystyrenes with heterocyclic chromophores, the T_g range observed for polymers **V 15** and **V 16** was 60-100^o C. Polymers **V 17**, **V 18** and **V 19** showed T_g in the range of 70^o C. In some cases exact determination of T_g was not possible and the values determined are approximately given in a broad range.

4.5.1.4 *Polymaleimides*

In an effort to synthesise novel materials which show significant SHG values and possess reasonable temporal stability, polymaleimide backbone has been evaluated using commercially available 4-cyano-4'-oxy biphenyl as the mesogenic chromophore (61). This polymer is smectic and has d_{33} values ranging from 10-20 pm/V.

Novel polymaleimides with azo and azomethine bridges were synthesised in the present study. Polymer **V 20** and **V 21** showed T_g in the range of 60-105^o C. The molecular weights were comparable with other systems, which could be due to the common method of polymerisation used. In case of polymers **V 22** and **V 23**, T_g obtained was 40^o C and 30^o C, respectively. In comparison to polymer **V 21** (105^o C), the lower T_g is because the hexamethylene spacer in polymer **V 23**, decouples the chromophore from the main chain to a larger extent, allowing its free movements and lowering the T_g.

Polymaleimides have comparatively higher T_g. The high dipole moment of the maleimide unit at right angle to the backbone and its cyclic structure impart great stiffness to polymer chain. The presence of aromatic rings and polar groups like carbonyl in the chain backbone increases the inflexibility of the chain and the T_g value increases. The comparatively higher T_g's obtained in these series could be attributed to the rigid ring structures in the macromolecular chain.

4.5.1.5 *Copolymers of substituted maleimide with styrene and N-vinyl carbazole*

Better T_g values were obtained for copolymers of styrene and substituted maleimide, poly[{N-[6-(4-cyano/nitro benzylidene aniline-4'-oxy)hexyl]maleimide}-co-styrene] (**V24**)/(**V25**). They ranged from 60-70^o C. All copolymers showed higher T_g irrespective of the chromophore present. Styrene and N-vinyl carbazole were

copolymerised with substituted maleimide. The T_g's are comparable to the reported values (62).

4.5.1.6 *Polyurethanes*

Polyurethane has moderate T_g and a structure that allows physical cross-linking using interchain hydrogen bonds. The T_g's of polyurethanes [**V 28** to **V 39**] ranged from 60-150^o C, which is higher than the glass transition temperature of common flexible polyurethanes (63). This can be attributed to the enhanced chain rigidity caused by incorporation of the substituted benzene ring. This rigidity could also be due to formation of interchain hydrogen bridges. T_g is noticeable in polyurethanes with azo chromophore whereas this is indistinguishable in the polyurethanes with azomethine chromophore which show a broad transition. Some polymers showed melting transition arising from side chain melting. Also, the polyurethanes prepared with MDI had higher T_g than the corresponding polyurethanes with TDI.

4.5.2 Thermogravimetric analysis (TGA) studies on polyurethanes

TGA studies of the polyurethane **V 32** indicate three weight loss processes (Figure 4.5) (temp. Range 25-800^o C, heating rate 10^o C/min, flow of 50 cm^3/min of N_2 gas).

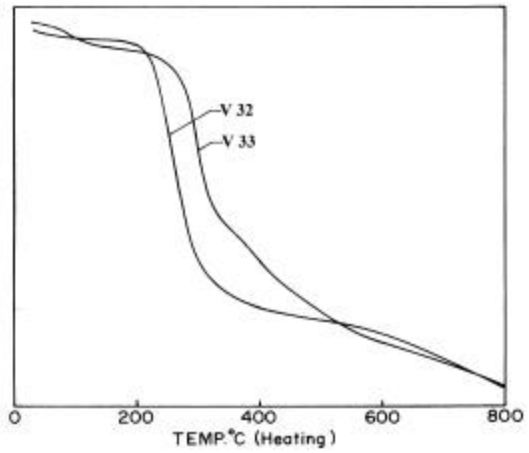

Figure 4.5 TGA curves of polyurethane V 32 and V 33 with a heating rate of 10^o C/min.

It shows an initial decomposition at about 183^o C due to the thermal breakdown of the azo group. The 19% weight loss corresponds to the thermal degradation of the nitrophenyl ring at the N=N linkage. Degradation or thermal decomposition of the

polymer backbone is almost complete (88 %) at 797^{o} C. Polymer **V 34** is stable up to 233^{o} C. Degradation of backbone is 83 % complete at 795^{o} C. Polymer **V 33** shows initial decomposition at 240^{o} C and 90 % degradation of backbone at 797^{o} C. Polymer **V 35** shows initial weight loss at 240^{o} C and 75 % thermal decomposition of the polymer backbone at 797^{o} C. **V 28** shows initial decomposition at 125^{o} C (10%) and 77 % degradation of backbone at 789^{o} C. Polymer **V 30** is stable upto 233^{o} C. Degradation of backbone is 78 % complete at 798^{o} C. Polymer **V 29** shows initial weight loss at 181^{o} C and 77% thermal decomposition of the polymer backbone at 791^{o} C. Polymer **V 31** is stable upto 258^{o} C. Degradation of backbone is 100% complete at 723^{o} C. Polymer **V 36** shows initial decomposition at 184^{o} C. Degradation of the backbone is 91 % complete at 798^{o} C. Polymer **V 37** is stable upto 280^{o} C and 79 % thermal degradation of the backbone is complete at 788^{o} C. Polymer **V 38** shows initial weight loss at 124^{o} C and 99% degradation of the backbone at 789^{o} C. Polymer **V 39** shows initial weight loss at 209^{o} C and 87% degradation at 789^{o} C.

4.6 Molecular weights

The kinetic chain length ν, in a polymerisation is defined as the average number of growth reactions which follow an initiation process. Normally the M_n is considered. ν is the number of monomeric units in the average polymer radical at the time of termination. It is related to the average degree of polymerisation (D_P) of the polymer by equation 4.1.

$$D_{Pn} = q\nu_n \qquad \textbf{4.1}$$

The value of q is 2 for termination entirely by combination since two radicals unite to give a single molecule; it is unity if disproportion is the sole mode of termination. Also D_{Pw} / D_{Pn} will be 1.5 for combination and 2 for disproportionation (64).

The number average molecular weight (M_n) of polymers were estimated by vapour pressure osmometry (VPO). The solvents were selected according to the solubility of polymers. Chloroform and dimethylsulphoxide were used at temperatures 40^{o} C and 80^{o} C respectively.

4.6.1 *Polymethacrylates*

Polymethacrylates [**V 1** to **V 5**] have shown M_n ranging from 5,600 to 7,200. The degree of polymerisation (D_P) ranged from 13 to 20. The maximum value was obtained for polymethacrylate with cyano as the electron withdrawing group. The lowest M_n value was obtained for **V 2** where barbiturate is used as the electron acceptor.

4.6.2 *Polyacrylates*

Polyacrylates [**V 6** to **V 8**] have shown M_n ranging from 2,710 to 3,200. The D_P ranged from 8 to 10. The maximum value (M_n = 3,200) was obtained for **V 6**, where aldehyde is the $\bar{e}$ acceptor. Not too high molecular weights were obtained for **V 7** and **V 8** with barbiturate as the e^- acceptor.

4.6.3 *Polystyrenes*

Polystyrenes [**V 9** to **V 19**] have shown M_n ranging from 4,750 to 11,050. The D_P ranged from 10 to 29. Polystyrenes have found to show higher molecular weights than polymethacrylates and polyacrylates. **V 12**, with cyano as the electron acceptor has the highest molecular weight and the lowest in this series was for polymer **V 14** (M_n = 4,750) with barbiturate as the electron acceptor.

4.6.4 *Polymaleimides*

The M_n of polymaleimides [**V 20** to **V 23**] range from 6,700 to 11,250 and D_P are in the range 18 to 33. Polymaleimides have the highest molecular weights within a series of homopolymers. The lowest M_n polymer was **V 20** with nitro as the acceptor. The highest molecular weight polymer in this series was for **V 21** with cyano as the electron acceptor group.

4.6.5 *Copolymers of substituted maleimide with styrene and N-vinyl carbazole*

M_n ranged from 4,255-7,100. The maximum value was obtained for **V 26** where the monomer units are 4-[6-(N-maleimido)hex-6-yloxy)-N-(4-cyano benzylidene)]aniline and N-vinyl carbazole; the lowest value of 4,255 for **V 25** where the monomer units are 4-[6-(N-maleimido)hex-6-yloxy)-N-(4-nitro benzylidene)]aniline and styrene. The D_P ranged from 8 to 12.

4.6.6 *Polyurethanes*

The molecular weights of polyurethanes [**V 28** to **V 39**], both from epoxy diols and ester diols, were better than the homopolymers synthesised in the other series, even

though they are lower compared to that observed for polyurethanes (65). They ranged from 7,100-16,200. The D_P ranged from 12 to 28.

Within a given structural entity, polymers with cyano as electron acceptor have the highest molecular weights in comparison to polymers with nitro and barbiturate as electron acceptor groups. This could be due to steric reasons as the latter groups are much bigger than cyano group. The barbiturate is the bulkiest and gave the lowest molecular weights. The chain transfer ability of –NH- group in barbiturate unit also contributes for lowering the molecular weights. The heterocycles gave molecular weights in the range of aromatic polymers. It is well established that the rate of free radical polymerisation is drastically decreased in the presence of azobenzenes and nitro substituents (20,56). The presence of functional groups with N and S atoms act as retarders, inhibitors or chain transfer reagents in the free-radical polymerisation. Also, the number of solvents for free-radical polymerisation is limited. The classical solvent used is benzene which shows very negligible chain transfer to various monomers. The chain transfer constant of tetrahydrofuran and dioxane are larger by a factor of 25 and 140 respectively and for dimethylformamide/ dimethylsulphoxide it is 200 fold the value of benzene (56). The molecular weights were found to increase with the rigidity of the backbone. On the basis of this observation, the copolymers of styrene and N-vinylcarbazole with maleimides were expected to give the highest molecular weights, but this was not observed. Polymaleimides gave the highest molecular weights. This discrepancy can be explained on the basis of steric reasons.

4.7 Solubility

Most of the polymers were soluble in common organic solvents either wholly or partially (Table 4.2). But the ones with barbiturate as the electron acceptor group were totally insoluble, probably due to the polar, bulky nature of the barbiturate moiety in the chromophore. Also, solubility may be reduced by intermolecular hydrogen-bonding between –NH- and C=O present in the barbiturate group.

The thin films were prepared by *spin coating technique* from dust free polymer solutions in an appropriate solvent and of correct concentration. Thus, the first step was to test for the solubility of polymers in all common solvents. The ideal polymer

Table 4.2 Solubility of polymers synthesised in the present investigation

Polymer code	$CHCl_3$	1, 1, 2, 2-TCE	DMF	DMSO
V 1	I	I	S	S
V 2	I	I	S	S
V 3	I	I	S	S
V 4	I	I	S	S
V 5	I	I	S	S
V 6	I	I	S	S
V 7	I	I	S	S
V 8	I	I	S	S
V 9	I	I	S	S
V 10	S	S	S	S
V 11	S	S	S	S
V 12	S	S	S	S
V 13	I	I	S	S
V 14	I	I	S	S
V 15	I	I	S	S
V 16	I	I	S	S
V 17	S	S	S	S
V 18	S	S	S	S
V 19	I	I	S	S
V 20	S	S	S	S
V 21	S	S	S	S
V 22	S	S	S	S
V 23	S	S	S	S
V 24	I	I	S	S
V 25	I	I	S	S
V 26	I	I	S	S
V 27	I	I	S	S
V 28	I	I	S	S
V 29	I	I	S	S
V 30	I	I	S	S
V 31	I	I	S	S
V 32	I	I	S	S
V 33	I	I	S	S
V 34	I	I	S	S
V 35	I	I	S	S
V 36	I	I	S	S
V 37	I	I	S	S
V 38	I	I	S	S
V 39	I	I	S	S
V 40	I	I	S	S
V 41	I	I	S	S

S = soluble, **I** = Insoluble

concentration was established to be in excess of 6-10 wt % for NLO measurements. 60 to 100 mg of polymer was used per mL of solvent. In case the polymer was not soluble in chlorinated solvents, then the dissolution is attempted first in a mixture of either 1,1,2,2-tetrachloroethane, 1,1,2-trichloroethane and dimethylformamide. The strategy that worked well in some cases was the addition of 1 drop of dimethylformamide (DMF) to wet the polymer and then the addition of the chlorinated solvent (to make up to 1 mL). On failing this, the polymer was solubilised in dimethylsulphoxide. The procedure was as follows: 60-100 mg of the polymer was weighed into clean sample tube, 1 mL of the solvent was added, tube was stoppered and set aside overnight. The polymer solution was taken in a syringe, attached with a 0.1 micron filter disc with the lowest void volume and

filtered slowly into a second clean sample tube avoiding back-pressure. To avoid back-pressure, the polymer solution (only those polymers soluble in chlorinated solvents) was usually pre-filtered in the following manner: Dilute polymer solution in dichloromethane was filtered using a pre-filter into a clean sample tube, covered with a tissue paper and allowed to evaporate in a dark room overnight to get cleaner polymer powder. Polymer solution made from this was easy to filter.

4.8 Spin coating

The spin coating was performed with a spin coating equipment. The cleaned glass slide was set on top of the spinner so that the centre of the rectangular glass slide coincided with the hole on the top of the spinner head. The polymer solution was added drop-wise using a clean pipette and evenly spread on to the glass slide to have a uniform thickness. After spin coating, the glass slide was removed, a mark was made on the top right corner on the underside of the glass slide. This was to ensure that the same side of the glass slide was positioned in the same direction in all poling experiments and UV/visible measurements. The speed, its gradient and time were established as: spinning time 60 sec; first 30 sec at 2000 rpm, quick acceleration to 4500 rpm and then 30 sec at this rpm. The spin coated film was dried for 24 hours at a temperature below the T_g to avoid plasticising effect arising from any residual solvent that would lower T_g. When dimethylsulphoxide was used as solvent, the solvent was evaporated simultaneously during spinning using a hot air-gun.

4.9 Polarisation

The Corona poling set up consists of two parts as shown in Figure 4.6. The first is the hot stage and the second a high-voltage unit. The polarisation unit consists of a needle pointing towards a copper plate mounted on a small platform and these were enclosed in a poly(methyl methacrylate) chamber with a vertically sliding front panel. The polymer coated glass plate was rested on the copper sheet with the polymer film side pointing up towards the needle and the needle positioned vertically above the centre of the glass plate. The temperature was set accordingly and the current was set to 0.003 milliamperes and the voltage was set to 6 kV. The polymer sample was allowed to reach the isothermal temperature for the first reading and the stopwatch was started. The sample was cooled to room temperature under the field and then the poling was stopped. Otherwise, the aligned

dipoles would relax back. The UV-visible absorption of the poled film was measured. During the second poling, the poling current and voltage were set at room temperature and then the sample was heated to the poling temperature, again to prevent the relaxation of the oriented dipoles. The poling was continued till no perceptible decrease in absorbence was noted.

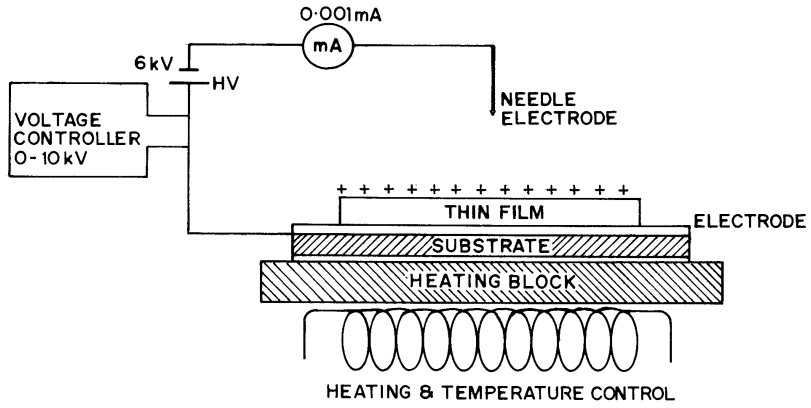

Figure 4.6 A schematic representation of corona poling set-up

4.10 Poling

Molecular motions begin at glass transition temperature. A polymer, having an intrinsic dipole and processed to a 1 micron (or so) thin film, can be oriented under a dc electric field just above the glass transition temperature. The order parameter (1 in perfect crystals and 0 in isotropic amorphous polymers) is enhanced by poling in an electric field and is indicative of the ability to align the sample. The order parameter is shifted from 0 to up to 0.4 for isotropic polymers and up to 0.6 for nematic polymers up on poling. Such poled films are essential to make NLO measurements. The important thing is to make 1 micron thick optically transparent film (transparency 0.92), having an absorbence in the UV/visible range (intrinsic to the sample) and with an absorbence of 1 to 1.5 (within Beer-Lamberts' law applicability). For this, the coating methodology to make around 1 micron thick transparent polymer film should be standardised. This would vary with the polymer sample, the solvent and the viscosity of the polymer solution.

4.11 UV measurements

The UV-visible spectrophotometer used for the absorption measurements of the film was Shimadzu UV-160. The standardisation was made with plain glass by

measuring absorbence at λ_{max} and correcting for any absorption of plain glass at λ_{max}. Later, the absorption of the spin-coated slide was measured. After poling, the measurement was repeated. The UV-visible spectra of polymers before and after poling are represented in Figures 4.7 to 4.19.

The UV-visible spectra of the as spin coated un-poled thin polymer film is scanned first against a similar glass slide (or the substrate used) to establish the λ_{max} and absorbence at λ_{max}. The as spun polymer film spin coated from an isotropic polymer solution would be isotropic due to a random distribution of the chromophores on the film surface. The absorbence of the film in the UV-visible range is essentially due to the chromophores. These chromophores would be present on the plane of the glass slide in an as spin coated isotropic polymer film. Hence, the absorbence of such a state will be the highest at λ_{max}.

On poling above the glass transition temperature, the dipoles will be aligned towards the electric field set normal to the plane of the glass plate. So the chromophores (some of them) will be aligned and will be dragged normal to the plane of the glass slide. On subjecting such an aligned sample to the UV-visible light only those dipoles normal to the light (unaligned ones) will contribute to the absorbence and hence absorbence intensity at λ_{max} would fall with increasing alignment. This alignment changes the order parameter, which can be extracted from a combination of poling and absorbence measurements. The global order parameter thus obtained is an indirect proof of the presence or absence of liquid crystallinity.

The variables involved in this series of experiments were poling temperature, poling time, applied voltage, and current density. The applied voltage was standardised to 6 kilovolts and the current density was standardised to 0.03 milliamperes. The distance between the two electrodes was also standardised. The optimum poling temperature and the optimum poling time were established by an iterative experimentation. One polymer film was used for each temperature. Solvent for the polymer, polymer concentration in the solution, spinning speed were other variables that were established to make polymer film of the desired quality and thickness.

Importantly, it can be seen that the linear optical absorption is far removed from 532 nm, the 2ω light generated in the SHG experiment performed with laser operated at 1064 nm. The chromophore absorption essentially reaches base line within 345-450 nm range for all polymers synthesised and evaluated in this study. Thus negligible resonant enhancement of NLO response and negligible photochemical damage of the chromophores can be anticipated. As a matter of fact from the resonant two-level model, the static value of the SHG co-efficients will be 0.48 of that measured actually at 1064 nm, the decrease being mainly due to the usual wavelength dispersion (66). The post poling spectrum reveals a noticeable reduction in the peak intensity in most cases and a small red shift in the band position in few cases. Similar electric induced changes are reported earlier (67) and are understandable as a simple case of dielectric anisotropy.

There is a strong tendency for an anisotropic dielectric to align in an electric field, so that the largest component of the dielectric constant coincides with the field direction. During corona poling, at T_g or temperatures slightly above that, the side chains tend to align along the direction of the poling field resulting in a decrease in the intensity of peak absorbence.

4.12 Order parameter $\langle P_2 \rangle$

The order parameter $\langle P_2 \rangle$ was calculated using the formula:

$$\langle P_2 \rangle = (A_i - A_p) / A_i \qquad \textbf{4.2}$$

where, A_p is absorbence of poled film and A_i absorbence of isotropic film. Films were polarised by corona poling (68) at temperatures above T_g of the polymer. The development of polar order was estimated by measuring the absorbence at λ_{max}. From the decrease in absorbence, the order parameter $\langle P_2 \rangle$ was estimated. Figures 4.20 to 4.31 show the development of order parameter $\langle P_2 \rangle$ against poling time for polymethacrylates, polyacrylates, polystyrenes, polymaleimides and for some copolymers.

The orientation time curves are fitted by the equation 4.3:

$$\langle P_2 \rangle = \langle P_2 \rangle_\infty (1 - e^{1/\tau}) \qquad \textbf{4.3}$$

Here, τ is a characteristic time for the process and describes the rate of orientation for a given set of conditions.

Alignment could not be achieved on a reasonable time scale at temperatures near or lesser than T_g as they are not very high in some of these systems. The kinetic limitation on polymer mobility is relieved at temperatures much above T_g, as noted in some polymers in DSC. The value of $<P_2>_{max}$ is the plateau level or orientation reached after sufficiently long time.

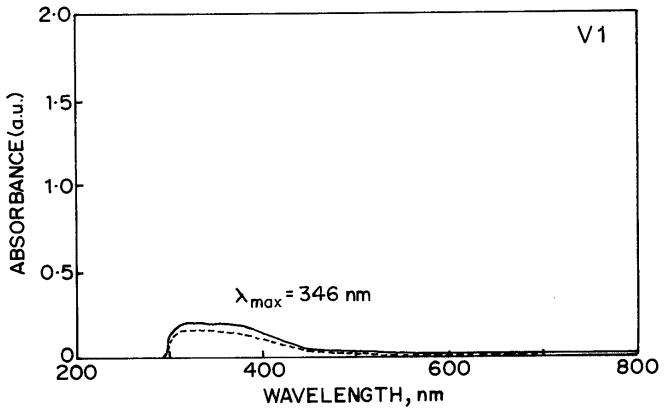

Figure 4.7 UV-visible spectrum of polymer V 1 before (—) and after (---) poling

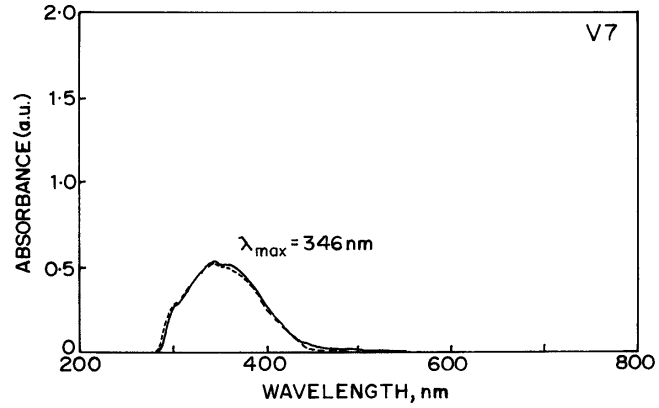

Figure 4.8 UV-visible spectrum of polymer V 7 before (—) and after (---) poling

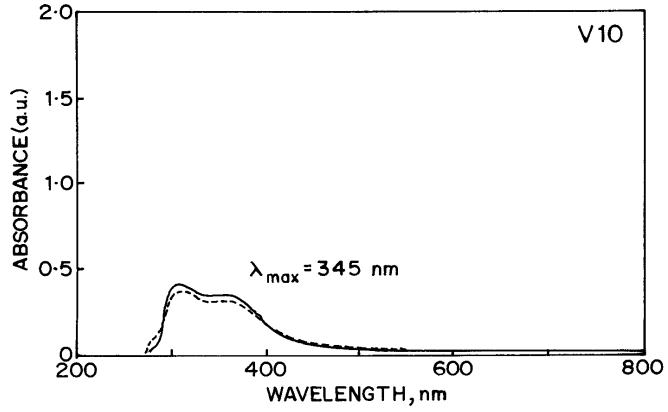

Figure 4.9 UV-visible spectrum of polymer V 10 before (—) and after (---) poling

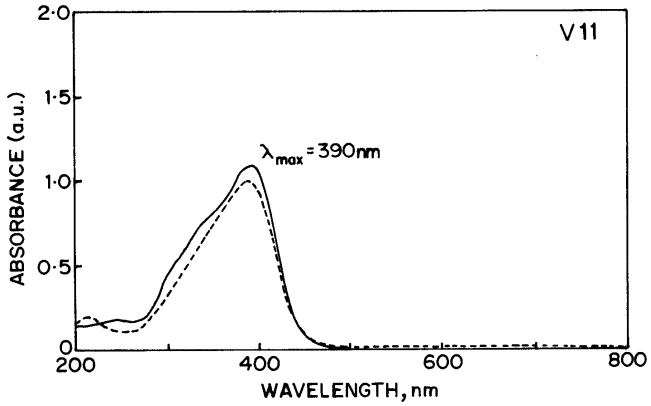

Figure 4.10 **UV-visible spectrum of polymer V 11 before (—) and after (---) poling**

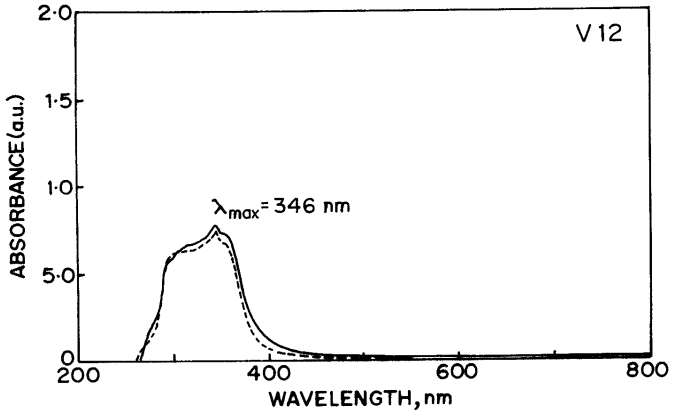

Figure 4.11 **UV-visible spectrum of polymer V 12 before (—) and after (---) poling**

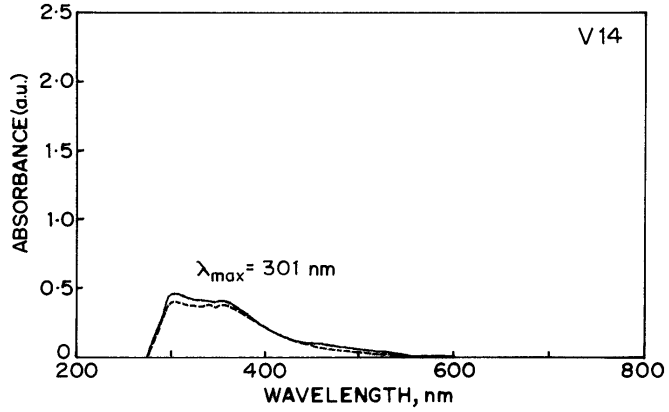

Figure 4.12 **UV-visible spectrum of polymer V 14 before (—) and after (---) poling**

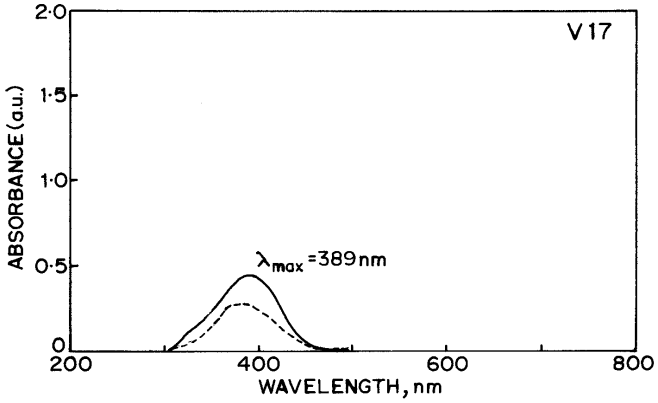

Figure 4.13 **UV-visible spectrum of polymer V 17 before (—) and after (---) poling**

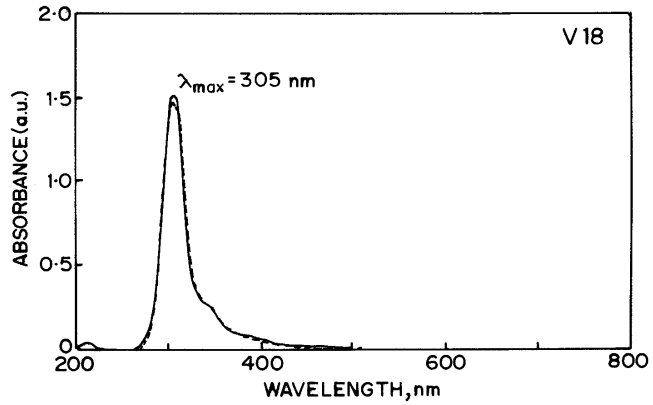

Figure 4.14 **UV-visible spectrum of polymer V 18 before (—) and after (---) poling**

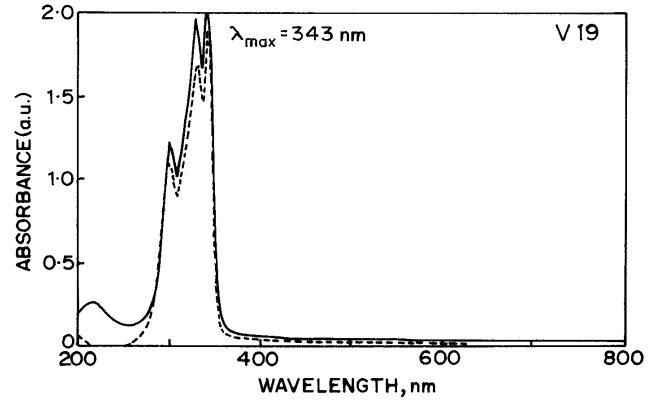

Figure 4.15 **UV-visible spectrum of polymer V 19 before (—) and after (---) poling**

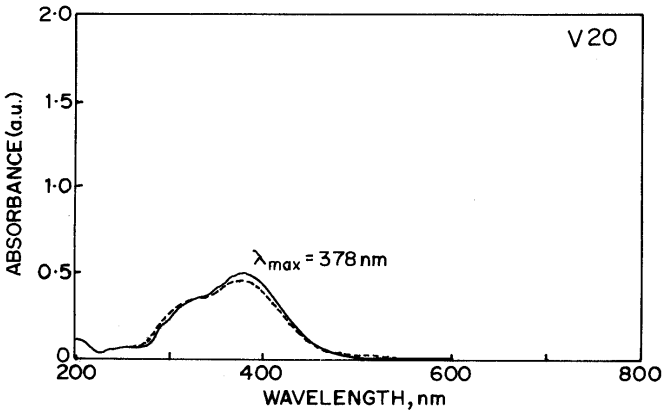

Figure 4.16 **UV-visible spectrum of polymer V 20 before (—) and after (---) poling**

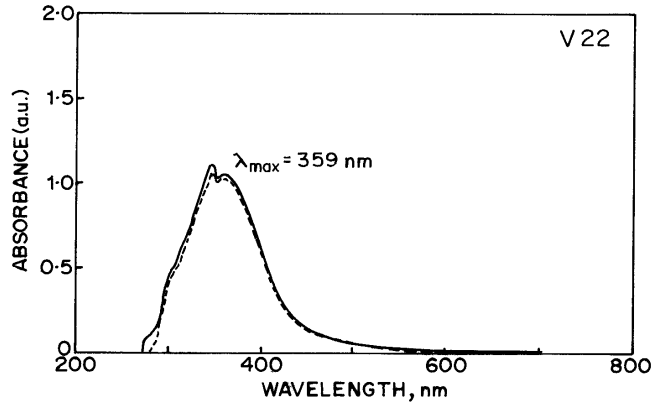

Figure 4.17 **UV-visible spectrum of polymer V 22 before (—) and after (---) poling**

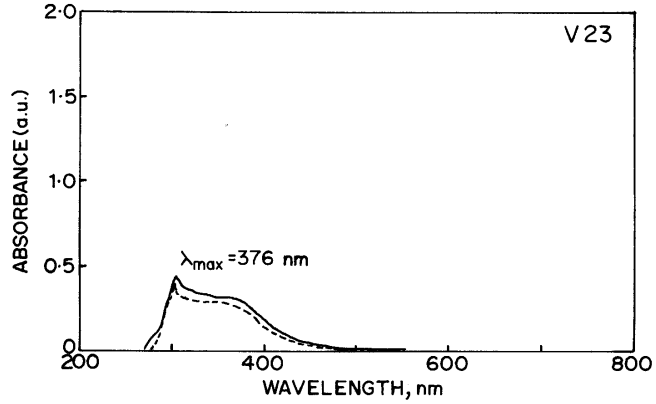

Figure 4.18 **UV-visible spectrum of polymer V 23 before (—) and after (---) poling**

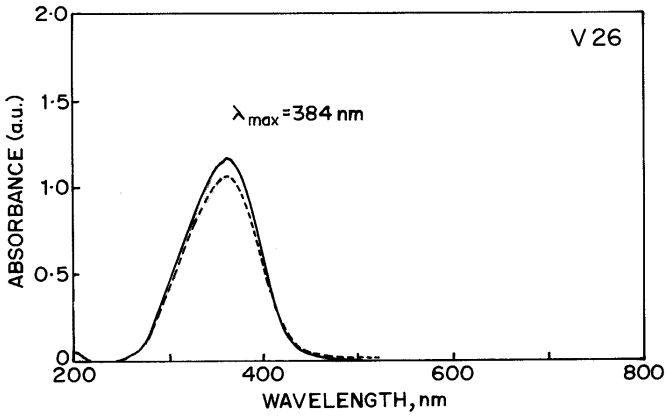

Figure 4.19 UV-visible spectrum of polymer V 26 before (—) and after (---) poling

The $<P_2>$ values observed for the polymers studied are comparable with that reported for amorphous homopolymers. The temperature used for poling was T_g + 10° C. The maximum $<P_2>$ value of 0.5 was obtained for **V 17**. Other Polymers also showed better values like 0.25 for **V 9**, 0.18 for **V 1**, 0.11 for **V 19** and **V 10** and 0.1 for **V 26**.

The lesser $<P_2>$ values ranging from 0.06-0.08 has been observed for polymers **V 5**, **V 11**, **V 12**, **V 18**, **V 21**and **V 20**. The lowest $<P_2>$ value was observed in the range of 0.02-0.05 for polymers like **V 17**. The lower $<P_2>$ values may be due to fast relaxation phenomena.

4.13 Substituted epoxy resins

Because of their extensive industrial application, thermosetting materials have been well investigated for many applications. One of the oldest and best studied classes are epoxy resins (69). These are multi-component systems consisting of polyfunctional epoxy monomers or prepolymers mixed with a variety of initiators, promotors, accelerators, etc. Polymerisation ultimately takes place by the opening of strained epoxy ring. The structure of final cured polymer depends on curing conditions, component structures, initiator type, functionality, etc.

One of the first NLO epoxy materials was described by Hubbard et al. (70). This was a crosslinked host-guest composite formed by the incorporation of the NLO chromophore (Here DANS) into a mixture of diglycidyl ether of bisphenol A and a diamine. The decay of polar order was dependent on size of chromophore i.e. large chromophores relaxed much slowly. Eich et al. discovered that the chromophore densities

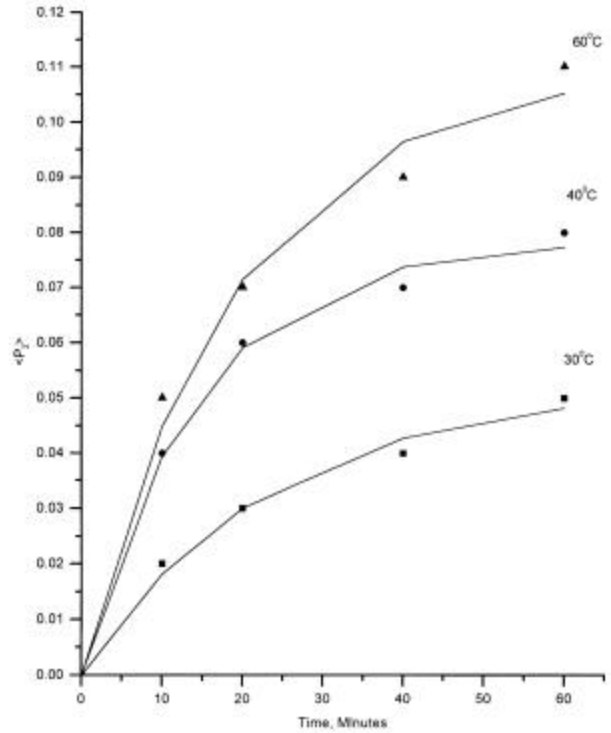

Figure 4.20 Development of order parameter against poling time for polymer V 10

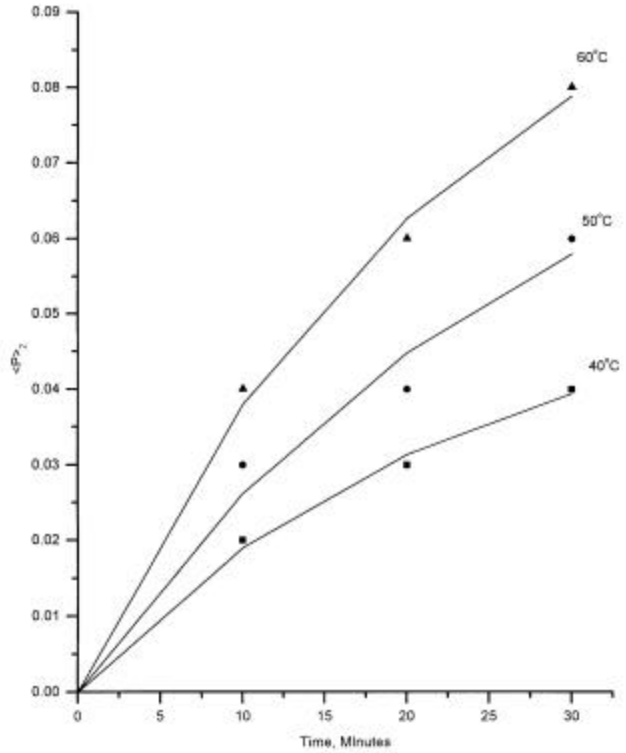

Figure 4.21 Development of order parameter against poling time for polymer V 11

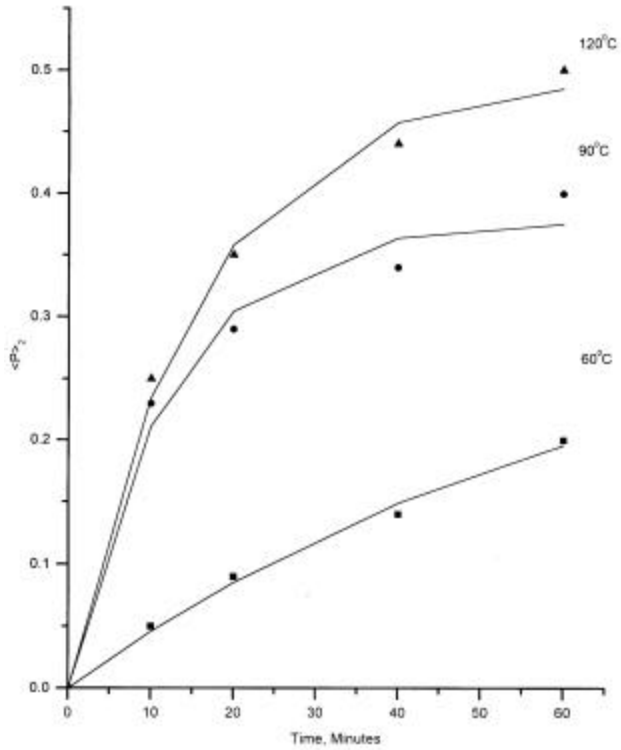

Figure 4.22 Development of order parameter against poling time for polymer V 17

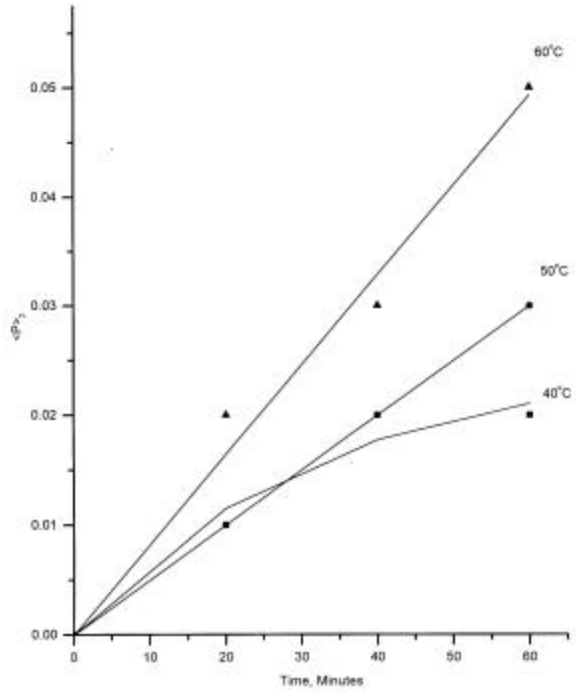

Figure 4.23 Development of order parameter against poling time for polymer V 18

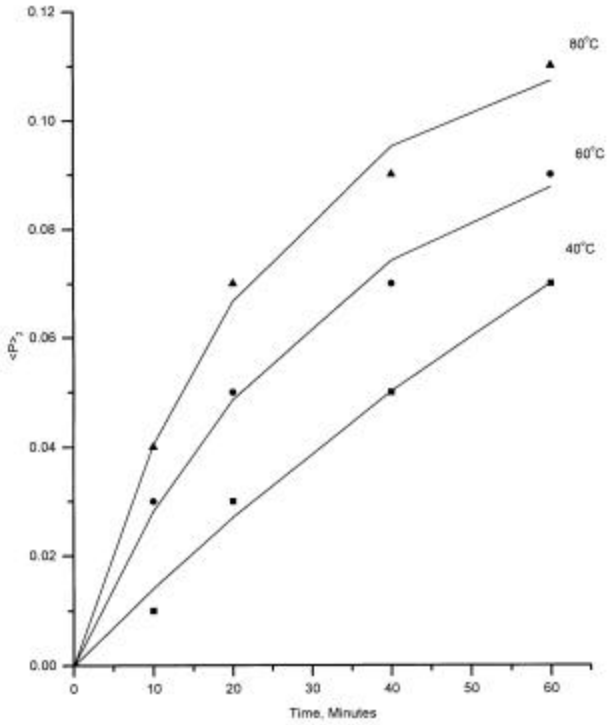

Figure 4.24 Development of order parameter against poling time for polymer V 19

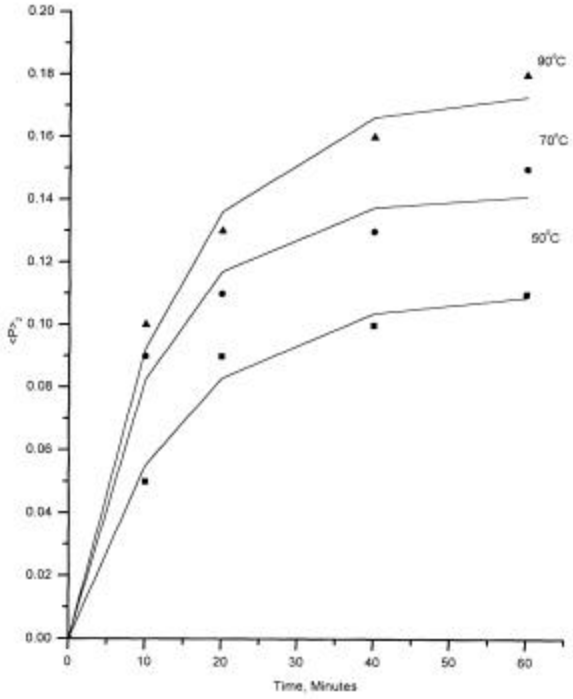

Figure 4.25 Development of order parameter against poling time for polymer V 1

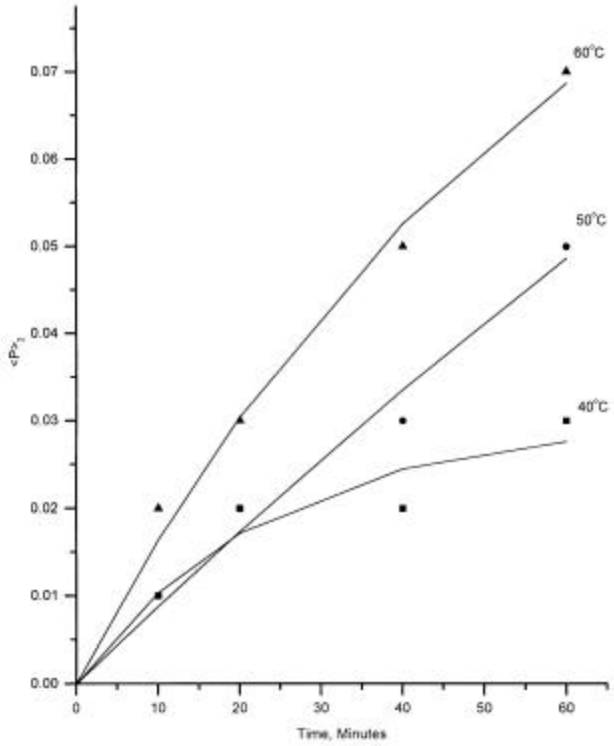

Figure 4.26 Development of order parameter against poling time for polymer V 20

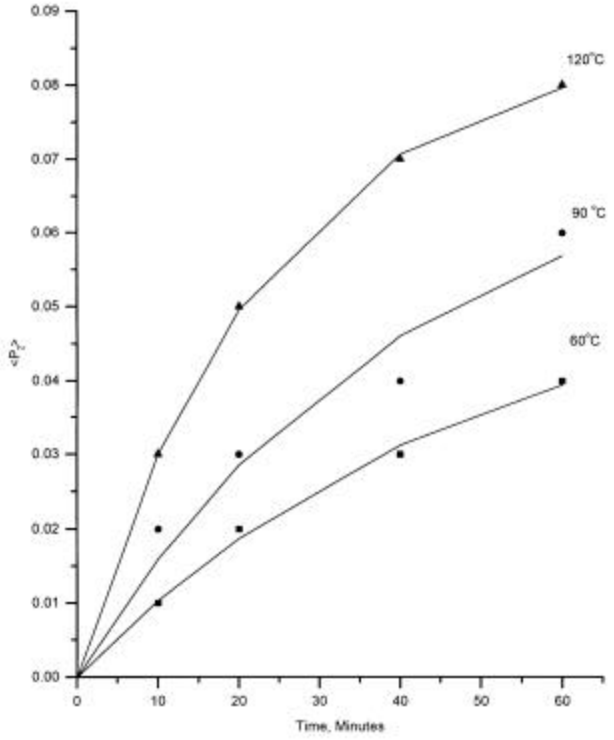

Figure 4.27 Development of order parameter against poling time for polymer V 21

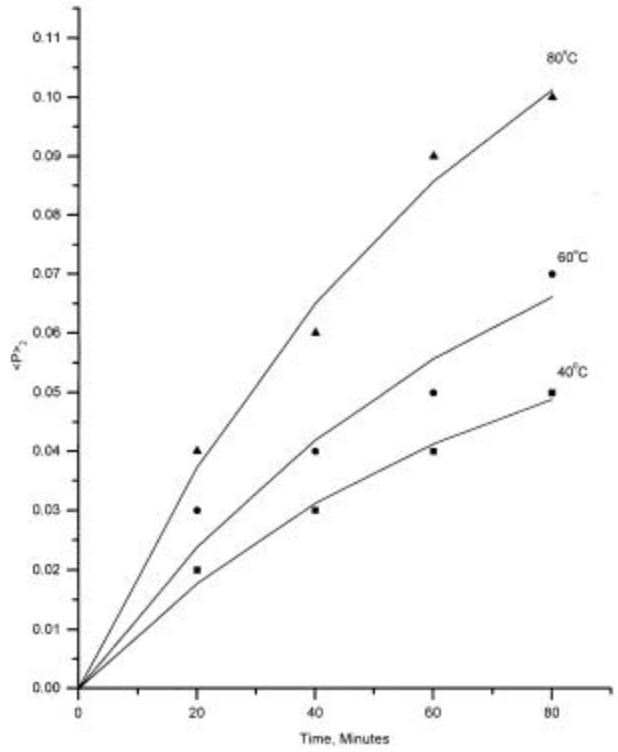

Figure 4.28 Development of order parameter against poling time for polymer V 26

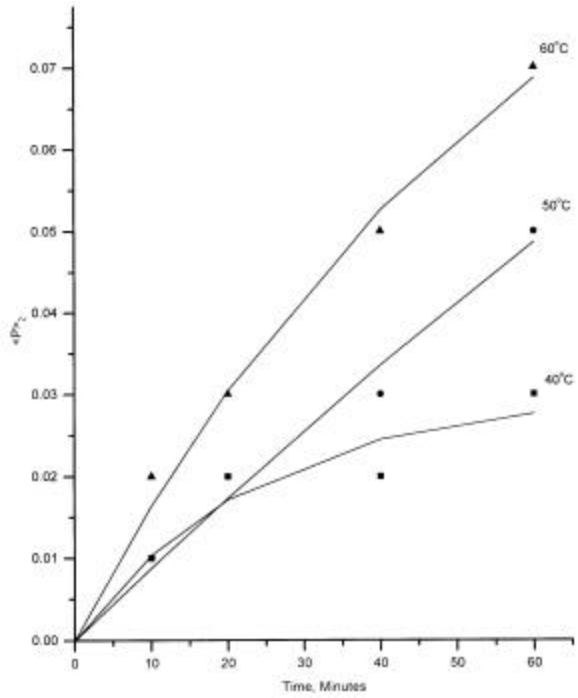

Figure 4.29 Development of order parameter against poling time for polymer V 5

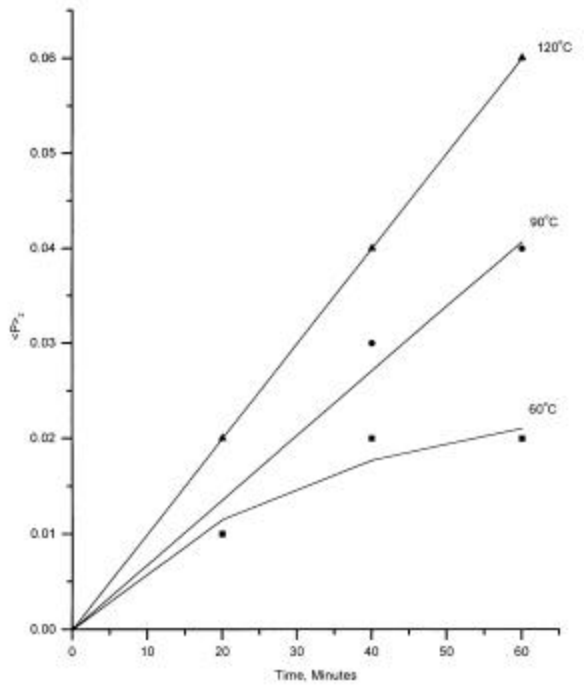

Figure 4.30 Development of order parameter against poling time for polymer V 12

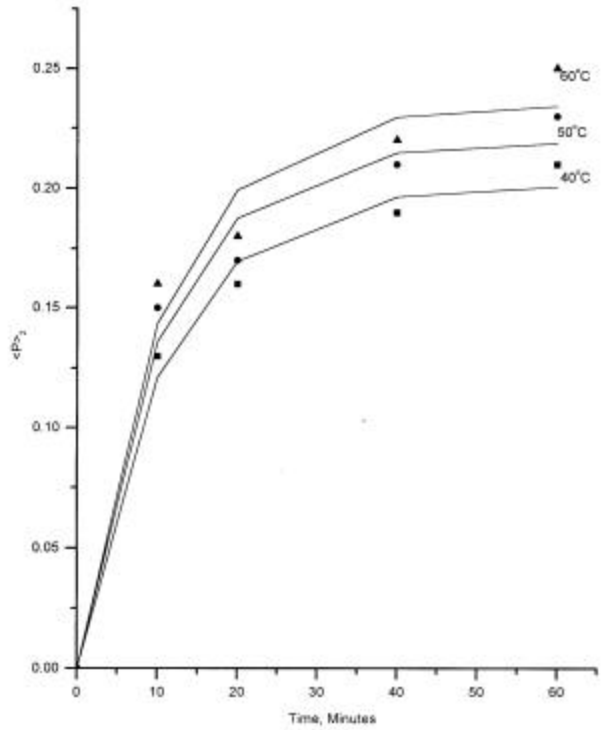

Figure 4.31 Development of order parameter against poling time for polymer V 9

and hence the poled nonlinearities in epoxy systems could be increased using a dual function initiator [i.e. an NLO initiator where the amino donor substituent functioned also as the nucleophilic initiator]. The authors (71) have also described cross-linking versions employing diamines. In our study, we have used some novel chromophores having azomethine bridge and nitro and cyano as e-accepting moiety. Also the size of the chromophore is big enough to prevent the decay of polar order. This dual function initiator was coupled with diglycidyl ether bisphenol A (BPDGE). The resultant polymers showed T_g of 89^o C for polymer **V 40** (NO_2 acceptor) and 58^o C for **V 41** (CN acceptor). They were spin coated to yield good optical quality films and their $<P_2>$ was calculated to be 0.3, which was comparatively better than the $<P_2>$ obtained for other systems.

Rigidity of polymers **V 40** and **V 41** can be further increased by using sol-gel technique. Sol-gel techniques have been investigated extensively for more than 2 decades and have been the subject of several symposia (72). A variety of synthetic routes have been used to prepare the functionalised organic-inorganic composites. The formation of a siloxane bond occurred at lower temperature to make it possible to prevent the decomposition of the organic component in the inorganic-organic composite. The hydrolysis from tri- or tetraalkoxysilane, accompanying with dehydration of silanol moieties by thermal curing, gave three-dimensional structures with excellent optical clarity.

Polymers **V 40** and **V 41** can be further modified to achieve stable second-order NLO polymers by hardening with a crosslinkable sol-gel system. Chong-Bok Yoon et al. (73) used (triethoxysilyl)propyl isocyanate as the sol-gel moiety. They observed that tethering the sol-gel moiety into the polymer backbone, followed by hydrolysis of the triethoxysilyl group to silanol resulted in three-dimensional crosslinking between the silanol groups that seemed like interpenetrating network (IPN).

4.14 Synthesis of siloxane polymers and elastomers

4.14.1 *4-[(S-1-Methylheptyl oxy)-3-nitro-1,4-phenylene carbonyloxy]-4'-(undec-10-enoxy) biphenyl* (**M34**) and *Poly{1-Methyl-1-[4-(S-1-methylheptyloxy)-3-nitro-1,4-phenylene carbonyloxy-4'-(undecamethyleneoxy)biphenyl]siloxane}*(**V 42**)

The synthesis of Monomer **M34** was first reported by Zentel (74). The synthetic scheme is given in Section 2.29. The –I (inductive) and –M (mesomeric) effect of the

laterally placed nitro group is expected to enhance nonlinear susceptibilities for oriented systems. The longer mesogen core (biphenyl) and the longer end group facilitates the formation of smectic C phases (75). Presence of chiral centre in the molecule is responsible for the C_2 symmetry. This C_2 symmetry implies that the untwisted S_C* phase can exhibit second order nonlinear optical (NLO) properties. In the first synthesis step Williamson's etherification was used. 1-Bromo undec-10-ene was reacted with 4,4'-dihydroxybiphenyl to give monoether 4-hydroxy-4'-(undec-10-enoxy) biphenyl (**I31**) (76). Diether was also formed in this reaction which was separated from the monoether by high temperature column chromatography. In the second synthesis step, the well known Mitsunobu reaction (77) was used. S (+) 2-Octanol was reacted with 4-hydroxy-3-nitro ethyl benzoate and the product was hydrolysed with sodium hydroxide to give 4-(S-1-methylheptyloxy)-3-nitro benzoic acid (**I32**). Finally, monoether 4-hydroxy-4'-(undec-10-enoxy) biphenyl (**I31**) and 4-(S-1-methylheptyloxy)-3-nitro benzoic acid (**I32**) were esterified by DCCI-esterification to give monomer 4-[(S-1-methylheptyloxy)-3-nitro-1,4-phenylene carbonyloxy]-4'-(undec-10-enoxy) biphenyl (**M34**). The structure of **M34** has been confirmed by ^{1}H NMR presented in Appendix I.

Monomer **M34** was then grafted unto poly(hydromethylsiloxane) using Pt-catalyst to give Polymer **V 42**. This polymer was first reported by Kapitza et al. (78). The progress of the polymerisation reaction was monitored by IR spectrum. The reaction was continued until no peak was observed at 1262 cm^{-1}, which is characteristic of the Si-H bond.

M34 shows liquid crystallinity as determined by polarising optical microscopy (POM) and DSC. The clearing temperature is 87^o C.

K 64 S_C* 78 S_A 87 I [^{o} C]

POM shows fan-texture between 78-86^o C, typical of smectic A systems (Figure 4.32 (a). Below 78^o C, fingerprint texture (Figure 4.32 (b)) is seen which could be due to Smectic C* phase. Crystallisation is seen at 64^o C with enthalpy of 37.2 J/g, as indicated by DSC.

Polymer **V 42** shows birefringence in POM. However, the nature of the texture could not be identified. DSC shows T_g at 32^o C with transition at 150^o (ΔH= 2.5 J/g) and

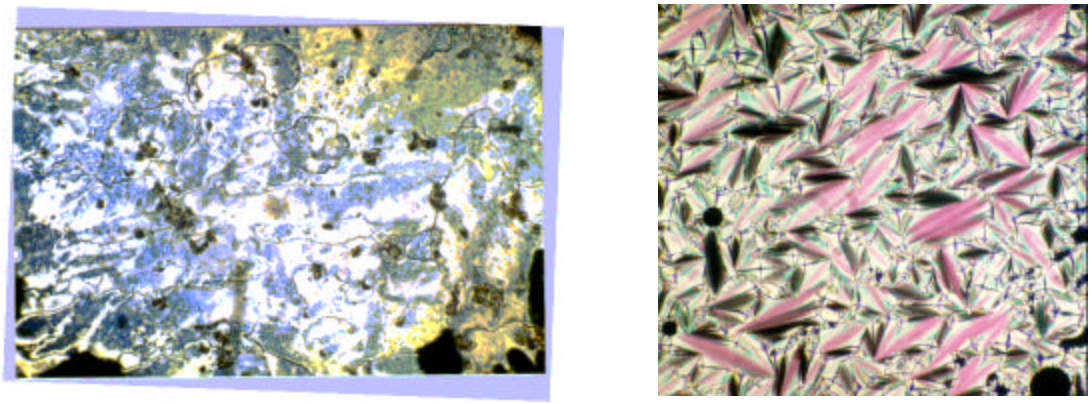

(a) **(b)**

Figure 4.32 Finger-print texture and fan texture for polymer V42; (a) at 75° C and (b) at 82° C.

clearing temperature at 180° C (ΔH = 4.0 J/g). From temperature dependent X-ray measurements, it was noted that the layer distance increases from 35.5 Å to 39 Å between 120 to 160° C.

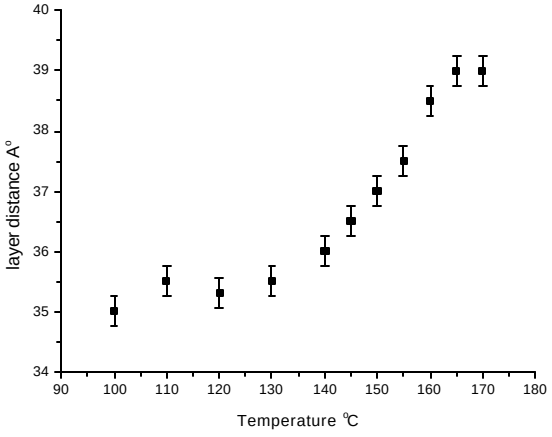

Figure 4.33 Plot of Temperature v/s layer distance

We can conclude from this that the tilt of mesogens with respect to the layer normal decreases on heating (Figure 4.33). The decrease in angle was found to be from 24.5° to 0°. From the enthalpy values obtained from DSC and X-ray results, transition from Sm_C* to Sm_A can be predicted.

G 32 S_C* 160 S_A 180 I [° C]

4.14.2 *1-[(S-2-Methylbutyl)oxycarbonyl-1,4-phenylene oxycarbonyl]-4-(hex-5-enoxy) phenylene* (**M35**) and *poly{1-methyl-1-[1-(S-2-methylbutyl oxycarbonyl-1,4-phenylene oxycarbonyl)-4-(hexamethyleneoxy)phenylene]siloxane}* (**V 43**)

In comparison to low molar mass and polymer systems, less work has been done on elastomers with S_C phases (79,80). Our aim is to use known polymer systems showing smectic C phases and to synthesise elastomers which also will show similar behaviour. Since the orientation measurement is done at room temperature, the selected system should show S_C* phase at ambient temperature. For this it is also essential that the T_g is well below room temperature. Monomer **M35** was grafted unto poly(hydromethylsiloxane) to give polymer **V 43** (Section 3.10).

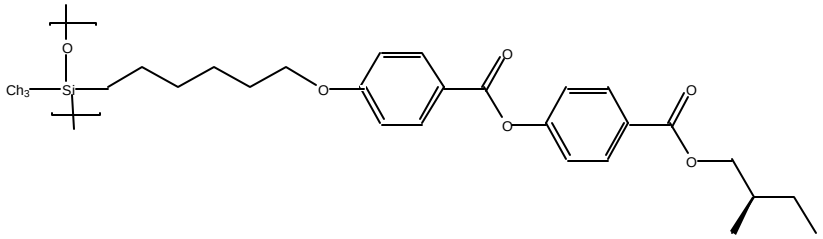

Polymer V 43

Polymer **V 43** shows a broad S_C* phase, with clearing temperature of 79^o C and a T_g of –11^o C. Therefore, we can predict that the elastomer prepared using monomer **M35** will also show similar properties and orientation should be possible at room temperature.

The synthetic scheme for monomer **M35** was shown in Section 2.30. S(+)-2-Methyl-1-butanol (amyl alcohol) was used as chiral end group. In the first synthesis step, 4-(hex-5-enoxy) benzoic acid (**I33**) was synthesised by Williamson's etherification from 6-bromo-1-hexene and 4-hydroxy methyl benzoate, followed by hydrolysis of the ether. In the second synthesis step, 4-(S-2-methylbutyl oxycarbonyl) phenol (**I34**) was synthesised by azeotropic esterification of amyl alcohol and 4-hydroxybenzoic acid. Monomer **M35** was synthesised by 1,3-dicyclohexylcarbodiimide (DCCI) mediated esterification of 4-(hex-5-enoxy) benzoic acid (**I33**) and 4-(S-2-methylbutyl oxycarbonyl) phenol (**I34**). The structure of **M35** was established by ^{1}H NMR given in Appendix I.

M35 does not show any liquid crystalline phases. But the polymer **V 43** is reported to show broad smectic C* phase (81,82) and hence it was decided to use the

monomer **M35** to synthesise elastomer. **M35** was grafted to siloxane backbone in presence of Pt-catalyst to give **V 43** (Section 3.10). Smectic phase in **V 43** was further confirmed by X-ray measurements. Inter-mesogenic distance was calculated as 4.5±0.5 Å and layer distance was 25.0±1.0 Å. From the model structure, the length of mesogen (all trans form) was calculated to be 27 Å. Since layer distance as measured by X-ray is only 25 Å, we can conclude that there is a tilt of the mesogen's long axis to the layer normal, indicating S_C phase.

4.14.3 *1-[(S-1-Methylheptyloxy)-3-nitro-1,4-phenylene-1-carbonyloxy]-4-(undec-10-enoxy) phenylene* (**M36**) and *poly{1-methyl-1-[1-(S-1-methylheptyloxy)-3-nitro-1,4-phenylene carbonyloxy-4-(undecamethyleneoxy)biphenyl]siloxane}* (**V 44**)

One of the main reasons for synthesising **M36** was to circumvent the use of biphenyl system which are difficult to work with due to solubility problems. Also being a fairly rigid system, the phase transition temperatures are higher. The use of more flexible system such as phenyl benzoate, brings down the phase transition temperature. The synthetic scheme is given in Section 2.31. For monoetherification of hydroquinone, we chose to first protect one hydroxyl group by esterification using one equivalent of benzoyl chloride (83-85). This was followed by Mitsunobu condensation reaction between the monoester and undec-10-en-1-ol. The product obtained was then hydrolysed to unprotect the hydroxyl group to give 4-(undec-10-enoxy) phenol (**I35**). Monomer (**M36**) was obtained by DCCI-esterification with 4-(S-1-methylheptyloxy)-3-nitro benzoic acid (**I32**) and 4-(undec-10-enoxy) phenol (**I35**). **V 44** was synthesised by grafting **M36** unto polysiloxane backbone using hydrosilylation reaction (Section 3.10).

4.14.4 *4-Nitro/cyano-4'-(undec-10-enoxy) azobenzene* (**M37**)/ (**M39**) and 2,5-*dimethyl-4-nitro-4'-(undec-10-enoxy) azobenzene* **(M38)**

Conjugated aromatic molecules such as stilbenes or azobenzenes with electron donor and acceptor substituents are frequently used as NLO active groups. The azo derivatives of phenol are reported to show smectic phases through hydrogen bonding under suitable conditions. An absence of extensive study in azo derivatives of phenol, its stability and the possibility to synthesise variety of monomers /polymers/ elastomers with azo chromophores were additional reasons to select azophenoxy chromophores for the synthesis of NLO active monomers. Common electron acceptor groups like the nitro and

cyano have been used in monomers **M37**, **M38** and **M39** to enhance the push-pull effect. The synthetic route for these monomers were presented in Section 2.32. 4-Hydroxy-4'-nitro azobenzene (**I36**), 2,5-dimethyl-4-hydroxy-4'-nitro azobenzene (**I37**) and 4-hydroxy-4'-cyano azobenzene (**I38**) were prepared using standard diazotisation procedure. Mitsunobu condensation was used to get **M37**, **M38** and **M39** by reaction between 4-hydroxy-4'-nitro azobenzene (**I36**), 2,5-dimethyl-4-hydroxy-4'-nitro azobenzene (**I37**) and 4-hydroxy-4'-cyano azobenzene (**I38**) respectively and undec-10-en-1-ol. Grafting of **M37** and **M38** to poly(hydromethylsiloxane) resulted in a solid mass which was difficult to characterise. The structures of these monomers **M37**, **M38** and **M39** were well characterised by ^{1}H NMR (Appendix I).

For **M37**, DSC did not reveal any mesophases. The melting point was 87^o C. However, in polarising microscope birefringence was noted just prior to isotropisation.

4.14.5 *1-{[(S-2-Chloro-4-methyl) pent-1-yloxy]-1,4-phenylene carbonyloxy}-4-(undec-10-enoxy) phenylene* (M40)

The synthetic route for **M40** was presented in Section 2.31. Copolymer of 1-{[(S-2-chloro-4-methyl) pent-1-yloxy]-1,4-phenylene carbonyloxy}-4-(undec-10-enoxy) phenylene **M40** with 1-[(S-2-methylbutyl)oxycarbonyl-1,4-phenylene oxycarbonyl]-4-(hex-5-enoxy) phenylene **M35** is known to give broad chiral smectic C phase (86).

4.14.6 *1,4-Bis(undec-10-enoxy) phenylene* (M41)

Synthesis of **M41** is shown in Section 2.34 (87). The crosslinker **M41** was synthesised using Williamson's etherification. 11-Bromo undec-1-ene was reacted with hydroquinone under argon atmosphere to give both monoether and diether. The diether was separated by column chromatography.

The crosslinker **M41**, which does not show any liquid crystalline phase, depresses the phase transformation temperatures of crosslinked systems relative to the linear ones of similar structure. The drawback in **M41** are the problems associated with orientation due to its longer side chain spacer length (11 methylene units) (85,88).

4.14.7 Elastomer E1

To observe frequency doubling, push-pull effect in the system is an obligatory factor, e.g. $-NO_2$ and $-NH_2$ (78). However, for systems with chiral smectic C phase

having C_2 symmetry, it is necessary to have the dipole moment of the system parallel to the smectic layers and hence the nitro group is laterally placed on the aromatic core. However, lateral substitution hinders the formation of S_C phases. To overcome this, the mesogens, spacers and chiral end groups should be longer, so as to stabilise the smectic phases. Such systems have a drawback of having high phase transformation temperatures and are likely to show not only smectic C but also other higher ordered smectic phases or crystalline phases. To lower phase transformation temperatures, only 40% of **M34** was used. Though the hyperpolarisability was not optimised, it was expected that the elastomer synthesised by mixing **M34** with **M35** would show the desired phase transformation temperatures.

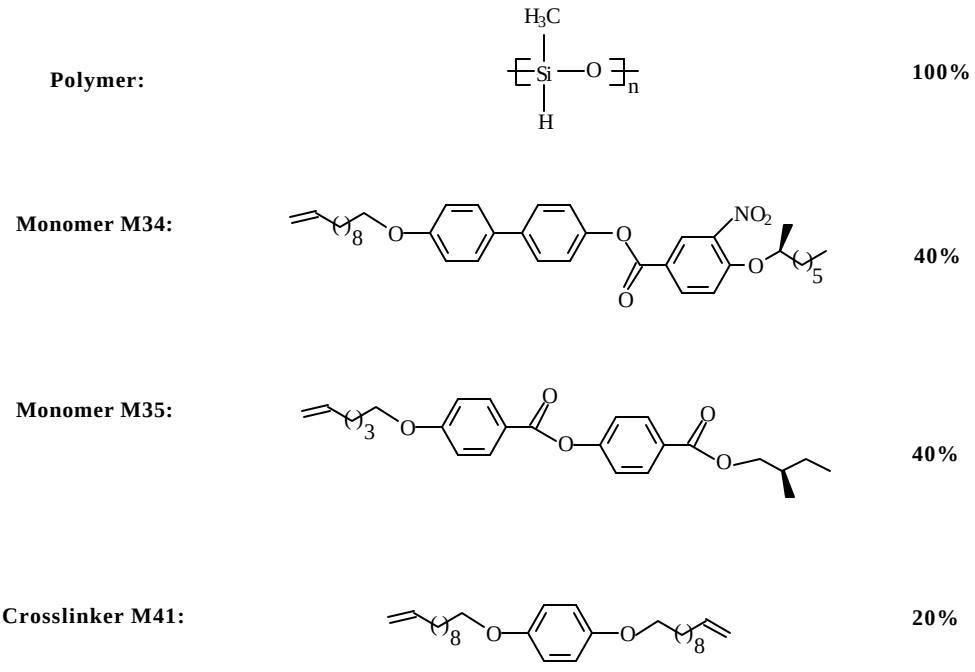

Figure 4.34 **Composition of smectic elastomer E1**

The LC elastomer (**E1**) (Figure 4.34) was synthesised as described previously (Section 3.11) (89). The elastomer contains two different mesogenic moieties statistically linked to a polysiloxane backbone. Although both mesogenic side groups provide a broad S_C* phase, the chiral benzoic acid phenyl ester (**M35**) was used to shift the LC to isotropic transition to lower temperatures. The chiral benzoic acid biphenyl ester (**M34**) was laterally substituted with a nitro group to improve the NLO response (90,91). The

elastomer film (thickness 200-300 μm) was prepared by spin casting technique in solution.

The other elastomers **E2**, **E3**, **E4** and **E5** were prepared using the procedure described in Section 3.11. The chiral benzoic acid biphenyl ester (**M34**) used in **E1** was replaced by chiral benzoic acid phenyl ester (**M36**) in **E2**. This helped to reduce the solubility problems associated with the use of biphenyl systems. Lateral substitution of this with a nitro group generated the tilted smectic C phase by creating a lateral dipole. Elastomers **E3**, **E4** and **E5** contain three different mesogenic moieties statistically linked to a polysiloxane backbone. Both the chiral benzoic acid phenyl esters (**M35**) and (**M40**) provide a broad S_C* phase. The achiral azo mesogen with acceptors like nitro and cyano were added to make the system compatible for NLO studies, wherein a push-pull effect is needed.

4.15 Alignment of elastomer

4.15.1 Uniaxial deformation of elastomer

Before the completion of crosslinking reaction, the swollen elastomer was removed from reaction vessel and simultaneously an uniaxial stress was applied to the isotropic sample, still containing the solvent, by carefully tensioning with weights. On further drying, the elastomer became liquid crystalline. Simultaneously, the elastomer becomes stretched with a stress of about $3x10^{-2}$ N mm^{-2} (Figures 4.35 and 4.36).

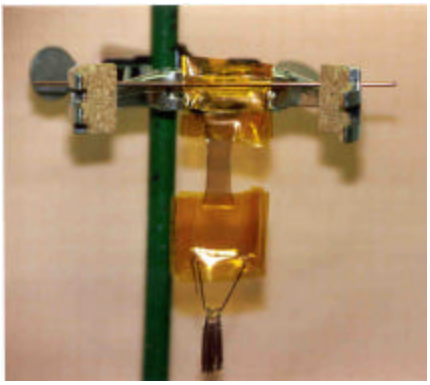

Figure 4.35 **Set-up for uniaxial deformation**

This uniaxial deformation leads to an uniform orientation of the preferred direction (director) of the mesogen long axis parallel to the stress direction and the smectic layers are ordered with an angle ψ of the layer normal to the mesogen long axis, where ψ is identical to the tilt angle of the mesogenic units in the smectic layer (chevron texture). Under these conditions, the cross-linking reaction proceeds and the mechanically induced anisotropic network structure and subsequent uniform director orientation are chemically locked in.

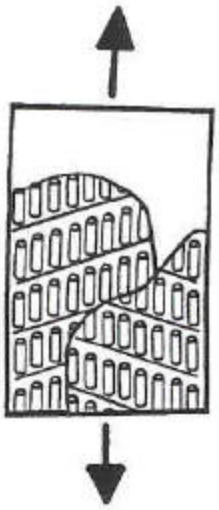

Figure 4.36 Orientation after uniaxial deformation in the swollen state

The samples were completely translucent, indicating "high order" in contrast to un-ordered turbid samples (Figure 4.37). However, due to the conic layer distribution, the elastomer does not exhibit macroscopical C_2-symmetry and therefore no SHG should be observable.

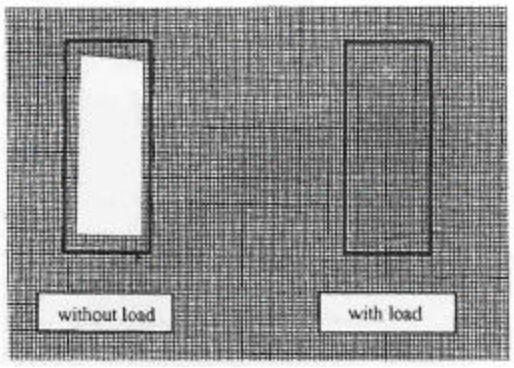

Figure 4.37 Photograph of the oriented S_C* elastomer corresponding to the unoriented polydomain sample

4.15.2 Shear deformation of the elastomer

The experiment clearly reveals that an uniaxial mechanical field is not suited to obtain a macroscopic uniform orientation of a S_C* system or that the layer normal of ~ ±

25^{o} remains with respect to the uniaxial stress axis. Considering the biaxial symmetry of the S_C*-phase it is obvious that a mechanical field, that is consistent with the LC phase symmetry, must be applied. As we have learnt from the strain experiment in the smectic phase, the mechanical field couples to the layer orientation (92). Consequently a suitable shear field (Figures 4.38 and 4.39) should result in an uniform layer orientation of the elastomer aligned with respect to the director.

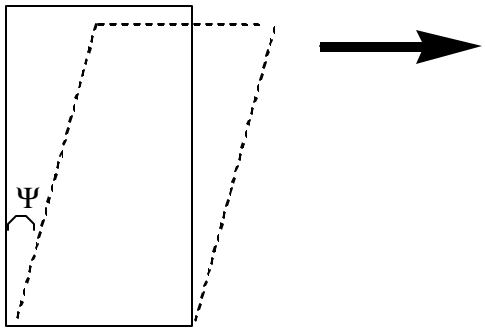

Figure 4.38 Shearing of the preoriented sample

For the shear experiment, the elastomer used was already aligned, with respect to the director, by the uniaxial field. The elastomer was gradually sheared with the angle Ψ and analysed by X-ray measurement after first annealing period of 6 h at room temperature and then at S_C* temperature range for another 6 h. On removing from the shearing machine, the sample continued to exhibit the macroscopical uniform orientation owing to the cross-linking process. Therefore, the elastomer now permanently displays the correct symmetry and is suitable for SHG experiments.

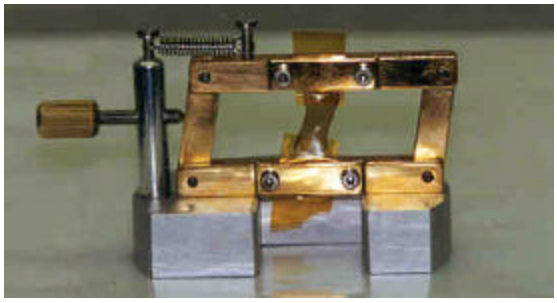

Figure 4.39 Set-up for shear experiment

4.16 Characterisation of E1

The transition temperatures were determined by differential scanning calorimetry and temperature-dependent X-ray measurements. Above the glass transition at -13^{o} C, the

elastomer exhibits a broad S_C* phase up to 57° C, followed by a S_A phase, with a clearing temperature of about 75° C. The elastomer with 10% of the cross-linking agent has a broad chiral smectic C phase in the temperature range -13° C (T_g) to 57° C and is therefore suitable for orientation experiments at room temperature.

To quantify the macroscopic orientation of the sample, the elastomer was analysed by X-ray measurements using a monochromator CuKα (λ=1.54 Å) beam. A two-dimensional image plate system (700 x 700 pixels, 250 µm / 125 µm resolution) was used as the director.

The smectic structure was confirmed by the X-ray pattern of the elastomer (Figure 4.40) that had not been mechanically loaded.

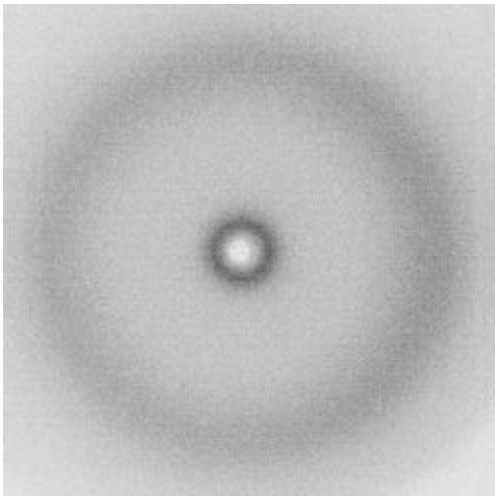

Figure 4.40 X-ray pattern of the chiral smectic polydomain

The X-ray pattern of the film, as obtained after the first deformation, is shown in Figure 4.41 (a). As expected, the azimuthal wide-angle reflections representing the mesogen-mesogen distance display clear horizontal maxima, indicating an uniform alignment of the mesogen long axes. The azimuthal small-angle reflections exhibit four maxima. The same pattern was obtained if the sample was rotated around the director of the mesogen long axis, indicating the conic layer orientation described earlier. The angle of the layer normal to the director has the value ψ = 25°. The X-ray pattern of the elastomer, as obtained after the shear experiment (alignment of the layer structure), is shown in Figure 4.41 (b). Whereas no changes in the wide-angle reflections can be observed, the small-angle reflections now exhibit an asymmetric distribution of the

intensities, indicating a nonsymmetric layer distribution. This procedure causes an excellent orientation of the layer structure and additionally induces a better orientation of the mesogen long axis, as indicated by the two sharp maxima in the small-angle reflection and by the curtailment of the wide-angle reflection.

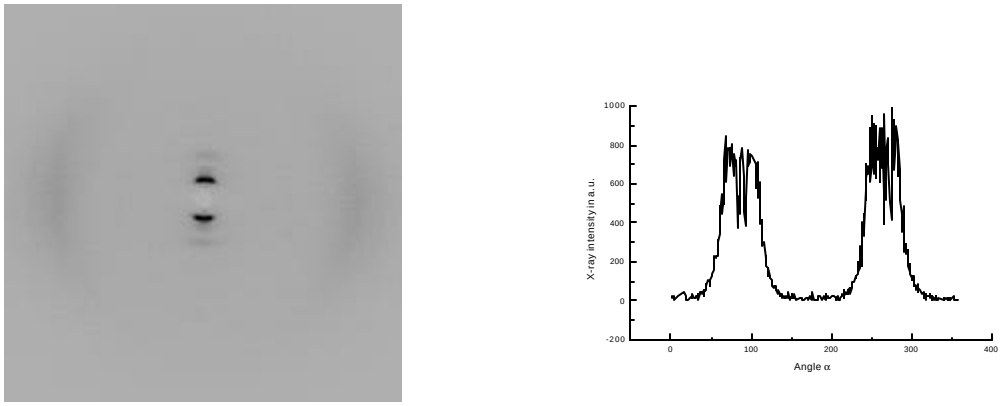

(a)

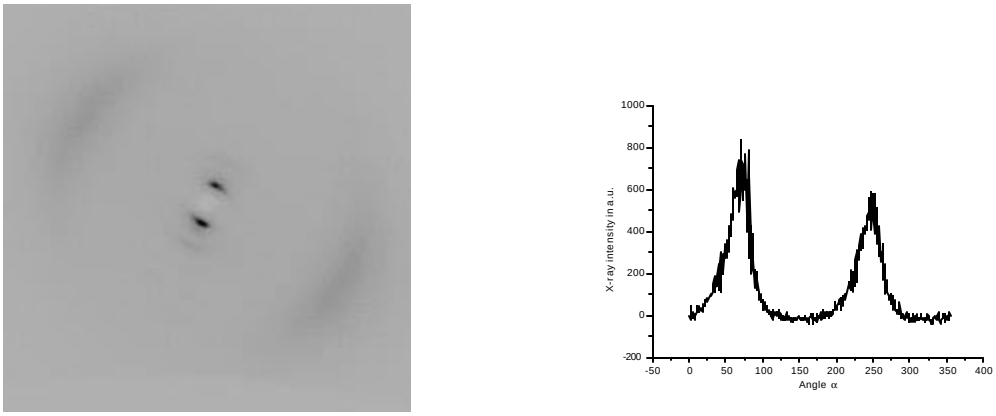

(b)

Figure 4.41 **Mechanical alignment of S_C* elastomer (E1); (a) Uniaxial elongation results in an uniform orientation of the mesogens while the orientation of the smectic layers shows a conical distribution. The X-ray pattern shows four small angle reflections of equal intensity. (b) A second elongation at an angle Y with respect to the axis of the first deformation leads to an almost uniform orientation of the layers, indicated by the suppression of two of the maxima in the X-ray pattern**

The transformation of **E1** from S_{C*} to S_A was confirmed by X-ray measurements. Uniaxially deformed elastomer **E1** was heated from room temperature (25^o C) to isotropic (75^o C). The X-ray pictures are shown in Figure 4.42. The X-ray diffractograms (a), (b),

(c), (d) and (e) in Figure 4.42 show two distinct small angle reflections, indicating a smectic C phase. On further heating transformation to smectic A phase is seen, as indicated by only two reflections in the small angle region (f), (g), (h) and (i). In (k) no reflections are seen in the small angle region, which indicates that the sample has become isotropic.

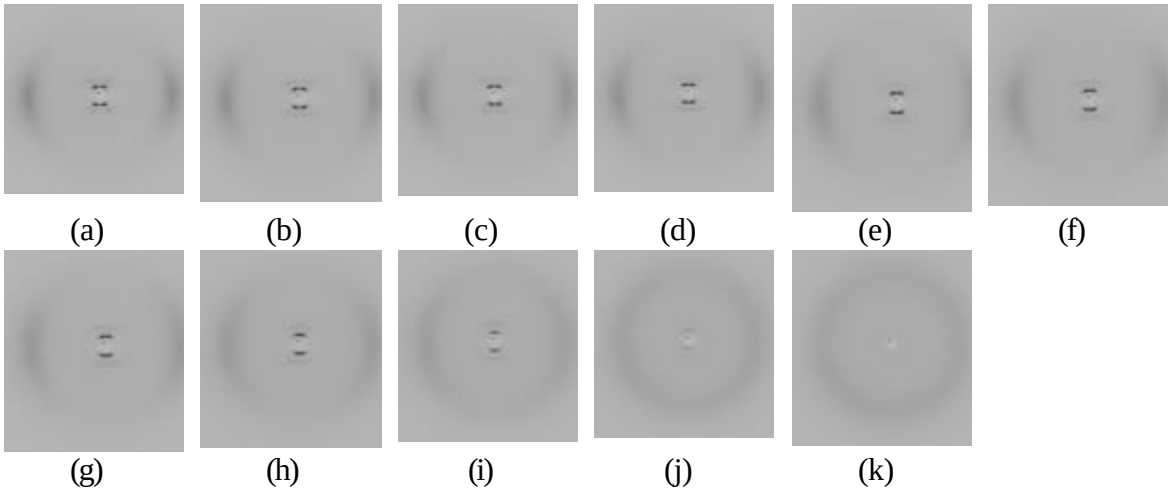

Figure 4.42 **X-ray diffractograms during first heating for elastomer E1 from room temperature [25° C, (a)] to isotropic [75° C, (k)]**

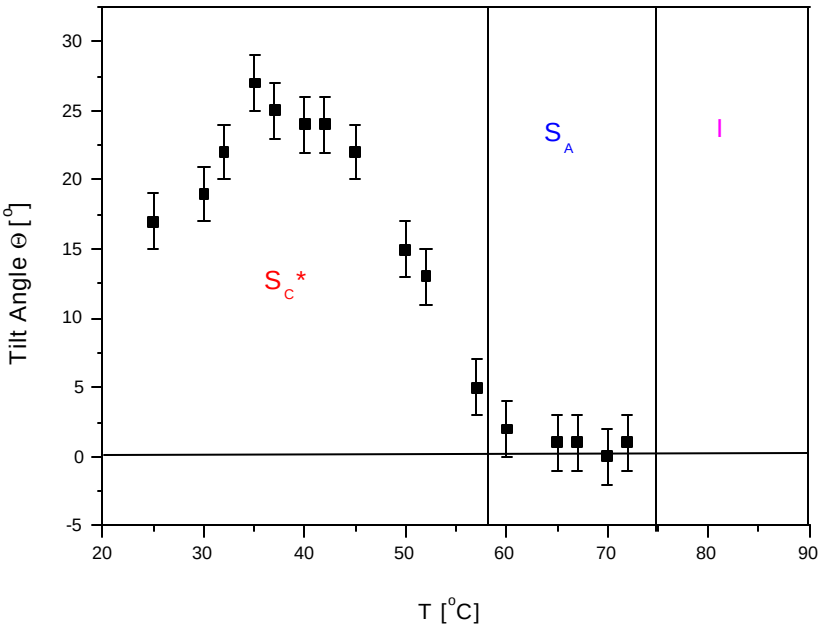

Figure 4.43 **Tilt angle plotted against temperature**

As seen from Figure 4.43, the tilt angle in the S_{C*} phase is ~25° at 35° C. Between 45-57° C, it falls to ~0°, indicating a transformation from S_{C*} to S_A phase. X-ray and DSC measurements do not show any biphasic system and hence the transformation is of the second order. At 75° C, transformation into the isotropic phase occurs.

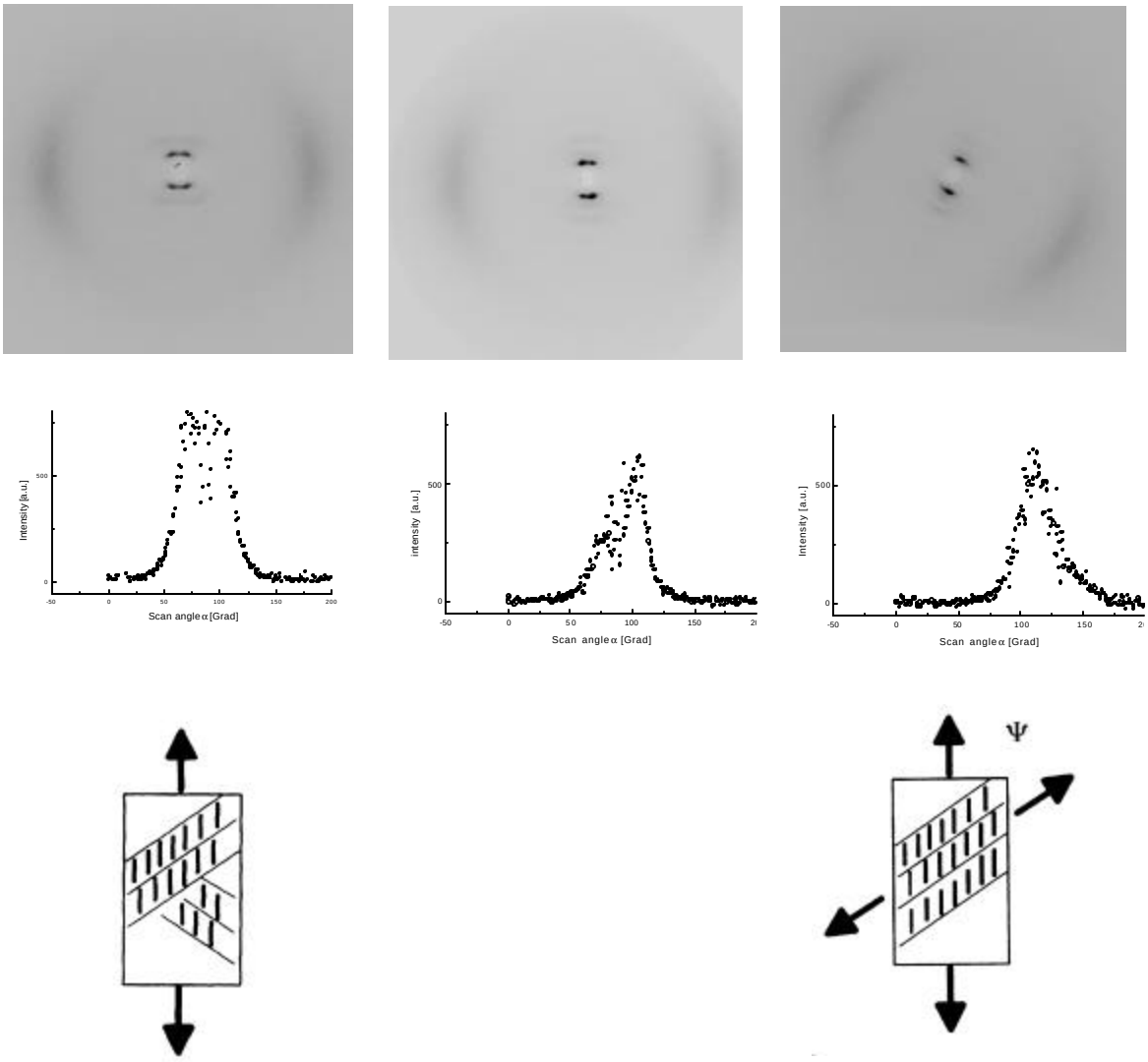

(a) **(b)** **(c)**

Figure 4.44 **X-ray patterns of elastomer E1 after uniaxial deformation (a), of the nonannealed sample after the second deformation (b) and of the annealed sample (c)**

It was observed that on annealing the elastomer within the S_C* phase (50° C) for 24 h causes an excellent orientation of the layer structure and additionally induces a

better orientation of the mesogen long axis as indicated by the small-angle reflection and by curtailment of the wide-angle reflection, as shown in Figure 4.44.

4.17 Characterisation of E3

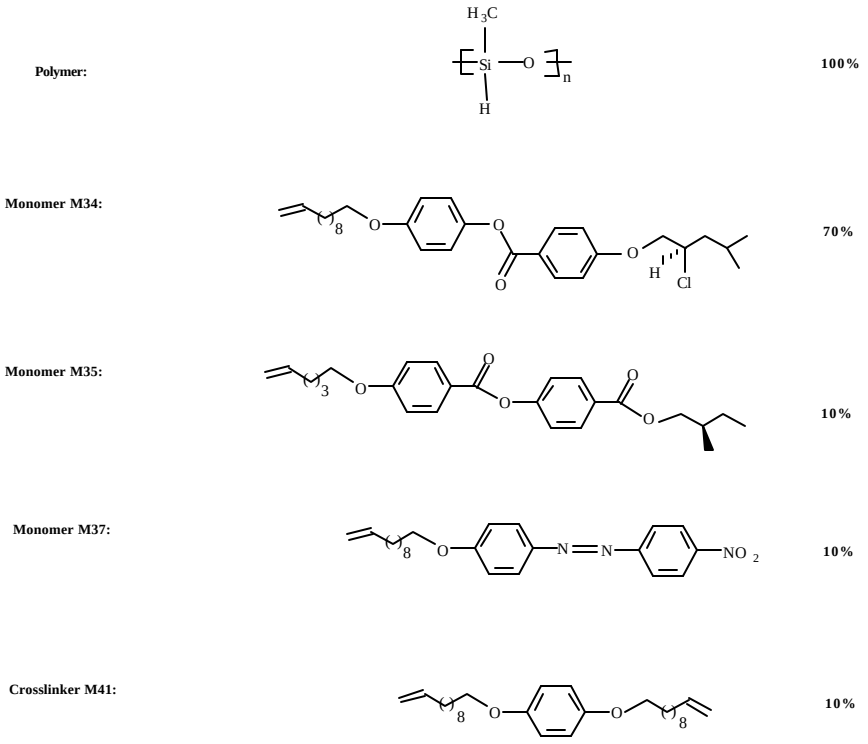

Figure 4.45 Composition of smectic elastomer E3

The synthesis of **E3** was described in Section 3.10. Above the glass transition temperature at -6±3° C, the elastomer **E3** exhibits a broad S_C* phase up to 40° C, followed by a S_A* phase, with a clearing temperature of approximately 100° C. The X-ray diffractogram of **E3** is shown in Figure 4.46. As expected, the azimuthal wide-angle relections display clear horizontal maxima indicating an uniform alignment of the mesogens long axis. The small angle reflections show 2 sharp maxima with a tilt of (-) 22.5° indicating an excellent orientation of the layer structure. The layer thickness obtained was 33.2 ±0.5 Å and the mesogen distance was 4.4 Å. It is noted that up to 30 mol% of the chromophore could be incorporated within the network without losing the chiral smectic C phase. However, approaching high chromophore contents, a tendency for the co-elastomer to form the ferroelectric smectic A phase could be detected. This is

Figure 4.46 X-ray pattern for elastomer E3 after second deformation

confirmed by temperature dependent X-ray measurements on Elastomer **E3,** which shows a transition from S_C* to S_A at ~40^o C. This transformation can be clearly seen in Figure 4.47. Figure 4.47 shows decrease in tilt angle from 22.5^o to nearly 0^o on heating from room temperature (25^o C) to isotropic (100^o C).

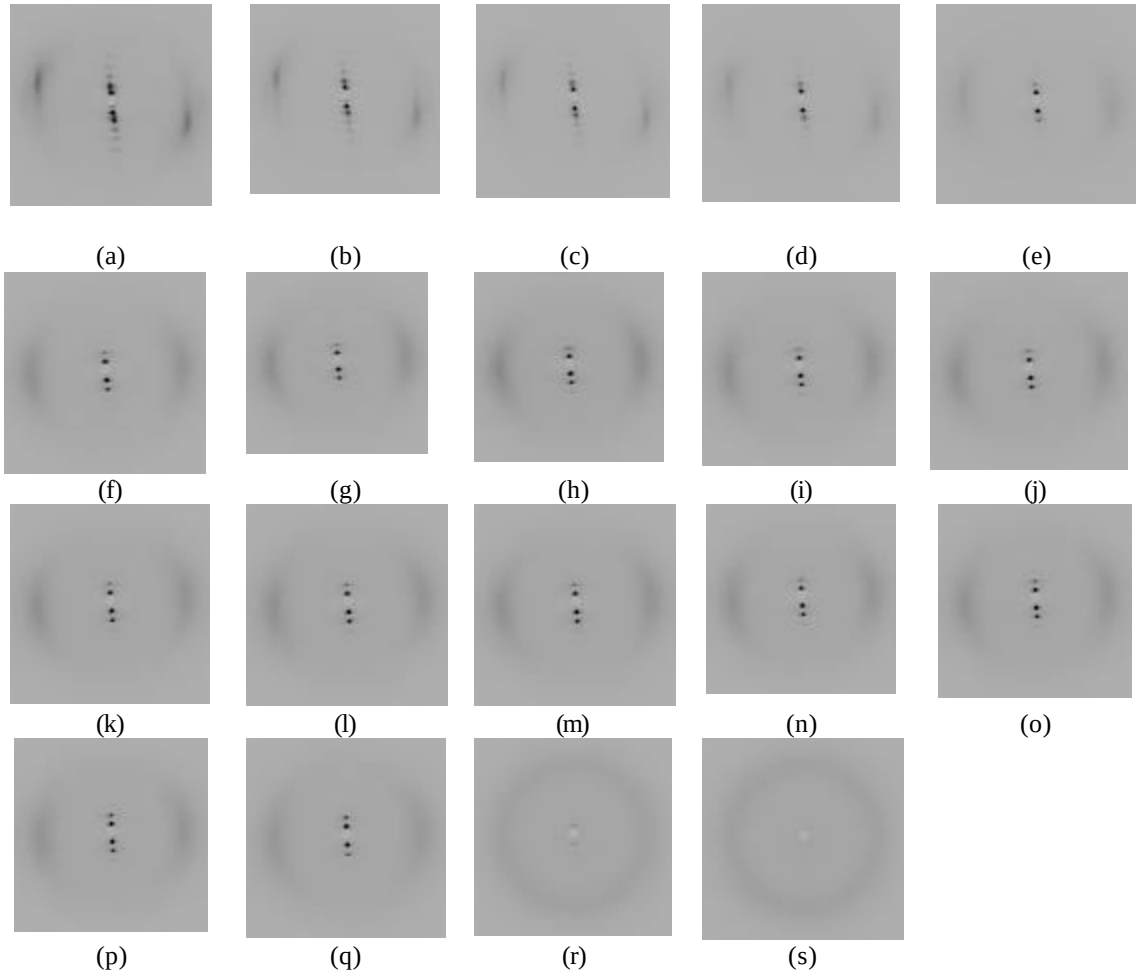

Figure 4.47 X-ray pictures during heating of elastomer E3 from room temperature [25^o C, (a)] to isotropic [100^o C, (s)]

4.18 Second harmonic generation (SHG) studies

4.18.1 Experimental techniques

A variety of experimental techniques have been used to obtain both qualitative and quantitative information about the second order nonlinearities of materials.

4.18.1.1 *Kurtz-powder technique*

A laser beam is directed onto a solid-powder sample. The emitted light is collected, filtered, detected and compared with a standard (usually urea is used as a standard d_{14} = 1.4 pm/V). The magnitude of response depends on particle size. Materials can be classified into phase matchable and nonphase matchable. For nonphase matchable, the second harmonic (SH) is only generated effectively over distances smaller than the coherence length. For light paths smaller than coherence length, the intensity of the SH increases with the square of interaction distance, so for small crystal size there is an increase of the SH intensity with the crystal size. But if the crystal size are of the order of the coherence length, there is no further increase of the light intensity with the propagation distance and powder SHG signal decreases.

For phase matchable materials, there is a direction of propagation for which the second harmonic intensity grows quadratically with the propagation path without a limit. It follows that the SHG intensity should not show a falling–off behaviour in such a case because the decrease in the number of crystallites, as they become bigger, will now be compensated by the contribution from phase matched interactions.

Results from Kurtz powder SHG studies do not have quantitative significance as the light intensities measured in the powder SHG technique depend on several factors (93). The magnitude of the tensor component of molecular hyperpolarisability 'β' is only one of these.

Molecular arrangement is important among these. In a centrosymmetric arrangement, the unit cell hyperpolarisability tensor component are all identically equal to zero; but even in non-centrosymmetric groups, there may be very substantial

differences in the nonlinear co-efficients arising from packing the nonlinear molecules in different ways.

The efficiency for SHG depends also on coherence lengths and reflection co-efficients. Given these complicating factors, the powder technique cannot be considered to give quantitative information about the molecular properties of molecules in the crystals being investigated. Therefore, observation of good powder SHG is a good indication of large β for a compound; whereas the absence of strong powder SHG does not necessarily preclude high molecular nonlinearities.

Despite the need for noncentrosymmetric packing and reservations concerning the quantitative nature of the results, the Kurtz powder technique has been used extensively to characterise organic compounds because it can be used to screen a large number of samples quickly and is a convenient method to study SHG materials without the need to grow large single crystals.

4.18.1.2 *Solvatochromism*

Solvatochromism is the shift of the absorption spectrum of a molecule with variance in solvent (94). The use of this phenomenon for the determination of β is based on the two level microscopic model of the first hyperpolarisability, in which the expression for β is reduced to ground and excited states. This model allows β_{CT} [β in direction of charge-transfer axis] to be determined in terms of other measurable microscopic quantities like transition energy ω_{eg}, translational dipole moment μ_{eg}, the ground-state dipole moment μ_g and μ_e. The μ_e is found by measuring the solvatochromic shift of λ_{max} of the solute, in solvents of varying polarity for which the dielectric constant and refractive index are known. This technique has been applied to organic compounds where charge transfer is dominated by one transition.

4.18.1.3 *Electric field induced second harmonic generation (EFISH)*

In EFISH technique, a liquid or solution sample is subjected to a high voltage dc pulse to align molecules (95). The pulse is synchronised with the laser beam pulse. $\chi^{(2)}$ then can be observed in what was previously an isotropic medium. All materials will produce an EFISH signal as it is formally a third order nonlinear process described by

susceptibility. The effective hyperpolarisability measured by the EFISH technique can be defined as β_{EFISH} and is given by equation 4.4.

$$\beta_{vec} = \mu\beta_{EFISH} \qquad \textbf{4.4}$$

In strong acceptor-donor molecules β_{CT} usually accounts for most of β_{EFISH}.

4.18.1.4 *Hyper Rayleigh scattering (HRS)*

HRS is due to orientational fluctuations of asymmetric molecules in solution that give rise to local symmetry on a microscopic scale in an isotropic liquid. The light scattered from such a system can have a component at the second harmonic that depends only on the first hyperpolarisability of the solute molecules and varies quadratically with the incident intensity (96). So measurements of different concentrations of solute allow β^2 to be extracted.

4.18.1.5 *Maker-Fringe analysis*

Detailed information about the components of second order susceptibility $\chi^{(2)}$ (-2ω, ω, 2ω) can be obtained from SHG measurements on well defined samples such as single crystals or oriented thin films (97). The oriented thin films can be obtained by procedures such as the asymmetric Langmuir-Blodgett [LB] deposition technique or electric–field poling of NLO chromophore doped polymers.

In the case of single crystals, the second harmonic is generated by a crystal with plane parallel surfaces and the distance of interaction of the fundamental and second harmonic radiation is varied by rotation of the sample about an axis perpendicular to the laser beam axis. This produces the maxima and minima of the second harmonic that are called Maker-Fringes.

Alternatively, a wedge made out of a crystal may be used to vary the interaction length. The amplitude of the second harmonic is proportional to $[\chi^{(2)}]\ [L_c Sin(L/L_c)]^2$, L being the variable interaction distance and L_c the coherence length. Comparison of the measurements with a well characterised material such as quartz, allows $\chi^{(2)}$ to be determined.

The major disadvantage of the technique is the requirement for large (of the order of cubic millimetres) single crystals. A second harmonic signal can also be obtained from thin films of some compounds if the films are made noncentrosymmetric. A technique

similar to that of Maker-Fringe can be used here. Rotating a second order optically nonlinear thin film deposited on a second order inactive substrate (glass) will result in an angularly dependent second harmonic with no fringes; where as glass plate covered on both sides with a NLO film shows an angular dependence of the second harmonic with fringes similar to those from a crystal. Here, the additional information about individual tensor components [$\chi^{(2)}$] can be obtained by varying the polarisation of the fundamental radiation. An important issue is that these measurements determine the macroscopic nonlinearity and obtain information about the molecular hyperpolarisabilities, with assumptions such as nature of local field corrections.

4.19 Mathematical models

During the last decade it was recognised that noncentro-symmetric organic materials exhibit pronounced second order nonlinear optical properties than conventional inorganic materials (98). The molecular, noncentro-symmetric, charge-transfer (CT) constituents can be considered as molecular diodes with enhanced polarisability in the CT direction. Therefore, the first molecular hyper-polarisability tensor β_{ijk} has a component β_{zzz} enhanced in the charge-transfer direction (z). Such charge-transfer molecules consist of a conjugated π electron backbone, terminated by an electron donating group and an electron-withdrawing group. In such systems the nonlinear optical response of the bulk material, important for device applications, depends on the ensemble addition of constituents. The simplest case is that of a single crystal. Here the macroscopic second order nonlinear optical susceptibility χ^2_{IJK} in the laboratory reference frame (IJK) is obtained by transforming the molecular first hyper-polarisability β_{ijk}. This β_{ijk} describes the second order NLO properties of a given molecule in molecular reference frame (ijk). For a three photon process ($\omega_3 = \omega_1 + \omega_2$), this is given by the following expression:

$$\chi^{2}_{IJK}(-\omega_3;\omega_1,\omega_2) = \sum_n N^n \sum_{ijk} f_i^{(n)\omega_1} f_i^{(n)\omega_2} f_k^{(n)\omega_3} a_{iI}^{(n)} a_{jJ}^{(n)} a_{kK}^{(n)} \beta_{ijk}^{(n)}(-\omega_3;\omega_1,\omega_2) \qquad \textbf{4.5}$$

where $N^{(n)}$ is the number density of molecular species (n) and $f^{(n)\omega}$ is their local field factor at frequency ω. For small molecules $f^{(n)\omega}$ is well approximated by the Lorentz-Lorenz formula:

$$f^{(n)w} = \frac{e+2}{3} \qquad \textbf{4.6}$$

In other cases, the second order nonlinear susceptibility is an average of all molecular orientations and is given by:

$$c^{2}_{IJK}(-w_3; w_1, w_2) = NF\left\langle b_{ijk}(-w_3; w_1, w_2)\right\rangle_{IJK} \qquad \textbf{4.7}$$

Thus, optimisation of second order nonlinear optical response requires the average value by a better polar orientation. In the case of anti-parallel orientation $\beta = 0$ and maximum orientation is attained when dipolar moments of all molecules are mutually parallel.

4.19.1 Second order nonlinear optical properties of poled polymers

The following expressions are possible for two different linear susceptibility tensor components for poled polymers with point symmetry (∞ mm), that are composed of rod-like type molecules having axial symmetry, with dipolar moment parallel to the z-axis of molecular reference frame:

$$\chi^{(1)}_{ZZ}(-\omega;\omega) = N\,F\left\langle \alpha_{XX} + (\alpha_{ZZ} - \alpha_{XX})\cos^2\theta\right\rangle \qquad \textbf{4.8}$$

and

$$c^{(1)}_{XX}(-w;w) = c^{(1)}_{YY} = N\,F\left\langle a_{XX} + (a_{ZZ} - a_{XX})\sin^2 q\right\rangle \qquad \textbf{4.9}$$

where, $\alpha_{xx} = \alpha_{yy}$ and α_{zz} are the molecular linear polarisability components in principal axes perpendicular and parallel to the symmetry axis, respectively.

Similarly, it follows from symmetry considerations and Kleinman conditions, that there are two non-zero $\chi^{(2)}$ tensor components: $\chi^{(2)}{}_{zzz}$ and $\chi^{(2)}{}_{xxx}$ for one dimensional charge transfer molecules ($\beta_{zzz} \neq 0$) and poled polymers with point symmetry (∞ mm), where Z is the poling direction (assumed to be perpendicular to the thin film surface).

$$c^{2}_{ZZZ}(-2w;w,w) = N\,F\,b_{ZZZ}(-2w;w,w)\left\langle\cos^3 q\right\rangle \qquad \textbf{4.10}$$

$$c^{2}_{XXZ}\left(-2w;w,w\right)=\frac{1}{2}N\,F\,b_{ZZZ}\left(-2w;w,w\right)\left\langle \sin^{2}q\cos^{3}q\right\rangle \qquad 4.11$$

where, F is the local field factor for SHG process

$$F=\left(f^{\omega}\right)^{2}\ f^{2\omega} \qquad 4.12$$

with $f^{\omega\,(2\omega)}$ given by equation. 4.6.

4.20 Statistical orientation models

The computation of corresponding configurational averages requires some assumptions on the orientation distribution function G(θ), which are listed below in the case of different statistical models proposed to describe the orientation mechanism and its efficiency under given assumptions.

The statistical average of different physical quantities, depending on orientation, can be obtained assuming a Gibbs-Boltzmann distribution function, given by:

$$G(\theta)=\frac{e^{\frac{-U}{kT}}}{2\pi\int_{0}^{\pi}e^{\frac{-U}{kT}}\ Sin\,\theta\,d\,\theta} \qquad 4.13$$

where, U is the potential energy of molecule; k is the Boltzmann factor; T is the poling temperature of the system.

In the simplest case, the energy of the permanent dipole μ_0 in the poling electric field E_p is:

$$U_{E}(\theta)=-\mu_{0}\,E_{P}\,cos\,\theta \qquad 4.14$$

Four different models have been proposed to describe the energy of an electric dipole moment in an orienting external field. These are Ising model, Isotropic model, SKS model and MSVP model.

4.20.1 *Ising model*

In this model a perfect molecular order is assumed ($\langle P_2\rangle = 1$) and two molecular orientations are possible with $\theta = 0$ and $\theta = \pi$. However, due to the thermal motions one

state is favoured more than the other one. The diagonal component of second order nonlinear optical susceptibility can be represented as:

$$\chi^{2}_{ZZZ}(-2\omega;\omega,\omega) = N F \beta_{ZZZ}(-2\omega;\omega,\omega)u \qquad \textbf{4.15}$$

where, $u = \mu_0 E_p/kT$.

4.20.2 *Isotropic model*

Isotropic model assumes no initial order ($<P_2> = <P_4> = 0$). The potential energy is given by equation 4.14 and the diagonal and off diagonal components of $\chi^{(2)}$ can be directly calculated from equations 4.10 and 4.11.

4.20.3 *Singer, Kuzyk and Sohn (SKS) model*

Singer et al. (98) consider an initial order of molecules, described by $<P_2>$ and $<P_4>$ parameters. This order introduces an additional potential energy term (θ) describing the tendency of molecules to align. One takes account of that by developing the orientation distribution function into the series, given by equations 4.10 and 4.11, with these order parameters. Introducing the so defined orientation distribution function into equations 4.10 and 4.11, one obtains the tensor components $\chi^{(2)}_{zzz}$ and $\chi^{(2)}_{zxx}$.

4.20.4 *Maier, Saupe, Vander Vorst and Picken (MSVP) model*

The natural tendency of rod-like molecules to order antiparallel in the external field was brought forth by Maier and Saupe who introduced an extra term into the potential energy of the following form:

$$U^{0}(\theta) = -\zeta \langle P_2 \rangle P_2 \cos\theta \qquad \textbf{4.16}$$

where, ζ is the parameter describing the size of this interaction. It takes a constant value for a given liquid crystal. In the Maier and Saupe theory, this parameter is proportional to the clearing temperature through the following relation:

$$k T_c = 0.22\zeta \qquad \textbf{4.17}$$

Van der Vorst and Picken generalised this model by introducing an extra term, that describes the energy of induced dipolar moment in the poled fields of the following form:

$$_i(\theta) = -\Delta\alpha E_P^2 P_2(\cos\theta) \qquad \textbf{4.18}$$

where, $\Delta\alpha$ describes the induced variation in molecular linear hyperpolarisability. The different orientational averages within four statistical models vary as follows:

1. Ising model $\langle P_2 \rangle = 1$.

2. Isotropic model $\langle P_2 \rangle = u^2/15$, where $u = \mu_0 Ep/kT$

3. In SKS model the order parameters $\langle P_2 \rangle$ and $\langle P_4 \rangle$ are assumed to be independent of electric field strength and are to be determined at zeroth poling field.

4. In MSVP model, the order parameter $\langle P_2 \rangle$ has to be determined self consistently by using numerical methods.

4.21 SHG results of selected synthesised polymers

A schematic representation of the SHG set-up is given in Figure 4.48. In this study, SHG experiments were performed in the transmission mode with a Nd:YAG laser at 1064 nm. The angle between the laser and the film surface was rotated and the SHG intensity $I^{2\omega}$ was recorded as a function of angle of incidence, as shown in Figures 4.49-4.66 for some of the polymers presented in Table 4.3. Both theoretical and experimental fits are shown in the Figures 4.49-4.66.

The two non-zero second order non-linear optical susceptibilities have been determined for the polymer thin films prepared in this investigation by comparing the SHG intensities from films with that from a reference done under the same conditions. An X-cut α-quartz single crystal was used as reference with d_{11}=0.5 pm/V. The incident fundamental beam polarisation was varied by rotating half wave plate. The SHG intensities were collected as a function of the incidence angle by rotating the sample around an axis perpendicular to the beam propagation direction at a given fundamental-harmonic beam configuration in order to extract the corresponding $\chi^{(2)}$ tensor components. The intensities were fitted using expression given by Swalen and Kajzar (99). The SHG experiments were conducted on fully poled films and the results are listed in Table 4.4.

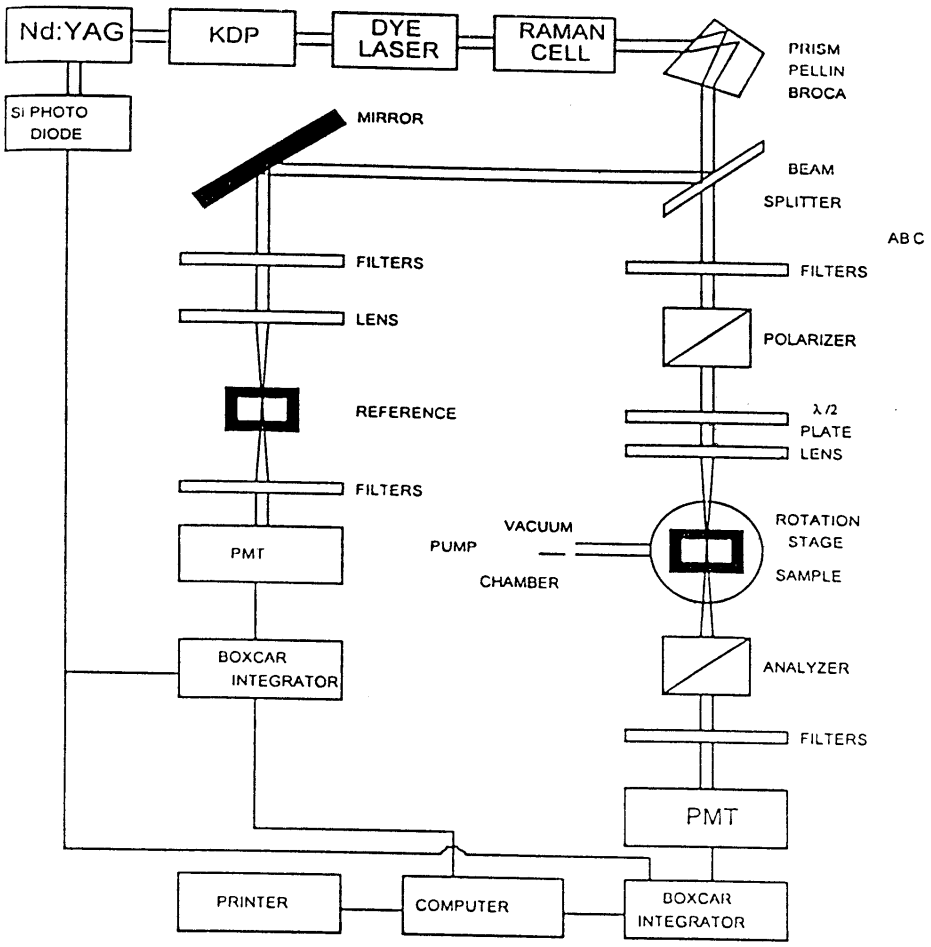

Figure 4.48 **Schematic representation of SHG-set-up**

Table 4.3 Structures of selected polymers studied for SHG

Polymer code	Structure
V 1	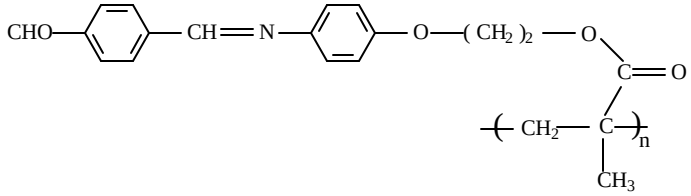
V 3	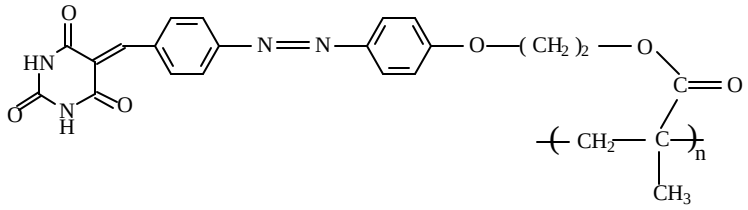
V 8	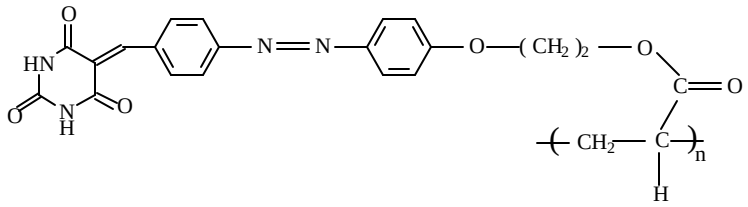
V 9	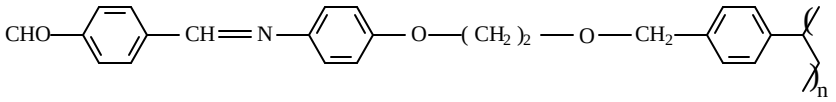
V 10	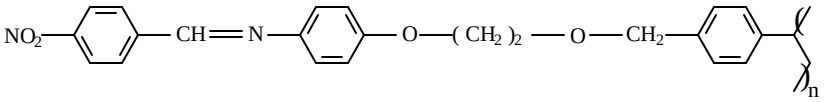
V 11	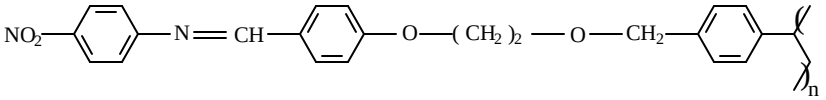
V 12	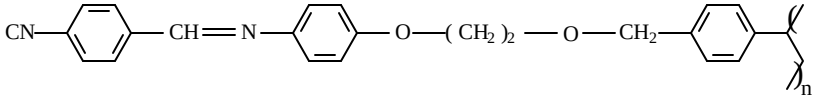
V-13	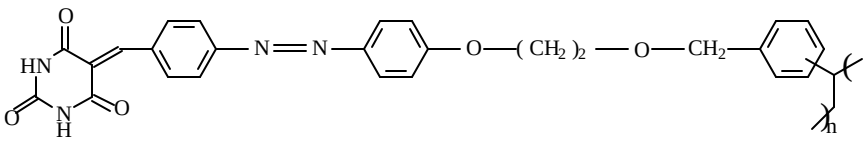

Contd…

Table 4.3 contd…

V 17	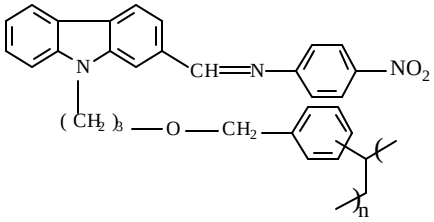
V 18	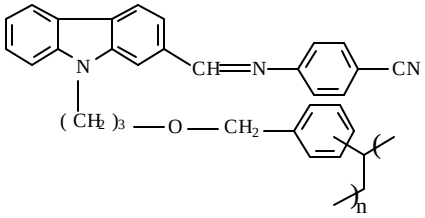
V-19	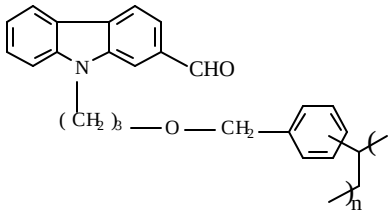
V-20	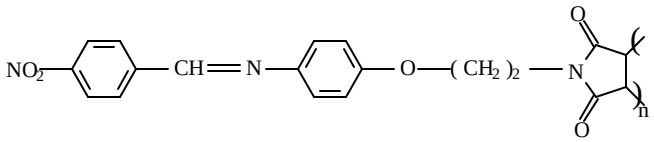
V-21	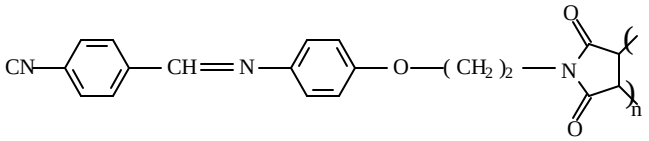
V-22	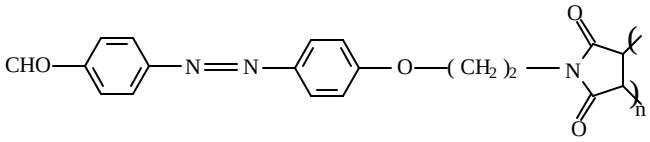

Contd…

Table 4.3 contd…

V-26

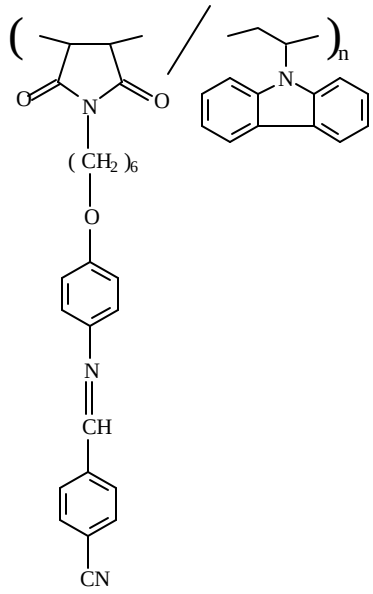

V 34

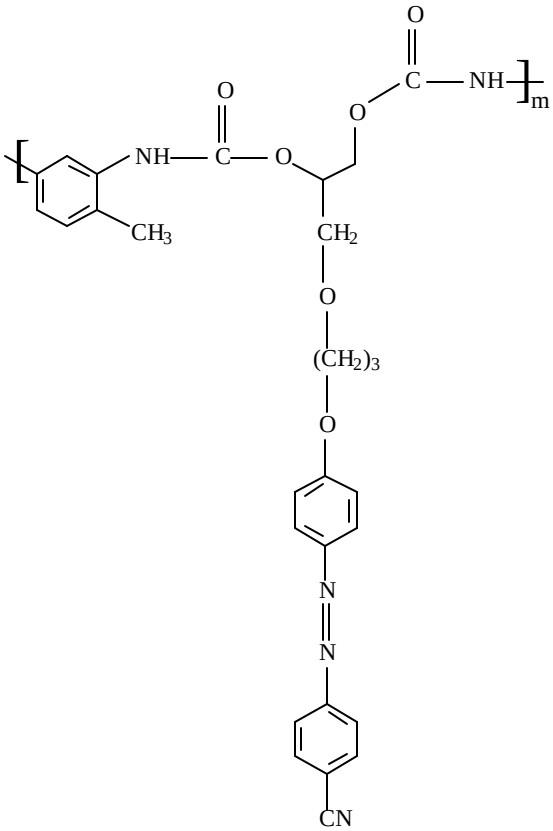

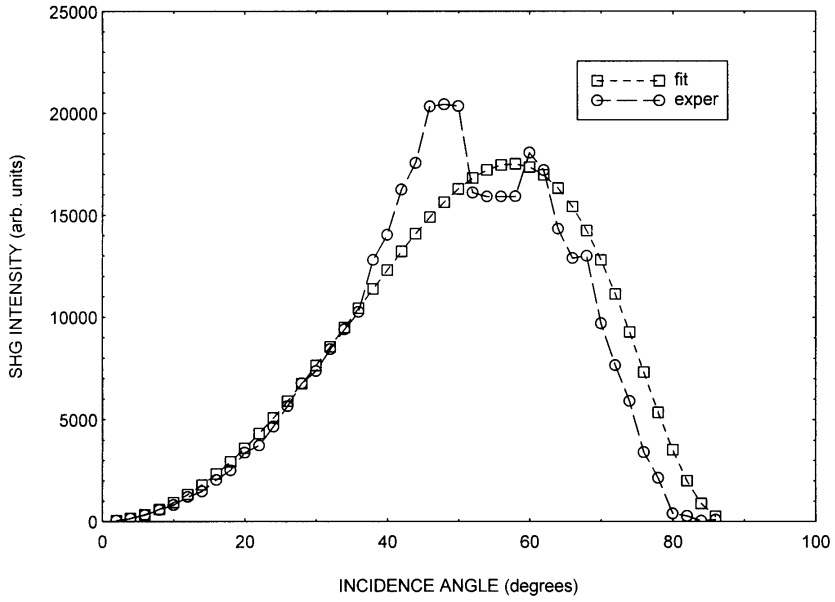

Figure 4.49 **Growth of SHG signal for polymer V 20 (p-p)**

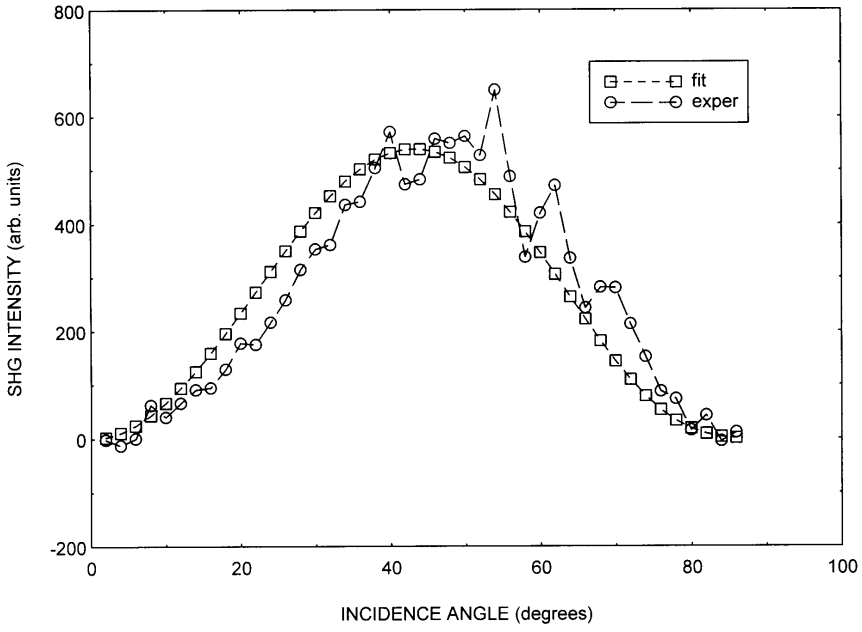

Figure 4.50 **Growth of SHG signal for polymer V 20 (s-p)**

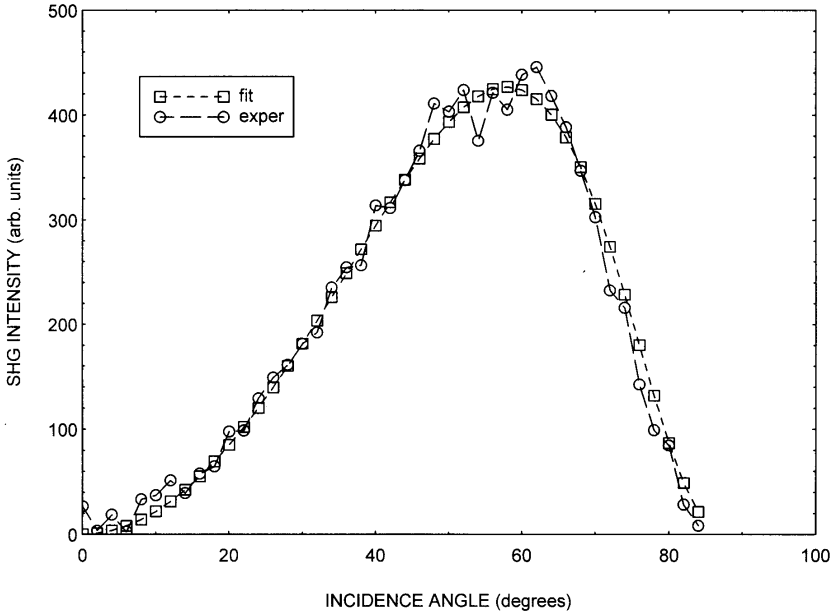

Figure 4.51 **Growth of SHG signal for polymer V 17 (p-p)**

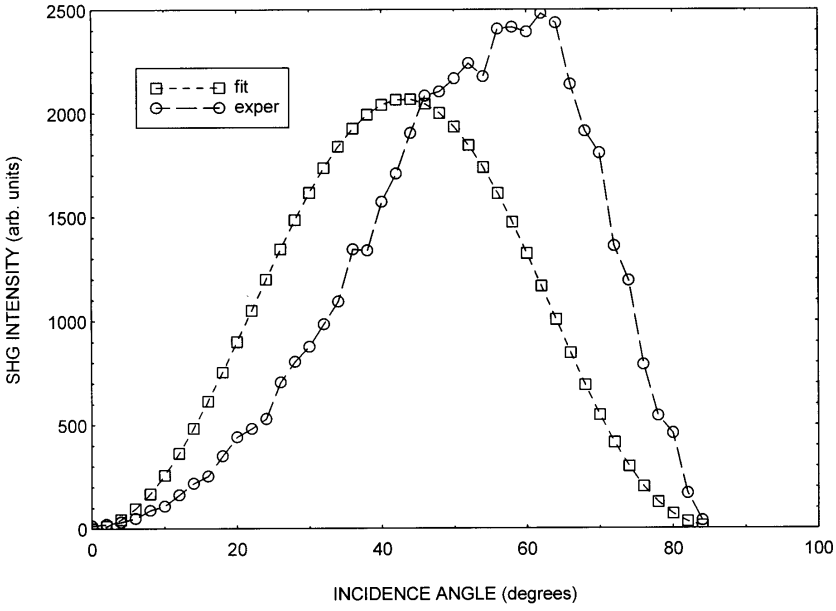

Figure 4.52 **Growth of SHG signal for polymer V 17 (s-p)**

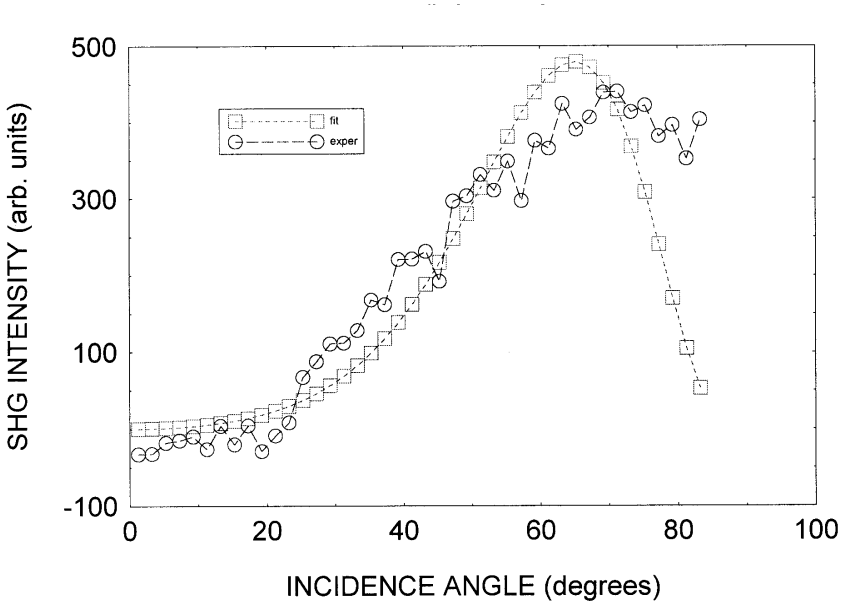

Figure 4.53 **Growth of SHG signal for polymer V 22 (p-p)**

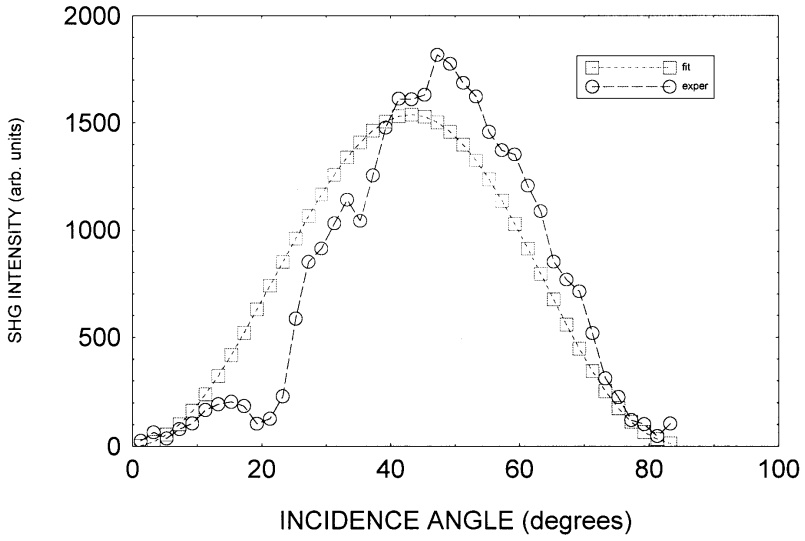

Figure 4.54 **Growth of SHG signal for polymer V 22 (s-p)**

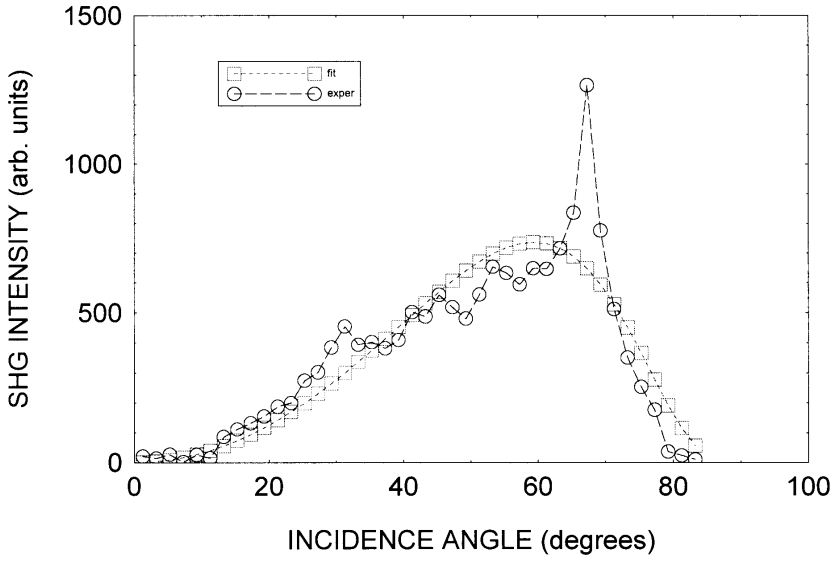

Figure 4.55 **Growth of SHG signal for polymer V 21 (p-p)**

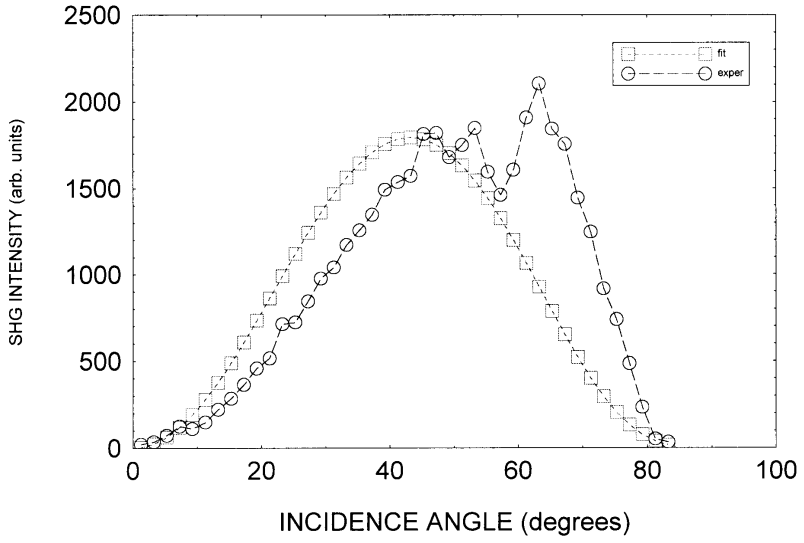

Figure 4.56 **Growth of SHG signal for polymer V 21 (s-p)**

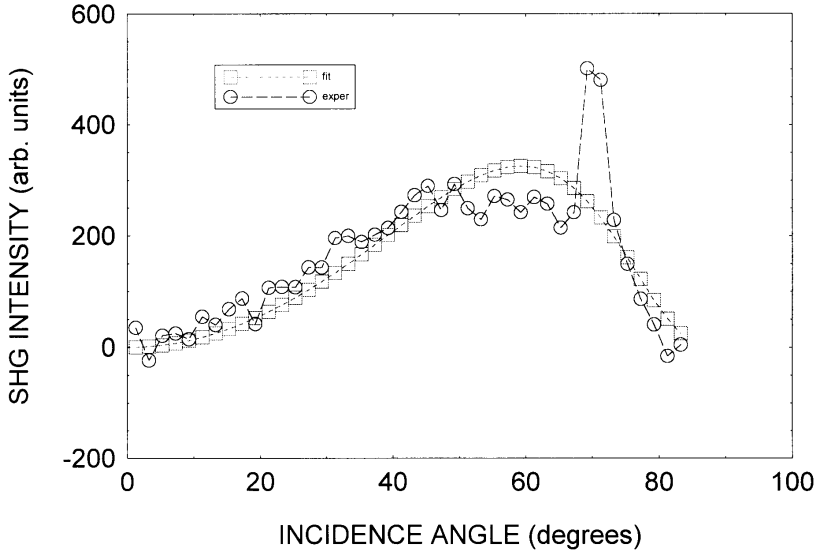

Figure 4.57 **Growth of SHG signal for polymer V 1 (p-p)**

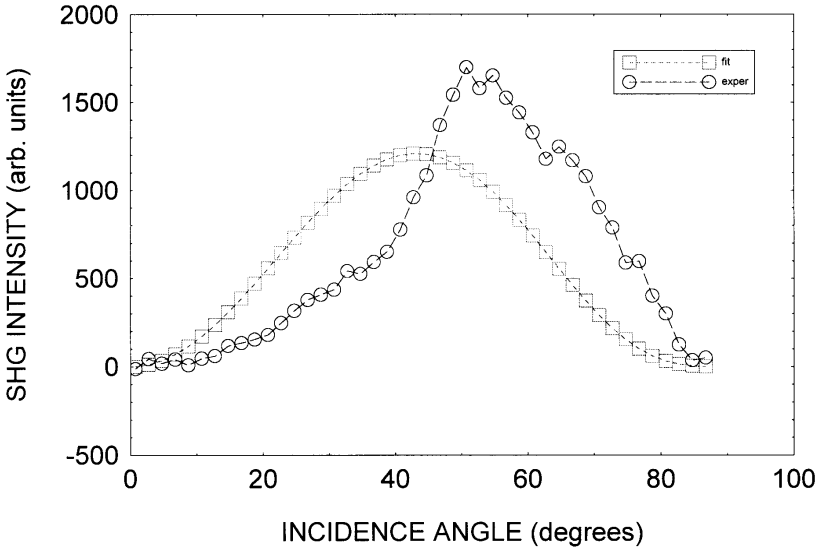

Figure 4.58 **Growth of SHG signal for polymer V 1 (s-p)**

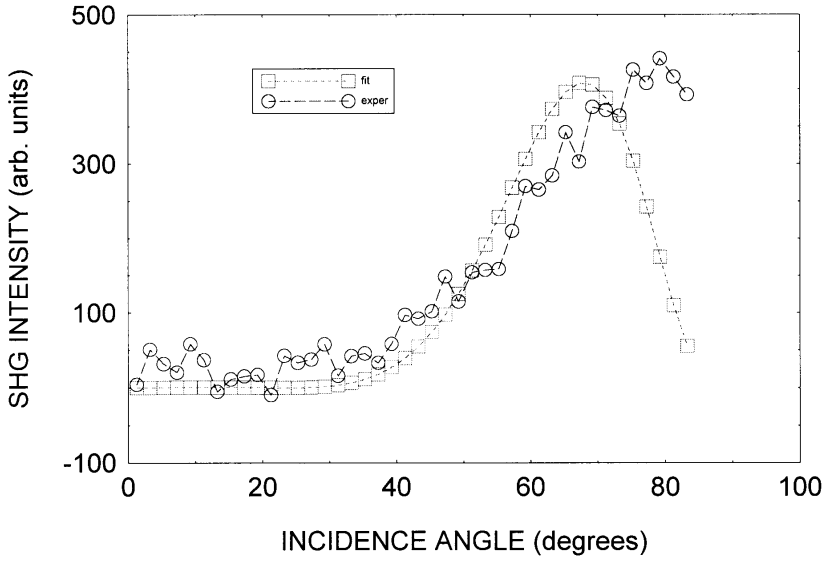

Figure 4.59 **Growth of SHG signal for polymer V 18 (p-p)**

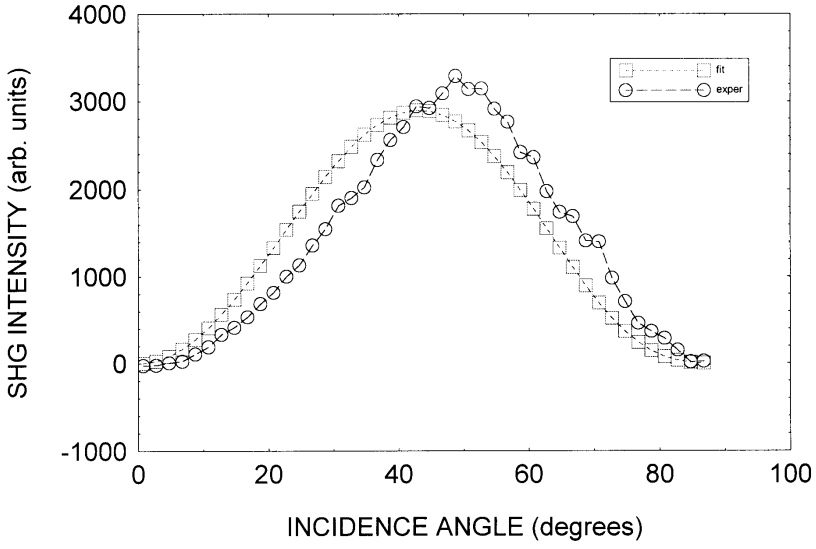

Figure 4.60 **Growth of SHG signal for polymer V 18 (s-p)**

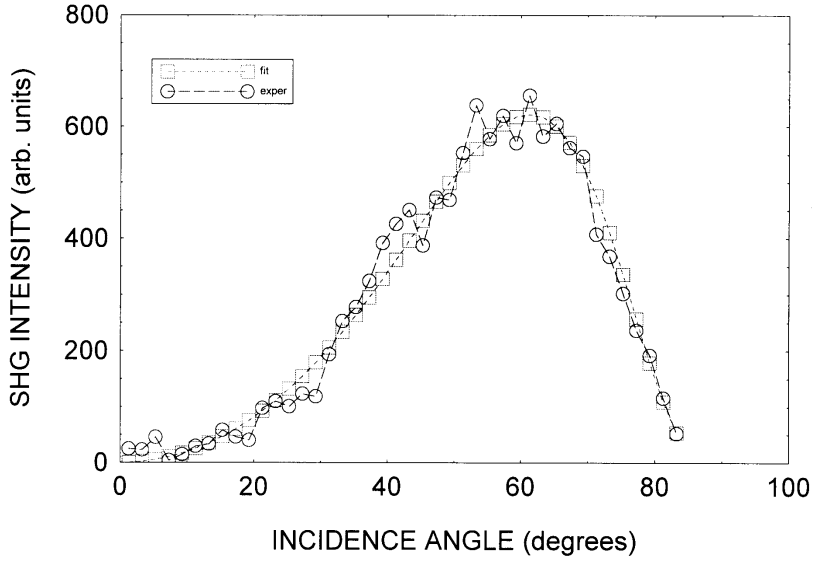

Figure 4.61 **Growth of SHG signal for polymer V 19 (p-p)**

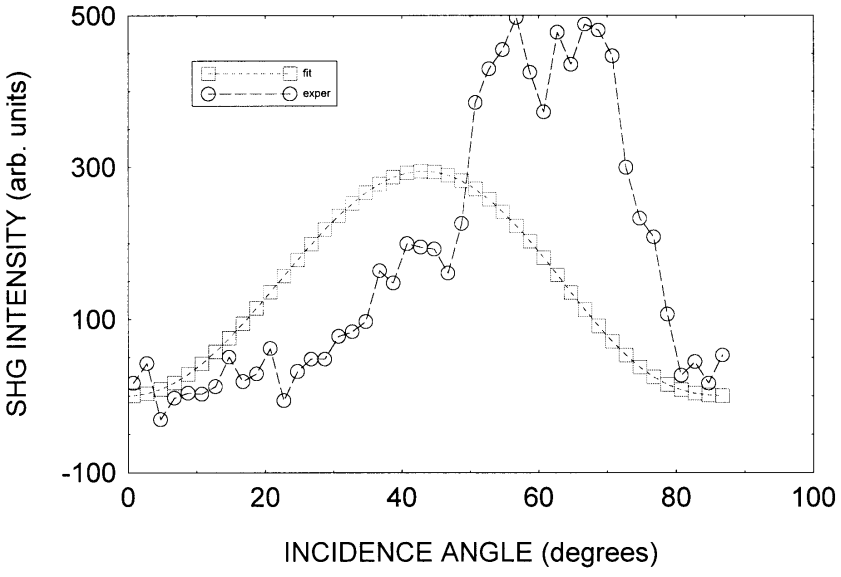

Figure 4.62 **Growth of SHG signal for polymer V 19 (s-p)**

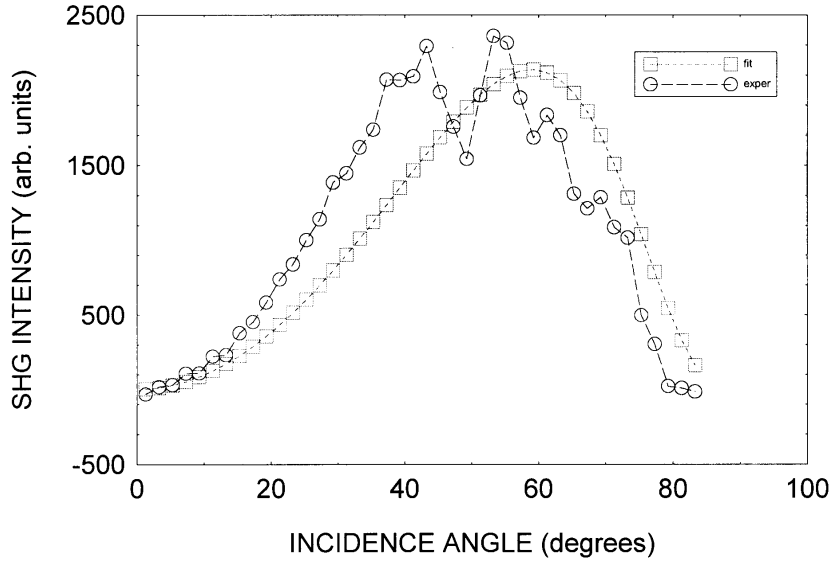

Figure 4.63 **Growth of SHG signal for polymer V 26 (p-p)**

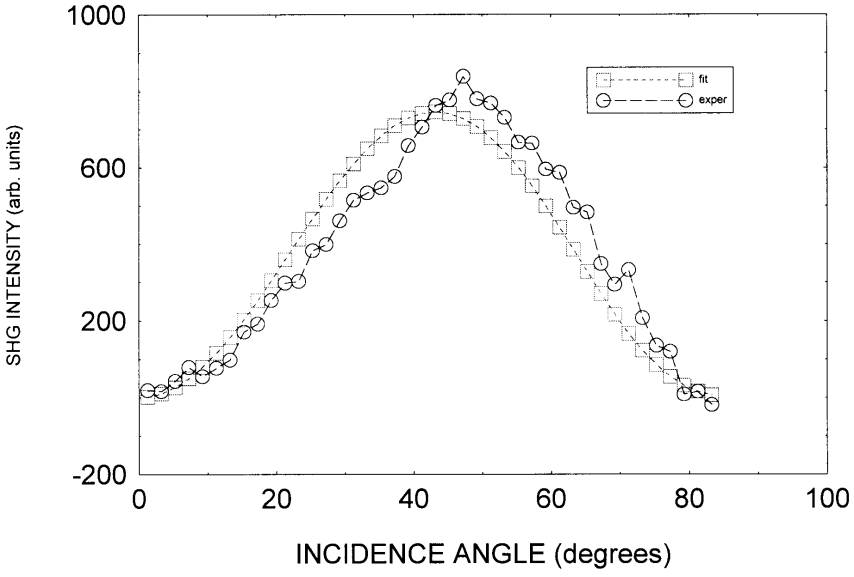

Figure 4.64 **Growth of SHG signal for polymer V 26 (s-p)**

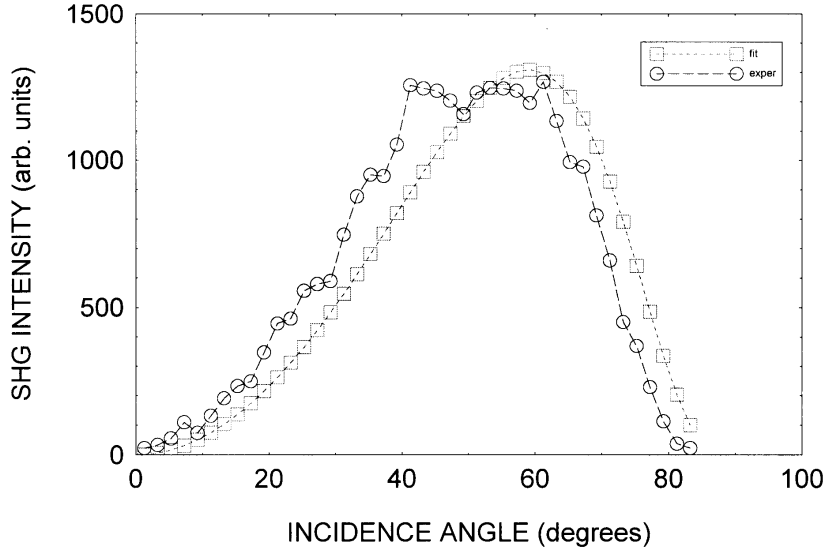

Figure 4.65 **Growth of SHG signal for polymer V 34 (p-p)**

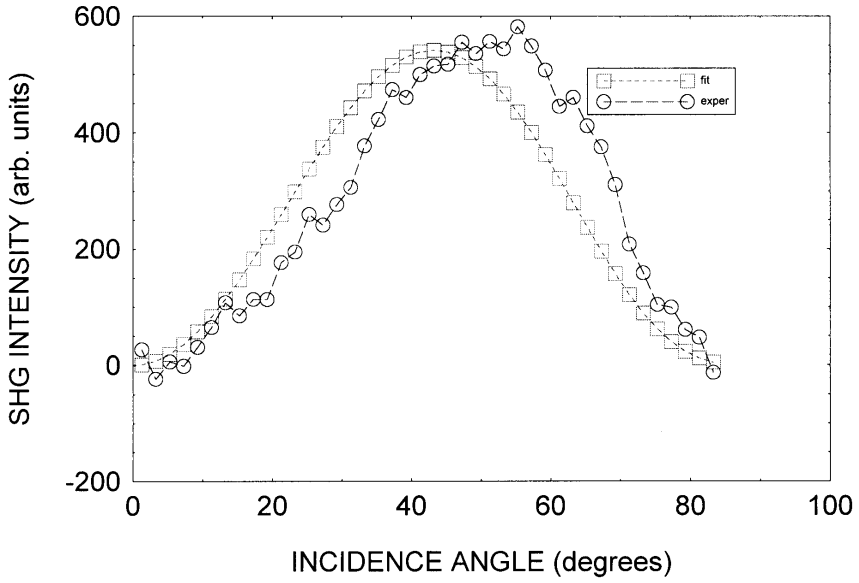

Figure 4.66 **Growth of SHG signal for polymer V 34 (s-p)**

Table 4.4 SHG results of selected polymers

Polymer code	Wavelength l_{max} (nm)	Thickness Å	d_{33} (pm/V)	d_{31} (pm/V)	d_{33}/d_{31}
V 1	378	500	2.426	0.809	3.0
V 3	352 ± 4	5849	0.418	0.105	3.8
V 8	356 ± 2	1278	0.148	0.049	3.0
V 9	357 ± 3	1388	0.013	0.004	3.25
V 10	358 ± 3	1000	0.186	0.061	3.2
V 11	390 ± 2	-	0.455	0.131	3.5
V 12	346 ± 1	4090	0.933	0.119	7.8
V 13	357 ± 2	2519	0.125	0.042	3.1
V 17	391 ± 3	962	10.617	3.539	3.0
V 18	348 ± 2	4382	2.704	0.901	3.0
V 19	331	8245	0.189	0.105	1.9
V 20	375 ± 3	2043	16.150	5.384	2.9
V 21	375	1389	1.499	0.500	3.0
V 22	349 ± 5	2316	6.393	2.131	3.0
V 26	341 ± 1	11818	1.169	0.237	5.0
V 34	360 ± 1	5390	0.485	0.237	2.04

Quartz single crystal was used as reference. The measurements were done at two different fundamental – harmonic beam polarisations: s-p and p-p. The first configuration allows to determine the d_{sp} susceptibility while the second the d_{pp} susceptibility, injecting the previously determined d_{sp} value.

There are 2 sets of data:

1. refractive index dispersion: The data were fitted by Sellmeier curve,

$$n^2 = A + B / (C - \lambda^2) \qquad \textbf{4.19}$$

where λ is wavelength in microns. It gives dispersion.

2. NLO data: These are measurements of 2 non-vanishing second order NLO susceptibility: d_{sp} and d_{pp}. There are 27 of such components, only two are non-zero due to thin film symmetry and Kleinman relations.

In most of the cases we have measured both components. In some however only diagonal d_{pp} was measured, assuming $d_{sp} = d_{pp}/3$ as it follows from isotropic model (gas model).

The d_{33} and d_{31} values were estimated by Maker-Fringe analysis. The ratio of d_{33} to d_{31} in some cases is higher than 3, a value predicted by molar statistical model for electric field poling of isotropic system (20). One of the assumptions made in the isotropic model, that the chromophores can rotate freely, may be responsible for this discrepancy. When the NLO chromophores are linked to the polymer backbone either directly or through short spacers, the motions of both the main chain and the side groups are coupled. This results in conformational constraints on chromophore ordering. Herminghaus et al. (100) and Robin et al. (101) developed simple models that take into account the effects of such conformational constraints to yield d_{33}/d_{31} ranging from 3 to 6.

Herminghaus et al. introduced a restriction parameter ν ($\nu \geq 0$) and developed a simple model to account for ratios ranging from 3 to 6. If all the dipoles participate in the poling process ($\nu=0$), the value $d_{33}/d_{31} = 3$ of the simple theory is retained. When $\nu=1$, only those dipoles rotating about an axis perpendicular to the applied electric field (i.e. parallel to the film) are involved in the poling process and results in $d_{33}/d_{31} = 6$. The experimentally determined d_{33} and d_{31} for some polymers agree with the theoretical prediction. In other cases, these values are less due to fast relaxation of poled polymer films.

SHG studies on Elastomer **E1** has been reported previously (92). The NLO

susceptibilities of the free-standing film were measured using a Maker-Fringe experiment.

To obtain the uniform layer orientation, a second uniaxial stress was applied instead of the (shear strain)⇒biaxial stress used in this study. Second uniaxial stress was applied under the angle $\Gamma = 90^{o} - \Psi$ to the first deformation direction (refer to Figure 4.67).

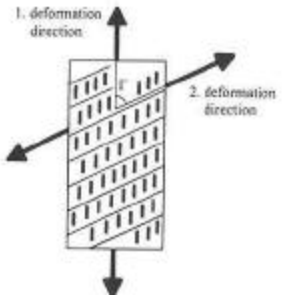

Figure 4.67 Structure of the chiral smectic C elastomer after the second deformation step

For the annealed, highly ordered sample the following values were obtained from Maker-Fringe curves theoretically fitted by known equation (92).

$$\mathbf{d_{22} = 0.10 \pm 0.05\ pm/V \text{ and } d_{23} = 0.15 \pm 0.05\ pm/V}$$

Although only 50% of the mesogenic units in the system contain the NLO-enhancing nitro group, these values are in the same order as the value of quartz (d_{11} = 0.5 pm/V) or those for nitro-substituted biphenyl chromophores in low molecular weight LC systems (102).

We could obtain excellent orientation of the layer structure by using shear fields and our X-ray results were comparable with those obtained for the Elastomer **E1** oriented by using uniaxial mechanical fields. This process also unwinds the helicoidal superstructure and accordingly, frequency doubling is observed where the intensity of the SHG is directly related to the perfection of the uniform smectic layer orientation. We can therefore conclude that similar SHG results could be predicted for our sample.

Thus samples exhibiting macroscopical C_2 symmetry are obtained without any external poling fields. The observed nonlinear susceptibilities are in the same order as those for similar chromophores in low molecular weight systems. It has to be noted that only 50% of the mesogenic units in our system are (not optimised) chromophores. Using more suitable chromophores much larger susceptibilities should be observed as already exemplified for low molar mass S_C* systems.

4.22 General conclusions

Several homo and copolymers were synthesised by free radical polymerisation from the corresponding monomers. The monomers were synthesised by simple organic transformations and purified and characterised. The polymers were precipitated and purified by reprecipitation. These were solubilised in common organic solvents and spin coated. The vacuum dried samples were electrically poled and their SHG was measured by Maker-Fringe analysis. Azobenzenes and azomethines were used as chromophoric moiety with A-D groups in para positions in the ring. Conventional electron withdrawing groups such as nitro, cyano as well as novel moiety like barbiturate were selected for the purpose. Oxy or thio groups were used as electron donating group. A variety of copolymers were synthesised. Also, novel heterocyclic moieties have been used as the chromophores. The spacer length used ranged from 2 to 6 methylene units. Polyurethanes were prepared from the synthesised novel diols by using simple organic reactions. These were characterised by IR and NMR. The d_{33} values were comparable with reported values. The experimentally determined 'r' value (d_{33}/d_{31}) for some polymers agreed with the theoretical prediction that onset of liquid crystallinity is desirable for high d_{33}/d_{31} ratio. Observation under crossed polarised light at different temperatures did not reveal any textures for the polymers. However, birefringence was observed for some spacer attached chromophoric units.

Bisstilbenes, bisazo or mixed stilbene/ azo compounds always absorb at higher wavelengths (472-528 nm) because of the rigid coplanar aromatic systems. But the two ring systems with azo and azomethine bridges absorbed at shorter wavelengths (<360 nm). This makes them useful for SHG applications. Also three or more ring systems face solubility problem. In this study, variety of chromophores with two ring systems have been synthesised.

The electron transmission follows the trend N=N > CH=CH > CH=N. The insertion of CH=N perturbs the conjugation to a limit. The rate of cross-linking is higher in stilbenes which paves way to CH=N and N=N.

Glass transition temperature (T_g) decreased with increasing spacer length and increasing flexibility of the polymer backbone. Isotropisation temperatures also decreased

with increasing spacer lengths. Spacer lengths of two, three or six methylene units have been used here. This was suitable for SHG, considering different factors and synthetic ease.

The backbones used in this study are polyacrylates, polymethacrylates, polystyrenes, polymaleimides and polyurethanes. More emphasis has been given on styrenes due to their good optical properties and higher T_gs compared to other systems. Also attempts were made to increase the rigidity of the polymer backbone by synthesising copolymers of styrene with maleimide.

Stronger acceptor generally leads to higher β values. The nitro group is an effective acceptor partially because it has the proper hybridisation to have effective overlap with the p orbitals of the benzene ring (103). Hammet constants with correlation between σ_R and β_0 provides the importance of nitro group for higher β value relative to groups like cyano, formyl, etc. Semi-empirical molecular orbital calculation predicts the electron-withdrawing (EW) effect of groups and thus barbiturate was considered.

Several chiral SmC* elastomers were synthesised and permanently oriented by suitable mechanical deformations. Thus samples exhibiting macroscopical C_2 symmetry were obtained without any external electric poling fields. Such systems therefore represent a new class of material for nonlinear optical applications.

In conclusion, this study presents synthesis, characterisation and properties of novel side chain polymers for NLO. Such basic research in hand with processing advancement will throw light into the research area of nonlinear optics.

4.23 Outlook

Non-linear optical materials are widely used in lasers and electro-optics, especially in solid-state lasers. They are extensively used for various applications including pure science, medicine, diagnostics, and entertainment. However, their most dominant market is in broad band telecommunications as optical switches and modulators. It is expected, based on the trend observed in recent years, that in general, the use of various types of non-linear optical materials will increase and dominate many fields especially in telecommunications. In particular, it is expected that by improving the

reliability of the materials, devices, electro-optical equipment and lasers, the market size of non-linear optical materials may increase significantly.

Some of the areas where focus for future research lies can be concluded as:

4.23.1 *Bio-medical applications*

The biomedical applications of non-linear optical (NLO) materials are still in infancy. Part of the problem concerns with difficulties of attaching (NLO) materials to tissue surfaces or to a specific organ. Development of the methods that will allow incorporation of NLO materials on proteins, tissue surfaces and specific organs (including bone surfaces) would be an important determinant in the future progress toward the use of NLO materials for biomedical use. The frequency doubling (or multiplication) effects can be used for diagnosis and also therapy of specific diseases.

4.23.2 *Applications of Optical Phase Conjugation*

Optical phase conjugation is a nonlinear optical process that generates the "phase-conjugate" or "time-reversed" replica of an optical wave front. A variety of nonlinear optical processes, including degenerate four-wave mixing and stimulated Brillouin scattering, can be used to perform the phase conjugation process. Applications of optical phase conjugation include aberration, correction of optical systems, distortion-free propagation through turbulence in the earth's atmosphere, construction of interferometers with novel operational characteristics, and the development of high energy laser systems.

4.23.3 *NLO in fiber optics*

A complete understanding of the origin of the nonlinear optical properties in optical fibers is needed to develop applications of optical fibers that make use of this nonlinear response. Examples of such applications include the development of sources of ultra-short pulses, the development of optical switches, and the development of optical solution transmission systems with enhanced data-transfer rates.

4.23.4 *Development of composite materials for NLO*

A basic question that is addressed by this work is whether it is possible to construct a composite material in such a manner that its nonlinear coefficients exceed those of the constituent materials, with the specific goal of developing materials with superior properties for use in photonic devices. Past work has demonstrated

experimentally that composite structures can be fabricated that possess enhanced third-order nonlinear optical response. Specific research projects which can excel in future include the following: (1) To perform laboratory studies of the second-order nonlinear response of composite materials, especially those fabricated from poled polymers; (2) To perform theoretical and experimental studies of composite materials possessing a fractal structure in an attempt to clarify the role of various distance scales in determining the level of enhancement of the nonlinear optical response; (3) To study the relationship between composite nonlinear optical materials and photonic band gap materials, for example, to determine whether the large spatial variations in electric field amplitude that occur near a photonic band gap be used to enhance the nonlinear optical response of such a material and (4) To develop layered structures with properties such that both quasi-phase-matching and enhanced nonlinear optical response occur.

4.23.5 *Basic NLO interactions*

There is a lot of room for the study of fundamental nonlinear optics such as: (1) Experimental studies of the efficiency of nonlinear optical interactions excited by beams brought to a focus by an axicon rather than by a spherical lens; (2) Studies of the noise properties of stimulated Brillouin scattering and the experimental determination of the noise figure of a beam of light amplified by this process; (3) Theoretical and experimental studies of the extent to which quantum mechanical fluctuations of the optical field can induce filamentation in an otherwise uniform laser field and (5) Studies of cascaded optical nonlinearities motivated particularly towards determining the role of cascading in self-induced second harmonic generation in optical fibers.

4.24 REFERENCES

1. Aurey, G., *Chem. Rev*., **63**, 645 (1963).

2. Hartzler, C. and Thaler, W., *J. Am. Chem. Soc*., **83**, 3877 (1961).

3. Kuwae, Y. and Kamachi, M., *Bull. Chem. Soc. Japan*, **62**, 2474 (1989).

4. Maillard, B., Ingold, K. U. and Scaiano, J. C., *J. Am. Chem. Soc*., **105**, 5059 (1983).

5. Bevington, J. C. and Troth, H. G., *Trans. Faraday Soc*., **58**, 186 (1992).

6. Tedder, J. M., *Angew. Chem. Int. Ed. Eng*., **21**, 401 (1982).

7. Mayo, F. R. and Walling, C., *Chem. Rev*., **46**, 191 (1950).

8. *Nonlinear Optical Properties of organic Molecules and Crystals*, Chemla, D. S. and Zyss, J., (eds.), John Wiley and Sons: NY (1991).

9. Prasad, P. N. and Williams, D. J., in *Introduction to Nonlinear Optical Effects in Molecules and Polymers*, John Wiley and Sons: NY (1991).

10. Williams, D. J., *Angew. Chem. Int. Ed*., **23**, 690 (1984).

11. *Nonlinear Optical Properties of Organic and Polymeric Materials ACS Symposium Series 233*, American Chemical Society: Washington DC (1983).

12. (a) Raimundo, J. –M., Blanchard, P., Ledoux-Rak, I., Hierle, R., Michaux, L. and Roncali, J., *Chem. Commun*., 1597 (2000). (b) Blanchard-Desce, M., Alain, V., Bedworth, P. V., Marder, S. R., Fort, A., Rusner, C., Barzoukas, M., Lebus, S. and Worthmann, R., *Chem. Eur. J*., **3**, 1091 (1997).

13. (a) Marder, S. R., Cheng, L.-T., Tiemann, B. G., Friedli, A. C., Blanchard-Desce, M., Perry, J. W. and Skindhoj, J., *Science*, **263**, 511 (1994). (b) Marder, S. R., Beratan, D. N. and Cheng, L.-T., *Science*, **242**, 103 (1991).

14. Risser, S. M., Beraran, D. N. and Marder, S. R., *J. Am. Chem. Soc*., **115**, 7719 (1993).

15. Levine, B. F. and Bethea, C. G., *J. Chem. Phys*., **63**, 2660 (1975).

16. Bethea, C. G., *Appl. Opt.*, **14**, 1447 (1975).

17. Meredith, G. R., Van Dusen, J. G. and Williams, D. J., *Macromolecules*, **15**, 1385 (1982).

18. Singer, K., Kuzyk, M. and Sohn, J., *J. Opt. Soc. Am. B*., **4**, 968 (1987).

19. (a) Guichard, B., Noël, C., Reyx, D., Chevalier, S., Senes, J. P. and Kajzar, F., *Macromol. Chem. Phys*., **198**, 3657 (1997). (b) Eckl, M., Müller, H., Strohriegl, P., Beckmann, S., Etzbach, K. H., Eich, M. and Vadra, J., *Macromol. Chem. Phys*., **196**, 315 (1995). (c)

Man, H. T. and Yoon, H. N., *Adv. Mater*., **4**, 159 (1992).

20. Miller, R. D., in *Organic Thin Films for Waveguiding Nonlinear Optics, Advances in Nonlinear Optics*, Vol. **3**, Kajzar, F. and Swalen, J. D., (eds.), Gordon and Breach Publishers: Amsterdam (1996); p.329.

21. Koga, T., Ohba, H., Takaze, A. and Sukagami, S., *Chem. Lett*., **11**, 2071 (1994).

22. Mortazavi, M., Knoesen, A., Kowel, S., Higgins, B. and Dienes, A., *J. Opt. Soc. Am. B*, **6**, 733 (1989).

23. (a) Shuto, Y., Amano, M. amd Kaino, T., *Jpn. J. Appl. Phys*., 30, 320 (1991). (b) Loucif-Saihi, R., Nakatani, K., Delaire, J. A., Dumont, M. and Sekkat, Z., *Chem. Mater*., **5**, 229 (1993).

24. Singer, K., Sohn, J. and Lalama, S., *Appl. Phys. Lett*., **49**, 248 (1986).

25. Singer, K., Kuzyk, M., Holland, W., Sohn, J., Lalama, S., Comizzoli, R., Katz, H., Schilling, M., *Appl. Phys. Lett*., **53**, 1800 (1988).

26. Meyers, F., Marder, S. R., Pierce, B. M. and Bredas, J. L., *J. Am. Chem. Soc*., **116**, 10703 (1994).

27. Bublitz, G. U., Ortiz, R., Runser, C., Fort, A., Barzoukas, M., Marder, S. R. and Boxer, S. G., *J. Am. Chem. Soc*., **119**, 2311 (1997).

28. Alain, V., Fort, A., Barzoukas, M., Chen, C., Blanchard-Desce, M., Marder, S. R. and Perry, J. W., *Inorg. Chim. Acta*, **242**, 43 (1996).

29. Shu, C., Tsai, W. J., Chen, J., Jen, A., Zhang, Y. and Chen, T., *Chem. Commun*., 19, 2279 (1996).

30. Jen, A., Cai, Y., Bedworth, P. V. and Marder, S. R., *Adv. Mater*., **9**, 132 (1997).

31. Guan, H. W. and Wang, C. H., *J. Chem. Phys.*, **98**, 3457 (1993).

32. Ye, C., Minami, N., Marks, T. J. and Yang, J., *Macromolecules*, **21**, 2899 (1988).

33. Jerphagnon, J. and Kurtz, S. K., *J. Appl. Phys*., **41**, 1667 (1970).

34. Noël, C., Gangadhara, Ching, K. C., Large, M., Reyx, D. and Kajzar, F., *Macromol. Chem. Phys.*, **198**, 1665 (1997).

35. Seava, F. D., (eds.), *Liquid Crystal: The fourth State of Matter*, Marcel Dekker Inc.: NY (1979); p.73.

36. McCulloch, I. A. and Bailey, R. T., in *Nonlinear Optical Properties of Organic Materials II, Proc. SPIE.*, **1147**, 134 (1989).

37. Morgan, P. W., Kwolek, S. L. and Pletcher, T. C., *Macromolecules*, **20**, 729 (1987).

38. (a) Prasad, P. N., Orezyk, M. E. and Zieba, J., *J. Phys. Chem.*, **98**, 8699 (1994). (b) Kippelen, B., Tamura, K., Peyghambarian, N., Padias, A. B. and Hall, H. K., *J. Appl. Phys*., **74**, 3617 (1993).

39. Page, R., Jurich, M., Reck, B., Sen, A., Twieg, R., Swalen, J., Bjorklund, G. and Wilson, C., *J. Opt. Soc. Am.* B, **7**, 1239 (1990).

40. Lindsay, G. A., Henry, R. A., Hoover, J. M., Knoesen, A. and Mortazavi, M. N., *Macromolecules*, **25**, 4888 (1992).

41. Dai, D., Marks, T. J., Yang, J., Lundquist, P. M. and Wong, G. K., *Macromolecules*, **23**, 1891 (1990).

42. Man, H. T., Chiang, K., Hass, D., Teng, C. C. and Yoon, H. N., *Proc. SPIE*, **1213**, 7 (1990).

43. (a) Duran, R., Guillon, D., Gramain, A. and Skoulios, A., *Makomol. Chem., Rapid Commun*., **8**, 321 (1987). (b) Finkelmann, H., Happ, M., Portugall, M. and Ringsdorf, H., *Makromol. Chem.*, **179**, 2541 (1978).

44. DeMartino, R. N., Khanarian, G., Leslie, T. M., Sansone, M. J., Stamatoff, J. B. and Yoon, H., *Proc. SPIE*, **1005**, 2 (1989).

45. Hayashi, A., Goto, Y., Nakayama, M., Kaluzynski, K., Sato, H., Kato, K., Kondo, K., Watanabe, T. and Miyata, S., *Chem.*, **4**, 555 (1992).

46. Monthéard, J. P., Booinon, B., Zerroukhi, A. and Cachard, A., *Polym.*, **33**, 3756 (1992).

47. Monthéard, J. P., Booinon, B., Zerroukhi, A. and LeBarny, P., *J. Appl. Polym. Sci.*, **44**, 1307 (1992).

48. Ahlheim, M. and Lehr, F., *Macromol. Chem. Phys*., **195**, 361 (1994).

49. Ahlheim, M. and Lehr, F., *Macromol. Chem. Phys*., **196**, 243 (1995).

50. Dörr, M. and Zentel, R., *Macromol. Rapid Commun*., **15**, 935 (1994).

51. Chang, J. Y., Kim, T. J., Han, M. J., Choi, D. H. and Kim, N., *Polymer*, **38**, 4651 (1997).

52. Sung, P. H., Chen, C. Y., Wu, S. Y. and Huang, J, Y., *J. Polym. Sci., Part A: Polym. Chem.*, **34**, 2189 (1996).

53. Noordegraaf, M. A., Kuiper, G. J., Marcelis, A. T. M. and Sudhölter, *Macromol. Chem. Phys*., **198**, 3681 (1997).

54. Strohriegl, P., *Makromol. Chem.*, **4**, 363 (1993).

55. Nalwa, H. S., Watanabe, T., Kakuta, A., Mukoh, A., Miyata, S., *Synthetic Metals*, 3895 (1993).

56. Muller, H., *Makromol. Chem. Rapid Commun*., **13**, 125 (1992).

57. Singer, K. D., *Appl. Phys. Lett*., **53** (19), 1862 (1988).

58. Samyn, C., Verbiest, T. and Persoons, A., *Makromol. Rapid Commun*., **21**, 1 (2000).

59. Goldstein, M. and Sinka, R., in *The glass transition and the nature of the glassy state*, New York Academy of Science: NY (1976).

60. Suresh, S., Vohra, V., Rajan, C. R., Ponrathnam, S., Large, M. and Kajzar, F. *Nonlinear Optics*, **19**, 367 (1999).

61. Gangadhara, Noël, C., Thomas, M., and Reyx, D., *J. Poly. Sci.: Part A: Poly. Chem.*, **36**, 2531 (1998).

62. Gangadhara, Ponrathnam, S., Noël, C., Reyx, D. and Kajzar, F., *J. Poly. Sci.: Part A: Poly. Chem.*, **37**, 513 (1999).

63. Tanaka, M. and Nakaya, T., *Kobunshi Ranbunshu*, **43**, 311 (1986).

64. Burnett, G. M., in *Mechanism of Polymer Reactions*, Interscience: NY (1954), p.76.

65. Frisch, K. C., in *Macromolecular design of polymeric materials*, Hatada, K., Kitayama, T. and Vogl, O. (eds.), Marcel Dekker, Inc.: NY (1997); Chap.31, p.523.

66. Kajzar, F., Horn, K., Nahata, A. and Yardley, J. T., *Nonlinear Optics*, **8**, 205 (1994).

67. Perplies, E., Ringsdorff, A., Wendroff, J. H., *J. Poly. Sci. Poly. Lett*., **13**, 243 (1976).

68. Comizzoli, R. B., *J. Electrochem. Soc*., **2**, 134, 424 (1987).

69. Hood, K., in *Comprehensive Polymer science: The Synthesis, Characterisation and Applications of Polymers*, Pergamon: Oxford (1989); Chap. 37.

70. Hubbard, M. A., Marks, T. J., Yang, J. and Wong, G. K., *Chem. Mater*., **1**, 167 (1989).

71. Eich, M., Reck, B., Yoon, D. Y., Willson, C. G., Bjorklund, G. C., *J. Appl. Phys*., **66**, 3241 (1989).

72. Kim, J., Plawsky, J. L., Laperuta, R. and Korenowski, G. M., *Chem. Mater*., **4**, 249 (1992).

73. Yoon, C. –B. and Shim, H. –K., *Macromol. Chem. Phys*., **199**, 2433 (1998).

74. Kapitza, H., Zentel, R., Twieg, R. J., Nguyen. C., Vallerien., S. U., Kremer, F. and Willson, C. G., *Adv.Mater*., **11**, 539 (1990).

75. Hikmet, R. A. M., Lub, J. and Higgins, J. A., *Polymer*, **34**(8), 1736 (1993).

76. Meerwein, H. in *"Houben-Weyl:Methoden der organischen Chemie"*, 6/3, 4. Auflage, Georg Thieme Verlag Stuttgart, 1965, S.55.

77. Mitsunobu, O., *Synthesis*, **1** (1981).

78. Schmitt, K., Herr, R. -P., Schadt, M., Fünfschilling, J., Buchecker, R., Chen, X. H. and Benecke, C., *Liquid Crystals*, **14** (6), 1735 (1993).

79. Brehmer, M. and Zentel, R., *Mol. Cryst. Liq. Cryst. Sci. Technol., Sect A.*, **243**, 353 (1994).

80. Finkelmann, H. and Rehage, G., *Makromol. Chem. Rapid. Commun*., **3**, 859 (1982).

81. Jákli, A. and Saupe, A., *Liq. Crystals*, **9**, 519 (1991).

82. Witt, O. N. and Johnson, S., *Chem. Ber*., **26**, 1908 (1893).

83. Hahn, G., Stenner, W. and Hoppe Seylers Z., *Physiol. Chem.*, **181**, 93 (1929).

84. Bredereck, H. and Heckh, H., *Chem. Ber*., **91**, 1416 (1958).

85. Semmler, K., Dissertation, Universität Freiburg (1994).

86. Hassner, A. and Alexanian, V., *Tetrahedron Lett.*, **46**, 4475 (1978).

87. Nishikawa, E., Dissertation, Universität Freiburg (1997).

88. Goodby, J. W., in *Ferroelectric Liquid Crystals*, Gordon and Breach Science Publishers: NY (1991), p.99.

89. Finkelmann, H., Kock, H. J. and Rehage, G., *Makromol.Chem., Rapid Commun*., **2**, 317 (1981).

90. Walba, D. M., Ros, M. B., Clark, N. A., Shao, R., Johnson, K. M., Robinson, M. G., Liu, J. Y. and Doroski, D., in *Materials for Nonlinear Optics*: *Chemical Perspectives*, Marder, S. R., Stucky, G. D. and Sohn, J. E. (eds.), ACS Symposium Series 455, American Chemical Society: Washington DC (1991).

91. Walba, D. M., Ros, M. B., Clark, N. A., Shao, R., Johnson, K. M., Robinson, M. G., Liu, J. Y. and Doroski, D., *Mol. Cryst. Liq. Cryst*., **198**, 51 (1991).

92. Benné, I., Semmler, K. and Finkelmann, H., *Macromolecules*, **28**, 1854 (1995).

93. Kurtz, S. K. and Perry, T. T., *J. Appl. Phys*., **39**, 3798 (1968).

94. Boshard, C., Knopfle, G., Pretre, P. and Gunter, P., *J. Appl. Phys*., **71**, 1594 (1992).

95. Chemla, D. S., Qudar, J. L. and Jerphagnon, *J., Phys. Rev. B*, **12**, 4534 (1975).

96. Clays, K. and Persoons, A., *Phys. Rev. Lett*., **66**, 2980 (1991).

97. Maker, P. D., Terhune, R. W., Nisenoff, M. and Sawage, C. M., *Phys. Rev. Lett*., **8**, 21 (1962).

98. Singer, K. D., in *Polymers for Light Wave and Integrated Optics: Technology and Applications*, Hornak, L. A., (eds.), Marcel Dekker: NY (1992); p.321.

99. Gonin, D., Noël, C. and Kajzar, F., in *Organic Thin Films for Waveguides in Nonlinear Optics, Advances in Nonlinear Optics*, Vol. **3**, Kajzar, F. and Swalen, J. D., (eds.), Gordon and Breach Publishers: Amsterdam (1996); p.221.

100. Herminghaus, S., Smith, B. A. and Swalen, J. D., *J. Opt. Soc. Am. B*, **8**, 2311 (1991).

101. Robin, P., Le Barny, P., Bronssoux, D., Pocholle, J. P. and Lemooine, V., in *Organic Molecules for Nonlinear Optics and Photonics*, Messier, J., Kajzar, F. and Prasad, P. N., (eds.), Kluwer Academic Publishers: Dordrecht (1991); p.481.

102. Yoshino, K., Utsumi, M., Morita, Y., Sadohara, Y. and Ozaki, M., *Liq.Cryst.*, **14**, 1021 (1993).

103. Monaco, R. R., Gardiner, W. C., *J. Phys. Org. Chem.*, **8**(10), 629 (1995).